NASA TECHNICAL MEMORANDUM

NASA TM X-71455

NASA TM X-71455

CENTAUR STANDARD SHROUD (CSS) CRYOGENIC UNLATCH TESTS

Titan/Centaur Project Office
Lewis Research Center
Cleveland, Ohio 44135
October, 1973

TABLE OF CONTENTS

ABBREVIATIONS

CSS	Centaur Standard Shroud
EMI	Electro-Magnetic Interference
ETR	Eastern Test Range
FBR	Forward Bearing Reactor
FSR	Forward Seal Release
GD/CA	General Dynamics' Convair Aerospace Division
GHe	Gaseous Helium
GN_2	Gaseous Nitrogen
LH_2	Liquid Hydrogen
LMSC	Lockheed Missiles and Space Company, Inc.
LN_2	Liquid Nitrogen
LOX	Liquid Oxygen
NASA	National Aeronautics and Space Administration
PYC	Pyrotechnic Control Unit
SFC	Squib Fire Circuit
SMDC	Single Mild Detonating Cord
TSAP	Tank/Shroud Annulus Pressure

I. PROGRAM SUMMARY

by S. V. Szabo, Jr.

SUMMARY

Cryogenic tanking and partial jettison (unlatch) tests were performed on a full scale Centaur vehicle and Centaur Standard Shroud (CSS) to develop and qualify the CSS insulation system, the CSS and Centaur ground-hold purge systems, and the Centaur hydrogen tank flight vent system. Operation of the shroud/Centaur pyrotechnic systems, seals, and the shroud jettison springs, hinges, and other separation systems was demonstrated by a partial jettison of the shroud into catch nets. The Centaur tanks were filled with liquid hydrogen and liquid nitrogen. Prelaunch operations were performed, and data taken to establish system performances. These tests were performed at the NASA Lewis Research Center's Plum Brook Station.

Results from the initial tests showed a higher than expected heat transfer rate to the Centaur hydrogen tank. In addition, the release mechanism for the forward seal between the Centaur and the CSS did not function properly, and the seal was torn during jettison of the shroud. Cross-wiring on installation of the shroud explosive separation system also caused the explosive containment tube to rupture. Extensive modifications were made to the insulation and the forward seal release mechanism. Changes were also made to prevent cross-wiring of the shroud explosive separation system on installation.

A series of special tests were performed to establish the effectiveness of insulation modifications and to demonstrate the satisfactory operation of the redesigned forward seal release mechanism.

Results from these tests showed that the forward seal release was satisfactory and that the heat transfer rate to the Centaur hydrogen tank was reduced by about 50 percent. A final cryogenic unlatch test was then performed with a successful shroud jettison and forward seal release. This concluded the cryogenic unlatch test portion of the CSS qualification program.

INTRODUCTION

All spacecraft require some form of protection from weather and a thermally controlled environment during prelaunch operations. In addition, protection is required from adverse aerodynamic and thermal environments during launch and ascent. These requirements are usually satisfied by a shroud or fairing attached to the launch vehicle and enclosing the spacecraft. This shroud is jettisoned after the most adverse conditions are passed in the launch and ascent phase of flight.

In addition to the spacecraft protection, space vehicles utilizing cryogenic propellants require thermal insulation during prelaunch operations to prevent excessive propellant boil-off. Insulation is also required during ascent for protection from aerodynamic heating.

The Centaur space vehicle, mated with the Titan IIID booster, was chosen to be the launch vehicle for the Viking spacecraft to orbit and soft land on the planet Mars in 1976. This Centaur vehicle is called the Centaur D-1T.

The Centaur was the United States' first upper stage vehicle using liquid hydrogen and liquid oxygen as the propellants. As the upper stage for the Atlas booster, this combination has been the launch vehicle for Surveyor, Mariner, Pioneer, OAO, and a series of communication satellites.

The current D-series Centaur vehicle, using the Atlas as the booster stage, utilizes one of several shroud designs for spacecraft protection dictated by spacecraft size and mission requirements. Thermal protection for the Centaur liquid hydrogen tank during prelaunch and ascent is provided by jettisonable insulation panels.

The Viking spacecraft requires a large diameter aeroshield for landing on Mars. This meant an increased diameter shroud, over those presently used, would be required for spacecraft protection. The larger diameter shroud would also be heavier than existing shrouds and aerodynamic loading during ascent would tax the strength of the Centaur. One possibility to enhance structural capability would be to make the Centaur tank heavier and make the present insulation panels capable of carrying a structural load. This, however, meant increased complexities in system designs and many modifications to existing designs.

Instead the shroud design that would cover the spacecraft and Centaur, and be a structural member along with providing insulation for Centaur's cryogenic propellant tanks, was conceived. This was the design finally chosen and Lockheed Missiles and Space Company, Inc. (LMSC) was awarded the contract to design and build the shroud. This shroud has been designated the Centaur Standard Shroud (CSS).

A test program consisting of the following three major series of tests was conducted at the Lewis Research Center's Plum Brook Station to qualify the CSS for flight.

1. Cryogenic unlatch tests to qualify the shroud insulation, purges, and jettison systems under cryogenic conditions.

2. Structural tests to establish the load carrying and structural capabilities of the shroud.

3. Heated jettison tests at altitude conditions, to demonstrate shroud jettison system operation after experiencing simulated aerodynamic heating during ascent.

This report presents the results of the cryogenic unlatch tests of the CSS completed in February 1973. Descriptions and tests results of the CSS, its

systems, and the applicable Centaur vehicle systems from the cryogenic unlatch tests are presented. Facility description and supporting test control and instrumentation systems are briefly described in the appendices to the report.

TEST HARDWARE CONFIGURATION

The test hardware for the Centaur Standard Shroud cryogenic unlatch test program consisted of the following major items and systems:

1. A Centaur Standard Shroud with the insulation, jettison and pyrotechnic systems, and all seals and bolt-on hardware installed.

2. A Centaur flight-weight tank with several major items and systems installed to configure it to a D-1T vehicle.

3. Centaur interstage adapter.

4. Titan skirt.

5. Viking payload envelope model.

The overall test configuration and assembly of this hardware in the Plum Brook B-3 facility is shown in Figures 1-1 and 1-2. A brief description of the shroud, tank, interstage adapter, Titan skirt, and Viking payload envelope model follows. Detailed descriptions of each of the supporting systems can be found in the respective sections of this report.

CENTAUR STANDARD SHROUD (CSS)

The Centaur Standard Shroud (CSS) encloses both the Centaur and the payload, and provides environmental protection for both while on the ground and in flight. The CSS general configuration is shown in Figure 1-3. The cylindrical portion of the shroud around the Centaur and spacecraft is 14 feet in diameter. Total shroud length is 58 feet.

The payload section (forward of station 2514.0) is about 31 feet long. The nose cap is made from corrosion-resistant stainless steel, with two aluminum radiation shields attached to the inside. (These radiation shields were not installed for the test.) The two conical sections forward of station 2680.66 are of magnesium semimonocoque construction. The cylindrical section between stations 2514.0 and 2680.66 is of aluminum semimonocoque, corrugated construction. Attached to internal rings in the conical and cylindrical section are one-inch thick fiberglass blankets. (These fiberglass blankets were also not installed for the test.)

The equipment section, from station 2459.14 to station 2514.0, allows access to hardware on the Centaur equipment module through doors in the shroud. This portion is also of aluminum, semimonocoque construction.

A forward bearing reaction system between the shroud and the Centaur at station 2459.14 reduces shroud/Centaur relative deflections during launch and ascent. The reaction path is released after maximum dynamic loading by a pyrotechnic system that severs the bearing struts, and they retract to a stowed position.

The cylindrical section around the Centaur LH_2 tank is also of aluminum, semimonocoque corrugated construction. The annular space between the shroud and the Centaur is isolated from the remainder of the shroud by flexible seals at stations 2241.78 and 2459.14. This annular volume is purged with helium during prelaunch operations. Fiberglass insulation attached to internal rings in this section of the shroud provides insulation for the Centaur LH_2 tank. This volume is isolated from the rest of the shroud until just prior to shroud jettison.

The remaining portion of the shroud below station 2241.78 is also of aluminum semimonocoque corrugated and skin-stringer construction. It contains the aft circumferential separation joint, hinges, and the interface to the Centaur interstage adapter.

The two halves of the CSS join along a longitudinal split line. Each half also joins to the fixed aft part of the shroud along the circumferential separation joint at station 2209.

At jettison, all separation joints are severed by a noncontaminating pyrotechnic system. The aft conical boattail is bolted to the Centaur interstage adapter and is jettisoned with the Titan stage. Eight compressed springs mounted longitudinally at the base of the shroud force the two halves to separate. Two hinges for each half are attached at the aft circumferential separation plane.

Centaur Tank

The Centaur tank assembly used was a flight-weight tank of the "D" series configuration. The basic tank configuration and dimensions are shown in Figure I-4. The tank assembly is made of type -301 stainless steel and is a completely monocoque structure requiring internal pressure to support its own weight. A common evacuated, double-walled bulkhead separated the forward liquid hydrogen tank from the aft liquid oxygen tank.

The basic Centaur tank had the following major items of hardware and systems installed to configure it partially to the D-1T design:

1. Payload truss adapter.
2. Centaur D-1T equipment module and dummy electronic/avionic packages.
3. Centaur stub adapter.
4. Hydrogen tank flight vent system.
5. Stub adapter radiation shield.

6. Hydrogen tank radiation shield (prototype).

7. Forward and aft shroud to Centaur seals.

8. Forward seal releaser system.

9. Forward bearing reaction struts.

10. Centaur/CSS purge systems.

11. Pyrotechnic system control boxes and harnessing (for forward bearing reaction struts and forward seal releaser).

12. Electrical, instrumentation, and RF disconnects between the Centaur and CSS.

Details and descriptions of each of these major items and systems can be found in other sections of this report.

Other Centaur D-1T systems not necessary for the conduct of the tests, such as propulsion, pneumatic, and propellant feed systems, were not installed.

Centaur Interstage Adapter

The Centaur interstage adapter is the structural item that the Centaur and shroud are attached to at their aft support points. It provides the interface between the Centaur, CSS, and Titan skirt. Details of its construction can be found in Section VIII of this report. It is manufactured by General Dynamics' Convair Aerospace Division.

Titan Skirt

The Titan skirt is another structural item providing an interface between the Centaur shroud hardware and the Titan vehicle. It is manufactured by the Martin Marietta Corporation.

Viking Payload Envelope Model

The Viking payload envelope model was a test peculiar item. It was mounted on top of the Centaur truss adapter in the flight location. Its purpose was to provide the dimensional envelope of the Viking spacecraft during shroud jettison to determine if clearance problems existed.

TEST OBJECTIVES

The cryogenic unlatch test program was part of the CSS qualification test program whose general test objective is to qualify for flight the Centaur Standard

Shroud and modified Centaur systems for the Titan/Centaur D-1T vehicle. The cryogenic unlatch test program general objectives were to:

1. Obtain data and evaluate the performance of the Centaur and shroud ground-hold systems.

2. Demonstrate proper operation of the shroud jettison systems.

To accomplish these overall objectives, the following detailed objectives were defined:

1. Evaluate the ground venting capability of the D-1T Centaur hydrogen tank vent system. (This objective required LH_2 in the Centaur hydrogen tank.)

2. Determine the heat transfer rate through the CSS and Centaur structure to the Centaur liquid hydrogen tank. Establish prelaunch thermal environments. (Required tanking LH_2.)

3. Evaluate the performance of the shroud/Centaur ground-hold purge systems.

4. Evaluate leakage of purge gases through the CSS and seals during ground-hold.

5. Demonstrate separation of the shroud/Centaur forward bearing reaction (FBR) struts when their pyrotechnic bolts are severed under temperature conditions that will be present when liquid hydrogen is in the Centaur tank.

6. Demonstrate the ability of the CSS to unlatch by the successful action of the pyrotechnic joints, springs, and hinges, and to begin jettison; demonstrate that appropriate electrical and mechanical connections separate properly during start of jettison, and measure shroud motion during this partial jettison.

7. Determine the transmissibility of the shock from the CSS pyrotechnic separation devices to areas of the Centaur, CSS, and the Titan skirt.

TESTS PERFORMED

A summary of all tests performed in the cryogenic unlatch test program is given in Table 1-1. The tests are listed chronologically.

The test program as originally conceived and defined in references 1 and 2 consisted of the combined system test and the three cryogenic unlatch tests. During the course of the program, however, a higher than expected heat transfer rate to the Centaur hydrogen tank, and problems with the forward seal release during jettison were encountered. Modifications were made to the shroud insulation and the forward seal release mechanism was redesigned. As a result of these changes, the ambient forward seal release test and the LN_2/LN_2 and LH_2/LN_2 tanking and seal release tests were added. Cryogenic unlatch test no. 3 was performed at the completion of these tests and was the final test in the program.

GENERAL TEST SEQUENCE

The general sequence of major events for all the cryogenic unlatch tests was the same. These were, in order:

1. Pretest test hardware and facility checkout.

2. Super-Zip and other ordnance loading and installation.

3. Initiation of countdown operations and GN_2 purge of tank/shroud annulus.

4. Transfer of tank/shroud annulus purge from GN_2 to GHe.

5. Ordnance system arming.

6. Test site evacuation.

7. Centaur propellant loading (LN_2 and H_2).

8. Cold soak to thermal equilibrium of test hardware.

9. Heat transfer tests and other tests of CSS and Centaur, including water spray or "rain" tests.

10. Detanking of Centaur LH_2 tank (for safety requirements)

11. Initiation of autosequence:

    a. Fire Forward Bearing Reactor (FBR) pyrotechnics and separate FBR struts.

    b. Fire Forward Seal Release (FSR) pyrotechnics and release forward seal (cryo-unlatch test no. 3 only).

    c. Fire Super-Zip and jettison shroud.

    Note: For tanking and forward seal release tests, (tests nos. 4, 5, and 6 of Table 1-1) only the FSR pyrotechnics were fired. See Appendix A for detailed autosequence.

12. Facility clean-up and inertion and safing of ordnance systems.

13. Preliminary inspection.

14. Firing of secondary Super-Zip cord with shroud in catch nets. (Cryo-unlatch tests nos. 2 and 3 only.)

15. Final inspection and facility shutdown.

16. Removal of shroud from test stand for refurbishment.

Chronological resumes of each cryo-unlatch test and the LN_2/LN_2 tanking and forward seal release and the LH_2/LN_2 tanking and forward seal release tests are presented in Appendix D.

Removal of the shroud, refurbishment, and reinstallation had to be accomplished between each test. Refurbishment consisted of repairing damage incurred during the test, changing expended hardware, instrumentation changes and any other modifications. The entire shroud was then reassembled in sections, in the test stand, and prepared for the next test. Average time for removal, refurbishment, and reinstallation was about six to seven weeks.

RESULTS AND CONCLUSIONS

The following is a summary of the results and conclusions drawn from the Centaur Standard Shroud cryogenic unlatch tests. Results and conclusions can also be found in each of the respective sections of the report.

1. The CSS, Centaur, and other hardware and systems as configured for the third cryogenic unlatch test, provide an acceptable thermal environment, shroud separation, and jettison.

2. The Centaur tank flight hydrogen vent system as redesigned for the D-1T vehicle has sufficient capacity to handle the expected range of flowrates.

3. The CSS/Centaur seals and forward seal release mechanism, as installed for the third cryogenic unlatch test, provided adequate sealing and performed satisfactorily during CSS separation and jettison.

4. The CSS/Centaur purge systems as configured and operated during the third cryogenic unlatch test met all requirements for the flight vehicle. However, during LH_2 tanking the high purge flowrate of 65 lb/hr. of GHe must be maintained in the forward purge system to prevent an uncontrollable collapse in shroud pressure around the Centaur tank.

5. The initial LH_2 tank fill rate must be slower than that used for present Centaur tankings, until the minimum pressure in the CSS/tank annulus has been reached.

6. All pyrotechnic devices as configured and installed for the third cryogenic unlatch test are acceptable for flight.

7. The insulation configuration tested in cryogenic unlatch test no. 3 provides a heat transfer rate to the Centaur LH_2 tank and ice accumulation on the CSS that is acceptable.

8. Motion of the shroud during the third cryogenic unlatch test was within acceptable limits regarding clearances to the Centaur and spacecraft envelope.

9. Measured shock loads from the pyrotechnic devices firing were less than qualification requirements for the Centaur equipment module and the Titan skirt.

10. The Centaur tank, truss adapter, equipment module, and the interstage adapter were all structurally adequate during this test program.

11. No structural degradation and/or anomalies occurred in the CSS structure as a result of the cryogenic unlatch tests.

TABLE I-1 CENTAUR STANDARD SHROUD CRYOGENIC UNLATCH TEST SUMMARY

TEST NO.	TEST DESCRIPTION	TEST DATE	PROPELLANTS		NUMBER OF FBR STRUTS	ELECTRICAL DISCONNECT MODE	HYDROGEN VENT DISCONNECT MODE	RADIATION SHIELD INSTALLED	FORWARD SEAL RELEASE SYSTEM TYPE	HYDROGEN TANK HEATING RATE @ MAX PURGE RATE BTU/HR	REMARKS AND COMMENTS
			LH_2 TANK	LO_2 TANK							
1	COMBINED SYSTEMS TEST	Sept. 20, 1972	LN_2	LN_2	6	N/A	N/A	YES	MECHANICAL	N/A	SYSTEMS CHECKOUT TEST
2	CRYOGENIC UNLATCH TEST NO.1	Sept. 28, 1972	LH_2	LN_2	6	PRIMARY	SECONDARY	YES	MECHANICAL	214,000	SHROUD JETTISONED INTO NETS HIGHER THAN EXPECTED H_2 TAN TANK HEAT RATE. SUPER-ZIP TUBE RUPTURED. FORWARD SEAL TORN DURING JETTISON.
3	CRYOGENIC UNLATCH TEST NO.2	Nov. 8,1972	LH_2	LN_2	6	PRIMARY and SECONDARY	PRIMARY	YES	MECHANICAL	200,000	SHROUD JETTISONNED INTO NET COLLIDED WITH PAYLOAD MODEL DURING JETTISON. HEAT RATE TO H_2 TANK STILL HIGH. NO SUPER-ZIP TUBE RUPTURE AT JETTISON. FORWARD SEAL DID NOT SEPARATE FROM ONE HALF AND WAS TORN.
4	AMBIENT FORWARD SEAL RELEASE TEST	Dec. 19,1972	N/A	N/A	N/A	N/A	N/A	YES	PYROTECHNIC	N/A	BASELINE CHECKOUT FOR NEW FORWARD SEAL RELEASE SYSTEM. RESULTS WERE SATISFACTORY.
5	LN_2/LN_2 TANKING AND FORWARD SEAL RELEASE TEST	Jan. 10,1973	LN_2	LN_2	N/A	N/A	N/A	YES	PYROTECHNIC	N/A	INDICATED LOWER H_2 TANK HEATING RATE. FORWARD SEAL RELEASE SATISFACTORY UNDER CRYOGENIC CONDITIONS.
6	LH_2/LN_2 TANKING AND FORWARD SEAL RELEASE TEST	Jan. 23,1973	LH_2	LN_2	N/A	N/A	N/A	YES	PYROTECHNIC	125,000	REDUCED H_2 HEAT RATE VERIFIED INSULATION MODS MADE. FORWARD SEAL RELEASE SATISFACTORY.
7	CRYOGENIC UNLATCH TEST NO.3	Feb. 7,1973	LH_2	LN_2	6	PRIMARY	PRIMARY	YES	PYROTECHNIC	125,000	SUCCESSFUL TEST.

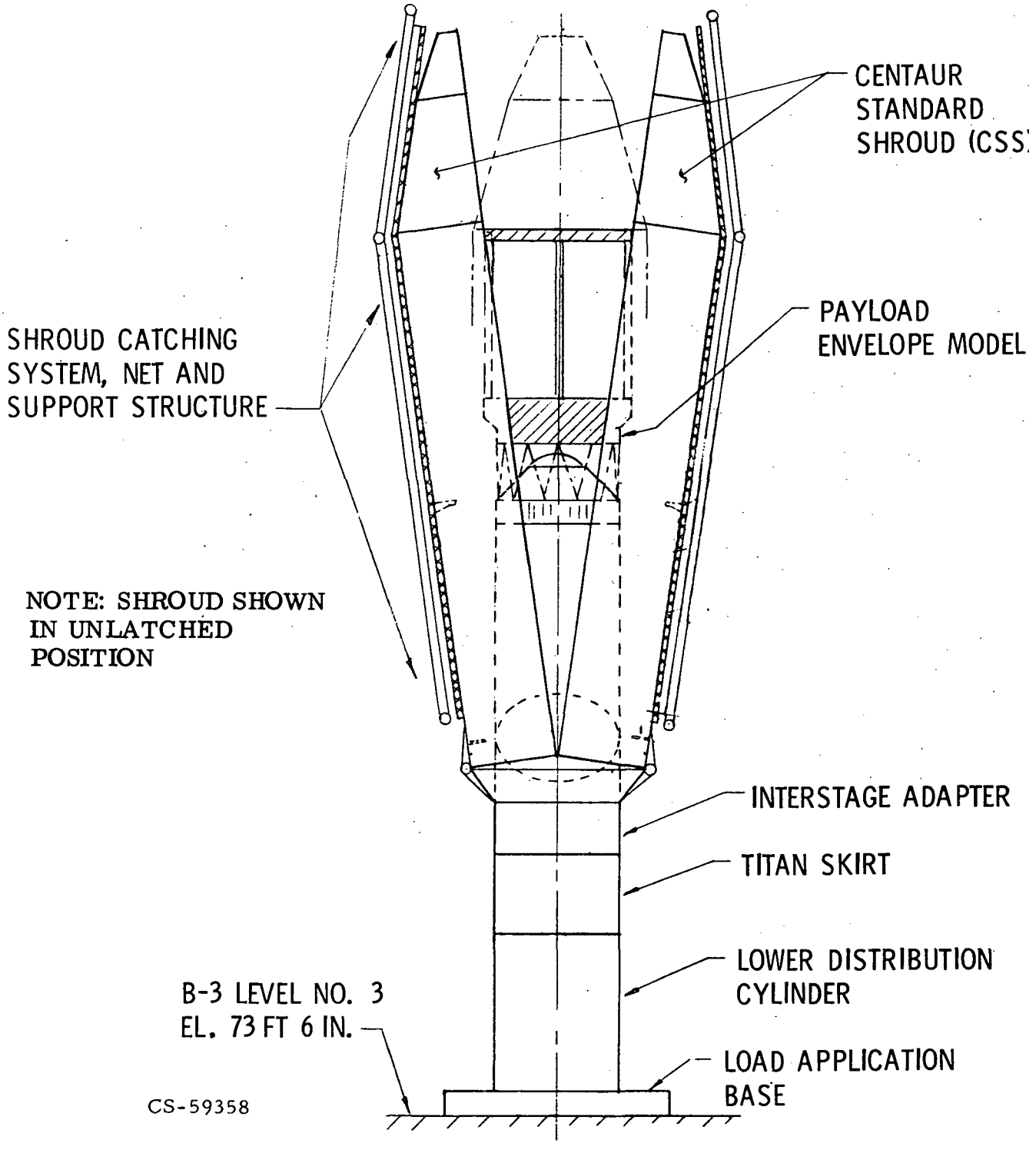

FIGURE I-1 TEST HARDWARE ASSEMBLY FOR CRYOGENIC UNLATCH TESTS

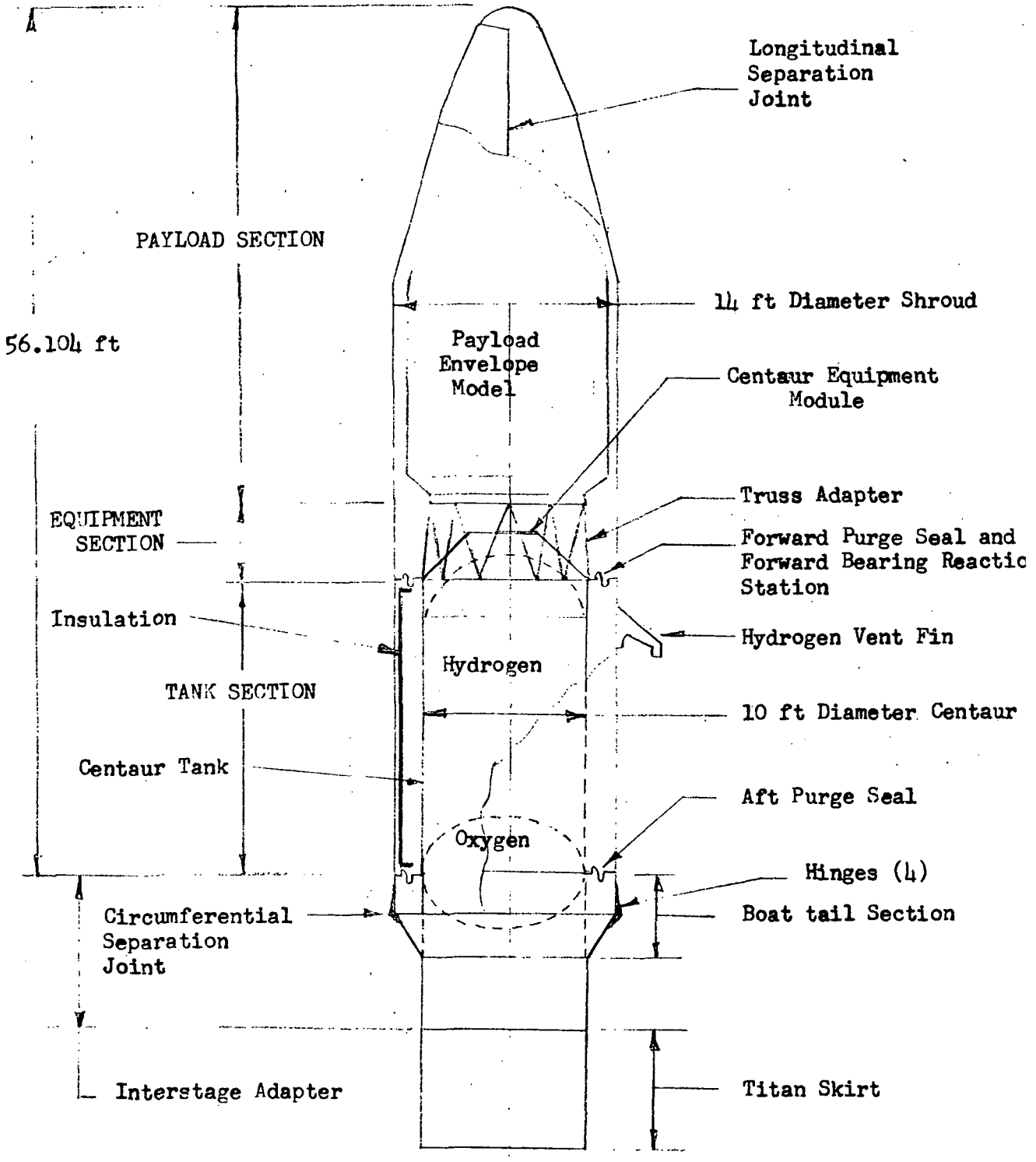

FIGURE I-2 OVERALL CENTAUR STANDARD SHROUD (CSS) CRYOGENIC UNLATCH TEST CONFIGURATION

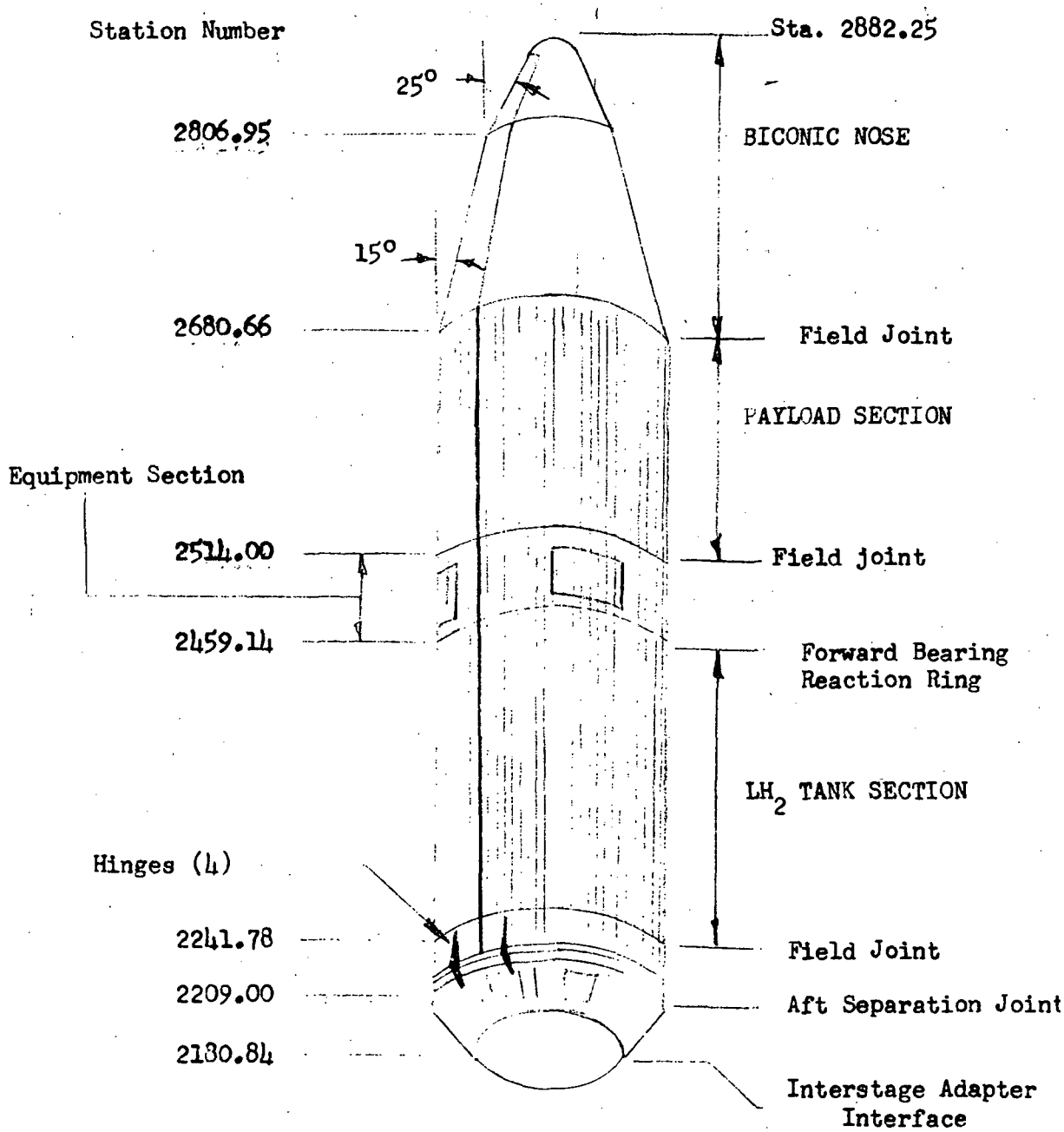

FIGURE I-3 CENTAUR STANDARD SHROUD (CSS) GENERAL CONFIGURATION

STAINLESS STEEL WELDED CONSTRUCTION; SKIN THICKNESS, 0.013 TO 0.026;
PRESSURE STABILIZED STRUCTURE; MODIFIED FORWARD BULKHEAD

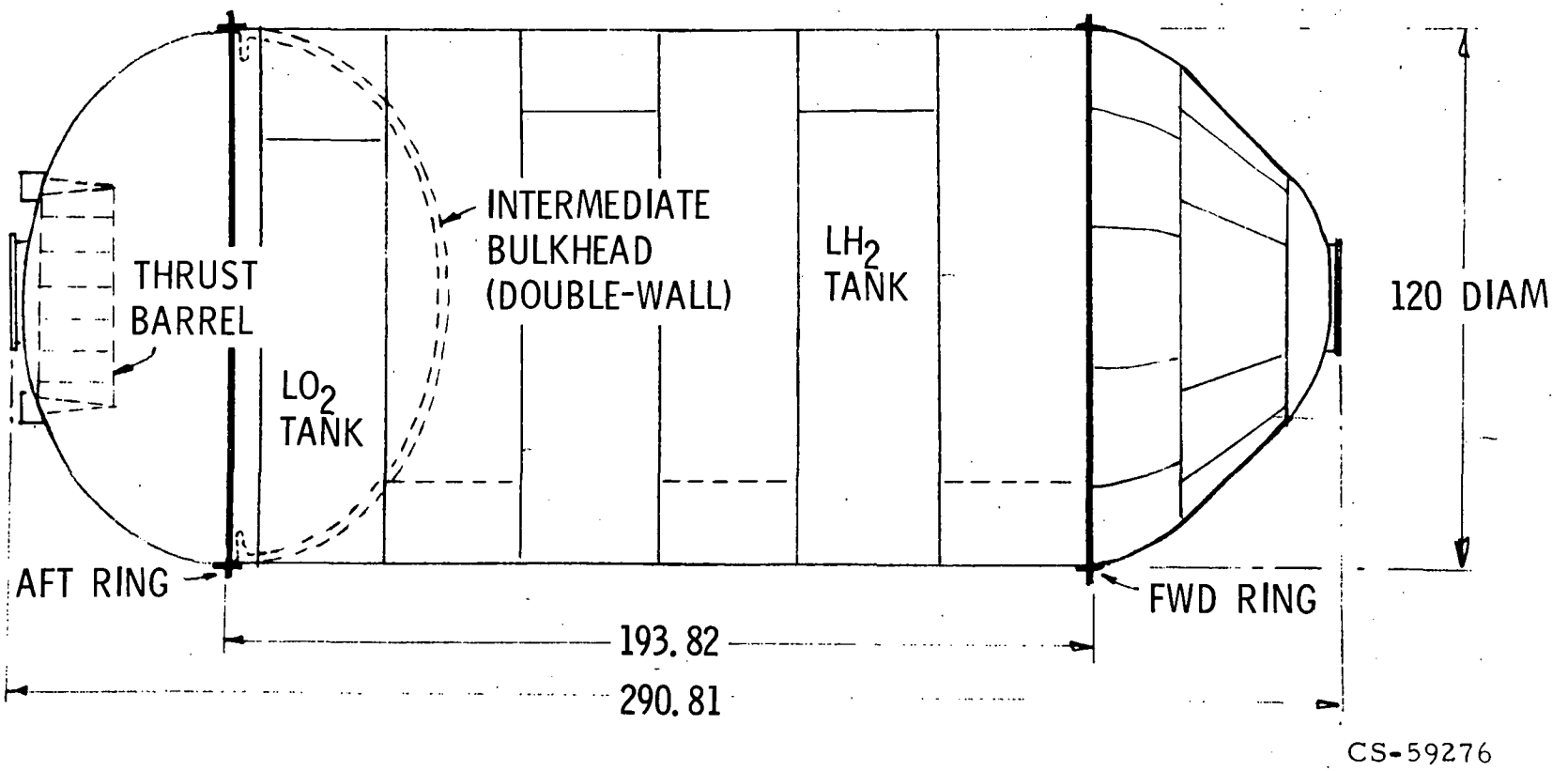

FIGURE I-4 CENTAUR PROPELLANT TANK CONFIGURATION

II. CENTAUR HYDROGEN TANK VENT SYSTEM

By W. A. Groesbeck

SUMMARY

The hydrogen tank vent system test results verified system performance capability for D-1T Centaur launch and flight operations. All test objectives were met. The vent disconnect release mechanism was exercised successfully in both the primary and secondary mode. Capacity of the system to vent boil-off gases was successfully demonstrated during all propellant tanking and tank pressurization sequences. Overall improvement in the D-1T vent system capacity, as compared to the D Centaur configuration, was verified in that for any given vent flow rate the corresponding ullage pressure was less.

SYSTEM DESCRIPTION

The test vehicle was configured with the flight hardware of a Centaur hydrogen tank vent system as shown in figure II-1. Components of the system comprised: (1) a primary vent valve and four inch diameter vent plenum assembly mounted to the forward tank door, (2) vent ducting (2 1/2 inch diameter) extending across and mounted to the forward bulkhead, (3) vent nozzle assemblies interfacing with the protruding stub ends of the vent ducting at the intersection with the stub adapter, (4) vent disconnect assemblies, one in each vent leg, interfacing between the vent nozzles and the Centaur Standard Shroud, and (5) a vent fin mounted exterior to the shroud.

An additional facility vent installation was also made to the tank to accommodate the test operations. This installation was accomplished by eliminating the secondary vent valve installation and blanking off the corresponding connections to the vent plenum. The opening in the hydrogen tank door for the secondary vent valve was not made. Instead, a 5 inch diameter hole was cut for the facility vent. The vent ducting was expanded to an 8 inch line, which was routed vertically through the nose section of the shroud on the vehicle centerline, and on up through a 6 inch line above the roof of the test stand.

The facility vent system was used during detanking and shroud jettison when the flight disconnects were separated. It was also available in case of any emergency requiring a high vent rate capability. Tank pressure control while on the facility vent was regulated by a facility vent valve. The vent valve could be remotely set to control at any desired pressure.

The vent disconnects which disengage at shroud disconnect are also illustrated in figure II-1. Basically each disconnect is a telescoping tube assembly with spherical ball attachments at each fixed end. Differential motion between the shroud and tank structure is accommodated by the sliding tube sections and ball joints. Seals at each spherical ball and between the telescoping tube sections prevent any leakage of hydrogen vent gas. The shroud end of the disconnect is fixed while the release mechanism is at the inboard end. As shown, this inboard end of the disconnect is bagged and purged with helium to keep the release mechanism ice free.

The release mechanism was designed for two modes of disconnect. In either mode the release mechanism is engaged by the outward extension of the telescoping tube sections during shroud jettison. As shown in figure II-1 the inner tube slides out until it engages the stops on the inside of the outer tube. When the tube movement bottoms out against the stops the moving shroud exerts a direct pull force through the tubes to the release mechanism. In the primary disconnect mode the outer tube force shears two phenolic-resin pins. By shearing the pins the outer tube is permitted to move out enough to release four mechanical fingers (latching lugs) that extend over the inboard end of the disconnect pulls clear of the vent nozzle. Should the pins not shear the pull force then acts directly on the latching fingers. This force bends the fingers back allowing the disconnect assembly to pull away from the vent nozzle in a secondary mode of separation.

SYSTEM OPERATION

The hydrogen vent system's performance was good and all test objectives were met. The first objective was to demonstrate successful operation of the new D-1T Centaur hydrogen vent disconnect at shroud jettison. A second objective was to verify the vent flow capacity of the new design vent system. These tests provided the first operational results on a full scale vehicle configured with flight hardware.

Vent System Disconnects

The vent system disconnects at the shroud vehicle interface separated successfully in the secondary mode during the first shroud unlatch test. The four latching lugs were bent back allowing the disconnect to become disengaged from the vent nozzle. Shear pins for the primary disconnect mode were partially fractured but did not shear. The reason for the disconnect separating in the secondary mode rather than the primary mode is attributed to the shroud rotational velocity being less than predicted for flight under space vacuum conditions. The predicted tangential velocity of the shroud at the disconnect location at the time of disconnect engagement is 20 inches/second. The measured velocity during the test was only about 6.5 inches/second (see Section X). Hence, a lesser velocity reduced the impact loading and the pins were not sheared. Under

flight conditions with a higher expected velocity the additional impact loading will shear the pins (before bending the latching lugs) and cause the release mechanism to separate in the primary mode. Similar results were demonstrated in the design proof test and were not in this test program.

Inspection of the vent nozzles after the first test revealed that the teflon coated nozzle surfaces were scuffed by the latching lugs as they pulled off. One nozzle was repaired by polishing the surface; but the other nozzle surface was scratched so deep that the nozzle was replaced. Damage of the teflon surface by the latching lugs would not be of any consequence on a flight operation. However, for further unlatch tests the replacement was necessary to insure a good sealing surface and prevent leaking hydrogen vent gas.

On the next two cryo-unlatch tests a retainer was installed between the fingers of the latching lugs to prevent bending. In this way the disconnect motion forced the pins to shear thereby releasing the four latching fingers and allowing the disconnect to separate in the primary mode. In both tests the primary mode of release was successfully demonstrated. Inspection of the vent nozzle surfaces following each of these two tests showed no evidence of any scuffing. The clean nozzle surfaces were further evidence of proper release of the vent disconnect in the primary mode.

Vent Systems Flow Capacity

The vent system demonstrated good flow capacity for all ground venting requirements of the Centaur D-1T vehicle. Hydrogen boil-off gas was vented through the flight vent system during tank chilldown, hydrogen tanking, topping operations and tank blowdown following vent valve lock-up tests to measure self-pressurization rates. The tank chilldown and propellant tanking were accomplished using current operational procedures for the Centaur vehicle.

Adequacy of the hydrogen vent system depends on the system pressure drop and is determined as a function of tank ullage pressure and vent boil-off rates. Large system pressure drops for a given flow rate result in high ullage pressures. The design objective was to provide a system capacitance equal to or better than that of the current D-Centaur configuration. Test results demonstrated that this design objective was met.

The test results showing the relation between tank ullage pressure and vent flow rate are given in figure II-2. As shown the test results are in good agreement with the design predictions and also represent an improvement over the earlier D-Centaur configuration vent system. During tank chilldown and hydrogen tanking the maximum ullage pressure was about 21.8 psia. Once the tank was filled and the vehicle was fully cold soaked the ullage pressure settled out between 20.5 and about 21.3 psia. The higher ullage pressure corresponds to the first two cryo unlatch tests wherein the heat input to the tank was a maximum. With a reduced heat input as on the third unlatch test the ullage pressure was appreciably less at about 20.7 psia.

The current stabilized ullage pressure for D Centaur during launch operations averages between 21.6 and 22.0 psia; the maximum permissible limit is 22.2 psia. If D-1T Centaur tank heating rates are reduced to about 150,000 BTU/Hr. as expected, based on these test results, the ullage pressure during Cape operations may well settle out less than 21.0 psia. Also, as noted in figure II-2, the data indicate that at very low vent rates the ullage pressure runs just slightly above the vent valve reseat pressure of 20.5 psia. Predicted ullage pressures for the D-1T Centaur prelaunch operations at cold stabilized conditions would be in the range between the vent valve reseat pressure and about 21.0 psia.

The maximum measured vent flow rate was 0.45 lb/sec following primary vent valve unlock after a self-pressurization test. Tank pressure blowdown upon unlocking the vent valve was normal and vent rates were well within range of the system capacity.

CONCLUSIONS

All test objectives were successfully demonstrated on the hydrogen tank vent system during the shroud cryo unlatch test program. The release mechanism for the vent disconnects was exercised in both the primary and secondary mode. In each mode the mechanism released properly allowing the disconnect to pull clear of the vehicle. System vent flow capacity was verified during all phases of propellant tanking and tank pressure blowdown following vent valve lockup periods. The improved design of the D-1T vent system has reduced system losses such that, in comparison to the D-Centaur configuration, the corresponding ullage pressure for any given flow rate will be less. Overall test results have verified system performance capability for D-1T Centaur launch and flight operations.

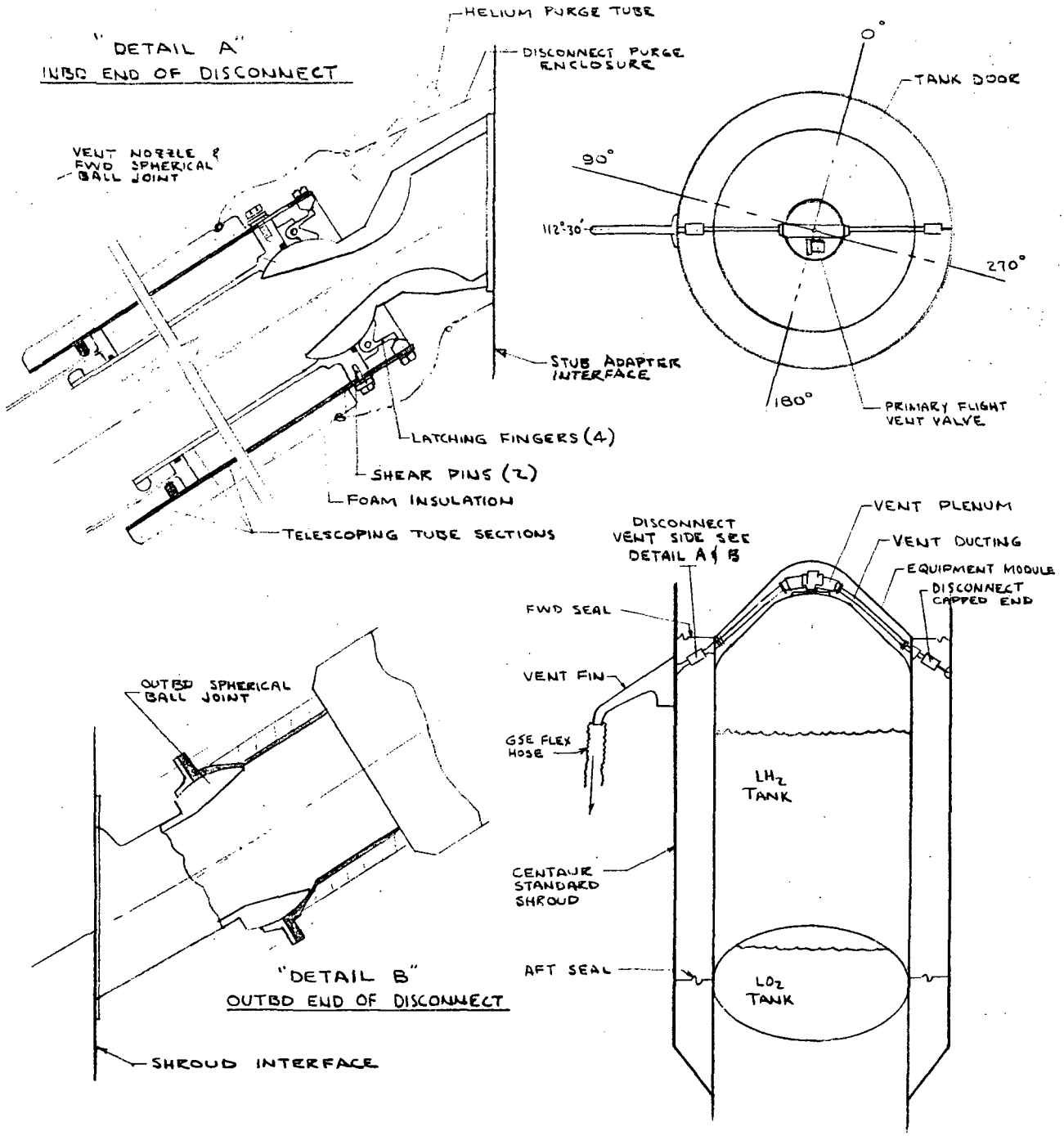

Figure II - 1 HYDROGEN TANK BALANCED THRUST VENT SYSTEM

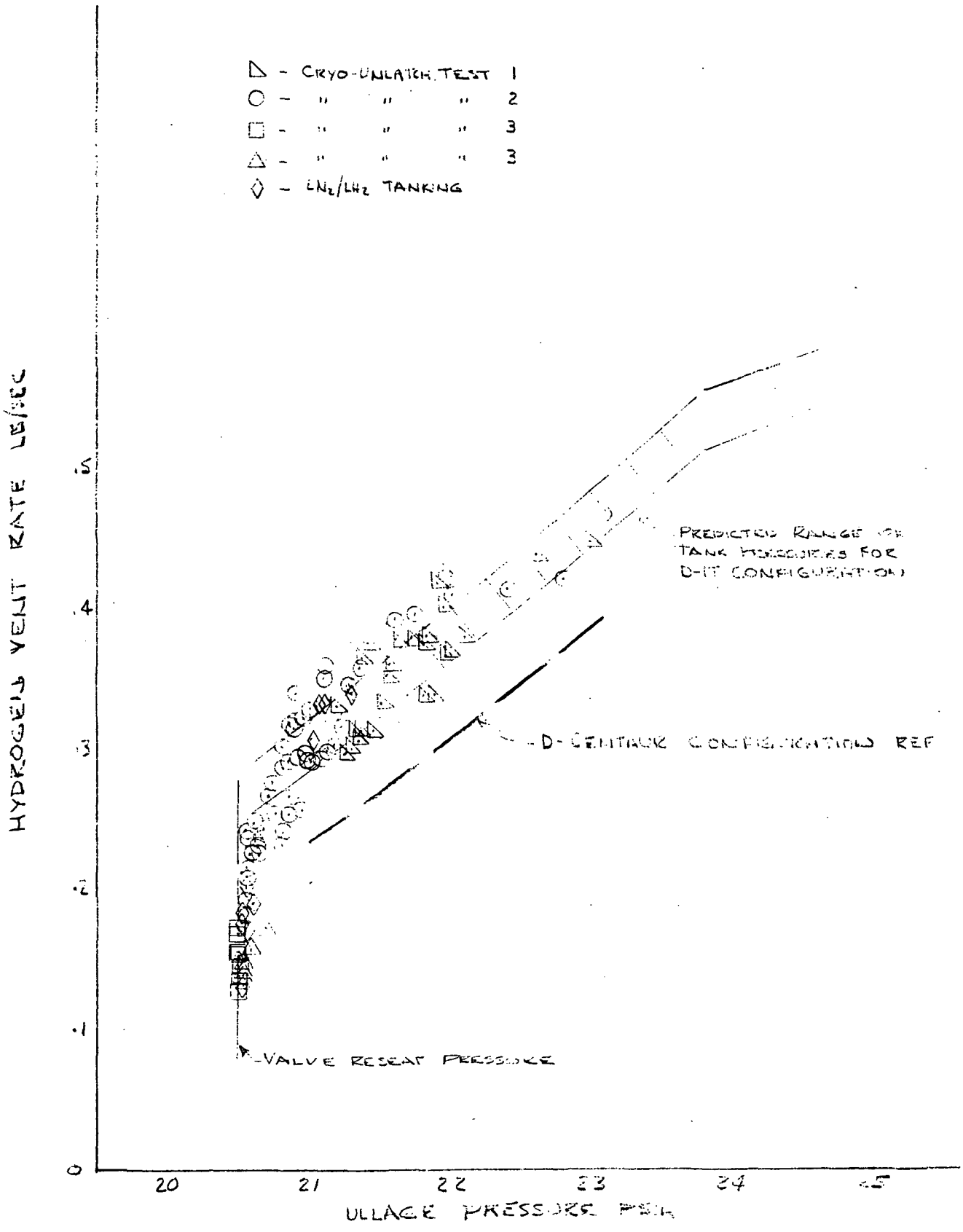

FIGURE II-2 H_2 VENT RATE & ULLAGE PRESSURE CORRELATION

III. SHROUD/CENTAUR SEALS

By T. L. Seeholzer, J. L. Collins, and S. V. Szabo, Jr.

SUMMARY

Significant modifications to the original CSS/Centaur seals were required to obtain satisfactory performance in the cryo-unlatch test program. The original aft split line seal used on cryo-unlatch test no. 1 was not used on further tests because the seal was redesigned. The redesigned seal was used on subsequent tests and will be used for flight. The aft circumferential seal was satisfactory. The forward circumferential seal encountered release difficulties, and the releaser mechanism was redesigned and operated satisfactorily.

SEAL LOCATIONS AND DESCRIPTIONS

The location of the CSS/Centaur seals is shown in figure III-1. There are four seals, which are:

1. Forward Circumferential CSS/Tank Purge Seal
2. Forward Split Line Seals (2)
3. Aft Circumferential CSS/Tank Purge Seal
4. Aft Split Line Seals (2)

The function of these seals is to provide a boundary between the CSS and the Centaur tank at each end of the CSS tank sections. During Centaur tanking and ground hold, the annular cavity between the CSS and the Centaur hydrogen tank is purged with helium gas. The adjacent equipment and boattail compartments are purged with nitrogen gas.

Minimum leakage of cold helium from the tank annulus to the equipment and boattail compartments is required. A minimum pressure level in the CSS/tank annulus is also required to prevent inflow of air. The seals are also required to allow separation of the shroud without imparting any unaccountable loads into the shroud during jettison.

Forward Seal and Releaser Mechanism

The forward seal, illustrated in figures III-2 and III-3, is located at station 2459 between the CSS and the forward end of the Centaur stub adapter. The seal consists of a silicone rubberized fabric attached to

the stub adapter by bolts, and retained on the CSS forward bulkhead by a cable and releaser mechanism. A bead on the CSS edge of the seal holds the seal under the cable.

The forward seal releaser mechanism was completely redesigned between cryo-unlatch test no. 2 and cryo-unlatch test no. 3. Therefore, the two systems tested will be described.

1. Bell Crank Releaser Configuration: The initial seal releaser design as shown in figure III-4 consisted of bell cranks at the CSS split lines which were held on rollers prior to CSS separation. The bell cranks were attached to the seal retaining cable which holds the seal in place (see figure III-3).

At CSS separation the bell cranks ride off the rollers allowing them to rotate and relieve the cable tension. Relief of cable tension permitted the seal to release from the CSS.

This system was employed in cryo-unlatch tests no. 1 and no. 2.

2. Explosive Bolt Releaser Configuration: A redundant explosive bolt system was used to release the seal for cryo-unlatch test no. 3. (For bolt details see Section VII.) Two bolts, one at each split line were attached to the seal retaining cables as shown in figure III-5. When the bolts were separated, the tension in the cable was relieved causing seal release. The bolts were actuated approximately 20 seconds prior to CSS separation. Seal release assist springs were located around the periphery of the seal to assist in raising the seal bead over the retainer lip (see figure III-6).

Forward Split Line Seal

The forward split line seal, shown in figure III-7, is formed from silicone impregnated dacron fabric arranged in a labyrinth of overlapping sections. The labyrinth is held between aluminum clips, and this assembly is bolted to the CSS forward bulkhead. The outboard edge butts against a silicone rubber block, and the inboard edge extends under the forward circumferential seal and restraining cable.

Aft Circumferential Seal

The aft circumferential seal is shown in figure III-8. This seal is basically a mylar membrane which is bolted to the CSS aft bulkhead. At the end of the mylar membrane is a slip joint which mates with the Centaur aft seal plate. With CSS rotation at jettison, the lanyard closest to the split line initiates a lifting force on the separable part of the slip joint (attached to the CSS shell) and the seal starts to separate.

Aft Split Line Seal

The aft split line seal is illustrated in figure III-9 and has basically the same cross section as the aft circumferential seal at the split line. Sealing is effected by the mylar/dacron laminated fabric which is folded together and restrained and compressed between stainless steel clips. The compressed assembly is bolted to the CSS aft bulkhead with silicone rubber blocks on the inboard and outboard edges to seal the ends. Upon separation of the CSS, the laminated fabric unfolds and separates.

SEAL OPERATION DURING TESTS

Forward Circumferential Seal and Releaser Mechanism

Cryogenic Unlatch Test No. 1: The operation of the forward seal during vehicle tanking and prelaunch hold conditions was satisfactory. Pre-test leak checks performed indicated that leakage through the forward seal installation was acceptable.

The operation of the forward seal releaser mechanism during shroud unlatch and jettison, however, was not acceptable. Movie camera data showed the forward seal "hung-up" at the 0^{o} axis split line. During shroud unlatch and jettison, the seal remained attached to one-half of the shroud, finally coming loose just before the shroud hit the catch nets. Post test inspection of the forward seal showed it had sustained a large tear about one foot long at the 0^{o} split line.

Examination of the seal release mechanism (refer to figure III-4) showed that the cable tensioning shoe on release had moved back and wedged between the shroud bulkhead lip and the bulkhead support gusset. This resulted in the seal being restrained between the cable tensioning shoe and the bulkhead lip, and then finally pulling free. (See figures III-10 and III-11 for details.)

As a result of this problem, the gusset was cut back to provide additional clearance. Also a spring was added to make the cam rotate faster allowing the cable tensioning shoe to release quicker. The seal itself was stitched and patched for use on the next test. This was the configuration tested on cryogenic unlatch test no. 2.

Cryogenic Unlatch Test No. 2: Pre-test leak checks made before this test showed again that leakage through and around the forward seal was minimal. The operation of the seal during tanking and prelaunch hold conditions was again acceptable.

The operation of the revised forward seal releaser again was not satisfactory during shroud unlatch and jettison. Movie camera data showed that 0^{o} split line of the shroud did not move for 0.9 seconds after the separation system had been fired and the separation joints severed. Also during

jettison, the forward seal did not come loose and remained attached to the shroud, sustaining a tear across the seal from the CSS edge to the equipment module. This also caused the shroud to be pulled over during jettison, colliding with the payload model. Further examination of movie data showed that the cable release toggles did not rotate. One of the factors contributing to the failure was the presence of a considerable quantity of ice and frost in the 0^{o} split line area. This ice and frost was formed by water leaking into the shroud in this area and freezing out on the split line seals and seal release mechanism. This test was performed in a driving rain with 20 mph winds blowing at the 0^{o} split line. The other factors contributing to the failure were an inadequate seal releaser design and an unreal environment in the equipment area. Based on these problems and the consequences noted, two courses of action to resolve this were taken. These were: (1) seal the shroud to prevent water leakage into the shroud and improve the environment in the equipment area to be more representative of the flight vehicle and (2) redesign the forward seal releaser mechanism to eliminate the pure mechanical device and replace with a pyrotechnic actuated device.

These changes were accomplished (the new seal release design is shown in figure III-5). Before proceeding into a third cryogenic unlatch test, three forward seal release tests were performed.

Forward Seal Release Tests: Three forward seal release tests were performed; one at ambient conditions, one with LN_2 in the Centaur LH_2 tank, and one with LH_2 in the Centaur LH_2 tank. In all three tests, the pyrotechnic releaser was actuated, and the seal came free from the shroud satisfactorily. Based on these test results, cryogenic unlatch test no. 3 was performed.

Cryogenic Unlatch Test No. 3: Seal operation throughout this test was completely satisfactory. The seal came free from the shroud quickly and easily based on movie data taken during unlatch and jettison.

Load cells under the seal retaining cable provided cable loads during this test. Figure III-12 and figure III-13 show that the cable load was 1,080 pounds at installation and varied only by 40 pounds during all phases of the test.

A photograph of the forward seal and releaser after cryo-unlatch test no. 3 is shown in figure III-14.

Forward Split Line Seals

The pretest leak check showed that the forward split line seals leaked at the interface with the silicone rubber blocks at the Super-Zip. After cryo-unlatch test no. 1, it was discovered that the rubber blocks did not part at the split line but were torn apart.

For cryo-unlatch test no. 2 a parting agent was used between the block and the blocks were repositioned at the interface between the Super-Zip and forward split line seals. This solved both the leak problem and separation problem which was demonstrated on cryo-unlatch test no. 2. An icing problem, developed during the tanking and heat transfer testing, in which the whole split line seal at the 0^{o} axis was covered with a block of ice. Rain water and water condensate from cold surfaces in the equipment compartment provided the water. Sealing the equipment compartment would eliminate one source of water but the other could not be totally eliminated. Specimen testing of iced split line seals showed that additional jettison forces up to approximately 800 pounds depending on separation rate, could develop. The area above the split line seals was filled with pour-type polyurethane foam to prevent possible ice formation and additional jettison forces.

For cryo-unlatch test no. 3, leakage was within specifications, no ice formed and the blocks and seals separated satisfactorily.

Aft Circumferential Seal

This seal performed exceedingly well during all phases of testing. Seal leakage was less than the design requirement and the seal separated satisfactorily. No design changes were made on the original seal configuration which is illustrated in figure III-8.

Aft Split Line Seals

The pretest leak check for cryo-unlatch test no. 1 showed that the aft split line seals leaked excessively and at random locations when the leak patterns of the two seals were compared. The seals were modified slightly to provide a tolerable leak rate and still allow the CSS to jettison. After the CSS was jettisoned, it was determined that an adhesive used in the fabrication of these seals had failed resulting in loose seal parts laying in the boattail compartment. After the first cryo-unlatch test, the aft split line seal was completely redesigned and is illustrated in figure III-8. This redesigned seal configuration was within the leakage specification and separated satisfactorily, as demonstrated on cryo-unlatch tests nos. 2 and 3. Figures III-15 and III-16 illustrate the motion of the inboard edge of the CSS aft bulkhead which provides the mounting surface for the aft split line seals. This illustrates the range of separation type motion (ambient to cryogenic temperature) that the seal must provide and still maintain its sealing integrity.

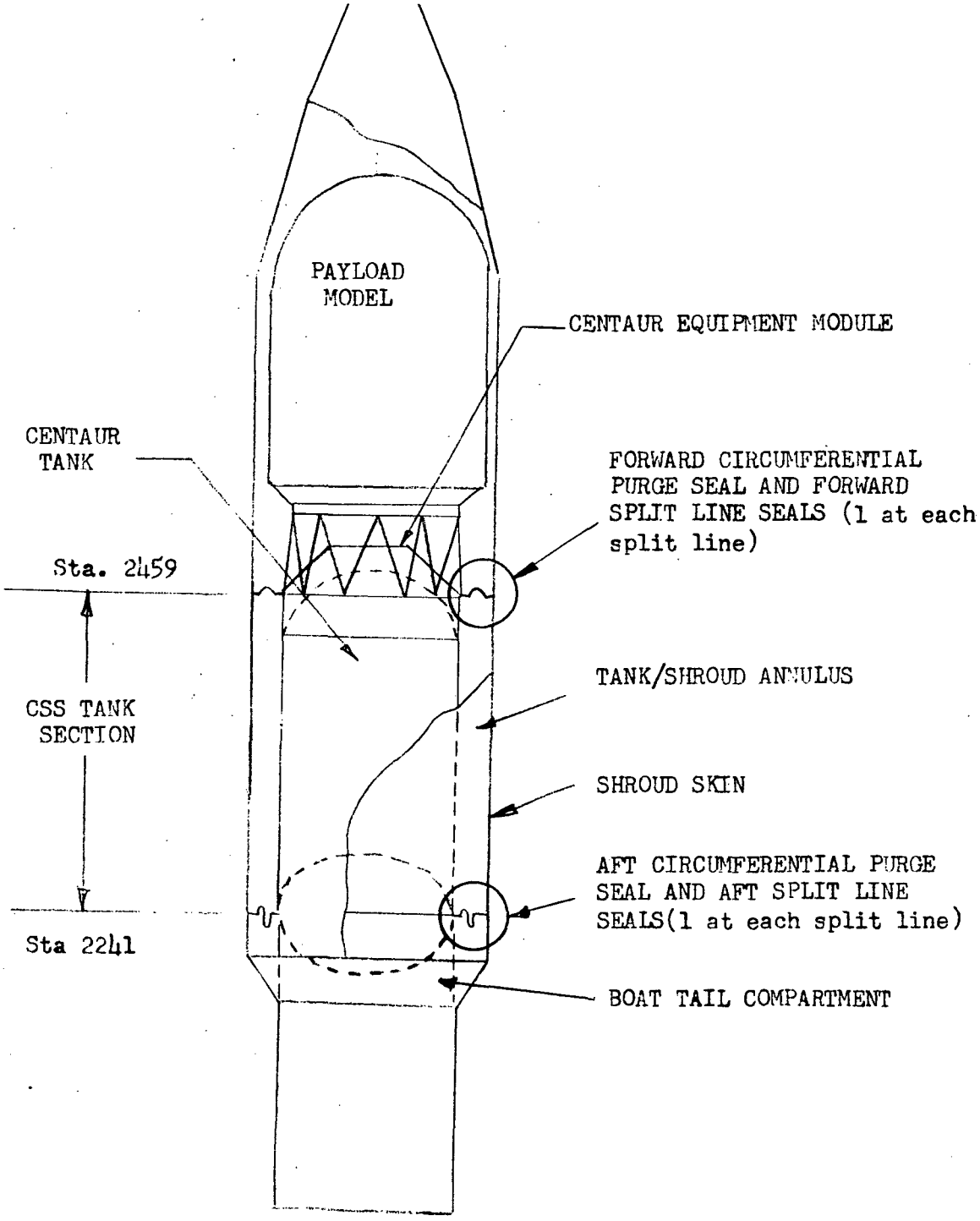

FIGURE III-1 LOCATIONS OF SHROUD/ CENTAUR SEALS

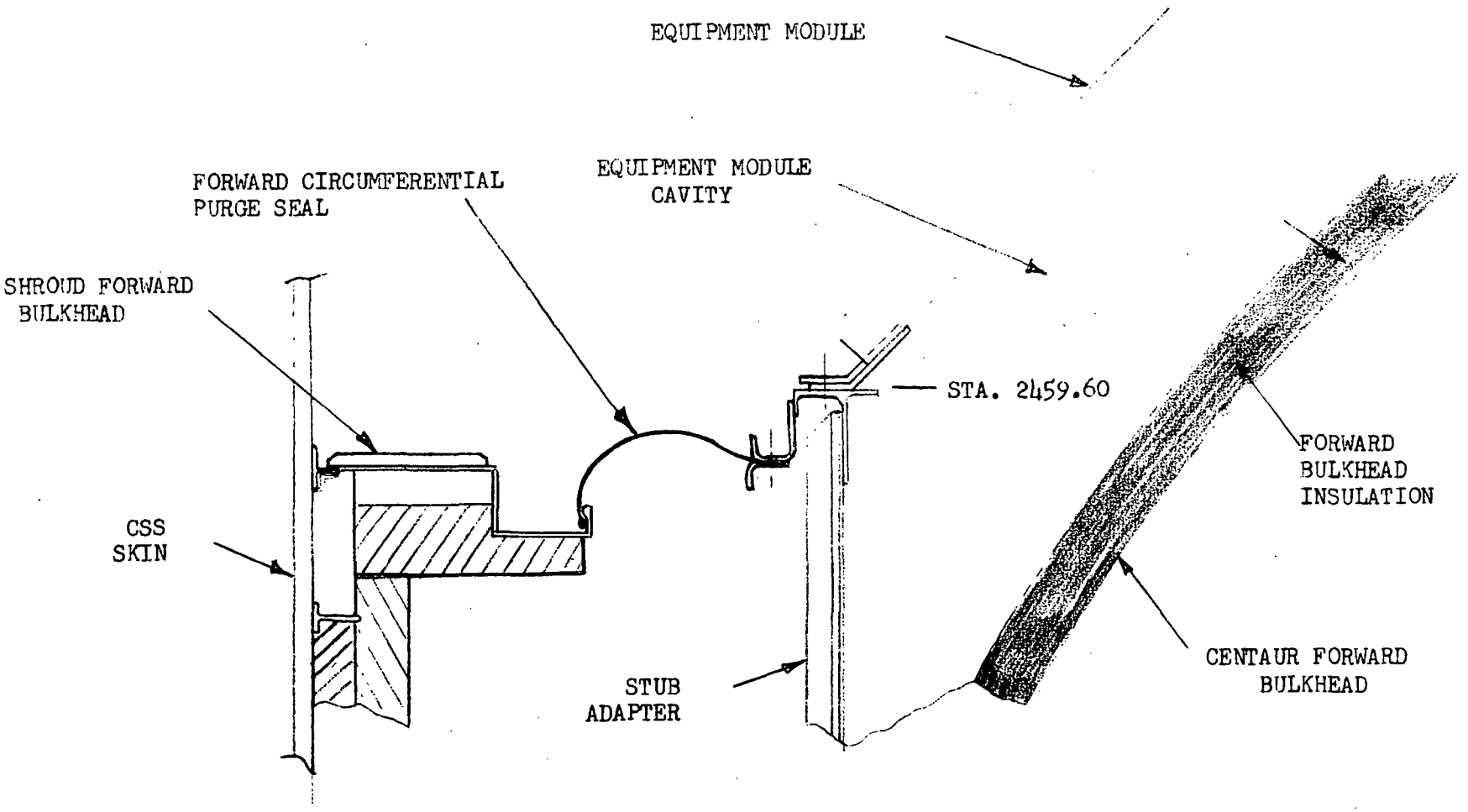

FIGURE III-2 SECTION THROUGH SHROUD/CENTAUR FORWARD CIRCUMFERENTIAL PURGE SEAL INSTALLATION

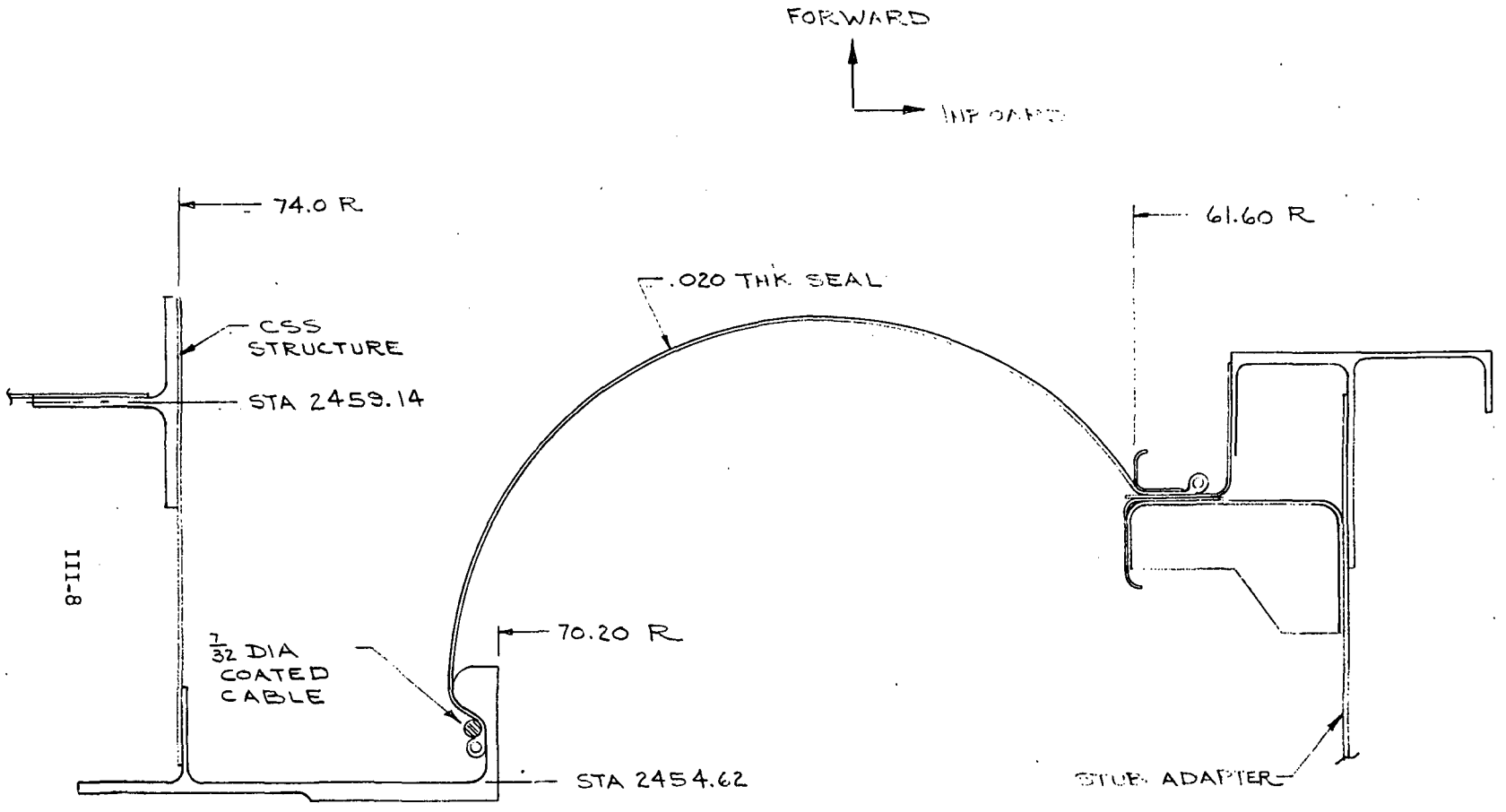

FIGURE III-3 FORWARD SEAL DETAILS

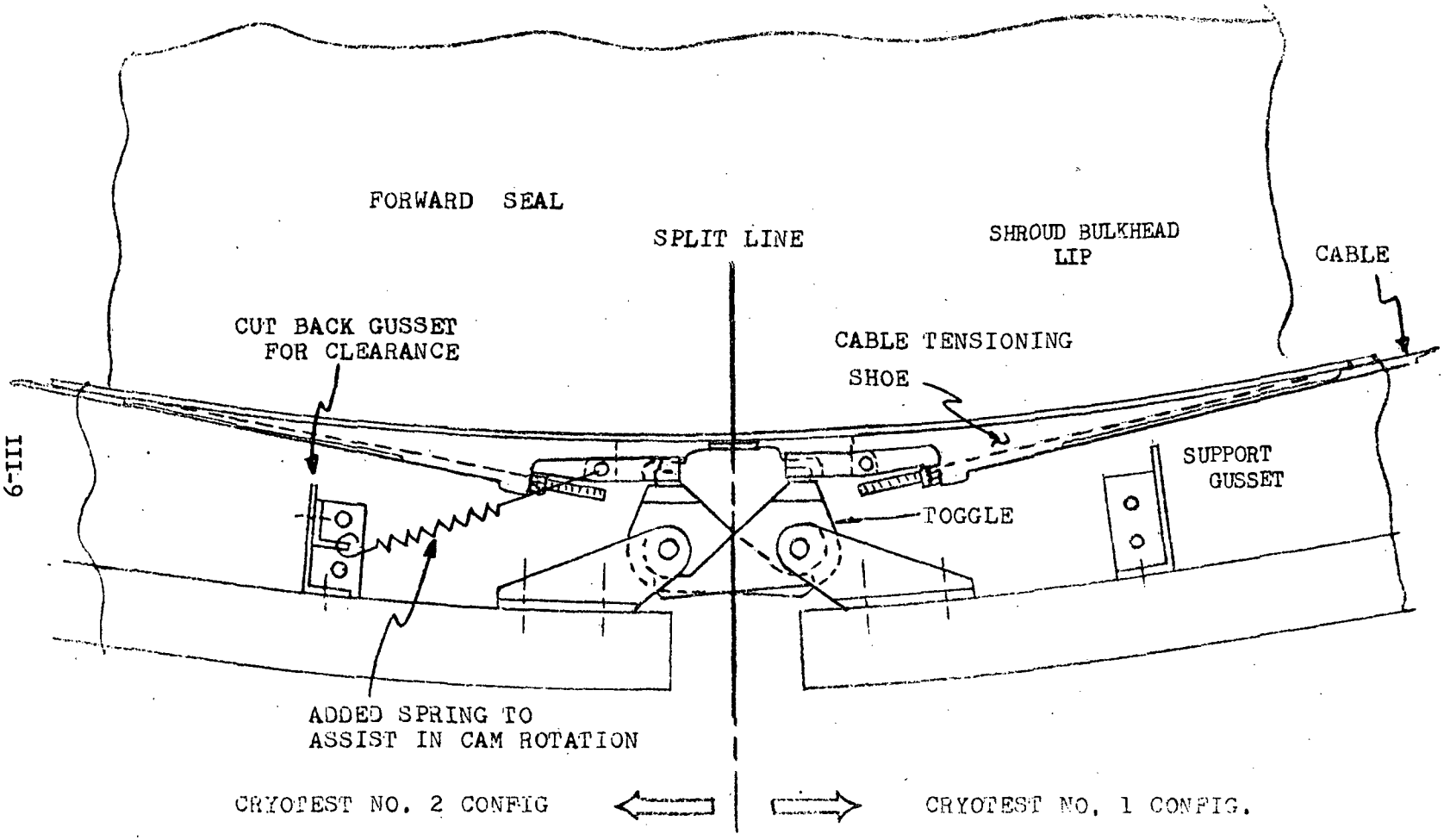

FIGURE III-4 FORWARD SEAL RELEASE MECHANISM - CRYO-UNLATCH TEST NO.1 AND TEST NO.2 CONFIGURATIONS

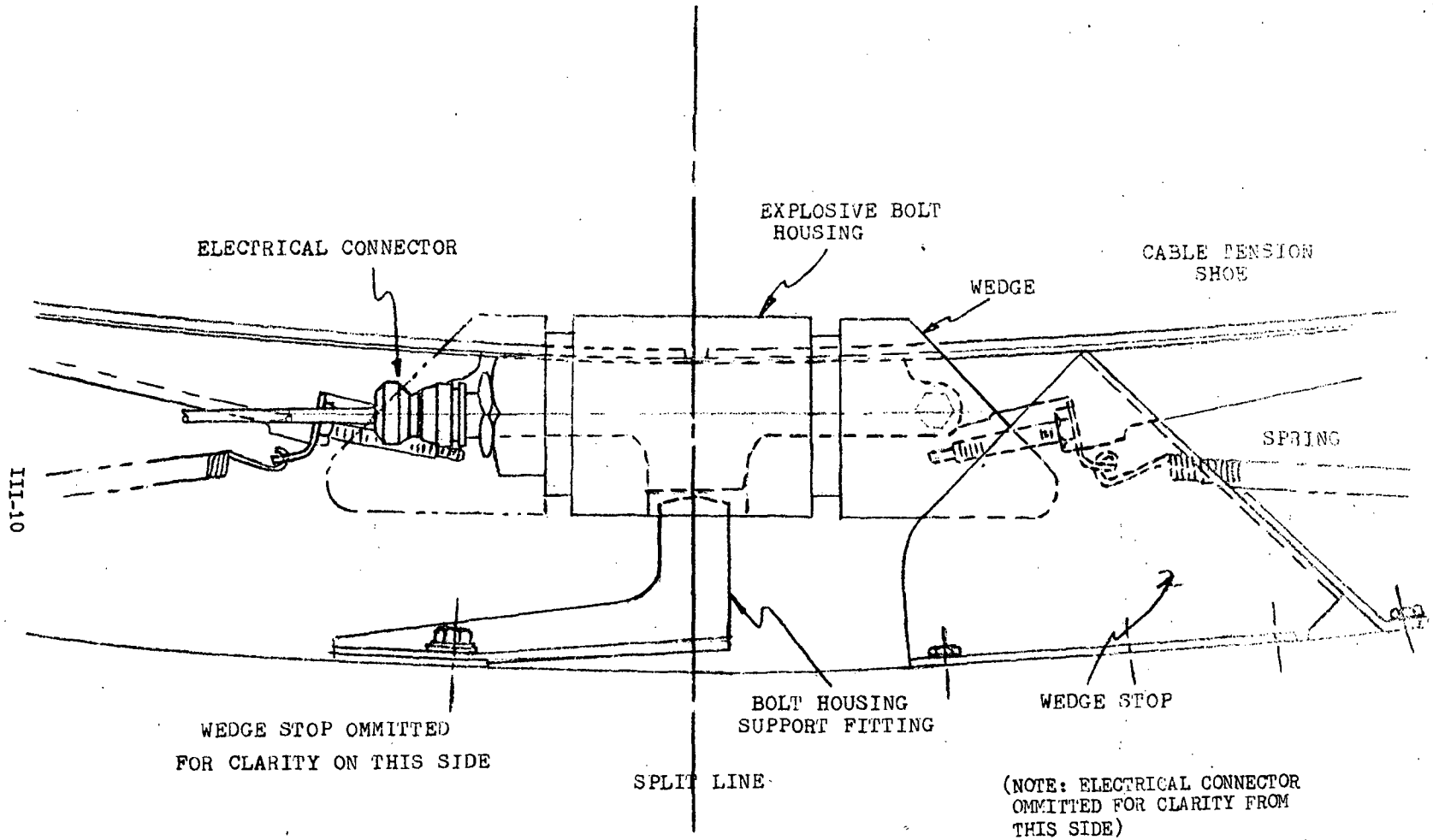

FIGURE III-5 PYROTECHNIC FORWARD SEAL RELEASE SYSTEM INSTALLED AFTER CRYO-UNLATCH TEST NO.2

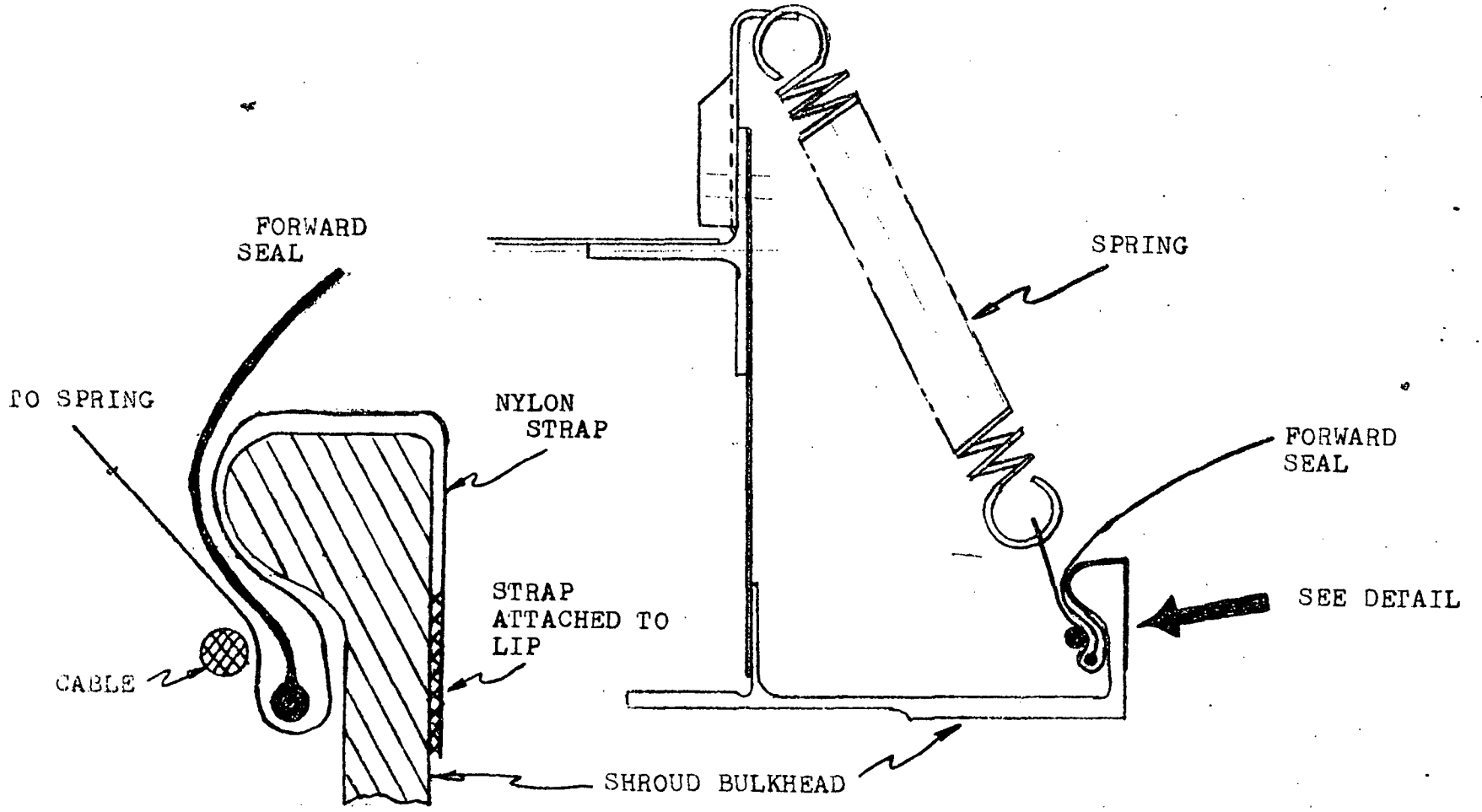

FIGURE III-6 FORWARD SEAL RELEASE ASSIST STRAP DESIGN INSTALLED AFTER CRYO-UNLATCH TEST NO.2

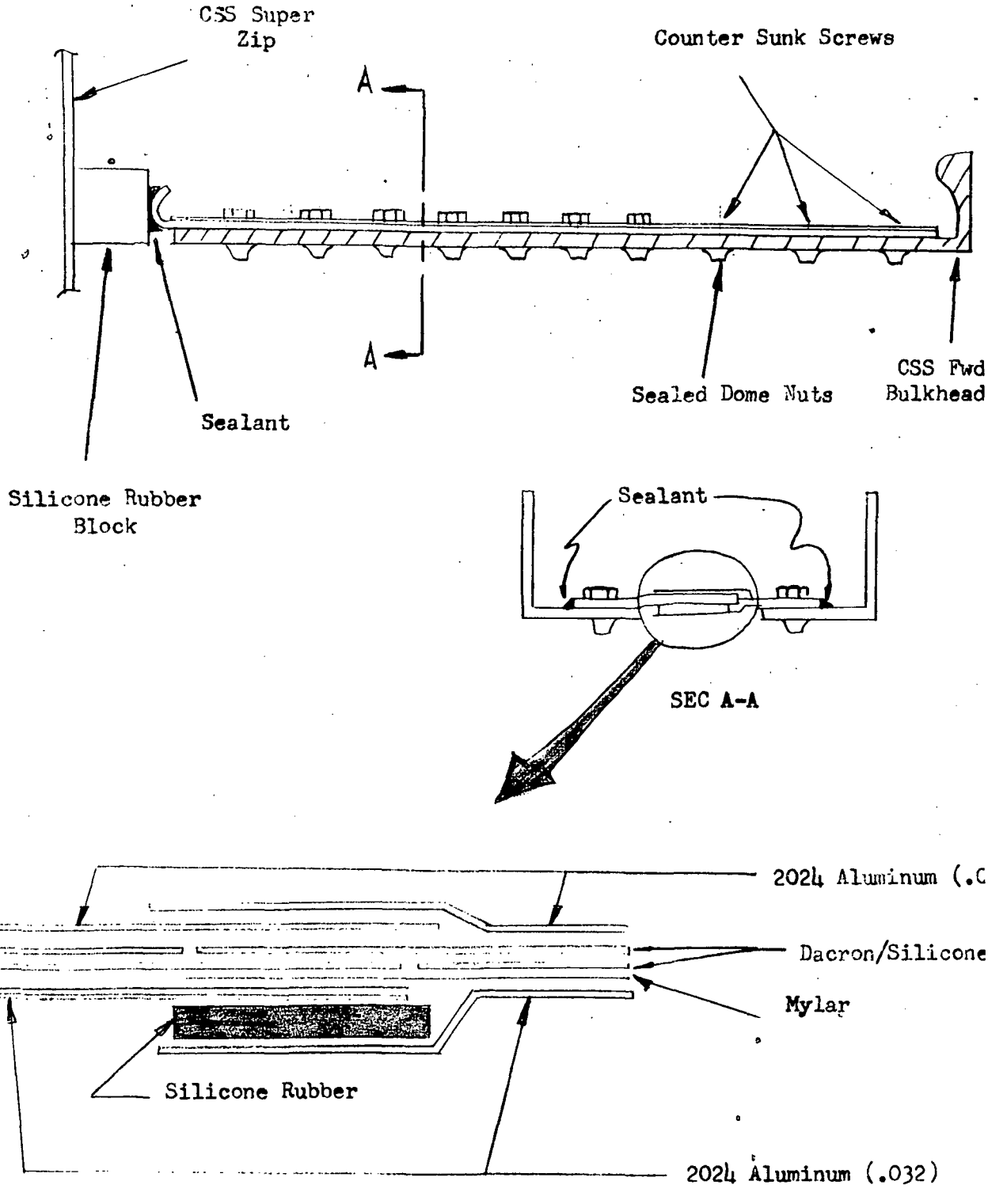

FIGURE III-7 FORWARD SPLIT LINE SEAL CONFIGURATION

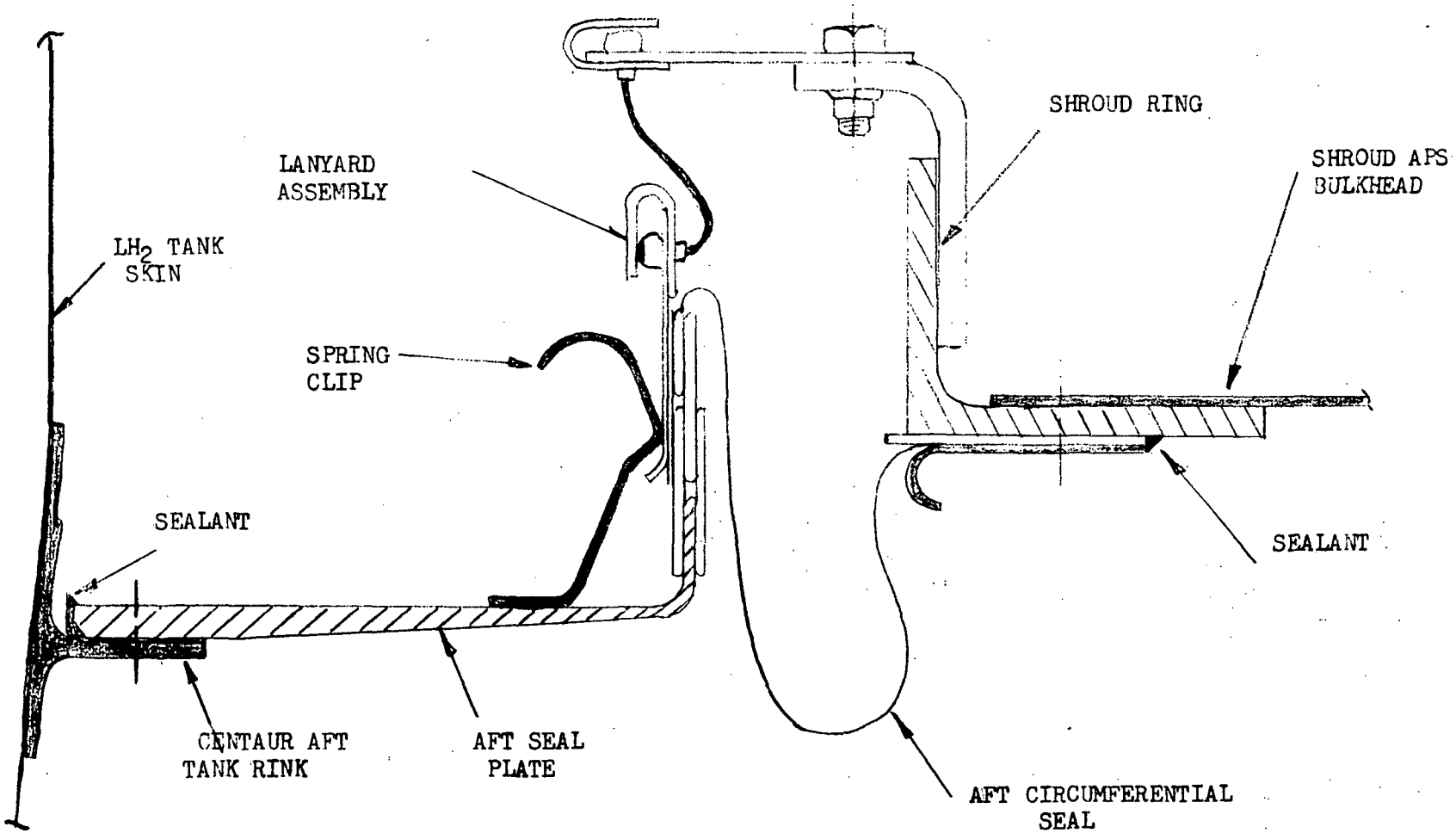

FIGURE III-8 SECTION THROUGH SHROUD/CENTAUR AFT CIRCUMFERENTIAL SEAL ASSEMBLY

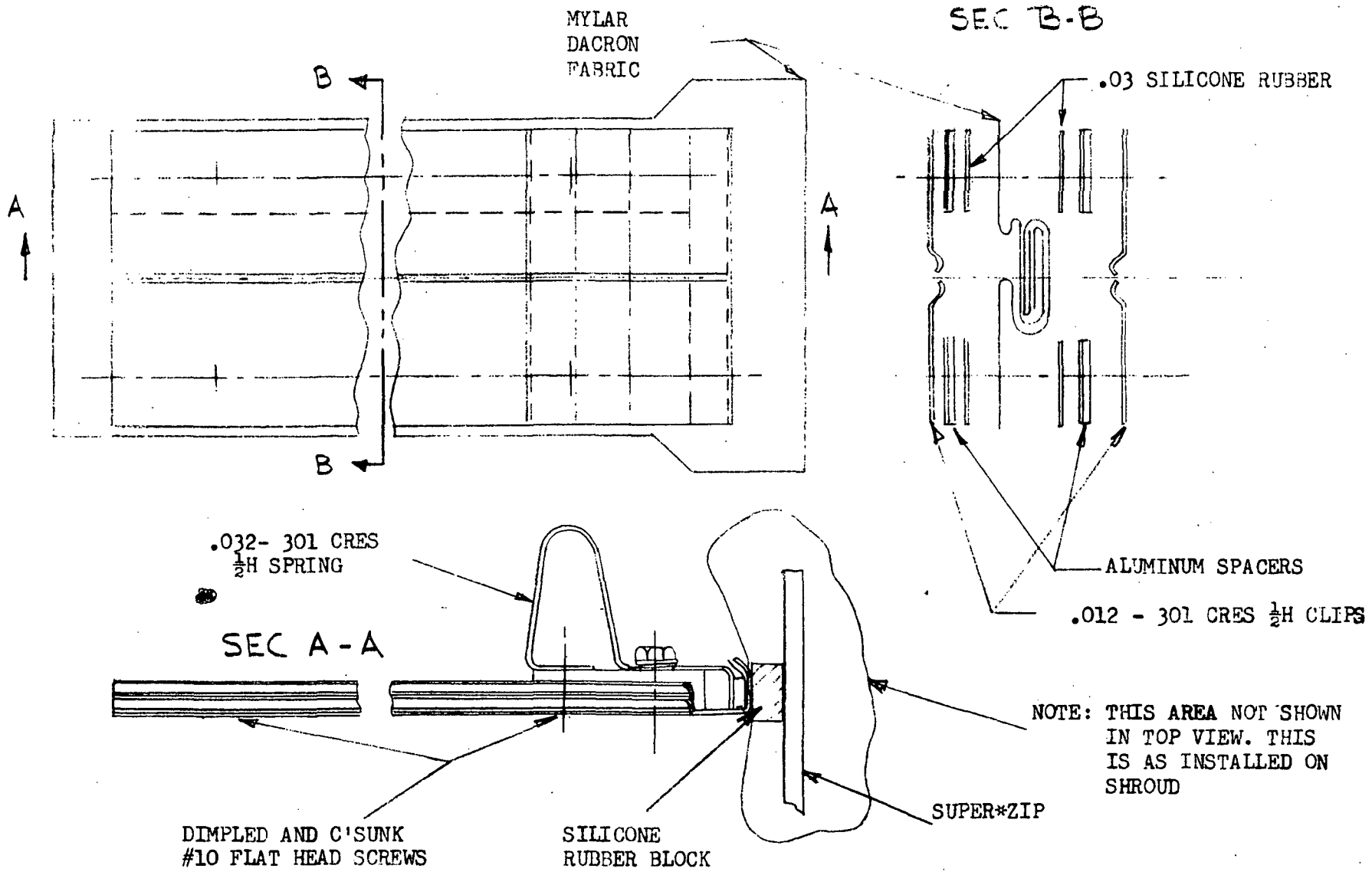

FIGURE III-9 AFT SPLIT LINE SEAL CONFIGURATION

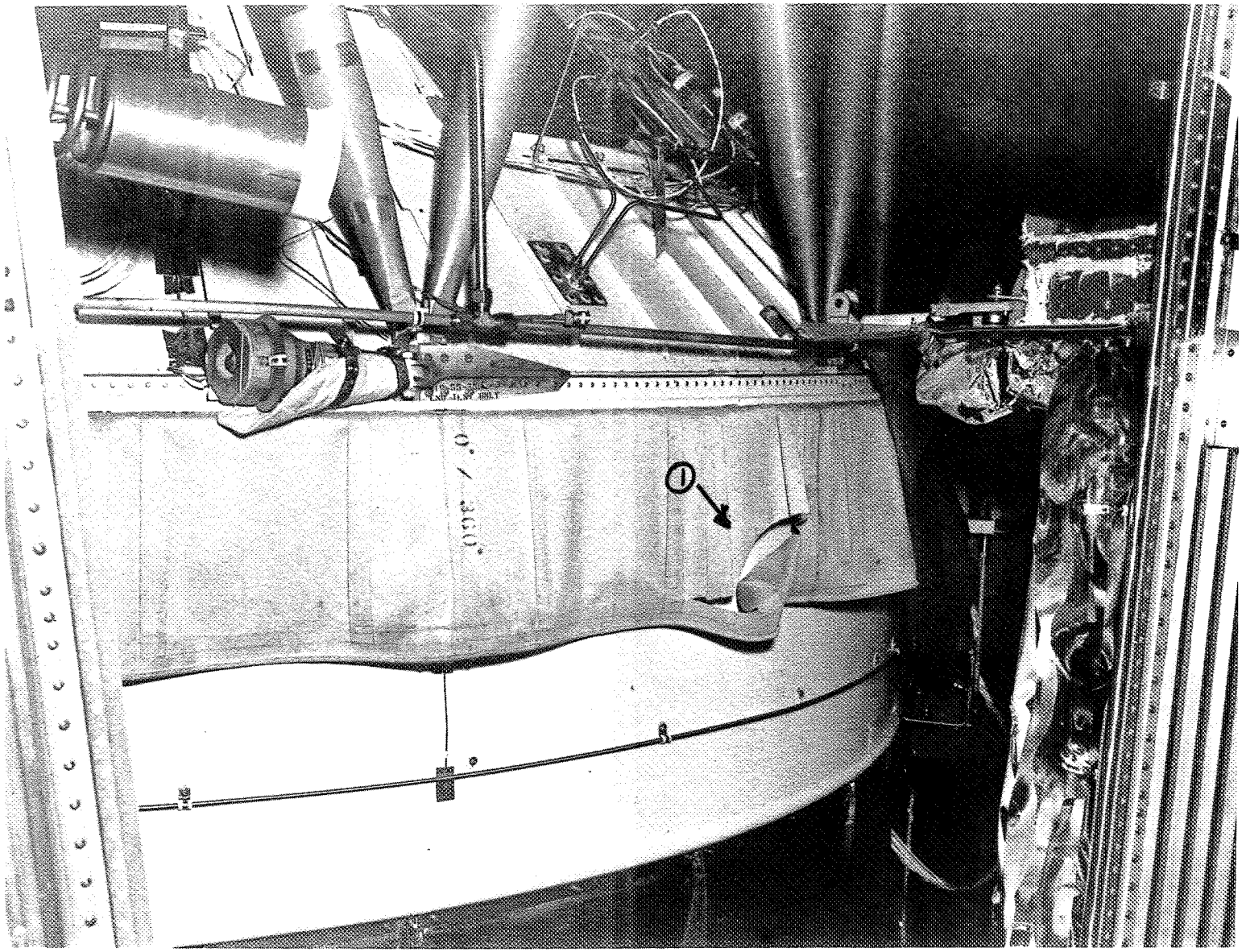

FIGURE III-10 FORWARD SEAL TEAR AFTER CRYOUNLATCH TEST NO. 1

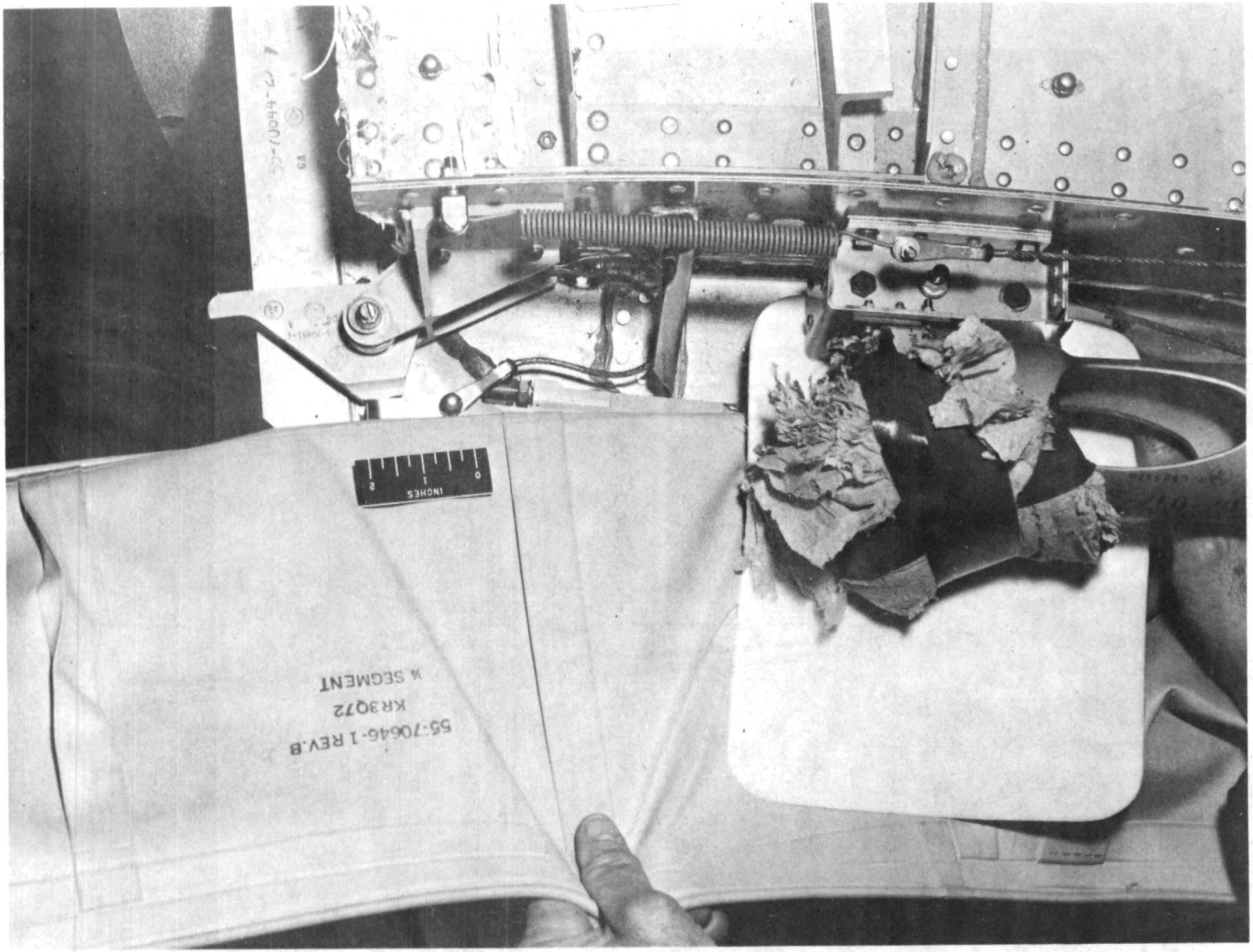

FIGURE III-11 PHOTOGRAPH SHOWING RESTRAINT OF SEAL ON CRYOUNLATCH TEST NO.1

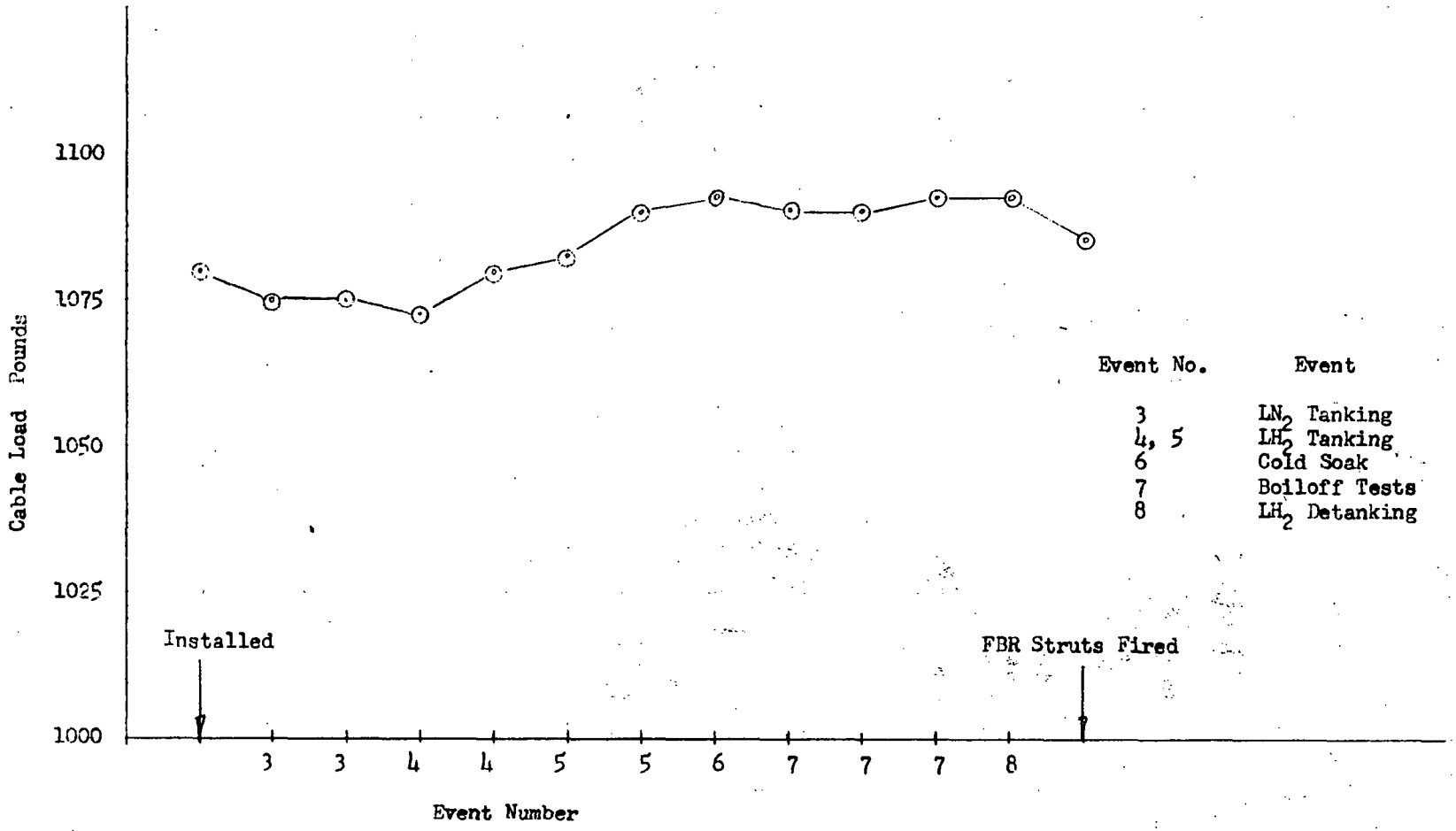

FIGURE III-12 FORWARD SEAL RETAINING CABLE LOADS DURING FIRST ATTEMPTED CRYOUNLATCH TEST NO.3

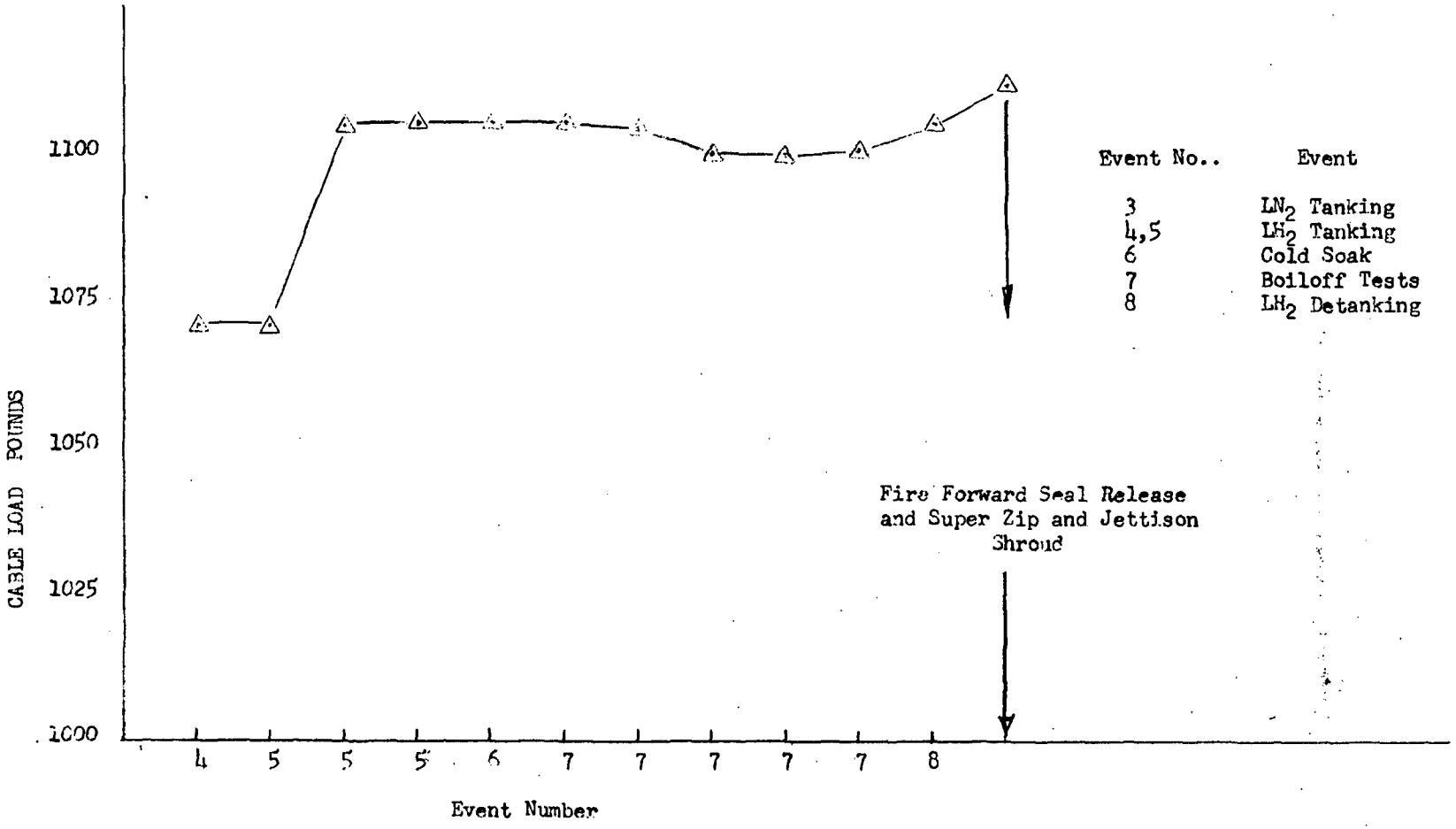

FIGURE III-13 FORWARD SEAL RETAINING CABLE LOADS DURING SECOND AND SUCCESFUL ATTEMPT OF CRYOUNLATCH TEST 3

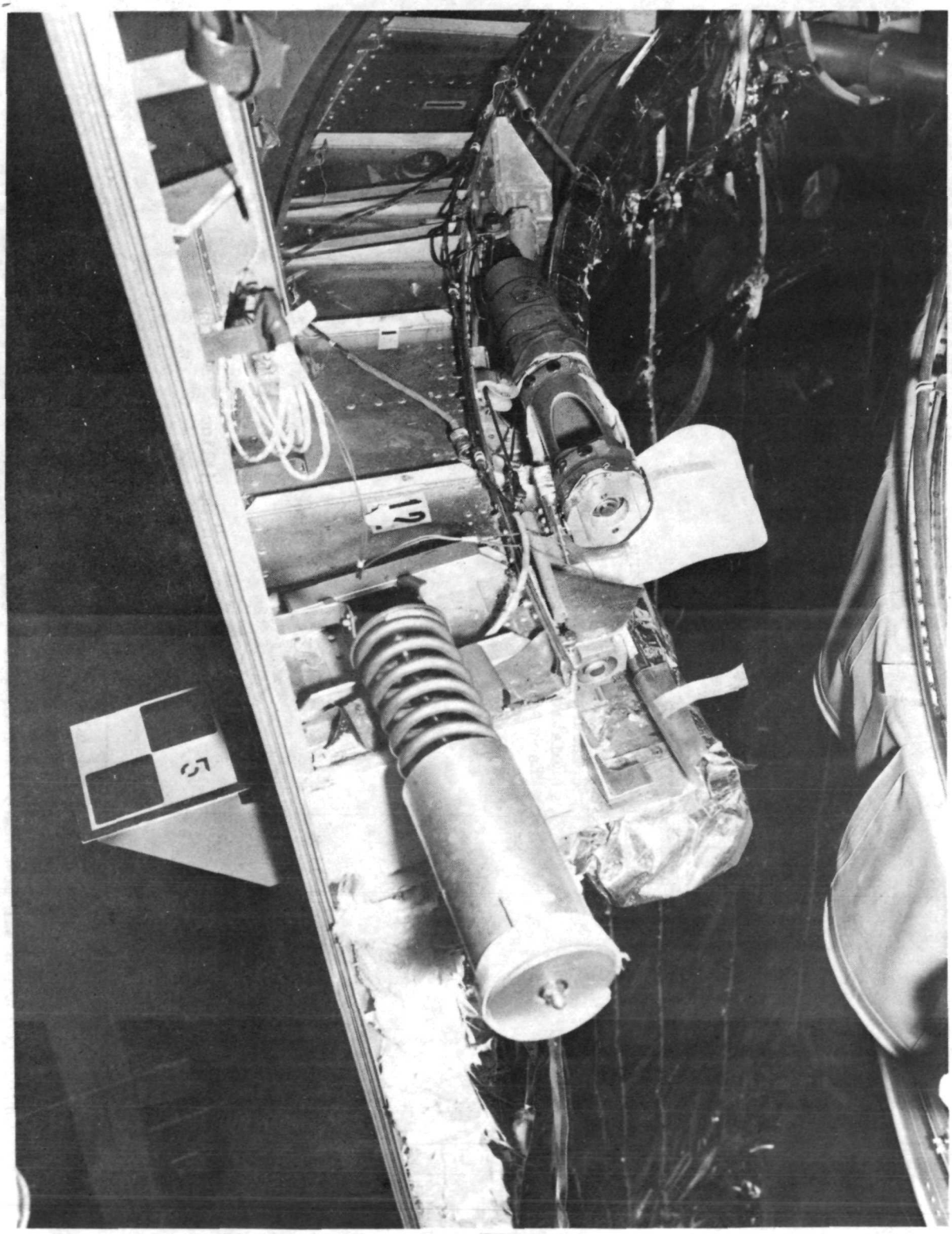

FIGURE III-14 FORWARD SEAL RELEASER AFTER CRYOUNLATCH TEST NO. 3

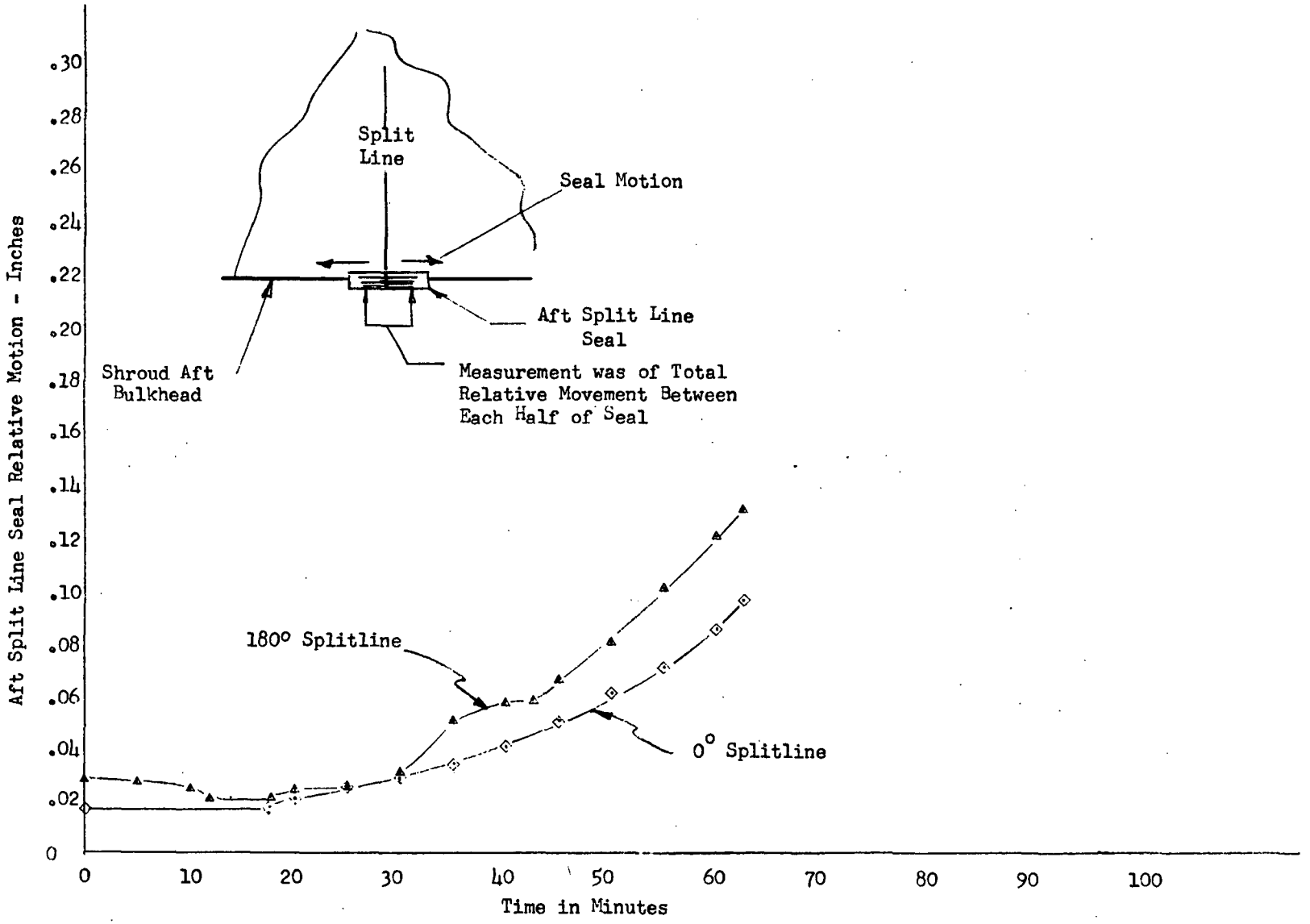

FIGURE III-15 AFT SPLIT LINE SEAL RELATIVE MOTION DURING FIRST LH2 TANKING FOR CRYO-UNLATCH TEST NO.3

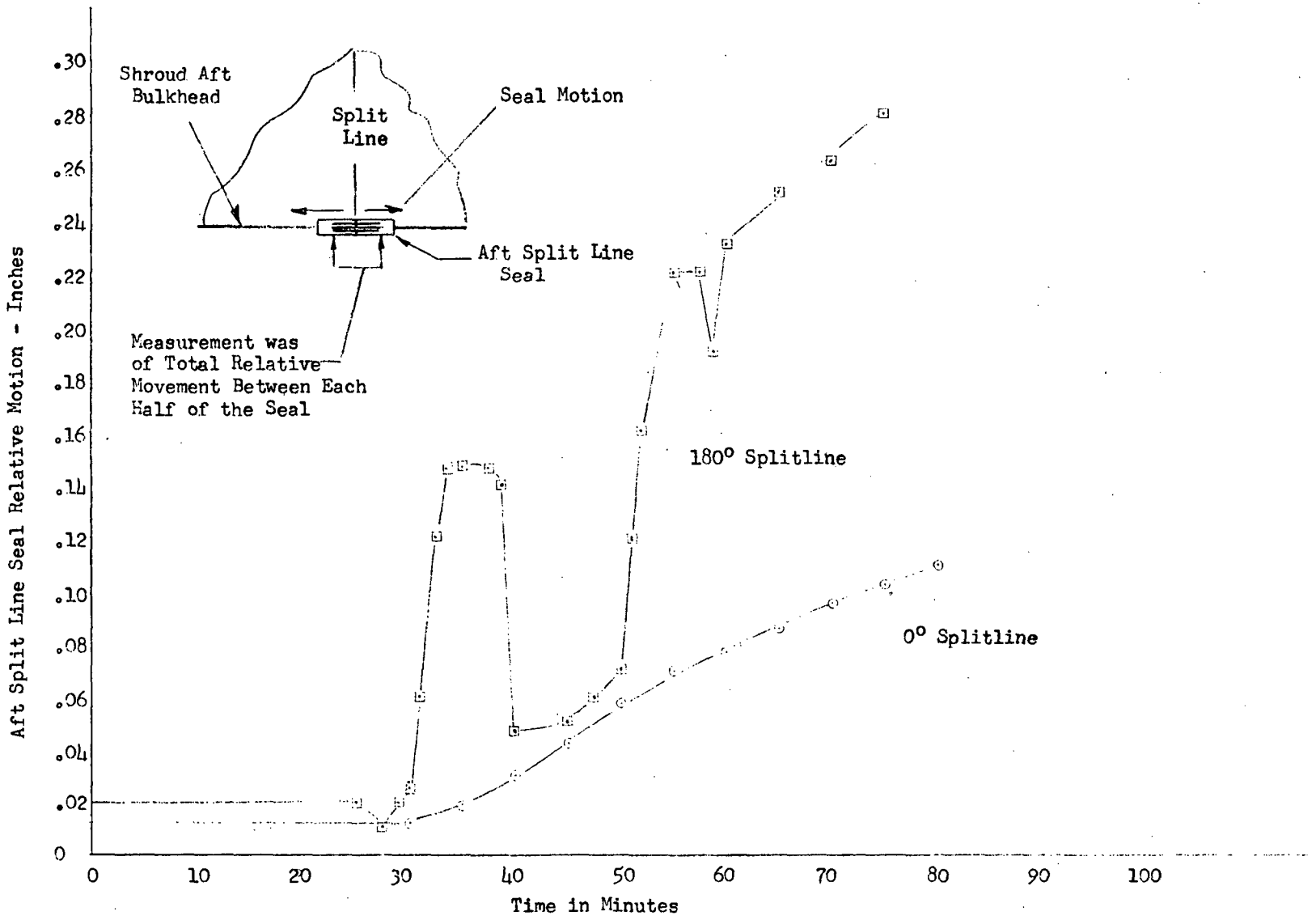

FIGURE III-16 AFT SPLIT LINE SEAL RELATIVE MOTION DURING SECOND LH2 TANKING FOR CRYO-UNLATCH TEST NO.3

IV. SHROUD/CENTAUR PURGE SYSTEMS

By S. V. Szabo, Jr. and R. W. Heath

SUMMARY

This section presents a description and test results of the shroud/Centaur purge system. These include both flight and test peculiar purges. Also presented are results of gas composition measurements made during the transfer of the tank/shroud annulus purge from gaseous nitrogen (GN_2) to gaseous helium (GHe).

All purges installed were of sufficient flow capability to perform their intended functions. Interactions between tank/shroud annulus purge flow, vehicle LH_2 tanking rate and tank/shroud annulus pressure were noted. Procedural changes were made and used to reduce the effects and severity of these interactions.

Gas composition measurements made during the purge gas transfer from GN_2 to GHe showed that a 90 percent concentration of helium in the tank/shroud annulus could be achieved in one hour at a flowrate of 52.5 lb./hr. GHe.

PURGE SYSTEMS DESCRIPTIONS

The purge systems for the CSS and other components as installed consisted of six basic systems. Of these, three were purges that will be used on the flight vehicle and three were test peculiar installations. These six purges were:

1. Forward Total Purge - Flight Purge
   a. Equipment Module
   b. Forward Purge Ring
2. Destructor Housing Purge - Flight Purge
3. LH_2 Fill/Drain Chute Purge - Flight Purge
4. Payload Area Purge - Test Peculiar
5. Forward and Aft Seal Warming Purges - Test Peculiar
6. Boattail Purge - Test Peculiar

A summary of each of these purges in terms of purge gas, flowrate and control, and for which tests they were used is given in Tables IV-1 and IV-2.

The shroud can be divided into four basic areas in which these purges are concentrated. These are; as shown in figure I-2.

1. Payload and Equipment Area.

2. Annular space between tank and shroud bounded by the forward and aft seals in tank section of shroud.

3. Under equipment module.

4. Boattail area.

The purges will be described in the above order.

Payload and Equipment Area

The two purges located in this area are the Payload and Equipment Area Purge and the Forward Seal Warming Purge.

Payload and Equipment Area Purge: - This GN_2 purge was installed after Cryogenic Unlatch Test No. 2 in order to maintain a positive pressure in this volume of the shroud. A schematic of the purge system showing its location is given in figure IV-1. The flowrate capability was up to 90 lb./min. of GN_2, entering into the shroud through two purge lines along the hydrogen vent line. The total flow was divided evenly between these two lines. The flow exited from the lines against deflector plates located immediately below the payload mounting ring. Flow control was maintained by a choked orifice with variable orifice inlet pressure set by a pressure regulator remotely controlled from the test control room.

Forward Seal Warming Purge: - This purge was active and used for all tests, and its location is shown in figure IV-1. GN_2 from a facility supply was distributed circumferentially by a purge ring as shown in figure IV-1. The GN_2 exited from the purge ring through a series of small holes located around the ring. The holes were aligned so that the GN_2 blew across the surface of the seal. Its function was to maintain the seal above minimum temperature requirements. The flow was preset prior to performing the test at 150 $\pm$ 10 lb./hr. This flow could not be remotely adjusted from the control room. It could, however, be turned on and off remotely.

Equipment Module and Tank/Shroud Annulus

The space between the equipment module and Centaur tank forward bulkhead, and the annular space between the tank and the shroud bounded by the forward and aft seals were purged prior to and during the test. These areas

are shown in figure IV-2. Gaseous nitrogen was used for pretest operations to displace all air and to dry the insulation located in this part of the shroud. This gaseous nitrogen was displaced by transferring the purge to gaseous helium before tanking the Centaur, since the GN_2 would liquify and freeze when LH_2 was loaded. Gas composition during the transfer was sampled, and tanking did not commence until 90 percent helium was achieved. The purge systems that provided gas to this area were:

1. Forward purge system which split flow into the equipment module and forward purge ring.

2. Destructor housing purge.

3. LH_2 fill/drain chute purge.

The purpose of these purges was to maintain a positive pressure under the equipment module and in the tank/shroud annulus to prevent air inflow, cryo-pumping and subsequent freezing. These purge gases exited from the tank shroud annulus through an adjustable vent in the LH_2 fill/drain chute, and through leaks in the seals, etc.

Forward Purge System: - The forward purge system is shown in figure IV-2. The system up to the flight disconnect, as shown on the figure, was facility supplied. All hardware downstream of and including the disconnect was flight hardware. As shown, the total flow was monitored and controlled by a choked orifice with a regulated upstream pressure. The total flow was split by orifices in the outlets of a tee on the equipment module. Part of the flow then went under the equipment module, through a single tube, and the remainder into the forward purge ring which distributed the flow circumferentially into the tank/shroud annulus. The purge under the equipment module flowed into the tank/shroud annulus through holes located in the stub adapter.

The total flow capability of the system was up to 100 lb./hr. of GHe and 25 lb./hr. of GH_2. Two flowrates were used during the test. A flow of 25 lb./hr. of GHe was used during Centaur LO_2 tank loading. During Centaur LH_2 tanking, when the greatest thermal transients were encountered, a high purge flow of 65 lb./hr. of GHe was used. After LH_2 had been tanked and thermal conditions stabilized, the flow rate was reduced to the 25 lb./hr. level. The equipment module/purge ring flow split ratio was 1/1 for Cryogenic Unlatch No. 1, and 1/5.25 for all subsequent tests as outlined in Table IV-1.

Destructor Housing Purge: - The destructor housing purge system is shown in figure IV-3. This purge serves two purposes. It provides warm purge gas to maintain the Centaur destruct unit above minimum temperature requirements, and also provides purge gas to the aft section of the tank/shroud annulus. Gaseous helium entered the shroud through a facility

line and then joined a flight insulated line near 90° on the shroud. The purge gas then entered the space between the destructor housing and the destructor unit located in the housing. It then exited the housing through a small hole in the bottom and dumped into the tank/shroud annulus. A purge flow of 27.5 ± 1.5 lb./hr. of GHe was used during all phases of testing. Flow control was through a choked orifice with regulated upstream pressure and temperature.

LH2 Fill and Drain Chute Purge: - Figure IV-4 shows a cross section through the LH_2 fill/drain chute. This chute is located on the side of the shroud at 155° and at station 2265.50 (centerline of fill/drain flange). The chute is an aluminum structure bolted to the shroud. The outer opening has a Mylar "ice-bag" covering. The LH_2 tank flight fill/drain line penetrates the bag, and attaches to the flight fill/drain valve located inside the chute. At vehicle liftoff, the fill/drain valve, line, and "ice-bag" are retracted and an internal door swings down and closes the opening. A preset 4.2 lb./hr. GHe purge is directed under the insulation covering the flight fill/drain valve and then dumps into the fill/drain chute. Located on the side of the chute, as shown, is an adjustable vent valve for purge gases from the tank/shroud annulus to also enter the chute. The 4.2 lb./hr. GHe purge and the purge gas from the tank/shroud annulus then exit through a hole in the "ice-bag."

For the Cryogenic Unlatch Tests, LH_2 fill/drain was accomplished through another tank opening, and the flight LH_2 fill/drain valve was not used. A simulated fill/drain line was installed that also served as a vent valve for emergency vent of the tank/shroud annulus.

Boattail Area

The boattail area of the shroud contained two purges as shown in figure IV-5. These are the aft seal warming purge and the boattail area purge.

Aft Seal Warming Purge: - This purge served the same purpose as the forward seal warming purge; to maintain the aft circumferential seal above a minimum temperature. GN_2 at 150 ± 10 lb./hr. from a facility supply was distributed circumferentially by a purge ring as shown in figure IV-5. The GN_2 exited from the purge ring through small holes located around the ring. The holes were aligned so that the GN_2 blew across the surface of the seal.

Boattail Area Purge: - This purge was not installed until after Cryogenic Unlatch Test No. 1. The function of this purge was to maintain a dry environment in the boattail and prevent freezing of water vapor on the aft seal and other cold surfaces. The purge was distributed into the boattail at four places, as shown in figure IV-5. Two flowrates were used. A flow of 200 lb./hr. of GN_2 was used during pretanking operations, and 400 lb./hr. during tanking and other portions of the test. Flow control was through a choked orifice with remotely controlled regulated upstream pressure.

SYSTEM OPERATIONS DURING TESTING

All purge systems operated satisfactorily and performed their intended functions throughout all tests. Reported in this section will be the results of the GN_2 to GHe purge transfer in the tank/shroud annulus, and the behavior and interaction of the tank/shroud annulus pressure with vehicle LH_2 tanking rate and changing of the forward purge system flowrate.

GN_2/GHe Purge Transfer and Gas Composition

As noted in the purge system descriptions, a GN_2 purge was used to remove all air, and dry the insulation prior to purging the tank/shroud annulus with gaseous helium (GHe). In transferring the purge from GN_2 to GHe, a limit of 90 percent GHe to GN_2 was set before Centaur tanking could commence. A goal of attaining 90 percent GHe to GN_2 in a time limit of one hour was established. To determine the gas composition with time, a gas sampling and analysis system was installed.

The purge gas sampler system used five pick-up points located around the tank as shown in figure IV-6. Two were placed under the equipment module; one in the free space and one inside the insulation blanket on the forward bulkhead. Two were located in the tank/shroud annulus, one at each end on the same axis. The fifth was placed behind the LH_2 tank radiation shield in the space between the shield and the tank, about midway up. Gas samples were drawn into these sense points and transferred through tubes to a gas analyzer which provide the percentage of gaseous helium to nitrogen (GHe/GN_2) using the thermal conductivity differences of the gases.

Gas samples were taken continuously from all locations except inside the insulation blanket on the forward bulkhead. Steady flow through this one sense line would have upset the gaseous diffusion process in that area. Consequently, one instantaneous data point was approximated in that area during each run. The sensor was opened at various times after the start of the purge and the "knee" of the resulting curve was taken as the instantaneous GHe concentration.

A variation was made in the GHe purge flow rates in order to evaluate the effects of reduced flow on gas exchange rates. Three different rates were used; 52.5 lb./hr. (which is the nominal flowrate), 26 lb./hr., and 13 lb./hr. The 52.5 lb./hr. flowrate gave satisfactory concentrations of GHe versus time. The 26 lb./hr. flowrate gave acceptable results, but the concentrations were marginal in some areas. One-quarter nominal flow gave unsatisfactory concentrations at the aft end of the tank/shroud annulus, and under the radiation shield. Table IV-3 summarizes the time to attain 90 percent GHe to GN_2 for different areas and purge flowrates. Typical concentrations versus time are shown in figures IV-7 through -10.

Clearly, the aft end of the tank/shroud annulus, and the volume under the radiation shield are vulnerable to a lowered purge flow.

The forward bulkhead insulation blanket should be completely purged free of GN_2 in one hour. As previously noted, time histories of the gas composition cannot be accurately made inside the forward bulkhead insulation; estimates of the GHe concentration can be made at given points in time. The GHe concentration inside the insulation is 90 percent after 10 minutes of purge at 52.5 lb./hr. flowrate. At 26 lb./hr. flowrate, the concentration is 90 percent after 20 minutes. At 13 lb./hr. flowrate, the concentration is only 50 percent after 24 minutes of purging.

Tank/Shroud Annulus Pressure Behavior During Centaur Hydrogen Tanking

During Centaur LH_2 tanking, it was expected that the Tank/Shroud Annulus Pressure (TSAP) would decay as the annulus gas temperature was decreased. An analysis performed (Reference 3) showed that the minimum TSAP would occur when the minimum temperature point was reached during the maximum weighted gas temperature decay rate during tanking. This analysis briefly follows:

The helium volume in the tank/shroud annulus at any given time is given by the perfect gas law:

$PV = WRT$

P = Annulus Pressure
V = Annulus Volume
W = Weight of Gas in Annulus
R = Gas Constant
T = Weighted Average Temperature

Differentiating with respect to time gives: (assuming R and V = constant)

$$V\frac{dP}{d\tau} = RT\frac{dW}{d\tau} + WR\frac{dT}{d\tau}$$

but $\frac{dW}{d\tau}$ is the helium purge gas flow rate into the shroud.

To obtain the minimum shroud pressure, we set $\frac{dP}{d\tau} = 0$, and using the perfect gas law for W at this time we get:

$$\frac{PV}{R}\left(\frac{1}{T^2}\right)\left(-\frac{dT}{d\tau}\right) = \dot{W}$$

or

$$P = \frac{\dot{W}RT^2}{V}\left(-\frac{1}{\frac{dT}{d\tau}}\right)$$

From this it can be seen that the minimum pressure will occur (for R, V and $\dot{W}$ = constants) when T is a minimum for the maximum $dT/d\tau$.

Using this equation, experience from other tests, and the known properties and pressure requirements for the shroud, the minimum purge flow of 52.5 lb./hr. of gaseous helium was established.

Data taken during Cryogenic Unlatch Test No. 3 show qualitatively that the minimum pressure does occur at the above stated temperature conditions. Figure IV-11 shows tank/shroud annulus pressure, LH_2 liquid level, purge flowrate, and shroud cavity weighted gas temperature for the first LH_2 tanking done for Cryogenic Unlatch Test No. 3. The initial tanking rate was 322 gal./min.

As can be seen, from the figure, the maximum temperature decay rate occurred between about 43 to 47 minutes on the figure, and was about 1100°R/hr. The minimum temperature point and minimum pressure point were reached at about 47 minutes at which time the annulus pressure started to increase. Minimum annulus pressure reached was measured at 0.015 psig.

As stated in Section I, of this report, problems were encountered and the vehicle had to be detanked and repairs made before proceeding. This meant another LH_2 tanking. For this tanking it was decided to reduce the initial tanking rate in order to determine the effect of tanking rate.

Figure IV-12 shows data from the second LH_2 tanking. As noted on the figure, the tanking rate was 157 gal./min. or half that of the previous tanking. The maximum temperature decay rate occurred between 37 and 50 minutes on the figure and was about 800°R/hr. The minimum pressure and temperature were reached at about 50 minutes. As can be seen, the annulus pressure did not experience as rapid a decay, and did not reach as low a pressure although both initially started at about the same pressure.

As both figures show, the purge flow was increased to the maximum prior to encountering severe pressure and temperature transients, and remained at this level throughout the tanking. This was not done on previous tankings, and purge flow was varied throughout the transient period, and obscured the behavior of the other parameters.

It can be concluded from these data that the analysis predicts, at least qualitatively, the mechanism and reasoning for the rapid annulus pressure decay. Assuming volume remains constant may not be valid since $dV/d\tau$ may be of the same order of magnitude or larger.

If on the flight vehicle, a rapid tanking rate, at least initially, is used, the annulus pressure may go below atmospheric pressure for a short period of time. This means that the equipment module cavity pressure may go negative and a crushing pressure experienced. A slower tanking rate, and the transfer to the high purge rate prior to filling the hydrogen tank is indicated.

Tank/Shroud Annulus Pressure Behavior When Changing Purge Flow Rates

After tanking LH_2 in the Centaur, and when thermal conditions had stabilized, the purge flow into the annulus was reduced from the high flow of 92.5 lb./hr. to 52.5 lb./hr. This reduction in purge flow had a significant effect on the annulus pressure as shown in figure IV-13. Plotted on figure IV-13 are total GHe flow into the equipment module cavity and the forward purge ring; the equipment module cavity pressure, and the tank/shroud annulus pressure against time in minutes. As seen from the figure, at about 21 minutes, the purge flow was reduced from 65 lb./hr. to about 26 lb./hr. in about 2 minutes. Both the equipment module cavity and the tank/shroud annulus pressure decayed very rapidly in response to the purge flow reduction, and then recovered and stabilized. The exact reasoning for this decay is not fully understood at this time. Here again on the flight vehicle, if the purge flow is reduced rapidly, the equipment module cavity pressure, and the tank/shroud annulus pressure could go negative, and a crushing pressure experienced. The purge system controls need to be designed so a **controlled reduction in purge flow** can be accomplished.

CONCLUSIONS AND RECOMMENDATIONS

Based on test experience and data obtained during the CSS Cryo-Unlatch Test Program, the following conclusions and recommendations are made:

1. The flight purge systems tested are of sufficient flow capability to perform their intended functions.

2. The requirement of 90 percent GHe to GN_2 in the tank/shroud annulus after purge gas changeover can be met in 1 hour using a flowrate of 52.5 lb./hr. total GHe.

3. Tank/shroud annulus pressure is very sensitive to LH_2 tanking rate. Because of this, the following recommendations should be incorporated:

   a. The tank/shroud annulus purge be increased to the high flowrate of 92.5 lb./hr. after LH_2 tank chilldown, and remain at this rate throughout vehicle tanking and the remainder of the countdown (unless a prolonged foreseeable hold occurs).

   b. The initial LH_2 tanking rate not exceed 175 gal./min. until the tank/shroud annulus pressure has reached its minimum point and has started to increase. After the minimum pressure has been experienced, LH_2 tanking can proceed at a rapid rate of about 500 gal./min.

4. Tank/shroud annulus pressure is sensitive to rapid changes in purge flowrate. Therefore, a system should be installed at ETR that allows an infinite number of flowrates over a specified range, rather than two fixed flows of 52.5 and 92.5 lb./hr. This can be accomplished using a

choked orifice and remotely controlling orifice upstream pressure. This type of control should be installed on both the forward purge and destructor purge systems. Also for this reason it is recommended that the purge flow be retained at the high rate throughout the countdown after LH_2 tanking, and not be reduced to the nominal flow of 52.5 lb./hr.

5. During detanking, such as after a vehicle tanking test or abort, the tank/shroud annulus pressure will increase rapidly due to warming of the gas. During detanking, the annulus pressure and purge flow should be watched closely, and purge flow reduced to maintain annulus pressure within acceptable limits. Although the shroud can structurally take pressures of 3 psig in burst, the tank/shroud annulus pressure should be limited to about 1 psig to prevent damage to split line seals and other sealing that may have been done to the shroud.

TABLE IV-1

SUMMARY OF CSS AND EQUIPMENT PURGES
USED FOR EACH CRYOGENIC UNLATCH TEST

	Destructor Housing Purge	Equip. Module Purge	Forward Annulus Purge	Eq.Mod. to Fwd. Purge Ratio	Seal Warming Purges		Payload Area Purge	Boat-tail Purge	LH_2 Fill Drain Chute Purge
					Aft	Fwd.			
Cryo-Unlatch Test No. 1	Yes	Yes	Yes	1/1	Yes	Yes	No	No	Yes
Cryo-Unlatch Test No. 2	Yes	Yes	Yes	1/5.25	Yes	Yes	No	Yes	Yes
LN_2/LN_2 Tanking	Yes	Yes	Yes	1/5.25	Yes	Yes	Yes	Yes	Yes
LH_2/LN_2 Tanking	Yes	Yes	Yes	1/5.25	Yes	Yes	Yes	Yes	Yes
Cryo-Unlatch Test No. 3	Yes	Yes	Yes	1/5.25	Yes	Yes	Yes	Yes	Yes

TABLE IV-2

CSS PURGE SYSTEM SUMMARY FOR CRYOGENIC UNLATCH TESTS

Purge System	Purge Gases	Flow Range	Flowrate During Test	Method of Flow Control	Comments
Payload Area Purge	GN_2	0-90 lb./min.	Flow varied to maintain positive press. in shroud.	Same as destructor housing purge.	
Fwd. and Aft Seal Warming Purges	GN_2	0-200 lb./hr.	150±10 lb./hr.	Choked orifice-Set upstream pressure. On-off control only.	Purge flow set before test
Total Forward Purge a) Equip. Module b) Fwd. Purge Ring	GHe GN_2 GHe GHe	2-100 lb./hr. 5-25 lb./hr. 1-50 lb./hr. .3-16 lb./hr. 1-50 lb./hr. 1.7-84 lb./hr.	25.0±1.5 lb./hr. 17.5±2.5 lb./hr. 12.5±1.0 lb./hr. *4.0±1.0 lb./hr. 12.5±1.0 lb./hr. *21.0±1.0 lb./hr.	Same as destructor housing purge. Total purge split by choked orifices into equip. mod. and purge ring flows.	GN_2 used for pretest purge only. *These purge rates used on Cryo-Test No.2 and on.
Destructor Housing	GHe GN_2	2-50 lb./hr. 5-20 lb./hr.	27.5±1.5 lb./hr. 7.5±2.5 lb./hr.	Choked orifice-Regulated upstream press. Remote control.	GN_2 used for pretest purge only.

TABLE IV-2 (CONTINUED)

Purge System	Purge Gases	Flow Range	Flowrate During Test	Method of Flow Control	Comments
LH_2 Fill/Drain Chute Purge	GHe	0-10 lb./hr.	4.2±0.2 lb./hr.	Choked orifice - Set upstream pressure on-off control only.	
Boattail Purge	GN_2	0-400 lb./hr.	200±10 lb./hr. and 400±10 lb./hr.	Same as destructor housing purge.	Thermal control purge.

TABLE IV-3

SUMMARY OF TIME REQUIRED TO ATTAIN
90% GHe TO GN_2 CONCENTRATION -
DATA FROM CSS CRYO-UNLATCH TESTS

Purged Area	Time to Attain 90% GHe to GN2 GHe Purge Flow Rate		
	52.5 lb./hr.	26 lb./hr.	13 lb./hr.
Equipment Module Cavity	5 Minutes	10 Minutes	25 Minutes
Forward End of Tank/Shroud Annulus	28 Minutes	38 Minutes	42 Minutes
Aft End of Tank/Shroud Annulus	52 Minutes	58 Minutes	180-190 Minutes
Behind Radiation Shield	58 Minutes	76 Minutes	190-200 Minutes

NOTE: Distribution of purges was always in the same proportion as 27.5 lb/hr. to the destructor, 4 lb/hr. to the forward bulkhead, and 21 lb/hr to the forward purge ring for purge rates less than 52.5 lb/hr.

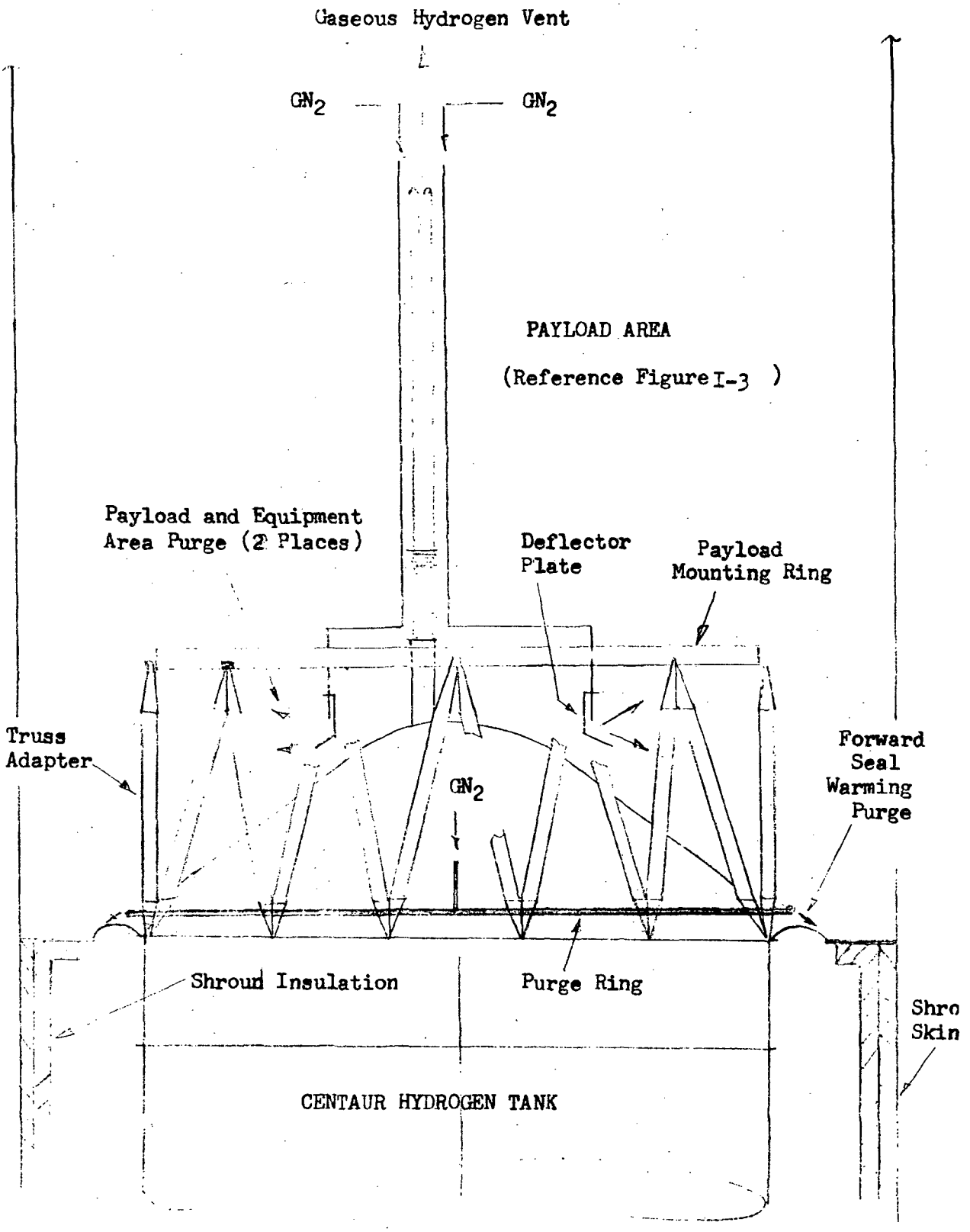

FIGURE IV-1 SHROUD PAYLOAD AND EQUIPMENT AREA PURGE AND FORWARD SEAL WARMING PURGE - CSS CRYOGENIC UNLATCH TESTS

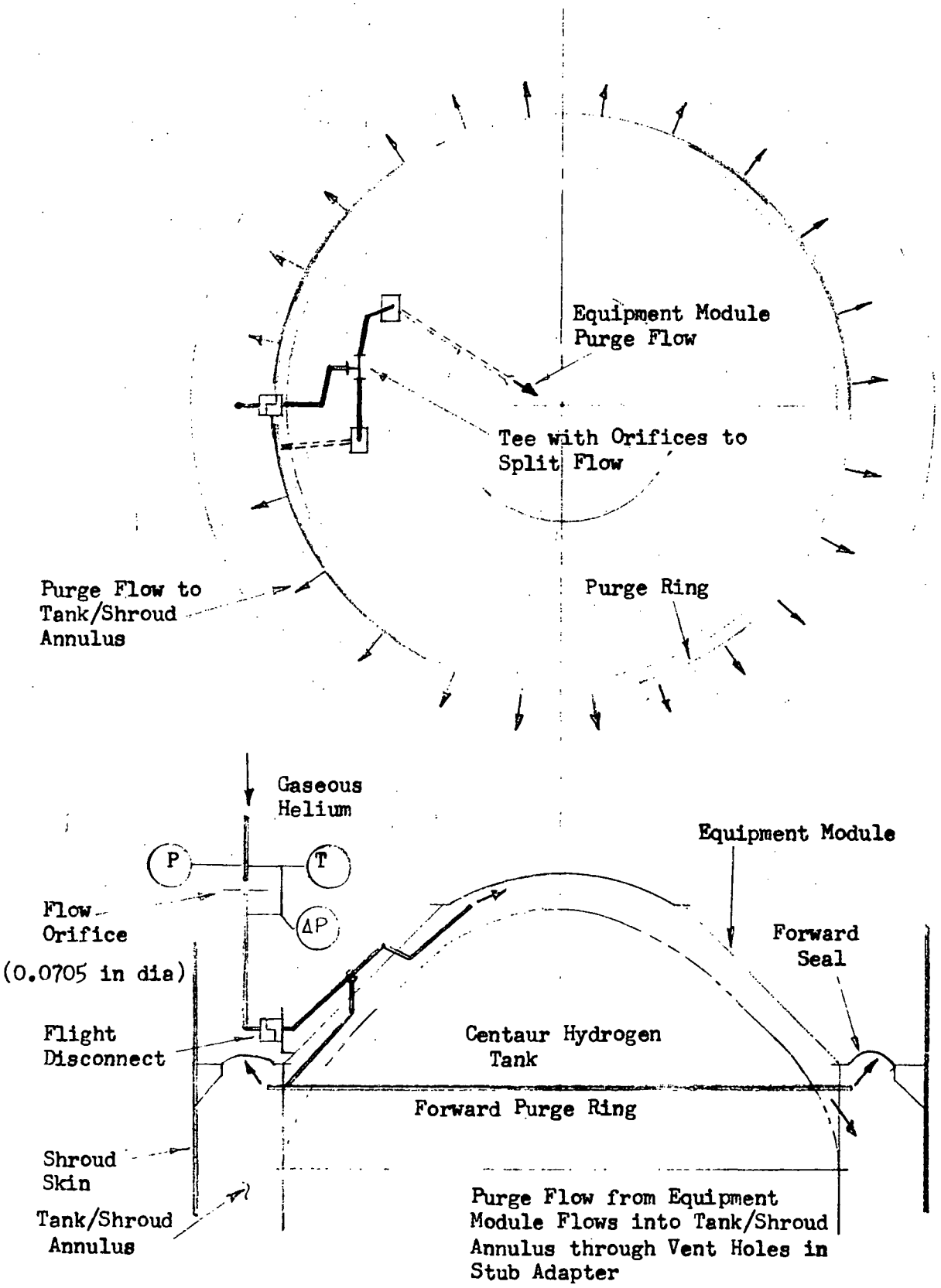

FIGURE IV-2 CENTAUR EQUIPMENT MODULE AND TANK/SHROUD ANNULUS FORWARD PURGE SYSTEM SCHEMATIC - CSS CRYOGENIC UNLATCH TESTS

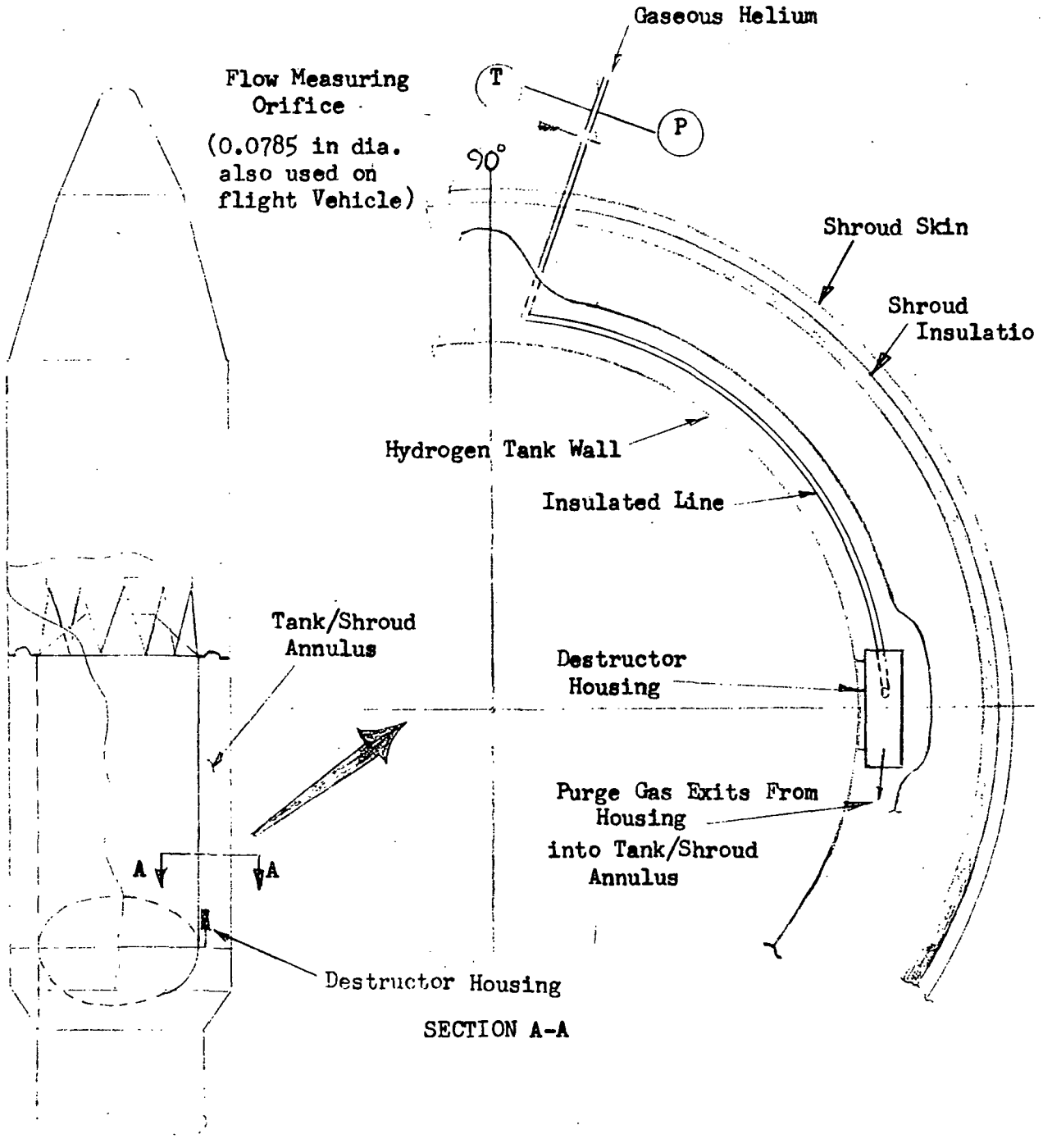

FIGURE IV-3 CENTAUR DESTRUCTOR HOUSING PURGE SYSTEM SCHEMATIC

CSS CRYOGENIC UNLATCH TESTS

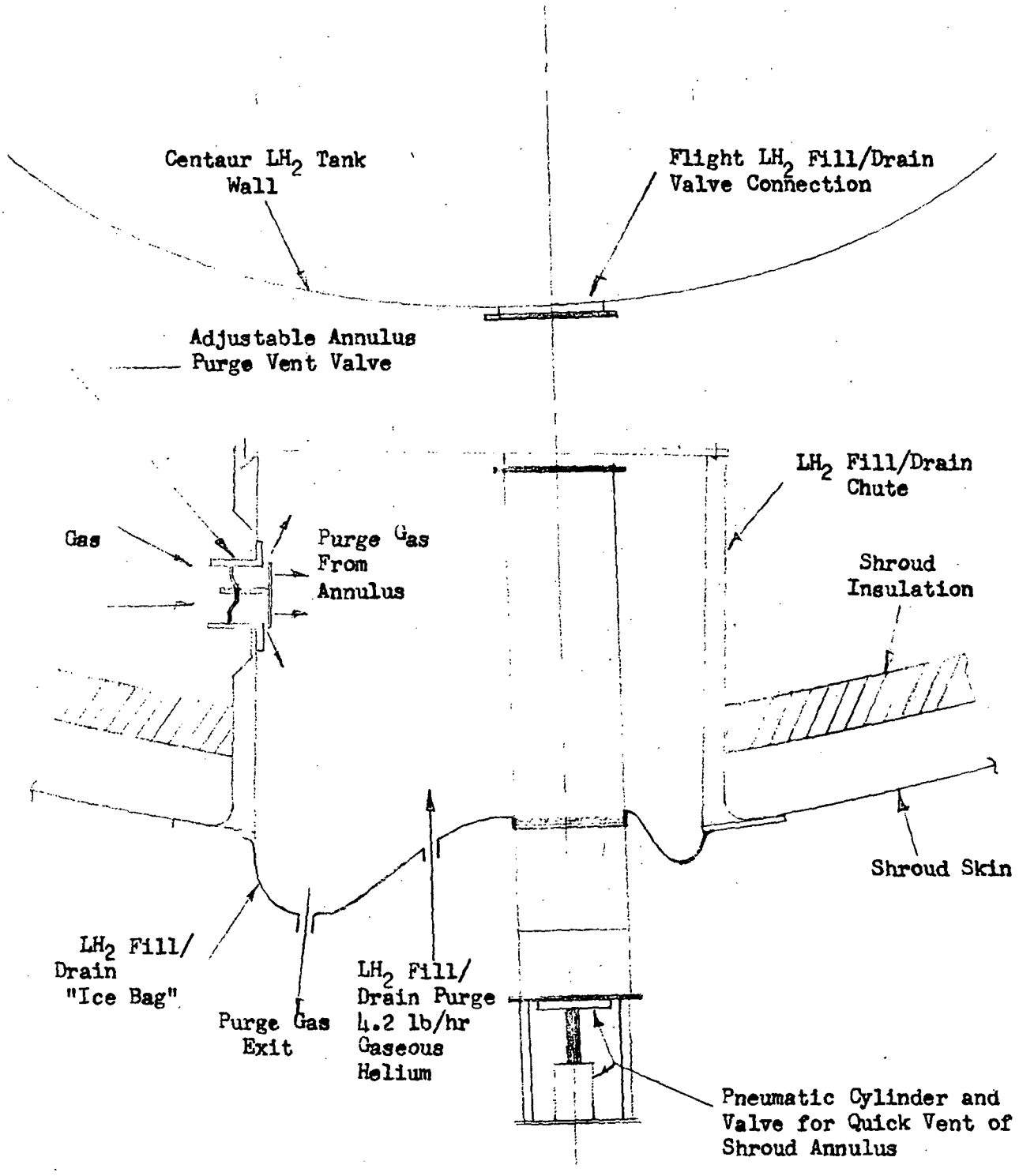

FIGURE IV-4 SECTION THROUGH LH_2 FILL/DRAIN CHUTE SHOWING PURGE GAS INLET AND EXIT. CSS CRYOGENIC UNLATCH TESTS

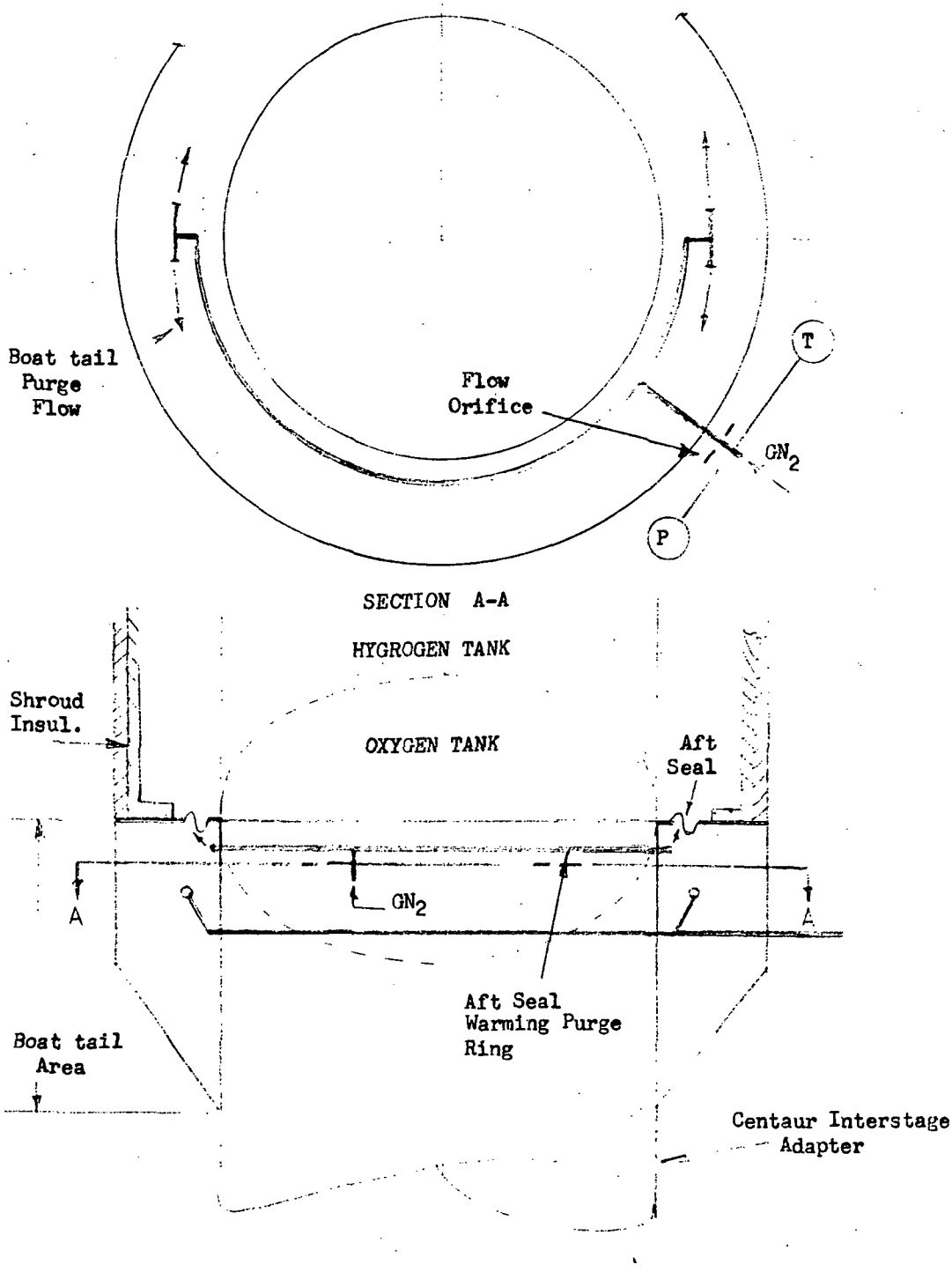

FIGURE IV-5 SHROUD BOATTAIL PURGE AND AFT SEAL WARMING PURGE SYSTEMS
CSS CRYOGENIC UNLATCH TESTS

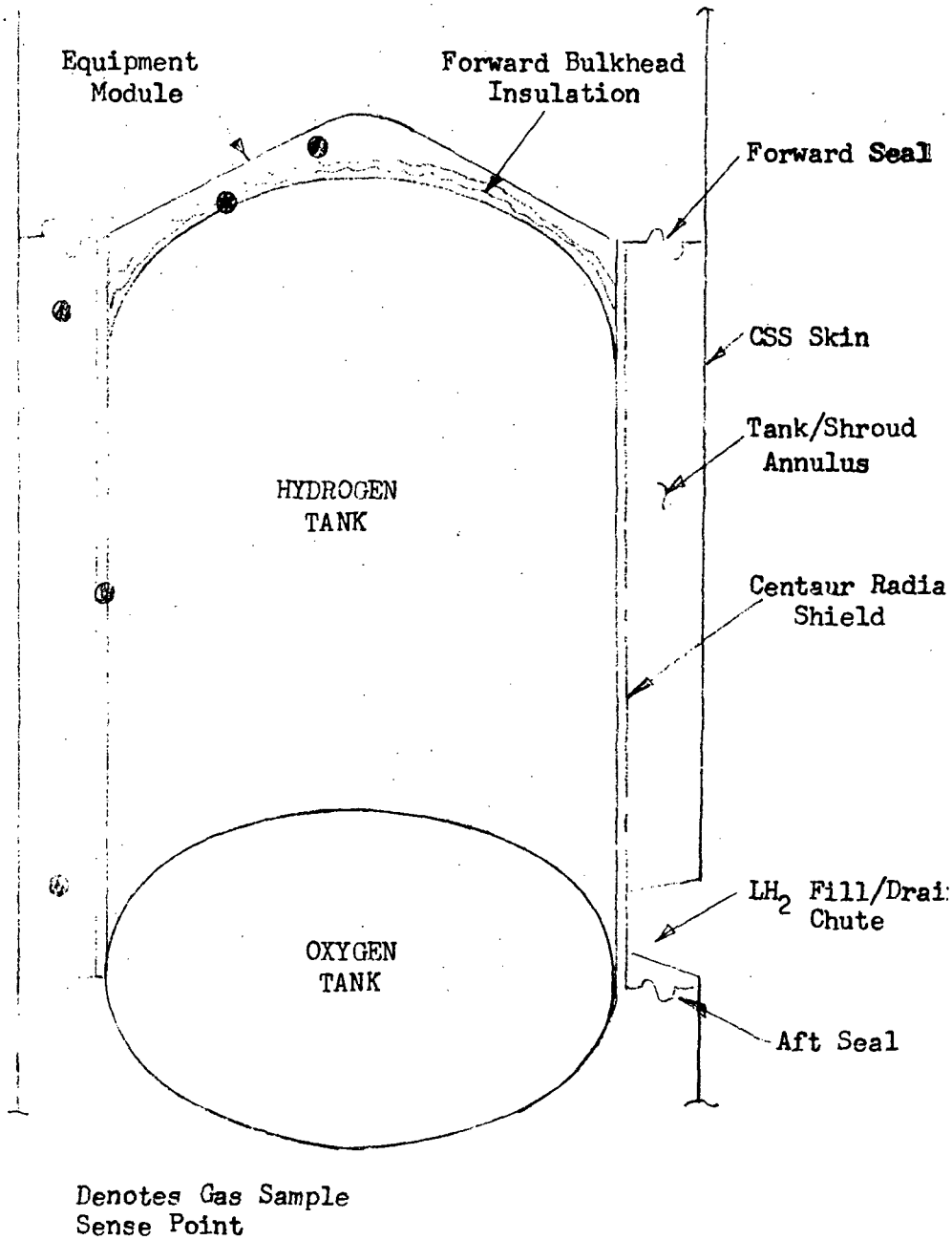

FIGURE IV-6 PURGE GAS SAMPLE SENSE POINT LOCATIONS - CSS CRYOUNLATCH TESTS

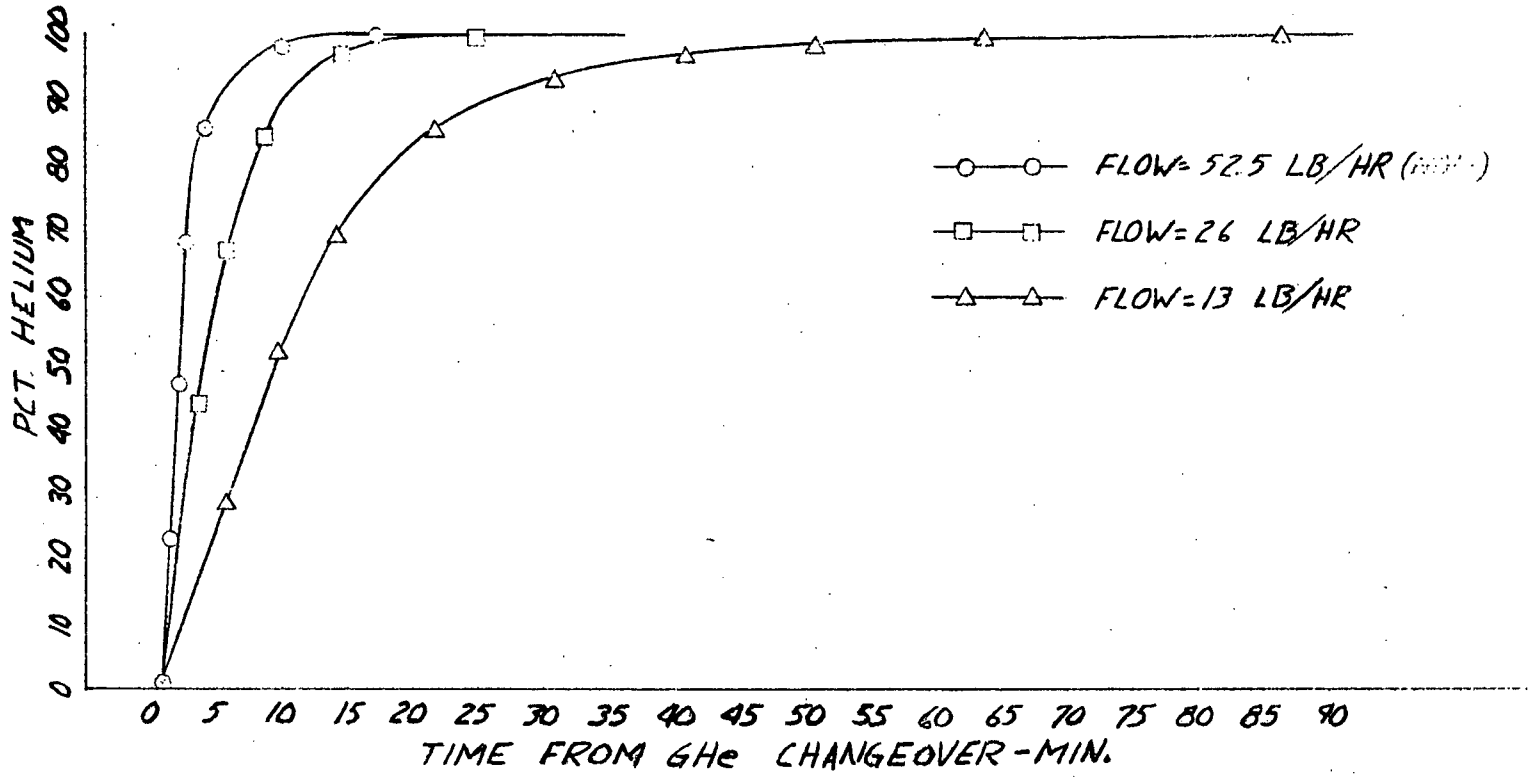

FIGURE IV-7 - PURGE GAS COMPOSITION UNDER EQUIPMENT MODULE

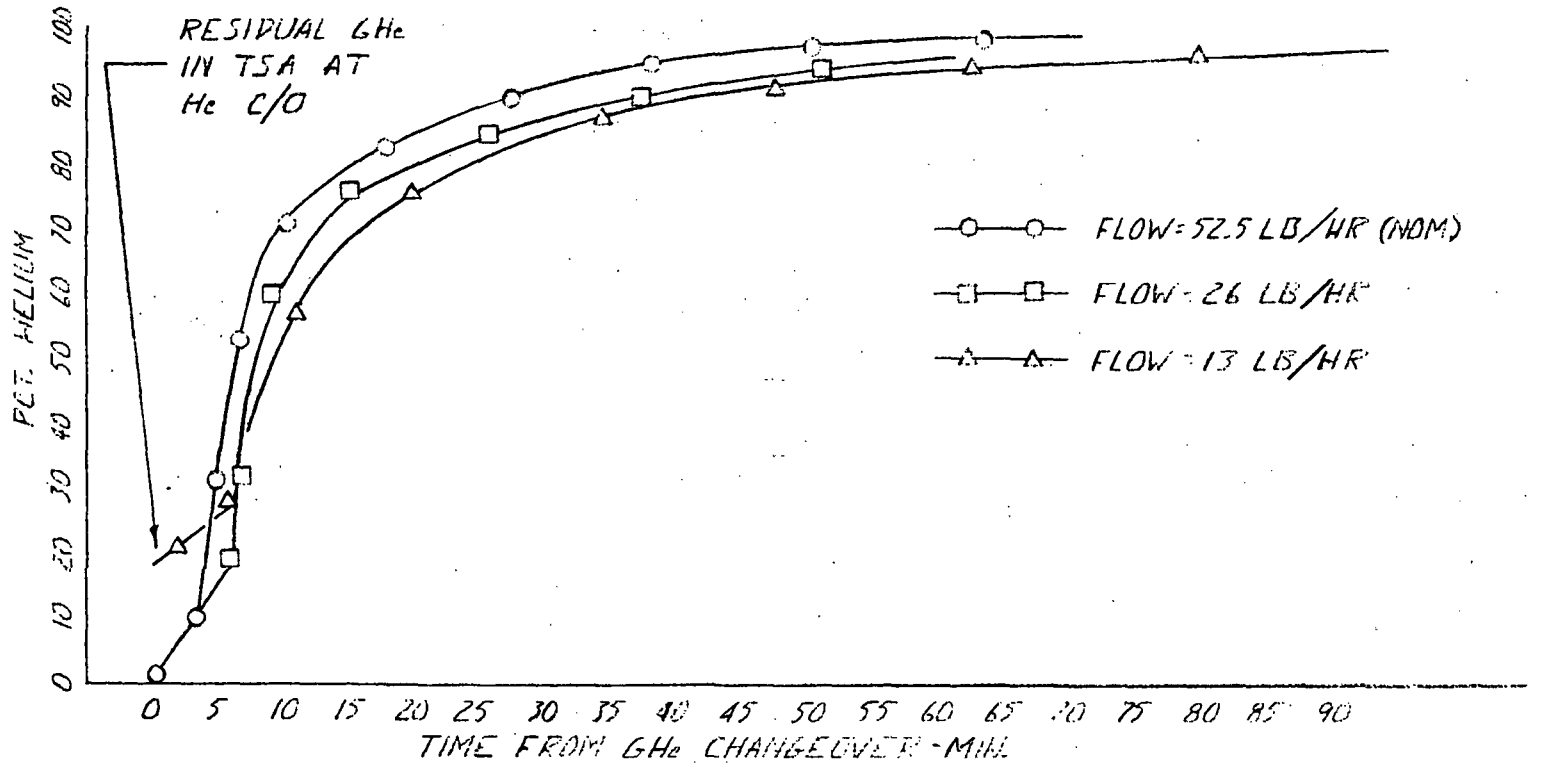

FIGURE IV-8 PURGE GAS COMPOSITION AT FORWARD END - TANK/SHROUD ANNULUS

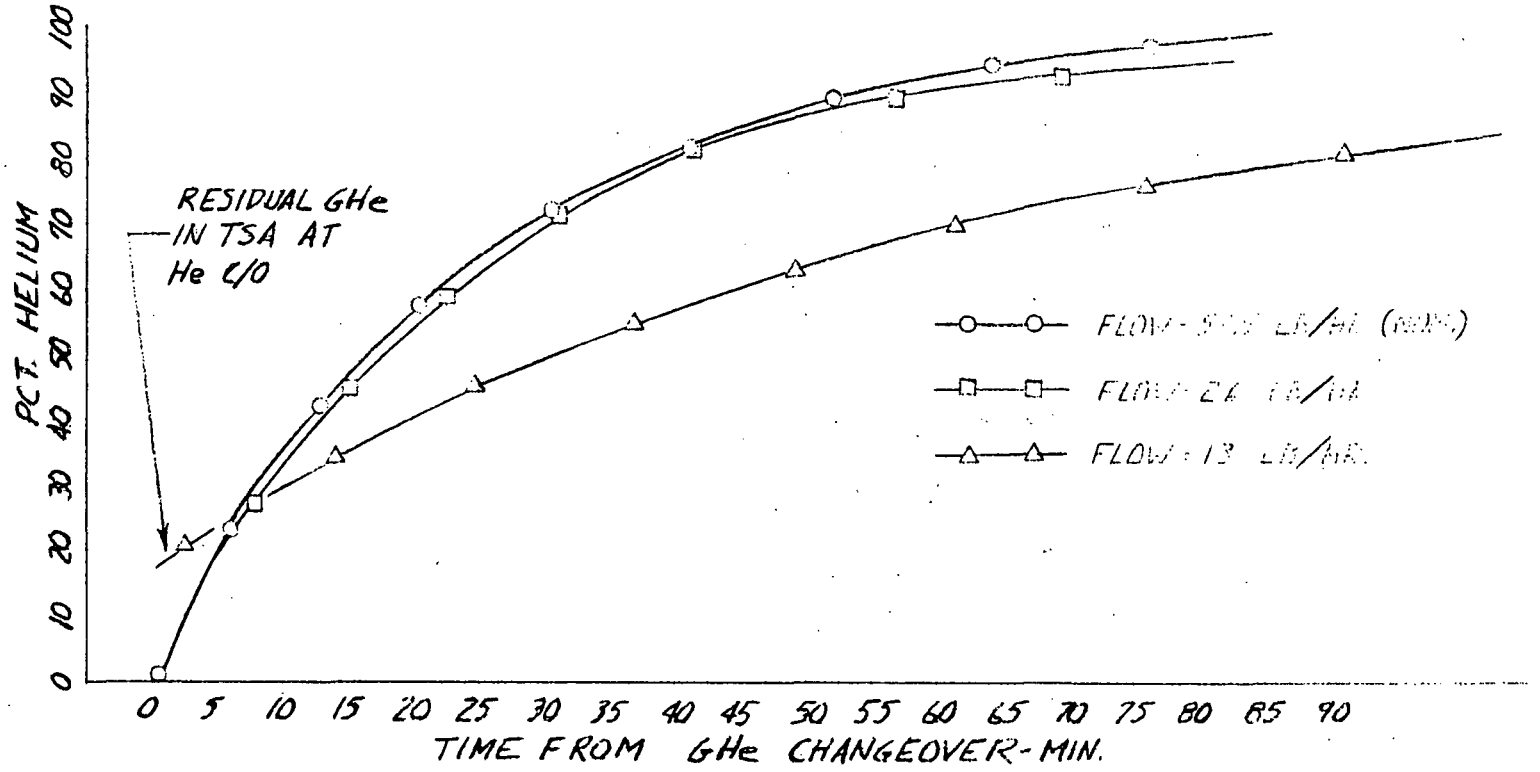

FIGURE IV-9 PURGE GAS COMPOSITION AT AFT END - TANK/SHROUD ANNULUS

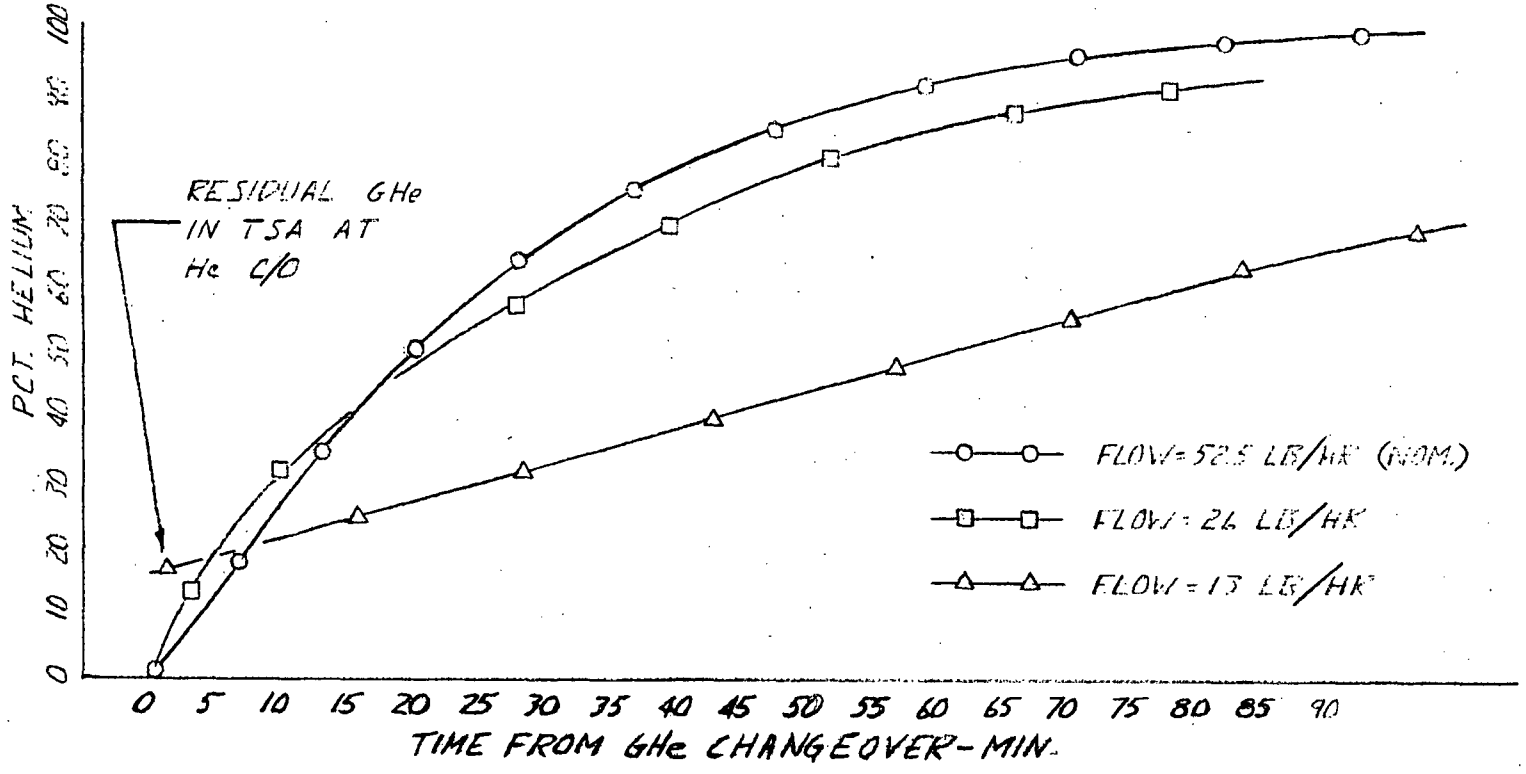

FIGURE IV-10 PURGE GAS COMPOSITION BEHIND RADIATION SHIELD

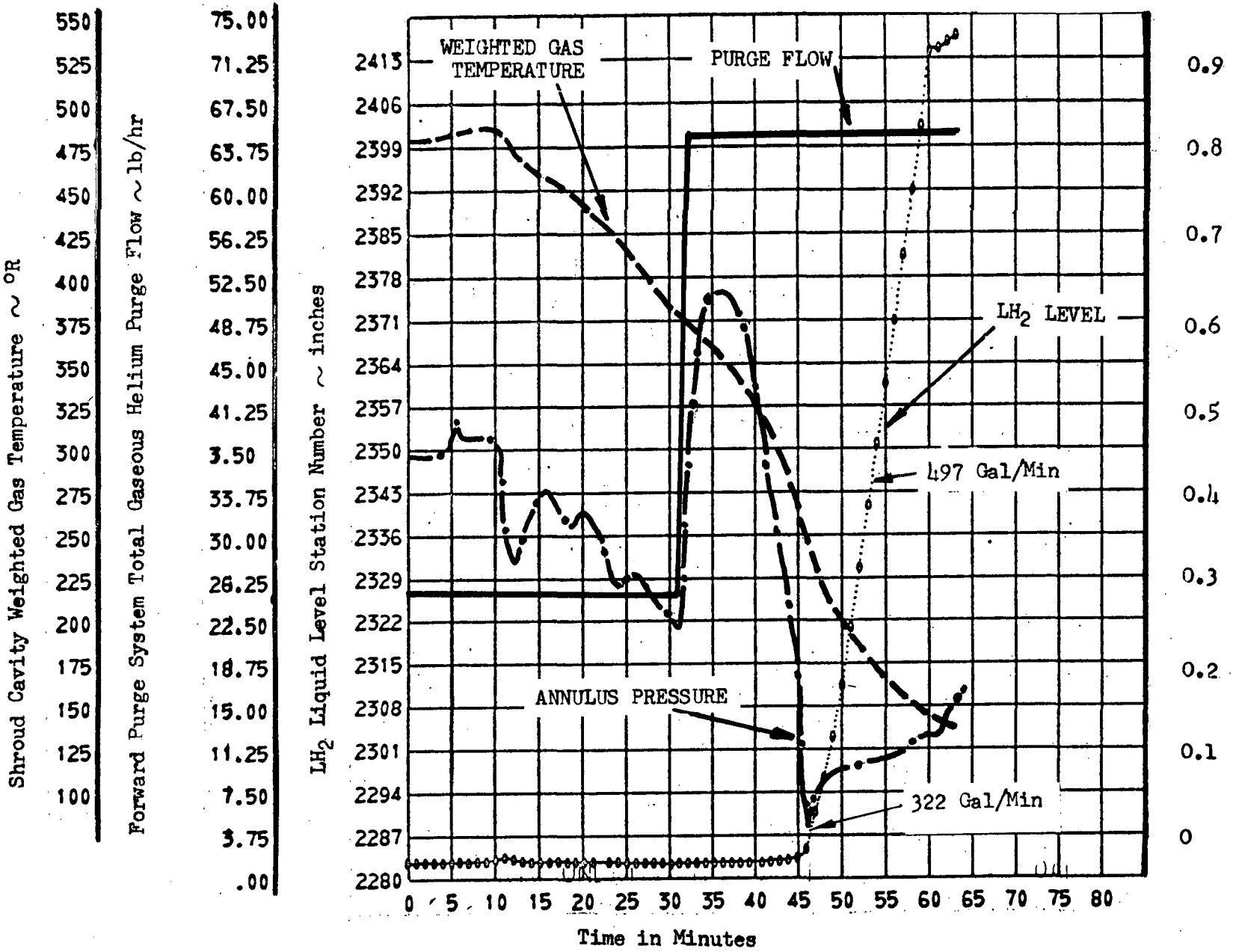

FIGURE IV-11 TANK/SHROUD ANNULUS PRESSURE DURING FIRST HYDROGEN TANKING FOR CRYOGENIC UNLATCH TEST NO.3

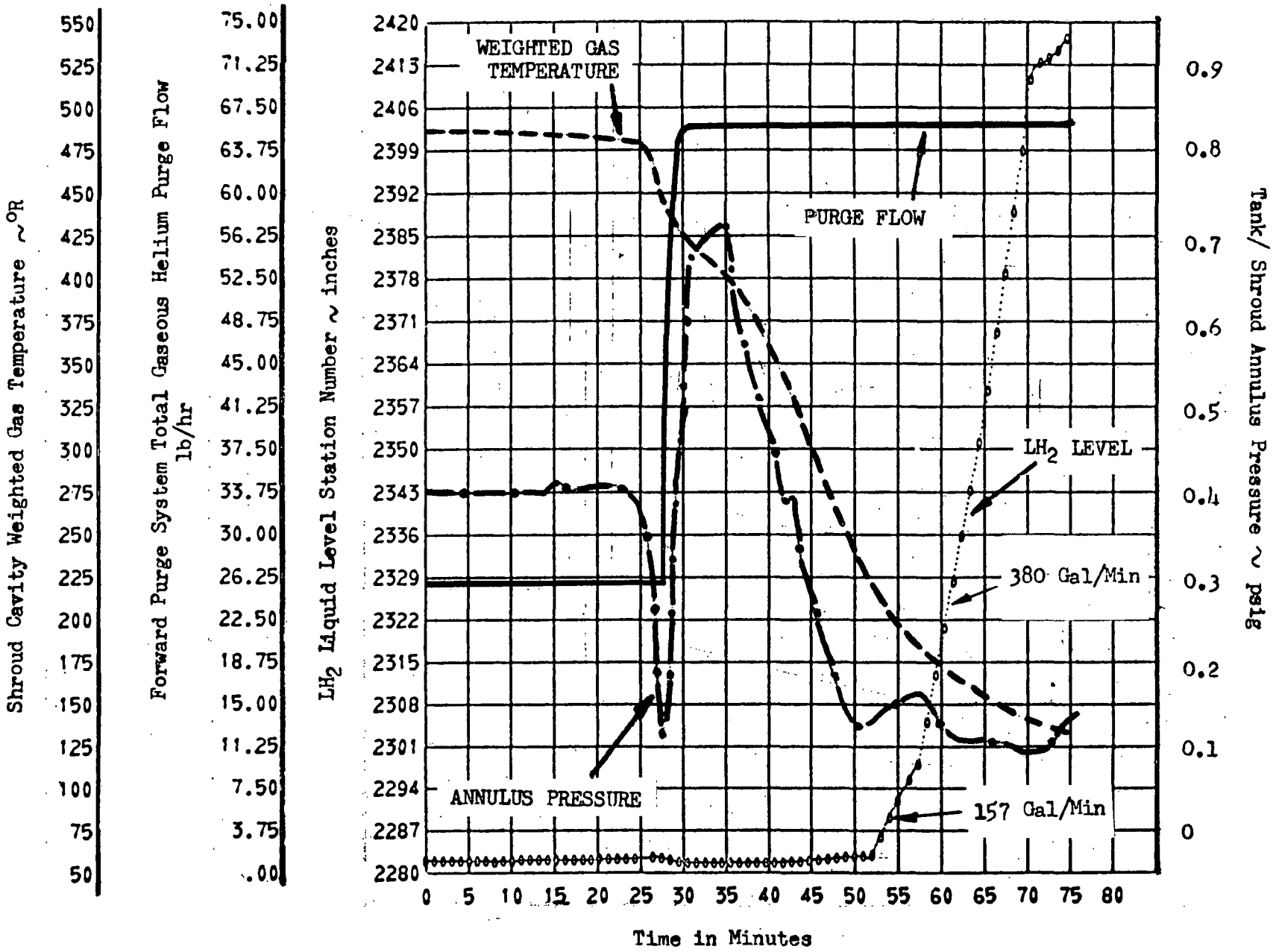

FIGURE IV-12 TANK/SHROUD ANNULUS PRESSURE DURING SECOND HYDROGEN TANKING FOR CRYOGENIC UNLATCH TEST NO.3

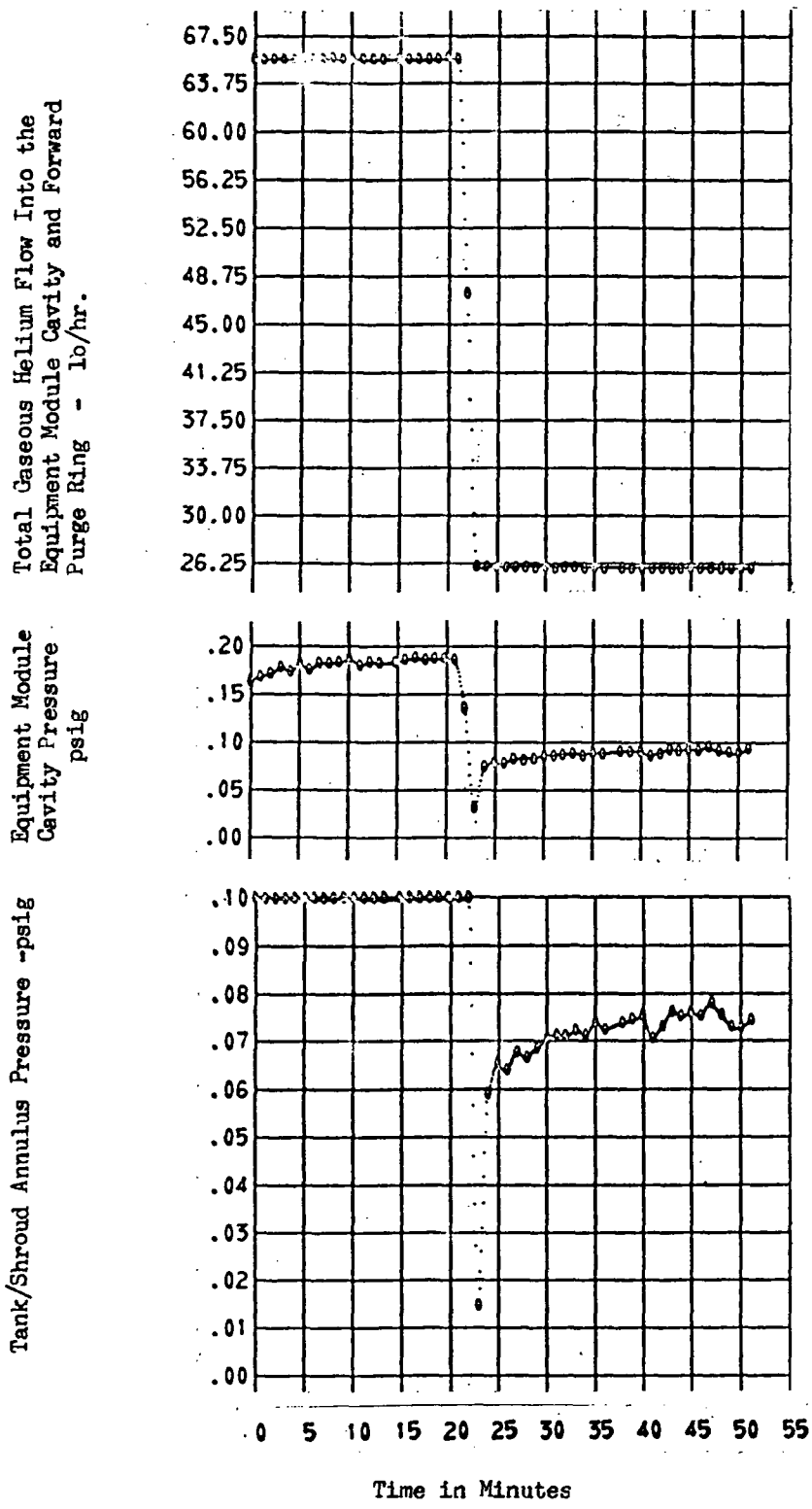

FIGURE IV-13 EFFECT OF CHANGING TANK/SHROUD ANNULUS PURGE FLOW ON EQUIPMENT MODULE AND ANNULUS PRESSURES. DATA FROM CSS CRYOGENIC UNLATCH TEST NO. 3

V. SHROUD/CENTAUR TEMPERATURE PROFILES AND HARDWARE THERMAL ENVIRONMENTS

by A. Fortini

SUMMARY

In order to determine the thermal performance of the Centaur Standard Shroud (CSS) during launch-hold conditions, thermocouples were strategically located about the CSS and the Centaur tank systems. Definition of temperature profiles, temperature distributions, and thermal environments were the objectives of the selected thermocouple locations. Instrumentation was placed in the following areas:

a. Equipment module/equipment area

b. Shroud tank section

c. Fill and drain chute

d. Shroud aft bulkhead and insulation

e. Centaur destruct box

f. Boattail area

By use of the above instruments, and as noted in Section VI, a helium purge circulation pattern about the tank section insulation was detected. Modification to the insulation design resulted in qualification of the shroud flight thermal system.

TEST METHODOLOGY

During each cryo-unlatch test, a series of LH_2 boil-off tests were made to determine the Centaur LH_2 tank heating rate. The criteria used for obtaining comparative data during each of the boil-off tests was to report all the data when the liquid level in the tanks was at the same height (LH_2 volume = 1141 $\pm$ 9 ft^3, LO_2 volume = 123 $\pm$ 12 ft^3) for each of the boil-off tests. In addition, only the first boil-off test of each cryo-unlatch was considered as a valid simulation of the two hour launch-hold requirement.

Data from other boil-off tests at the same tank liquid level as noted above are also reported. The objective is to study the effects of certain system variables; e.g., forward and aft seal warming purges, boattail purge, tank annulus purge, etc.

Finally, data during autosequence or during LH_2 detanking is reported in order to compare minimum temperatures of system components with design specifications.

TEMPERATURE PROFILES, DISTRIBUTIONS, AND THERMAL ENVIRONMENTS

Equipment Module/Equipment Area

As described in Section I, the equipment module/equipment area consists of:

a. Forward seal

b. FSR releaser blocks

c. FBR's

d. Shroud forward bulkhead

e. H_2 vent system insulation and Centaur forward bulkhead insulation

Forward Seal: The seal and its environment temperatures were measured at each quadrant axis in order to determine the heat transfer through the seal and to make a comparison with the design specifications. The heat transfer results are reported in Section VI.

A schematic of the seal assembly and the associated thermocouples is shown above Table V-1. The temperatures reported in Table V-1 are the minimum temperatures attained during all boil-off tests during cryo-unlatch tests as well as the LH_2/LN_2 tanking and forward seal release test.

As the test program developed, additional thermocouples were added for determination of temperature uniformity around the CSS and to detect leakage past the forward seal and/or the forward bulkhead split line seal area. The areas for additional instrumentation were at the 0^o and 270^o azimuth as shown in Table V-1.

A study of Table V-1 indicates that for cryo-unlatch test no. 1, the seal temperature was relatively warm. This fact can be attributed to the helium purge gas circulation pattern as stated in Section VI. For cryo-unlatch test no. 2, the seal temperatures were much colder than test no. 1 even though the helium circulation pattern still existed. These low temperatures were due to ice and frost formation upon the seal surface because the test was conducted during a rain storm and water entered the shroud equipment area; in addition, excessive leakage past the seal contributed to lowering the seal temperature.

With the added insulation as described in Section VI, the seal temperatures during the LH_2/LN_2 test were somewhat warmer even with seal leakage at the 0^o and 180^o azimuths. When the leakage was minimized, Table V-1 shows the seal temperatures to be much warmer.

Even though the seal and its environment temperatures were lower than the design specifications, the seal material maintained its structural integrity.

From the results of Table V-1 and the discussion above, the conclusions reached for the flight vehicle configuration are:

a. The air conditioning of this assembly must provide a sufficient quantity of dry, warm GN_2 (or air) to maintain a positive pressure above ambient in order to prevent rain and/or humid air from entering this area.

b. Leakage past the forward bulkhead split seal and the seal perimeter must be held to a minimum.

If these conditions are met, the heat leak through the forward seal will be less than 4,000 BTU/hr.

Table V-2 presents the forward seal assembly temperatures during the first boil-off tests for each of the cryo-unlatch tests. The liquid level in the tanks is about the same for these tests and the purge flows are as given in Table VI-2.

By comparing the temperatures of Table V-2 with those of Table V-1, the results show the seal temperatures in Table V-2 to be slightly warmer than those in Table V-1. This is expected because the temperatures of Table V-1 are minimums which occurred when the warming purge was off and the forward annulus purge flow was set for minimum requirements. The important conclusion from this comparison is that the heat transfer through the seal is not a strong function of the helium purge flow rates.

Forward Seal Releaser Blocks and FBR's: The temperatures of these components were measured for comparison purposes with design specifications ($360^{o}F$) for the pyrotechnics. The releaser blocks and FBR clevis attained a minimum temperature of $389^{o}R$ and $442^{o}R$, respectively.

Shroud Forward Bulkhead: A schematic of the bulkhead and the seal ring along with thermocouple locations is shown above Table V-3. This table presents the temperatures at the same liquid levels during the first boil-off tests for each of the three cryo-unlatch tests.

The data show that the added insulation (test no. 3 data) reduced the internal temperature significantly which again indicates the purge gas circulation had been eliminated. Although circulation existed during tests nos. 1 and 2, the lower temperatures occurred for test no. 2. This result was again due to the frost and ice formation upon the bulkhead because of the rain entering the shroud as explained previously.

A closer examination of the data indicates that annulus purge gas leakage occurred at the 180^{o} split seal during all tests. This fact is obvious by comparing the temperature difference between G and J at 180^{o} and 270^{o} for a test and comparison from test to test. Also, by comparison with E and the resulting temperature difference of A, B, C, and D with E, the data show temperature E decreased and the various temperature differences increased from test no. 1 to test no. 3 because the added insulation reduced the purge gas circulation.

From the above discussion and the results of Table V-3, the conclusions reached for the launch site conditions are the same as mentioned for the forward seal. If these conditions are met, the heat leak through the forward bulkhead and tank shroud seal ring will be less than 5,000 BTU/hr.

H_2 Vent System: The H_2 tank flight vent system, its insulation, and thermocouple locations are shown schematically above Table V-4. The table lists the temperature reading for the three tests having the same conditions of tank liquid level but at different purge flow rates.

For the first test, the exit orientation of the purge tube caused the purge gas to impinge against the equipment module bulkhead and thereby bypassing the insulation blanket. This conclusion was reached by comparing temperatures B, C, E, and F of test no. 1. For test no. 2 and no. 3, the orientation of the exit was altered and the purge flow rate was reduced to 4 lbs/hr. from 12 lbs/hr. As noted in the table, temperature B increased but temperature E decreased significantly. In addition, by comparing the temperature difference between B and C for each test, the temperature drop is in the correct direction. This cannot be said for E and F. Finally, comparing the increase of the venting H_2 gas temperature (D and A), indications are that no heat is being added to the venting H_2 gas via the venting duct wall and surrounding insulation.

The conclusions reached for this insulation system are:

a. The vent valve area causes an unbalanced circulation pattern of the purge gas which is difficult to explain, and

b. The insulation around the vent duct is adequate.

Because of the complexity of this thermal system, no attempt was made to calculate the heat leak into the tank. Instead, direct measurement of the leak was made through boil-off measurements (see Section VI).

Centaur Forward Bulkhead: Depicted in the figure above Table V-5 is shown the insulation system for the Centaur forward bulkhead. It consists of a multi-layer Mylar blanket laid against the tank bulkhead and purged with the same helium gas as discussed in the flight H_2 vent system. Here again, the purge flow was high for test no. 1 and low for nos. 2 and 3, and the liquid level in the tank was the same for all three tests.

At the high purge flow rate, the exit gas temperature, A, was $10^{\circ}R$ higher than its inlet temperature, F. Such results indicated that the gas picked up heat from the equipment module, and did not impregnate the blanket. This conjecture is substantiated by the data of Table V-5 as follows:

a. Average temperatures of the equipment module bulkhead (L, M, and N) is $408^{\circ}R$.

b. The average temperature of the purge gas is $374^{\circ}R$.

c. Average temperature of the external surface of the blanket (C, E, H, K) is $349^{\circ}R$.

d. Compare the temperature difference between equipment module bulkhead average temperature and the average temperature of the purge gas (difference is 34°R) with that of the temperature difference between the average temperature of the purge gas and the average temperature of the blanket surface (25°R).

e. Surface area of the module is larger than the blanket surface.

f. Conclusion: more heat is transferred to the gas than the gas can transfer to the blanket because of the smaller temperature driving potential and the smaller surface area.

All temperatures of Table V-5 were recorded when the liquid level was at station no. 2448 in order to observe the temperature gradients across and along the thermal system. These gradients indicate the heat path into the ullage and into the liquid.

The heat flow into the liquid via conduction potential of the Centaur forward bulkhead skin can be seen by noting the temperature differences between D and B, G and J, and the fact that the skin is thin. The resulting small temperature difference, the long heat path to the liquid, and the small skin cross-section area which the heat must travel through indicates a low heat leak into the liquid.

Longitudinal and transverse gradients of the multilayer Mylar can be computed from the table. The data show that the longitudinal gradients are small when compared to the transverse gradients. Considering the large transverse gradients (approximately 250°R) and the fact that the thermal conductivity of the blanket is that of helium because of impregnation, the resulting heat flow through the blanket is small.

The amount of enthalpy entering the liquid from the helium purge gas can be computed from the recorded data. For test no. 3, the temperature change of the gas is 97°R and the gas flow rate was 3.5 lbs/hr. as stated in Table VI-2 giving a heat flow into the tank of 421 BTU/hr.

Indications are that the major heat leak into the liquid hydrogen from this thermal system occurs through the equipment module bulkhead, traveling down through the stub adapter and entering the tank at station no. 2434.60.

Since this is a very complicated system to accurately predict the heat leaks because of unknowns, i.e., actual blanket thickness, gas flow characteristics within and surrounding the blanket, the thermal contact resistance between the tank bulkhead and blanket, and the temperature profile of the ullage gas, the sum total heat leakage was determined experimentally as explained in Section VI.

In attempting to analytically predict component heat leaks of this system, it should be noted that the data of test no. 2 were affected by the frost and ice upon the equipment module bulkhead.

From the data and the above discussion, the conclusions are:

a. Purge gas flow rates greater than 4.0 lbs/hr. are not required.

b. The stub adapter attachment at station no. 2434.6 is a heat leak path into the hydrogen tank.

c. The heat flow through the insulation blanket is small.

son.

Considering this data, the boil-off data, and the analysis as discussed in Section VI along with the data of this section, the boil-off rate attributed to the insulation system for the H_2 vent system, Centaur forward bulkhead, and stub adapter should be less than 22,000 BTU/hr. for the two hour launch-hold conditions.

Shroud Tank Section

This thermal insulation system is shown schematically in Figure VI-1 except for:

a. The added insulation between "Z" ring as required in test no. 3 to prevent the purge gas circulation.

b. The fill and drain chute.

c. The Centaur destruct box unit

d. Super-Zip

CSS Tank Section: As explained in Section VI, this thermal system had to be modified because of the helium purge gas circulation pattern within the shroud cavity not complying to the design model. This fact was obvious by noting the ice and frost formation pattern on the shroud skin, and the measured temperature profiles and distribution of the various components of the thermal system. These profiles and distributions are shown in Figures V-1 and V-2.

Plotted on the figures are the temperatures at four azimuths (0^o, 90^o, 180^o, and 270^o) for each component (tank, radiation shield, annulus gas, inboard insulation surface, outboard insulation surface, and shroud skin) and at longitudinal locations along the shroud axis. Also shown is the hydrogen liquid level in the tank at the time of data recording and is common to all data presented in the figure.

Figure V-1 is for test no. 1. No figure is presented for test no. 2 since the "quick type" modification to the circulation pattern, as mentioned in Section VI, was not successful and resulted in the same profiles and distributions as in Figure V-1.

The variations in the circumferential distribution of a component at a station is depicted by the data spread at that station. The temperature gradient through the system (from skin to tank) at any station is also depicted. Finally, the figures show the longitudinal temperature gradient for each component.

A detail study of Figure V-1 does show a flow circulation pattern of the purge gas. Considering first, the longitudinal temperature gradients of each component; second, consider the radial temperature gradient across the system; and finally, the circumferential distribution of a component.

Starting with the tank wall as a constant longitudinal boundary of $40^{o}R$ and noting the large temperature difference between the radiation shield and the tank, the decreasing difference shows that a downward gas flow exists between the tank and the radiation shield. This gas temperature was not measured during the tests. Also, the gradual longitudinal temperature profile of the radiation shield shows the gas not to be stagnant nor laminar free convection. Such a gas condition would result in a steep gradient from the aft seal area to the stub adapter interface area. At the interface juncture, the curve should then bend rapidly toward higher tempeatures.

From the longitudinal temperature profile of the gas and the gas being colder than the radiation shield at the forward end along with the fact of the inboard insulation temperature is nearly the same as the radiation shield temperature, indications are that two discrete large circulation flow fields exist within the shroud tank gas annulus. In order for the gas to be colder than its containing boundaries, a cold gas must be pumped into and mixed with the entering gas. This condition does exist by the shearing action of two or more adjacent toriodal vortexes having different energy levels and depicted in Figure VI-3.

The outboard insulation longitudinal temperature profiles indicate a stronger upward circulation flow at the 180^{o} azimuth than at the 0^{o} or 270^{o}. Since the shroud skin "Z" rings were not continuous at the 0^{o} and 180^{o} because of the longitudinal Super-Zip, a non-restrictive flow channel existed at 0^{o} and 180^{o}; whereas, at 90^{o} and 270^{o} the "Z" ring and its many venting holes cause some flow restriction. Therefore, there should be a steeper slope in the profiles for the 0^{o} and 180^{o} azimuth. The data do show this when the 0^{o} and 270^{o} azimuths are compared; but the data show a much steeper slope for the 180^{o} than for the 0^{o} azimuths. This is explained by the leakage of cold purge gas through the 180^{o} aft split seal and aft bulkhead insulation. This leakage was detected during the pressure check tests of the shroud cavity made before the test.

Since the shroud skin longitudinal temperature profile is not vertical and shows a convergence tendency toward the outboard insulation profile at the forward end, this shows that the cold gas at the aft end is picking up heat from the skin, rising in temperature, and flowing toward the forward end. Also, the data show that the severe leak at 180^{o} caused the skin temperature to be very cold.

In summary of Figure V-1, the data show a complex and interacting purge gas circulation flow field within the shroud tank annulus which bypasses the effectiveness of the radiation shield and insulation batting. In addition, severe leakages are detrimental to this thermal system.

By fully packing insulation between the outboard side of the original insulation batting and the skin and sealing the aft end of the radiation shield, the temperature profiles, gradients, and distributions were much improved during test no. 3. This is depicted in Figure V-2 and emphasized by comparison with the data of Figure V-1.

In light of the discussion of Figure V-1, Figure V-2 shows no major existence of purge gas flow circulations around the radiation shield nor between the outboard side of the original insulation batting and the skin. However, the data do indicate two or more minor vortex circulation patterns in the foward end of the tank shroud gas annulus. Also, the skin temperature profile for 180^{o} azimuth again indicates a purge gas leak but not as severe as depicted in Figure V-1.

Note the variation in circumferential distribution of temperatures near the stub adapter interface and the aft seal area. The variation at the interface area is due to mixing of the colder equipment module purge with the foward annulus purge gas; the variation near the aft seal area is the result of mixing the warm purge gas from the Centaur destruct box with the cold annulus gas.

From the data of this figure, calculations show that the heat flow into the tank from the helium purge gas and through the shroud skin are 21,000 BTU/hr. and 38,200 BTU/hr., respectively.

The conclusions reached from the data of these two figures are:

a. Qualification of the shroud for the two hour launch hold required additional insulation in the shroud skin cavities and sealing the aft end of the radiation shield.

b. Purge gas leakage is to be minimal.

c. The total purge flow should be 52 lbs/hr.

From the above data, the heat flow through this system should be less than 60,000 BTU/hr. at the launch pad during the two hour hold.

Fill and Drain Chute: This chute system serves a dual purpose; the line to fill or drain the H_2 tank passes through this chute on the flight vehicle, and the tank shroud purge gas vents through this chute via an adjustable purge vent valve attached to the chute wall. A schematic of the system is shown above Table V-6. Also shown schematically is a system for rapidly venting the tank shroud annulus that was installed where the flight fill line goes. The method of preventing ice formation within the chute via a helium warming purge is also shown.

Table V-6 presents the temperature distribution for various component parts of this system during the three tests wherein the liquid tank levels were the same.

The data show the components to be colder for test no. 2 than for test no. 3. Since test no. 2 occurred during a rain storm, the chute frontal area

became heavily iced and frosted resulting in lowering the internal temperature.

Test no. 3 again shows ice and frost to exist about the chute frontal area (compare temperatures A and F of test no. 2 with A and F of test no. 3). However, the total area was reduced (detected by TV cameras) because of the added insulation between the original insulation batting and the CSS skin.

All heat leaks for this system must pass through the aluminum surfaces of the chute boundary. Considering the data of test no. 3 only and comparing temperatures A and F with C, D, and E, large temperature difference exists. By averaging A and F and subtracting the average of C, D, and E, the resulting temperature difference is 74°R. This possible heat leak driving potential of 74°R is removed by venting the tank shroud purge gas into the chute cavity and exiting through the ice bag surface. By this technique, the entering heat flow through the ice bag surface is absorbed by the entering purge gas and returned to its source by dumping the purge gas outside of the ice bag surface. Such a method of producing a heat flow barrier is known as transpiration or film cooling. The effectiveness of this method is shown in Table V-6 by noting the small temperature difference between temperature B and C or D or E. Because the temperature differences across the aluminum were small, no calculation for the heat leak was made.

The conclusions reached for this system are:

a. If possible, all cold purge gases should exit through the ice bag surface in order to buck the possible heat leak.

b. Ice and frost will form over and about the chute area.

Centaur Destruct and Destruct or Housing: Temperature distribution about this system is presented in Table V-7 along with a schematic. The destruct unit was heated by a helium purge gas which exited into the aft section of the tank shroud annulus between the tank radiation shield and the inboard surface of the insulation batting.

As mentioned previously, this exiting purge does cause a variation in the circumferential temperature distribution of the shroud thermal system.

Table V-7 shows for test no. 1 that the skin temperature of the destruct unit is the same as the surrounding purge gas temperature C, and that the insulation of the purge line is effective, i.e., temperature B is colder than C with only a 5°R difference while temperature A is at 513°R. Also, the heat leak (enthalpy change) into the shroud annulus may be computed by use of the listed temperature data A and C.

Due to the need of additional instrumentation for investigation of the circulation problem, temperatures B and D were moved to other locations for tests nos. 2 and 3.

Test no. 3 shows that the heat leak due to the purge gas warming the destruct unit is 1,394 BTU/hr. This heat leak is not expected to change at the launch site.

The conclusion reached for this system is that it is qualified for flight.

Super-Zip and Detonators: Minimum temperatures during all boil-off tests and at the time of all firings of the Super-Zip detonators are listed in Table V-8. Also shown in this table are the locations of the temperature measurements. In addition, the minimum design temperature specifications are listed. Finally, there are three temperatures which exceeded the recording system range; however, the environment may be estimated from Figure V-1.

Table V-8 shows that the actual temperatures of the detonator blocks during boil-off or at the time of firing were greater than the respective design temperature specifications. For the Super-Zip at the time of detonator firing, the actual temperatures were greater than the design specifications. During boil-off, the Super-Zip temperatures measured were greater than the design specification. However, in the aft bulkhead area purge gas leakage and purge gas circulation bypassing the insulation batting may have caused low temperatures, exceeding the design specification.

For the 0^{o} azimuth and at station no. 2256.78, the outboard temperature reads $279^{o}R$ and the inboard temperature is lower than minimum recording level of $272^{o}R$. Because of the Super-Zip cross section geometry, the inboard temperature should not be much different from the outboard temperature as substantiated by the data at station no. 2361.78. A good estimate of the temperature can be obtained from Figure VI-1 by assuming the longitudinal temperature profiles of the outboard insulation and skin for the 180^{o} azimuth were similar to the Super-Zip at 0^{o} azimuth. Therefore, the inboard Super-Zip temperature must be greater than $250^{o}R$ and does not exceed the minimum design temperature.

For the 180^{o} azimuth and at station no. 2256.78, the table shows the temperatures to be less than $272^{o}R$. Applying the same logic as for 0^{o} azimuth, the inboard and outboard temperatures could not exceed the lower design temperature limit of $140^{o}R$.

Finally, these low temperatures at station no. 2256.78 occurred in test no. 2 during the second and third boil-off tests when large amounts of ice were formed along the Super-Zip because of the rain storm. Now that the circulation pattern has been eliminated, these temperatures should be much higher and proved to be so by a simulated rain test during test no. 3.

From the data and the simulated rain tests, it can be concluded that the temperatures of the system are greater than the minimum design temperature specifications.

Aft Bulkhead Area

This area consisted of three major components: a flexible seal, an insulated bulkhead attached to the cylindrical part of the shroud, and an aft seal plate attached to Centaur tank.

Aft Seal Plate and Seal: A schematic of this thermal system is shown above Table V-9. Depicted are temperature measurement locations and the manner of retaining the flexible seal to the aft seal plate.

Table V-9 presents the temperature data during the first boil-off tests of each of the three cryo-unlatch tests. A comparison of the temperatures for test no. 3 with those of tests nos. 1 and 2, indicates that the added insulation to the shroud resulted in warmer temperatures for these components. However, temperature B at the 180° azimuth for test no. 3 is colder than the prior test. This lower temperature is the result of a split seal leak previously mentioned in the discussion of Figure V-2.

The effect of the warming purge exiting from the Centaur destruct box, altering the circumferential temperature distribution is shown in test no. 3; note that temperature B at the 0° azimuth is greater than all other circumferential temperatures.

Temperature C is located between the Centaur tank and its radiation shield. The vertical temperature profile through the aft seal plate is shown by temperatures C, D, and E. Although this profile is steep, the heat flow into the shroud tank annulus is small because of the minimal area for heat penetration through the plate. This heat flow rate was calculated to be 950 BTU/hr. ft^2.

From an average seal temperature and the weighted average annulus gas temperature, the computed heat flow rate should be 480 BTU/hr. ft^2.

The minimum temperature during all boil-off tests for the seal and interface fingers were 144°R and 86°R, respectively. The design temperature limits for the seal and interface fingers are 100°R to 580°R. Although the minimum specification was exceeded, the components functioned well.

CSS Aft Bulkhead: This component consisted of a reinforced and stiffened thin diaphragm to which mounting brackets were attached for support of insulation blankets. Reinforcement was accomplished by a hollow epoxy glass strut tying the inboard bulkhead flange to the cylindrical part of the CSS shroud.

A schematic of this component and the thermocouple locations are shown above Table V-10. The table presents temperature measurements at five azimuth locations during all three tests wherein the liquid level in the tanks are the same during each test.

An overview of the data again indicates the temperatures of tests nos. 1 and 2 were much colder than test no. 3; also, a temperature distribution comparison of test no. 1 with test no. 2 shows very little improvement and conclusively proves the "quick-fix" for prevention of purge gas circulation between insulation and CSS skin failed.

By observing the temperature differences at specific locations within the aft bulkhead area for tests nos. 1 and 2, the original insulation batting was ineffective because of the gas circulating between the batting and aft bulkhead and traveling upward between the batting and the CSS skin. The most severe indication of circulation occurs at 0° and 180° azimuths and at penetrations of the struts through the batting due to leak paths.

When additional insulation was placed between the batting and CSS skin and bulkhead (test no. 3), the temperature differences increased and, therefore, the circulation path was eliminated. However, the data indicate leakage at the 180° azimuth (see temperatures A, B, E, G, H, and I at 180° relative to other azimuths) due to a leak in the aft split seal.

A calculation of the heat transfer through the aft bulkhead shows the heat leak through this area amounts to 1250 BTU/hr.

Table V-11 is presented for the purpose of indicating the lowest temperatures attained for the various components of this thermal system when certain variables were changed; e.g., warming purge flow rates, shroud purge flow rates, simulated rain tests, etc. These data should not be used for heat transfer calculations because the data were not recorded at the same common time interval nor when the liquid level in the tanks were the same, and because of the long testing time (beyond two hours), much ice had formed on shroud skin. However, this data can be used for noting the severity of the circulation problem, its solution comparison, and the minimum temperatures for comparison with design specifications.

Boattail Area

The Centaur LOX tank, CSS shroud jettison springs, CSS shroud boattail, and the Titan interstage adapter were the components of this area. No insulation was applied to the LOX tank.

Temperatures were recorded of the internal areas and components for environmental reasons. Because of the exposed surface of the LOX tank, the boattail area is cold.

Table V-12 presents the measured temperatures within the boattail for tests nos. 1, 2, and 3. Here again, test no. 1 showed colder temperatures than test no. 3. Prior to test no. 2, venting holes within the boattail area were sealed in order to contain the warming purge gas. As noted from the temperature readings, the sealing did raise component temperatures while decreasing gas temperatures. For the actual flight configuration with the LOX tank being insulated, the components and environments will be much warmer than shown in Table V-12.

EFFECT OF AMBIENT ENVIRONMENT UPON VEHICLE TEMPERATURES AT LAUNCH SITE

Predictions of the heat transfer through the CSS shroud can now be made with a high degree of certainty based upon the tests at B-3. As stated in Section V, the highest heat leaks occur across the tank section of the shroud and by the helium purge gas. Assuming the forward and aft seal conditioning purge at the launch site have the same flow rates and temperatures, the heat leak through forward and aft bulkhead areas should be the same as in B-3 tests. In addition, the helium purge conditions of the shroud annulus should not be far different than those at B-3; therefore, the heat leak because of the helium purge should be very close (within 10 percent) of what was measured at B-3.

By use of the above assumption, a simple heat-transfer model can be made wherein a constant sink temperature of 40°R is used, an overall heat transfer coefficient, U, determined from cryo-unlatch test no. 3 is assumed constant, the shroud surface area is used, and the independent variable would be the skin temperature because of ambient conditions.

Figure V-3 gives a prediction of the heat leak into the LH_2 tank for various CSS skin temperatures. Also shown is a band for the expected variation of U because of emissivity of shroud surface and the change in film coefficients of purge gas being different than those of B-3 tests. Finally, plotted is the measured heat leak as determined from the boil-off test during cyro-unlatch test no. 3.

From Figure V-3, the heat rate is slightly sensitive to skin temperature but a 10 percent change in U causes a direct change of 10 percent in the heat rate. In addition, if the LH_2 propellant feed system was the same as those in B-3 configuration, Figure V-3 could be used as good prediction of the boil-off rate at the launch site. However, the configuration is much different and the air conditioning in the boattail section could not be simulated; therefore, the heat rate will be higher than shown in Figure V-3 and the expected rate is discussed in Section VI.

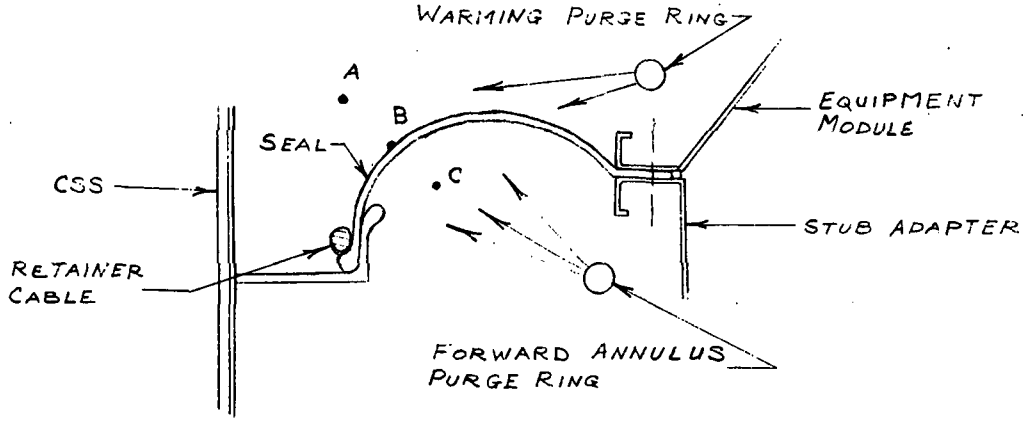

TABLE V-1 FORWARD SEAL MINIMUM TEMPERATURES, °R, DURING ALL BOILOFF TESTS

ITEM	TEST No. 1		TEST No. 2				LH_2 / LN_2				TEST No. 3				DESIGN
	AZIMUTH		AZIMUTH				AZIMUTH				AZIMUTH				
	180°	270°	0°	90°	180°	270°	0°	90°	180°	270°	0°	90°	180°	270°	
A	N/A	N/A	N/A	N/A	N/A	N/A	417	N/A	N/A	442	425	N/A	N/A	445	510
B	437	414	348	336	328	367	352	367	344	366	419	381	374	410	395
C	N/A	N/A	N/A	N/A	N/A	N/A	287	N/A	N/A	332	350	N/A	N/A	360	N/A

TABLE V-2 FORWARD SEAL TEMPERATURES, °R, DURING FIRST BOILOFF TESTS FOR CRYO-UNLATCH TESTS NO. 1, 2, & 3

ITEM	TEST No.1		TEST No. 2				TEST No. 3			
	AZIMUTH		AZIMUTH				AZIMUTH			
	180°	270°	0°	90°	180°	270°	0°	90°	180°	270°
A	N/A	N/A	N/A	N/A	N/A	N/A	447	N/A	N/A	449
B	438	416	359	337	330	378	420	384	378	416
C	N/A	N/A	N/A	N/A	N/A	N/A	370	N/A	N/A	369

N/A = NOT APPLICABLE

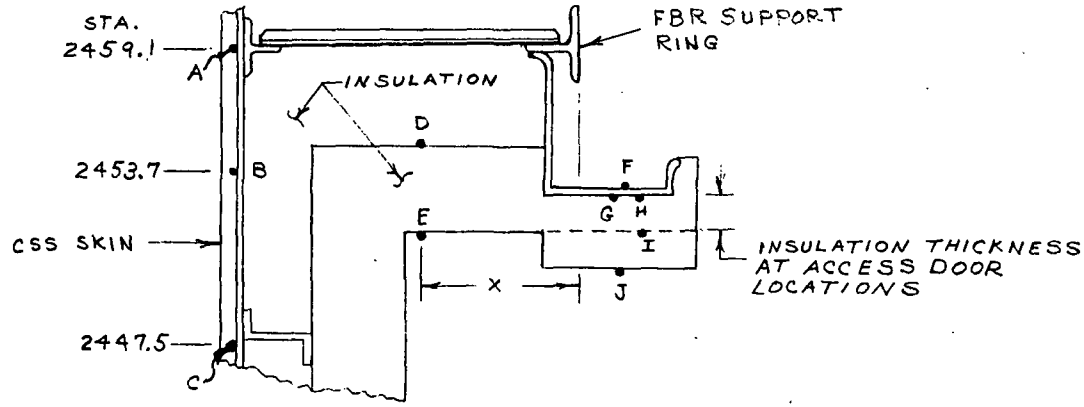

TABLE V-3 FOWARD BULKHEAD AND TANK SHROUD SEAL RING TEMPERATURES, °R, DURING FIRST BOILOFF TESTS FOR CRYO-UNLATCH TESTS No. 1, 2, & 3

ITEM	TEST No. 1 AZIMUTH				TEST No. 2 AZIMUTH					TEST No. 3 AZIMUTH					
	166°	180°	270°	300°	90°	166°	180°	270°	300°	0°	90°	166°	180°	270°	300°
A	N/A	N/A	506	N/A	N/A	N/A	N/A	493	N/A	N/A	N/A	N/A	N/A	483	N/A
B	↓	↓	510	↓	496	↓	↓	498	↓	↓	478	↓	↓	487	↓
C	↓	↓	N/A	↓	N/A	↓	492	N/A	↓	487	477	↓	482	N/A	↓
D	↓	495	485	↓	↓	↓	460	471	↓	N/A	N/A	↓	436	456	↓
E	↓	434	442	↓	↓	↓	404	405	↓	↓	↓	↓	355	385	↓
F	↓	N/A	N/A	↓	↓	↓	N/A	N/A	↓	↓	419	392	410	422	422
G	↓	426	441	↓	↓	↓	387	410	↓	↓	N/A	N/A	407	405	N/A
H	442	N/A	N/A	446	↓	428	N/A	N/A	422	↓	↓	389	N/A	N/A	415
I	401	↓	↓	430	↓	362	↓	↓	413	↓	↓	356	↓	↓	371
J	N/A	426	408	N/A	↓	N/A	363	360	N/A	↓	↓	N/A	392	349	N/A
X	↓	3.0"	2.0"	↓	↓	↓	3.0"	2.0"	↓	↓	↓	↓	3.0"	2.0"	↓

N/A = NOT APPLICABLE

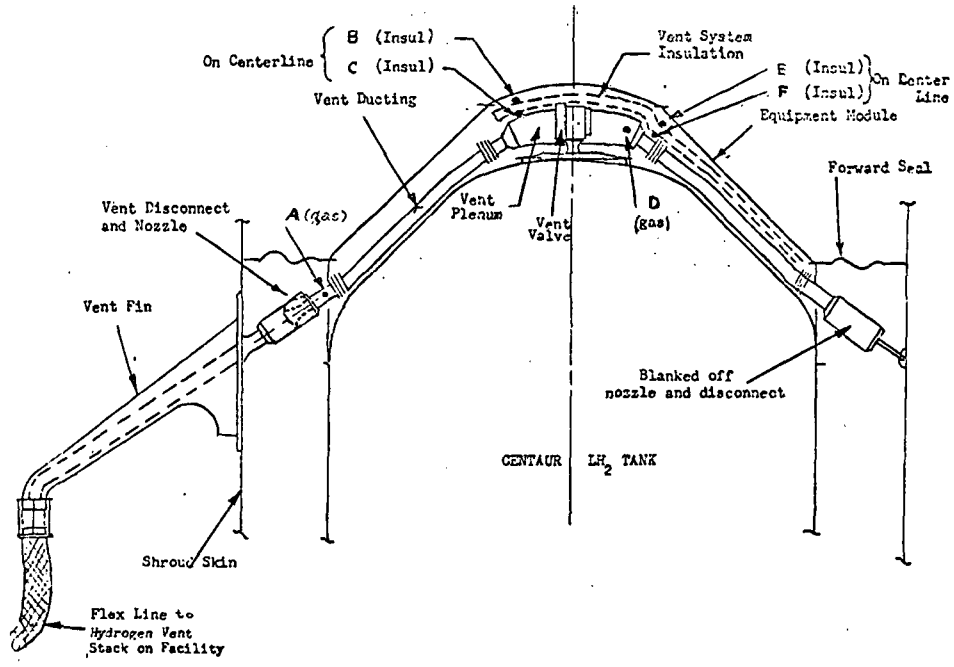

TABLE V-4 H_2 TANK FLIGHT VENT SYSTEM INSULATION TEMPERATURES, °R, DURING FIRST BOILOFF TESTS FOR CRYO-UNLATCH TESTS NO. 1, 2, & 3

ITEM	TEST No.1	TEST No.2	TEST No.3
A	45	43	48
B	378	417	400
C	91	76	81
D	44	42	47
E	364	74	67
F	247	78	105

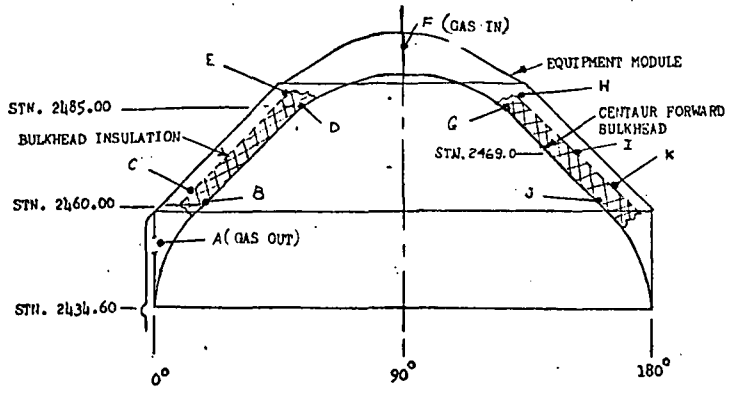

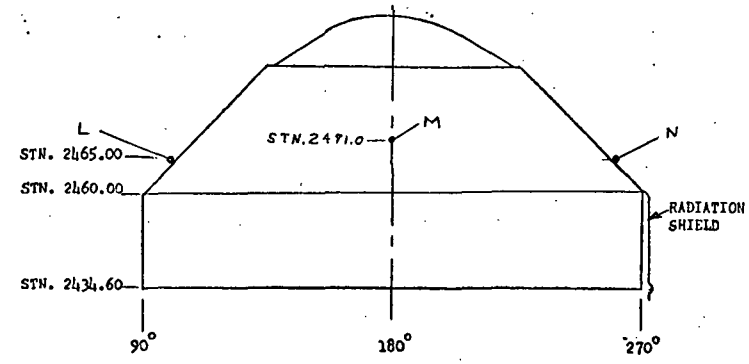

TABLE V-5 FORWARD BULKHEAD INSULATION AND EQUIPMENT MODULE SKIN TEMPERATURES, °R, DURING FIRST BOILOFF TESTS FOR CRYO-UNLATCH TESTS NO. 1, 2, & 3

ITEM	TEST No. 1	TEST No. 2	TEST No. 3
A	379	334	344
B	77	69	74
C	304	290	307
D	91	96	99
E	364	372	363
F	369	458	441
G	91	92	94
H	371	359	340
I	370	312	322
J	80	76	77
K	357	289	308
L	417	402	425
M	408	416	415
N	400	386	426

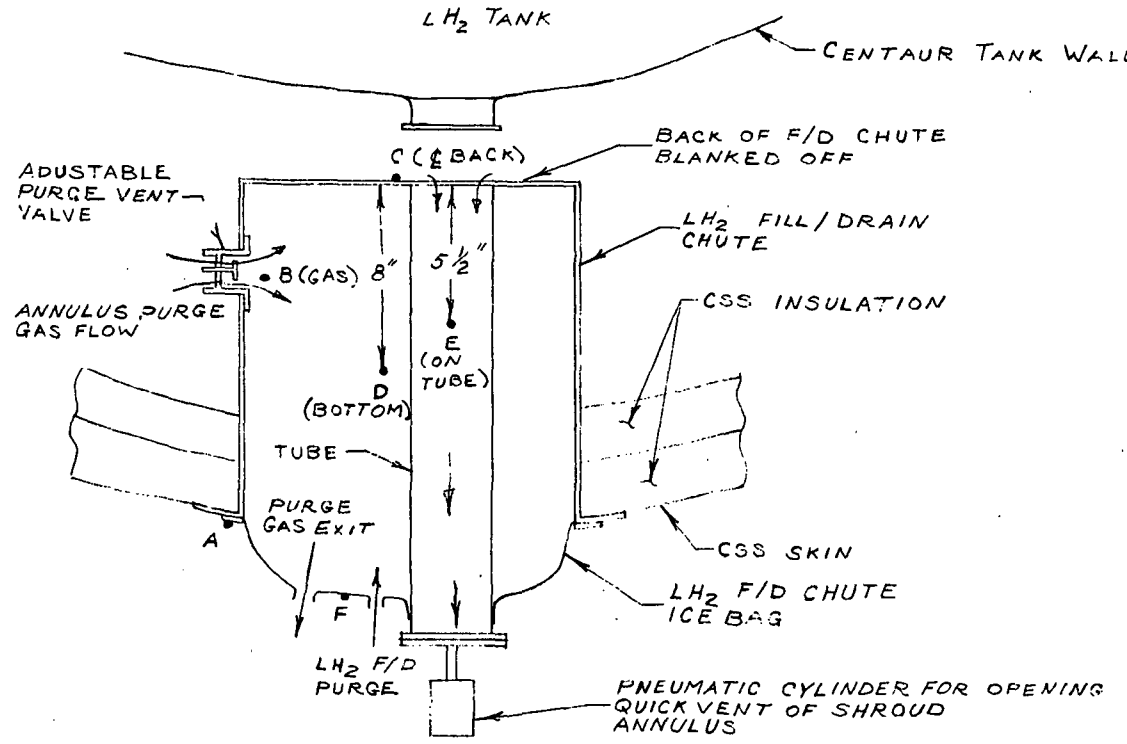

TABLE V-6 FILL / DRAIN CHUTE TEMPERATURES, °R, DURING FIRST BOILOFF TESTS FOR CRYO-UNLATCH TESTS No. 1, 2, & 3

ITEM	TEST No. 1	TEST No. 2	TEST No. 3
A	NG	256	257
B	237	140	160
C	N/A	144	155
D	N/A	136	146
E	N/A	142	162
F	N/A	180	199

N/A = NOT APPLICABLE
NG = NO GOOD

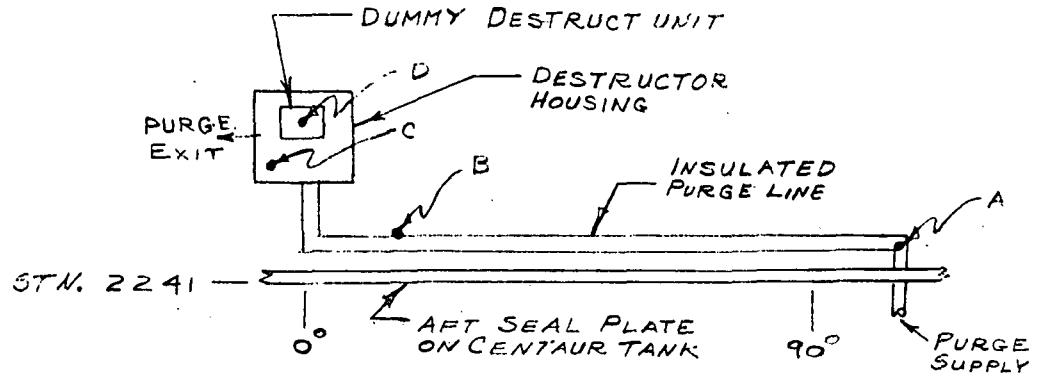

TABLE V-7 CENTAUR DESTRUCTOR SYSTEM TEMPERATURES, °R, DURING BOILOFF TESTS FOR CRYO-UNLATCH TESTS NO. 1, 2, & 3

ITEM	TEST NO 1	TEST NO 2	TEST NO 3
A (GAS)	513	489	483
B (LINE)	462	N/A	N/A
C (GAS)	467	444	446
D (SKIN)	468	N/A	N/A

N/A = NOT APPLICABLE

TABLE V-8 DETONATOR BLOCK & SUPER ZIP MINIMUM TEMPERATURES, °R, DURING ALL BOILOFF TESTS AND AT TIME OF ALL FIRINGS

ITEM & STATION NO.	DESIGN		0° AZIMUTH		180° AZIMUTH	
	BOILOFF	FIRING	BOILOFF	FIRING	BOILOFF	FIRING
DETONATOR BLOCKS @ 2215	210	340	451	436	365	368
SUPER ZIP INBOARD @ 2233	140	260	302	346	289	354
" " " @ 2361.78	↓	↓	456	469	386	413
" " OUTBOARD @ "			450	460	390	417
" " INBOARD @ 2256.78			<272	312	<272	284
" " OUTBOARD @ "			279	312	<272	279

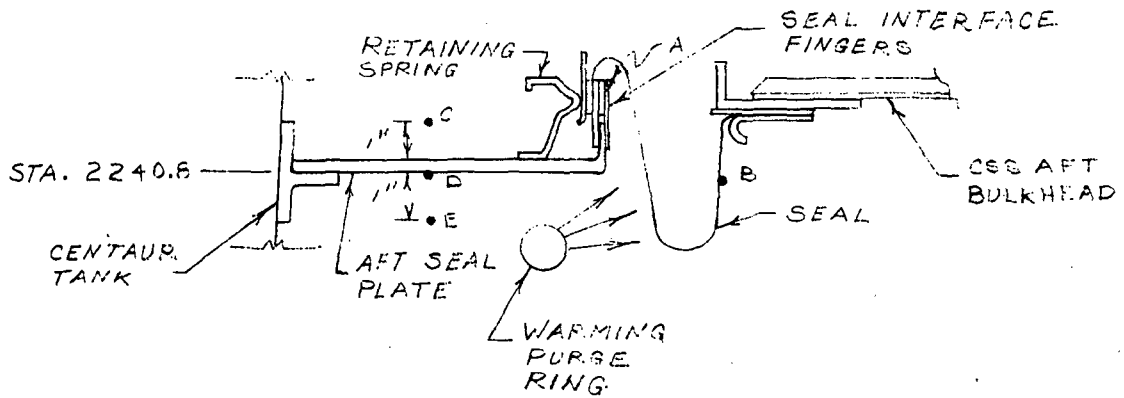

TABLE V-9 AFT SEAL PLATE AND FLEXIBLE SEAL TEMPERATURES, °R, DURING FIRST BOILOFF TESTS FOR CRYO-UNLATCH TESTS NO. 1, 2, & 3

ITEM	TEST NO. 1		TEST NO. 2				TEST NO. 3			
	AZIMUTH		AZIMUTH				AZIMUTH			
	180°	270°	0°	90°	180°	270°	0°	90°	180°	270°
A	105	133	N/A	N/A	120	192	N/A	N/A	140	N/A
B	257	288	267	335	302	267	383	375	193	362
C	N/A	N/A	N/A	N/A	N/A	N/A	N/A	N/A	N/A	120
D	↓	↓	↓	↓	↓	↓	↓	↓	↓	326
E	↓	↓	↓	↓	↓	↓	↓	↓	↓	396

N/A = NOT APPLICABLE

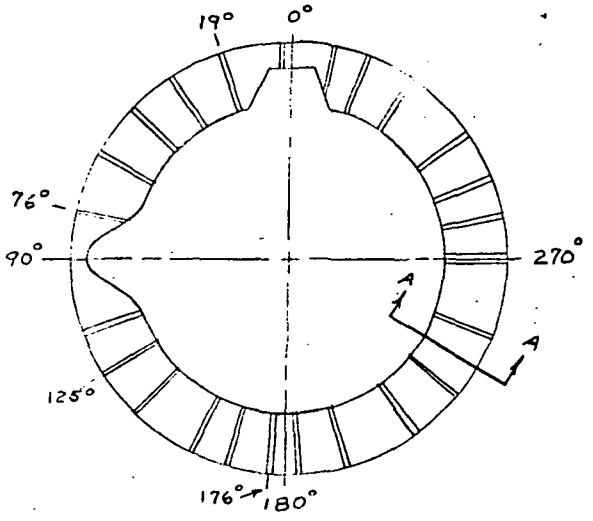

VIEW LOOKING AFT

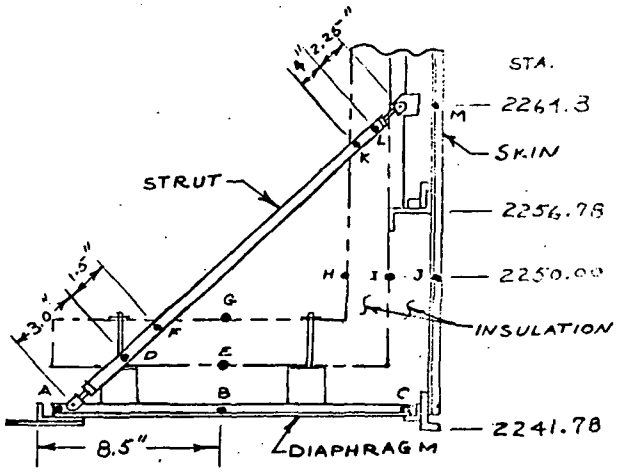

SECT A-A

CSS AFT SEAL AREA

TABLE V- TEMPERATURE, °R, DISTRIBUTION DURING FIRST BOILOFF TESTS FOR CRYO-UNLATCH TESTS NO. 1, 2, & 3

ITEM	TEST NO.1		TEST NO. 2					TEST NO. 3				
	AZIMUTH		AZIMUTH					AZIMUTH				
	176°	270°	19°	76°	125°	176°	270°	19°	76°	125°	176°	270°
A	164	224	N/A	N/A	N/A	194	278	340	298	N/A	196	N/A
B	N/A	N/A	↓	↓	↓	N/A	N/A	372	358	367	241	371
C	250	N/A	↓	↓	↓	273	N/A	422	N/A	N/A	N/A	N/A
D	N/A	115	↓	111	↓	137	134	N/A	N/A	N/A	N/A	236
E	133	229	158	N/A	299	150	281	328	254	310	171	296
F	N/A	108	N/A	↓	N/A	N/A	109	N/A	N/A	N/A	N/A	N/A
G	105	111	116	↓	115	106	111	133	109	119	115	119
H	N/A	N/A	N/A	↓	N/A	N/A	N/A	150	120	110	121	133
I	↓	↓	↓	↓	↓	↓	↓	215	412	257	266	462
J	↓	↓	↓	↓	↓	↓	↓	464	452	462	425	464
K	111	113	↓	↓	↓	↓	166	N/A	N/A	N/A	N/A	N/A
L	120	168	↓	430	↓	234	434	↓	↓	↓	N/A	325
M	315	382	↓	485	↓	331	493	↓	480	↓	406	476

N/A - NOT APPLICABLE

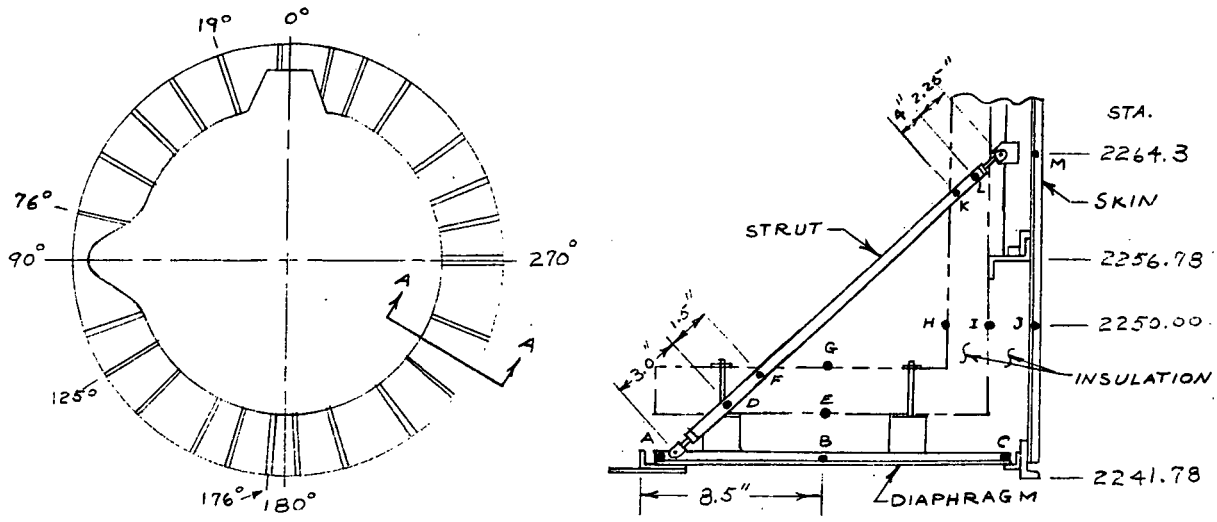

CSS AFT SEAL AREA

TABLE V-11

MINIMUM TEMPERATURE, °R, DISTRIBUTION DURING ALL BOILOFF TESTS FOR CRYO-UNLATCH TESTS NO. 1, 2, & 3

ITEM	TEST No.1		TEST No. 2					TEST No. 3				
	AZIMUTH		AZIMUTH					AZIMUTH				
	176°	270°	19°	76°	125°	176°	270°	19°	76°	125°	176°	270°
A	164	210	N/A	N/A	N/A	155	260	319	280	N/A	166	N/A
B	N/A	N/A	↓	↓	↓	N/A	N/A	354	337	357	210	354
C	250	N/A	↓	↓	↓	243	N/A	399	N/A	N/A	N/A	N/A
D	N/A	113	↓	103	↓	115	125	N/A	N/A	N/A	N/A	222
E	133	220	131	N/A	271	122	268	313	236	309	151	278
F	N/A	107	N/A	↓	N/A	N/A	103	N/A	N/A	N/A	N/A	N/A
G	105	110	109	↓	109	97	105	129	107	118	110	115
H	N/A	N/A	N/A	↓	N/A	N/A	N/A	128	118	107	116	128
I	N/A	N/A	↓	↓	↓	↓	↓	182	399	286	259	417
J	N/A	N/A	↓	↓	↓	↓	↓	409	437	461	422	419
K	111	112	↓	↓	↓	↓	129	N/A	N/A	N/A	N/A	N/A
L	120	168	↓	394	↓	164	419	↓	↓	↓	N/A	293
M	315	369	↓	433	↓	273	487	↓	478	↓	409	447

N/A = NOT APPLICABLE

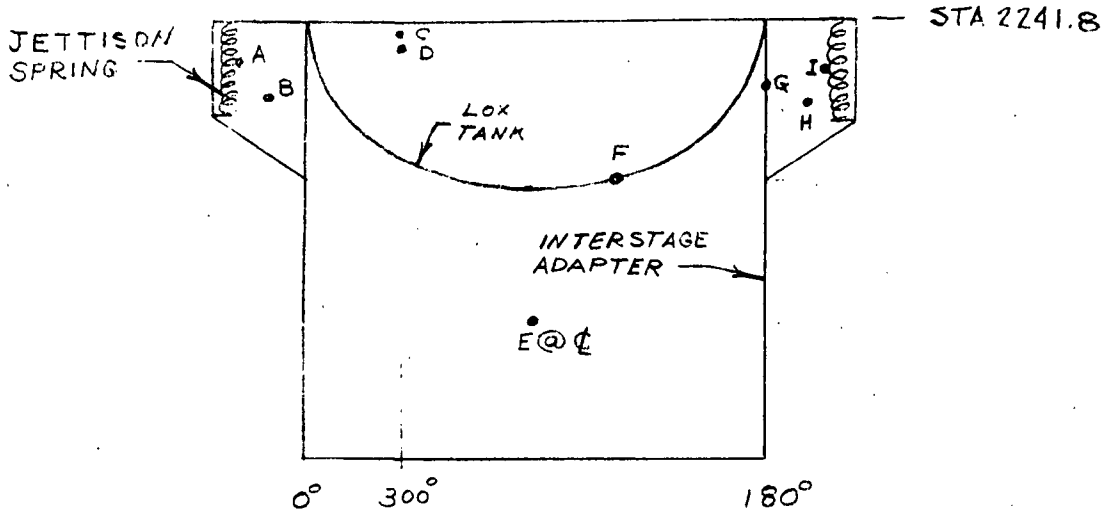

TABLE V-12 TEMPERATURE, °R, DISTRIBUTION IN BOATTAIL AREA DURING BOILOFF TESTS FOR CRYO-UNLATCH TESTS No. 1, 2, & 3

ITEM	TEST No.			STATION LOCATION
	1	2	3	
A (SPRING)	N/A	428	N/A	MID-COIL
B (GAS)	459	412	412	2197.2
C (ADAPTER SKIN)	351	361	363	2234.8
D (ADAPTER SKIN)	368	389	380	2230.8
E (GAS)	461	398	350	2142.0
F (TANK SKIN)	159	N/A	N/A	2180.5
G (ADAPTER SKIN)	342	394	393	2220.8
H (GAS)	282	399	405	2197.2

N/A = NOT APPLICABLE

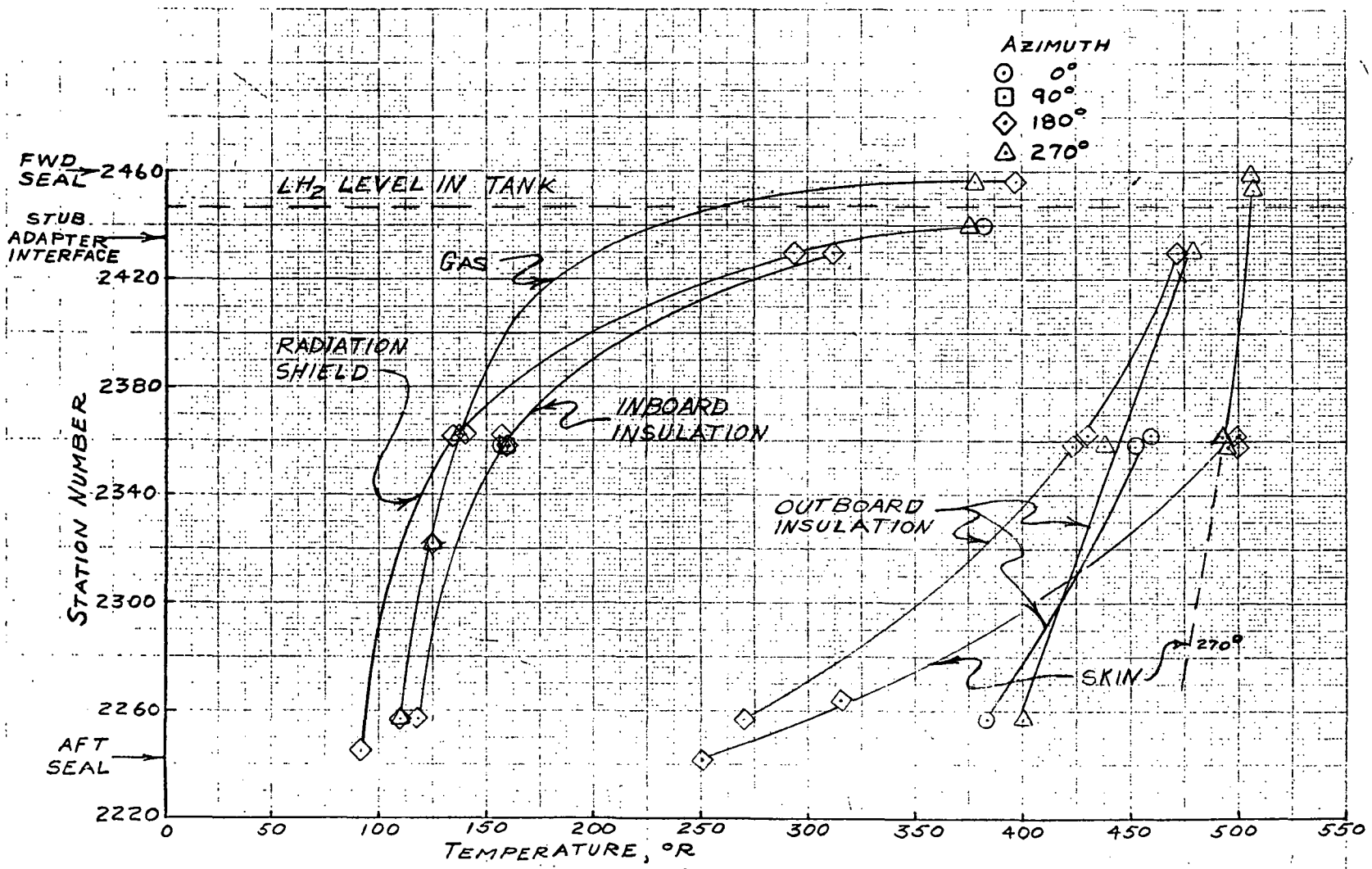

FIGURE V-1 TEMPERATURE PROFILES, CRYO-UNLATCH 1, BOILOFF TEST 1

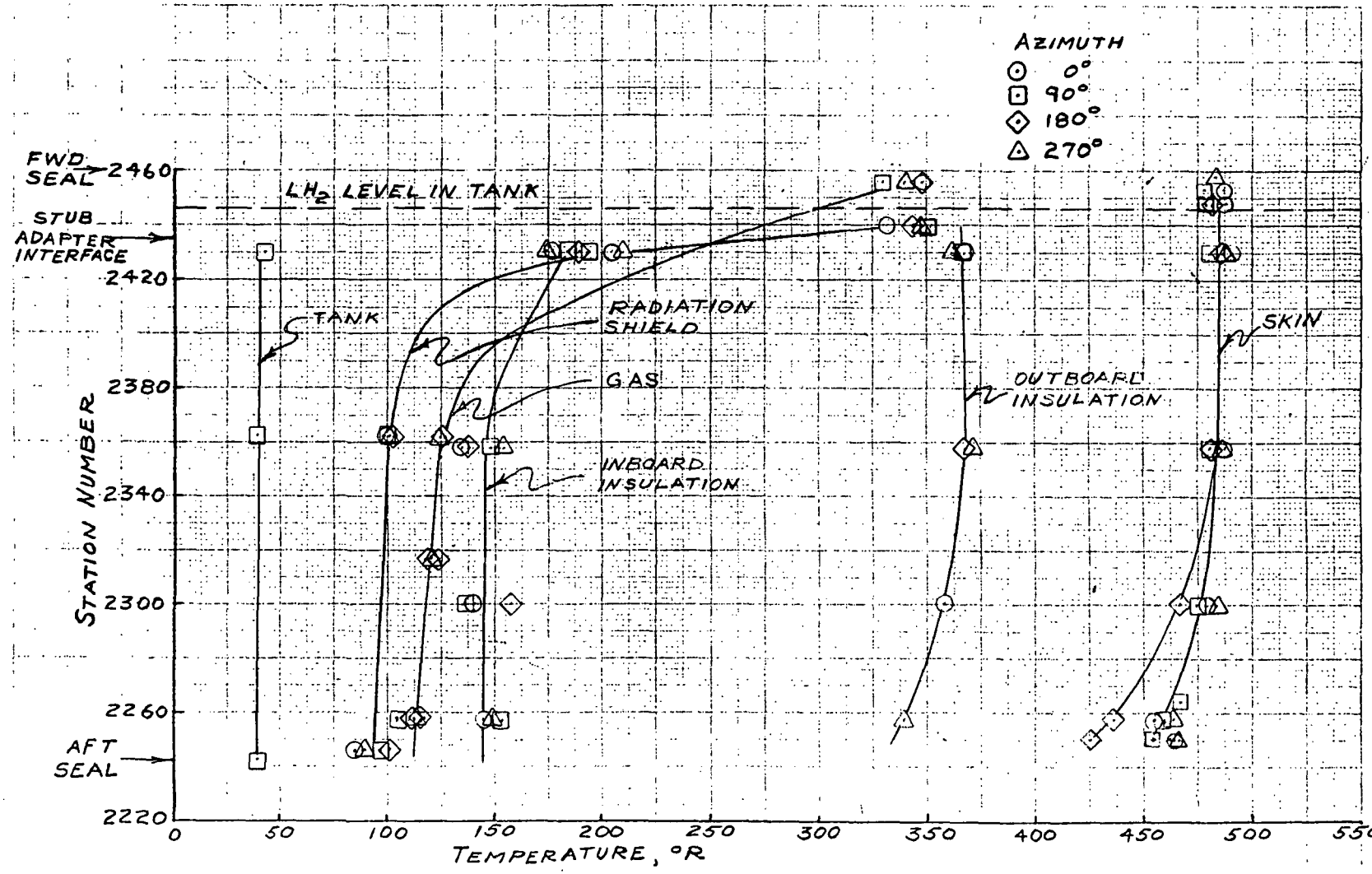

FIGURE V-2 TEMPERATURE PROFILES, CRYO-UNLATCH 3, BOILOFF TEST NO. 1

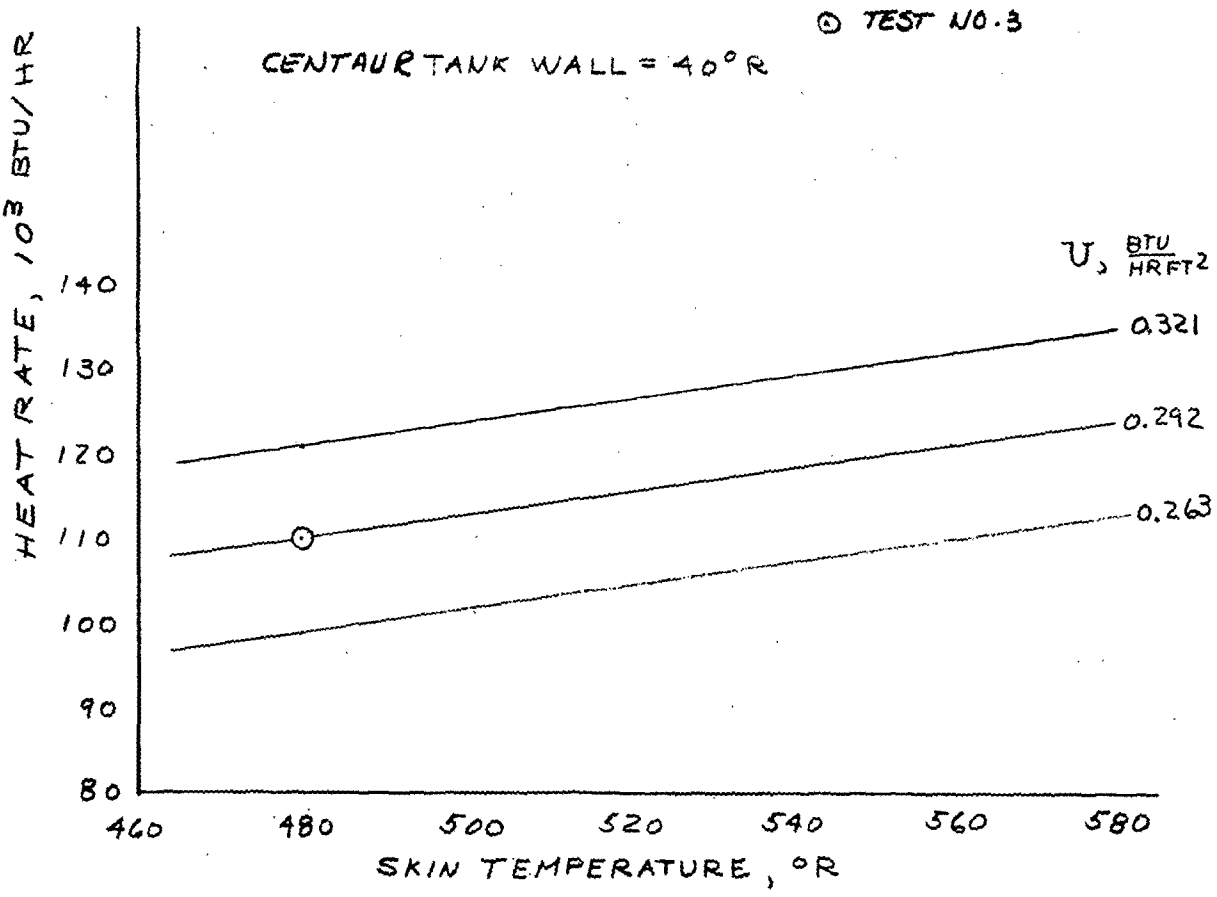

FIGURE V-3 LH_2 TANK HEAT RATE VARIATION DUE TO CSS SKIN TEMPERATURE - BASED ON CRYO-UNLATCH TEST NO.3.

VI. SHROUD/CENTAUR HEAT TRANSFER AND THERMODYNAMICS

by Raymond F. Lacovic

SUMMARY

This section presents the results of the Centaur LH_2 tank boiloff tests performed during the Cryogenic Unlatch Test Program. These tests were performed in order to determine the LH_2 tank total heating rate, and to assess the thermal adequacy of the CSS-LH_2 tank system for ground hold operations for the flight vehicle at the Eastern Test Range (ETR). During the course of the program four major thermal problems were discovered. Briefly, these problems were:

1. Helium purge gas recirculation from the shroud insulation - tank radiation shield annulus to the shroud skin - shroud insulation annulus.

2. Helium purge gas circulation from the tank - tank radiation shield annulus to the shroud insulation - tank radiation shield annulus.

3. High helium purge flow velocity and forced convection in the stub adapter - equipment module - LH_2 tank cavity.

4. Helium stratification and stagnation in the shroud insulation - tank radiation shield annulus.

The first three of these problems were eliminated by configuration changes to the CSS-LH_2 tank system. These changes were:

1. Filling the annulus between the shroud skin and shroud insulation with fiberglas batting.

2. Completely closing off the bottom of the LH_2 tank radiation shield.

3. Adding a diffuser at the end of the equipment module purge line and reducing the purge rate.

The fourth problem is the result of a natural phenomena which apparently cannot be corrected by a simple configuration change. This phenomena results in the formation of a large stagnant mass of cold helium ($<150^{o}R$) in the shroud insulation - tank radiation shield annulus which does not participate in the annulus convective flow processes.

Heat transfer tests with the final insulation configuration, indicated that the LH_2 tank total heating rates for the Cryogenic Unlatch Test No. 3 configuration are 121,400 BTU/hr. and 100,300 BTU/hr. at the high

helium purge rate and low helium purge rate respectively. If these heating rates are extrapolated to the flight vehicle configuration and conditions, values of 148,000 BTU/hr. and 122,000 BTU/hr. can be expected. These heating rates, together with the required configuration changes, indicate that the CSS-LH_2 tank system is thermally acceptable for ground hold operations at the Eastern Test Range.

PRE-TEST HEAT INPUT PREDICTIONS

The Centaur liquid hydrogen (LH_2) tank in the D-1T configuration receives heat inputs from eight major sources during a ground hold condition. These heat sources, which are indicated in figure VI-1, were analyzed prior to the Cryogenic Unlatch Test Program in order to estimate the total tank heating, and to assess air conditioning, icing, and tank self-pressurization behavior and requirements. While this report is not intended to present the details of these analyses, it is important to summarize the pre-test heat input predictions and heat transfer model in order to provide an understanding of the thermal problems that occurred with the CSS-LH_2 tank system.

The overall convection heat transfer model used is shown in figure VI-1. As indicated in this figure by the flow arrows, the convective flows were assumed to be neatly compartmentized by the various components of the CSS-LH_2 tank system. Each flow compartment was analyzed to determine its effective heat transfer coefficient and to determine its contribution to the total tank heating rate. The heat transfer model was two dimensional and no circumferential flow was assumed. The external flows were assumed to be forced convection, and the internal flows were assumed to be free convection. The helium gas between the radiation shield and the tank was assumed to be stagnant. This heat transfer model was logical in view of past D-Centaur experience and in comparison with analyses from somewhat similar systems available in the literature. Consequently, the model was essentially the same for the NASA, LMSC, and GD/CA independent pre-test analyses of the LH_2 tank ground hold heat transfer condition.

The individual heat input rates determined from the pre-test calculations are summarized in table VI-1. These rates were predicted to be the maximum LH_2 tank heat input rates for the Cryogenic Unlatch Test configuration. The maximum total heat input rate was predicted to be 122,000 BTU/hr., but the actual total heat input rate was expected to be significantly lower than this value.

METHOD OF DETERMINING LH_2 TANK HEAT RATE

The total heat input rate to the LH_2 tank was determined from boiloff tests performed prior to the shroud unlatch. In a boiloff test, a nearly full tank of liquid hydrogen is permitted to vent continuously at constant tank

pressure. As the liquid boils, the liquid level in the tank will decrease. This liquid level decrease was measured directly by a LH_2 tank capacitance liquid level sensor and indirectly by LH_2 tank vent flow rate. In this manner, the amount of LH_2 boiloff in a given time period was accurately obtained. This LH_2 boiloff is directly related to the total LH_2 tank heat input by the latent heat of vaporization. A summary of purges and ambient conditions for all boiloff tests performed is given in table VI-2.

TEST RESULTS - CRYOGENIC UNLATCH TEST NO. 1

The data from boiloff test no. 1 during Cryogenic Unlatch Test No. 1 is summarized in figure VI-2. In this figure the measured heat input rates at various liquid levels are plotted against the wetted surface area of the tank forward bulkhead and sidewall. Based on this data the actual heat transfer rate for a fully loaded tank can be obtained by extrapolating the curve to the proper wetted surface area. In addition, the individual heat input contributions of the forward bulkhead and stub adapter can be determined from the plot. The heat input rate for a fully loaded LH_2 tank, with the test configuration, was thus determined to be 214,800 BTU/hr. This heat rate was about 93,000 BTU/hr. greater than the maximum pre-test prediction.

In order to evaluate the sources and consequences of this large heat input the magnitudes of the individual heat input sources were calculated from the test data. These calculated heat input rates are also listed in table VI-1 in order to facilitate comparisons with the pre-test predicted values. As shown by this comparison, the calculated heat input rates were greater than the predicted rates for each one of the major heat sources and, in addition, the total calculated heat input rate was less than the total measured heat input rate by more than 42,000 BTU/hr. (which meant that there was a large unaccounted heat source).

After an examination of the test data and test hardware the unexpected large LH_2 tank heat transfer rate was attributed to four distinct, new, convective flow patterns which had greatly affected the assumed internal convective flow model (figure VI-1). These four flow patterns were as follows:

1. There was a forced convection flow path between the tank skin and the radiation shield instead of the assumed stagnant helium condition. The installation of the radiation shield resulted in an open area of 50 $in.^2$ at the bottom of the shield (required open area was only 1.5 $in.^2$) which permitted warm helium to flow behind the shield and to set up a volumetric collapse, forced convection "pumping" action behind the shield.

2. The flow in the equipment module cavity was forced convection instead of the assumed free convection. The equipment module cavity was purged with a maximum of 36 pounds/hour of helium through an open line which produced an inlet Mach No. of 0.5 and resulted in high velocity

circulating currents in the cavity. The heat transfer coefficients were, consequently, greater by a factor of three than the pre-test estimate.

3. The helium in the shroud insulation - radiation shield annulus stratified and did not readily mix with the incoming purge gas. This "natural" phenomena resulted in a much lower helium temperature in the annulus than predicted at the aft end of the annulus. This lower temperature not only increased the heat transfer through the aft seal (by increasing the temperature difference) but also set up a large gas density difference between the top and bottom of the annulus which served as the driving force for aft area leaks.

4. There was an additional convective flow path from the shroud insulation - radiation shield annulus to the shroud insulation - shroud skin annulus. The test temperature data (see section V) indicated that cold helium ($60^{o}R$) was driven into the shroud insulation - shroud skin annulus at the aft end where it picked up heat as it flowed up the annulus through the split line cavities and through manufacturing holes in the "Z" rings. It then added this heat to the tank as it re-entered the shroud insulation - radiation shield annulus through leaks along the shroud insulation boundary. Analyses showed that this "recirculation" flow pattern could easily account for the 42,000 BTU/hr. difference in predicted and measured LH_2 tank heating.

These four convective flow patterns resulted in the heat transfer convective flow model shown in figure VI-3. This flow model is considerably different than the assumed pre-test flow model shown in figure VI-1 and it resulted in a number of adverse consequences for the LH_2 tank ground hold condition. These consequences were as follows:

1. The increased heat input results in a payload loss by decreasing the quantity of LH_2 that can be tanked.

2. The heat input rate for the D-1T Centaur LH_2 tank would be a wide variable dependent on internal leak areas. The "unaccounted" heat input could just as easily have been zero, or 100,000 BTU/hr., or greater.

3. The unaccounted heat input is a heat sink at the shroud skin. This heat sink can freeze any water that may exist on the skin surface. The 42,000 BTU/hr. heat sink could freeze 300 pounds of water per hour.

4. The very large forward bulkhead heating rates would greatly affect the LH_2 tank self-pressurization rate and selected pre-launch vent valve lockup times.

5. The 250 percent increase in the aft seal heat loss could affect thermal conditioning in the boattail area.

6. The extremely cold helium in the aft end of the shroud insulation - radiation shield annulus can promote aft area leaks and unacceptably low structural temperatures. As a result of these leaks the tank shroud annulus

pressure was also unacceptably low after LH_2 tanking, even with the high helium purge rate.

In order to reduce or eliminate these adverse consequences, three easily implemented fixes were proposed. Briefly these were:

1. Add a diffuser at the end of the equipment module cavity purge line and reduce the purge flow rate.

2. Seal off the bottom of the radiation shield to prevent helium flow behind the shield.

3. Block off the helium flow path in the shroud skin - shroud insulation annulus.

These fixes were made and tested during the second Cryogenic Unlatch Test.

A number of LH_2 tank self-pressurization tests were performed during Cryogenic Unlatch Test No. 1. These tests were performed in order to evaluate the performance of the LH_2 tank flight vent system during blowdown and to aid in determining the vent valve lockup time prior to liftoff. The LH_2 tank pressure rise rates obtained during the self-pressurization tests were more than twice as great as expected. Analyses indicated that these high pressure rise rates were a result of the Centaur tank vent configuration. The test tank in addition to the flight vent also had facility vent line eight inches in diameter with a shutoff valve 60 feet downstream from the tank. The volume of this line ($21\ ft.^3$) was equal to the tank ullage volume ($21\ ft.^3$) for the full tank self-pressurization tests. Thus, the facility vent line heating was of equal importance to the forward bulkhead heating in establishing a tank pressure rise rate. This type of heating configuration deviates so far from a flight configuration that the tank pressure rise rate data is useless for any extrapolation to the flight vehicle. Consequently, a number of LH_2 tank self-pressurization tests will have to be performed at ETR during the first D-1T Terminal Countdown Demonstration (TCD) in order to establish the LH_2 tank vent valve lockup time.

There is a "phenomena" which was found to occur during a LH_2 tank self-pressurization test. As the tank pressure increased the Tank Shroud Annulus Pressure (TSAP) also increased. An example of this behavior is shown in figure VI-4. As shown in this figure, TSAP increased almost 50 percent during the LH_2 self-pressurization test. An analyses of the system showed that this behavior is "natural" for the LH_2 tank in the D-1T configuration. Since the tank is completely contained by the shroud and equipment module, any tank volumetric increase, or decrease, resulting from a change in tank pressure will change the volume of the cavity surrounding the tank. The effect of this volumetric change on TSAP is given by the following equation:

$$\Delta P_{TSAP} = P_{ABS} \times \left(\frac{\Delta V_{TANK}}{V_{CAVITY}}\right) \quad \text{where}$$

P_{ABS} = absolute TSAP

ΔP_{TSAP} = change in TSAP

V_{CAVITY} = contained volume surrounding tank (nominally 1237 $ft.^3$)

ΔV_{TANK} = change in tank volume resulting from change in tank pressure.

As indicated by this equation, even a small change in tank volume (such as 2 $ft.^3$ for the LH_2 tank Self-Pressurization Test) can greatly change TSAP. This same TSAP "phenomena" is expected to occur at ETR during LH_2 tank self-pressurization tests and lockup operations.

TEST RESULTS - CRYOGENIC UNLATCH TEST NO. 2

Three LH_2 boiloff tests were conducted during Cryogenic Unlatch Test No. 2 in order to determine the LH_2 tank heat input under various conditions. The heat input rates determined from each of the boiloff tests are summarized in table VI-3. As with the boiloff test during Cryogenic Unlatch Test No. 1, the LH_2 was permitted to boiloff to below the tank forward ring (Sta. 2434.6) for each boiloff test in order to obtain a measure of the forward bulkhead heating and to permit extrapolation to a fully loaded condition. The plots of the LH_2 tank heat input versus the tank wetted surface area for the three boiloff tests are shown in figure VI-5. If the curve from boiloff test no. 3 is compared with the curve from boiloff test no. 1 during Cryogenic Unlatch Test No. 1 (figure VI-2) it appears that a sizeable reduction in total heat input had been achieved. However, a close examination of the test data showed that the two tests were not directly comparable, and that at least 25,000 BTU/hr. would have to be added to the boiloff test no. 3 LH_2 tank heat input total. The explanation for this additional heat input is as follows:

The boiloff tests during Cryogenic Unlatch Test No. 2 were performed in a heavy rain under 20 knot winds with an ambient temperature of 46°F. These adverse weather conditions resulted in considerable ice buildup on the shroud skin (800 pounds, minimum). Temperature profiles around the shroud insulation indicated that cold helium was again circulating through the shroud skin - shroud insulation annulus, thus providing a large heat sink for the ice formation and accumulation. This ice accumulation closed the shroud skin external leaks and consequently forced a large percentage of the helium purge to leak past the forward seal. It is estimated that 50 percent of the helium purge exited through the forward seal area and, consequently, did not add its sensible heat to the LH_2 tank heating

(estimated at 15,000 BTU/hr.). In addition, the leakage of this low density helium had the effect of pumping air to the seal area. The moisture from the air condensed on the seal and insulated the seal from the nitrogen warming purge. The forward seal temperature was thus 60°F colder than for shroud unlatch no. 1 and the forward seal heat input was calculated to be 1000 BTU/hr. as compared with 10,600 BTU/hr. for shroud unlatch no. 1. This 9,600 BTU/hr. difference in forward seal heating plus the 15,000 BTU/hr. difference in helium purge sensible heat must be added to the LH_2 tank heat input totals shown in figure VI-5. Thus, the LH_2 tank total heat input was still much greater than expected and desired.

An examination of the test data and test hardware indicated that two of the three fixes incorporated after Cryogenic Unlatch Test No. 1 for reducing the LH_2 tank heat input did not work. The seal at the bottom of the radiation shield had cracked and areas of the shield had torn open. The attempt to block off the helium flow path in the shroud skin - shroud insulation annulus had also failed completely. Only the diffuser and reduced purge fix in the equipment module cavity worked properly. (A comparison of figure VI-5 and VI-2 shows that a 15,000 BTU/hr. reduction in forward bulkhead and stub adapter heating was achieved.) It was concluded that the helium flow in the shroud skin - shroud insulation annulus could not be blocked (the helium driving force is such that it would seek a leak path around the blockage) and that a much more positive seal must be devised for the bottom of the radiation shield. With the tremendous ice accumulation on the shroud skin and the resulting effects of the forced cold helium leakage into thermally controlled areas, some of the consequences of the cold helium recirculation heat transfer flow model became all too obvious.

For Cryogenic Unlatch Test No. 3 two fixes were proposed and made which were intended to definitely eliminate the helium recirculation concern. These fixes were:

1. To completely fill the shroud skin - shroud insulation annulus with fiberglas insulation.

2. To absolutely seal off the bottom of the radiation shield by foaming the bottom of the shield.

TEST RESULTS - LH_2/LN_2 TANKING AND FORWARD SEAL RELEASE TEST

After Cryogenic Unlatch Test No. 2, a LH_2/LN_2 tanking was performed to test a redesigned forward seal release mechanism. This test also afforded an excellent opportunity to check out the thermal fixes made to reduce the LH_2 tank heat input. So, as part of the LH_2/LN_2 tanking, four LH_2 boiloff tests were performed. The results of these tests are summarized in table II-4 and in figure VI-6. Boiloff tests no. 1 and no. 2 were of sufficient duration to provide a complete heat input plot of the forward bulkhead and stub adapter areas, as was performed for the preceding boiloff tests during Cryogenic Unlatch Tests No. 1 and No. 2. Boiloff test

no. 1 was performed at the maximum helium purge rate expected for use at ETR, and boiloff test no. 2 was performed at the nominal helium purge rate expected for use at ETR. Boiloff tests no. 3 and no. 4 were of short duration and were performed to give added insight to the effects of the helium purge, and GN_2 seal conditioning on the LH_2 tank total heat input.

A comparison of the boiloff test no. 1 results with the boiloff test no. 1 results from Cryogenic Unlatch Test No. 1 is also given in table VI-1. This comparison shows that a considerable reduction in total LH_2 tank heat input had been achieved (about 93,000 BTU/hr.). As indicated in this table, the calculated individual heat input rate total was 120,700 BTU/hr., as compared with the measured total heat input rate of 121,400 BTU/hr. This excellent agreement indicated that there was no longer a significant unaccountable heat source. This heating total is also very close to the maximum pre-test predicted total heat input of 122,000 BTU/hr. However, a comparison of the individual source heat input rates in table VI-1 shows that this close agreement is rather coincidental. Only the forward bulkhead and stub adapter heating is as predicted. The shroud sidewall heating is much less than predicted because of the added insulation. The forward seal heating is much less than predicted because of the extremely cold GN_2 used to simulate the forward air conditioning ($-12^{\circ}F$ as compared to $65^{\circ}F$ nominal for pre-launch). The aft seal and helium purge heating are much greater than predicted because of the cold helium temperatures in the shroud insulation - radiation shield annulus. This cold temperature results from the natural helium "stratification" phenomena reported earlier, which produces a much colder helium exit temperature and a greater temperature difference across the aft seal than predicted.

It may be possible to reduce this helium "stratification" by changing the distribution of the purge gas, but no attempt was made to investigate this possibility during this test program. As it stands now, the helium purge does little to affect the stratification. A comparison of the annulus weighted helium temperature for each of the four boiloff tests is given in table VI-4. As indicated in the table, a three-fold increase in the helium purge rate only affected the weighted temperature by $6^{\circ}R$. Thus, it appears that the annulus helium temperature will always be very cold ($< 150^{\circ}R$), even at the warm ambient ETR conditions. This cold helium may be a nuisance if it leaks out and impinges on thermally controlled components. Since some of this helium should exit through the adjustable vent in the fill and drain chute, the surrounding structural area will be especially cold during a ground hold operation, and large quantities of ice will probably accumulate on this structure during a humid day.

The thermal fixes implemented after Cryogenic Unlatch Test No. 2 had worked. The helium circulation through the shroud skin - shroud skin annulus had been greatly reduced and the total LH_2 tank heat input rate, while not as low as pre-test predictions, had been reduced to acceptable and understandable values. We could now extrapolate the LH_2 tank heating results for the B-3 configuration and environment to the flight vehicle configuration and ground hold conditions at ETR. Two estimates of the flight vehicle LH_2 tank heat input at ETR were made based on an extrapolation

of the boiloff test results. These estimates, listed in the table VI-4, are 148,000 BTU/hr. and 122,000 BTU/hr. based on a helium purge rate of 92.5 #/hr. and 52.5 #/hr. respectively. The estimates take into account the ETR ambient temperature, air conditioning, and configuration, but they are intended to serve only as a guideline. Any excessive deviation from these estimates, obtained from boiloff tests at ETR, should be investigated.

No additional thermal fixes were proposed for Cryogenic Unlatch Test No. 3.

TEST RESULTS - CRYOGENIC UNLATCH TEST NO. 3

Two additional LH_2 tankings, together with two more boiloff tests, were performed during Cryogenic Unlatch Test No. 3. These tests were of short duration and were performed to check the adequacy of the thermal fixes for normal ground hold times. For the last half of each boiloff test, water was sprayed along the shroud split lines in order to check for leaks under simulated rain conditions. The water flow had no measurable effect on the LH_2 tank total heating rate. The two boiloff test conditions (helium purge, GN_2 conditioning, ambient temperature) were identical with boiloff test no. 2 from the LH_2/LN_2 tanking. Thus, a direct comparison could be made of the LH_2 tank heating rates after three separate LH_2 tankings. This comparison is given in figure VI-7. As shown in the figure the LH_2 tank total heating rate increased slightly (approximately five percent) for each successive tanking. This kind of comparison could give some insight as to how the shroud - tank thermal systems degrade with repeated tankings. An examination of the temperature data (see section V) indicates that most of the heating rate increase between these three tests occurred from a degradation in the aft seal. As more and more cold helium leaked through the aft seal a pumping action was set up in the boattail area which increased the GN_2 flow over the seal surface and increased the heat transfer through this area. Based on the aft seal temperature data, it is estimated that about 70 percent of the heating rate increase can be attributed to this effect.

Regardless of the 10 percent increase in tank heating rate for the boiloff tests during Cryogenic Unlatch Test No. 3, the thermal fixes incorporated after Cryogenic Unlatch Test No. 2 are still considered to be completely adequate. The LH_2 tank total heating rate expected at ETR for the D-1T configuration should still be significantly less than for the current D-Centaur configuration, even if the 10 percent heating increase is added to the heat input estimates listed in table VI-4.

The water spray testing during these last two boiloff tests showed that the tendency for an ice buildup on the shroud skin has been extensively decreased. Even though the ambient temperature was 34°F, water droplets would not freeze on the skin. The shroud skin heat sink is probably no longer sufficient to freeze large water droplets. However, the shroud skin did sustain a slight "fuzz" layer of frost over most of the surface

area, and ice did accumulate at local cold spots such as the aft circumferential joint and the LH_2 tank fill and drain chute frame. The ice accumulation on the fill and drain chute frame may be of concern because it can affect aerodynamic flow.

CONCLUDING REMARKS

With the addition of fiberglas insulation to the shroud, the closing of the bottom of the radiation shield, and the reduced helium purge in the equipment module cavity, the CSS-LH_2 tank system appeared to be thermally acceptable. This conclusion is justified for the test vehicle configuration, but whether it applies for the flight vehicle configuration remains to be seen. The CSS-LH_2 tank system thermal performance was highly sensitive to such variables as helium leak paths and area, installation techniques, and the configuration and environment itself. The differences between the test and the flight vehicles in these areas can be considerable and even though no major thermal problems are expected with the CSS-LH_2 tank system for flight operations there are still some areas of concern that can be resolved by thermal testing at ETR with the full flight configuration.

In order to assess the thermal performance of the CSS-LH_2 tank system for ground operations at ETR, it is recommended that a number of thermal tests be performed during tanking tests at ETR. These tests should consist of at least one boiloff test and at least two LH_2 tank self-pressurization tests.

The boiloff tests would provide a rough measure of the total LH_2 tank heating which could be compared to the 11 boiloff tests performed during the Cryogenic Unlatch Test Program. This "rough measure" could be refined extensively if the LH_2 tank vent flow rate could be measured. This could be accomplished by incorporating the flow venturi from B-3 in the Complex 41 facility LH_2 vent line and by adding pressure, delta pressure, and temperature instrumentation to the present landline measurements. The use of this flow venturi would obtain an accurate measurement of the LH_2 tank heating for each D-1T TCD and launch, and to assess the vehicle to vehicle tank heating dispersions which are expected to be large for the CSS-LH_2 tank configuration. This venturi would also eliminate the need for future D-1T boiloff tests after D-1TPF. The vent flow measurement, together with the extensive instrumentation already available on D-1TPF, would permit a good assessment of the overall thermal behavior, and a reaffirmation of the convective thermal model, of the CSS-LH_2 tank system.

The LH_2 tank self-pressurization tests are required in order to determine the D-1T LH_2 tank vent valve lockup time. Since no acceptable self-pressurization test data was obtained from the Cryogenic Unlatch Tests, these tests are mandatory. In order to reduce the dispersions normally associated with LH_2 tank self-pressurization rates only the high helium purge rate should be used for a lockup prior to liftoff. A fixed purge

rate would eliminate the pressure rise dispersions resulting from the differences in forward bulkhead heating between high and low helium purge rates (estimated at 33 percent). The choice of the high purge rate will keep the pressure rise times reasonably short, and will provide a better comparison with D-1A Centaur experience. Since the high helium purge rate is also required for LH_2 tanking, the question may arise as to whether or not to return to the low purge rate between the completion of tanking and vent valve lockup. However, if the high purge rate is used continuously, a much greater quantity of cold helium would leak through the forward and aft seals into the thermally controlled forward and aft compartments. This additional leakage was not accounted for in the thermal analyses for these areas and could be of concern during long hold periods. Consequently, it is recommended to use the low helium purge rate, as originally planned, during a long hold period after tanking.

TABLE VI-1 - COMPARISON OF PRE-TEST PREDICTED AND CALCULATED AND MEASURED LH_2 TANK HEAT RATES FROM TEST DATA (1)

Heat Source	Centaur LH_2 Tank Heat Rates BTU/Hr.		
	Predicted Maximum	Calculated from Boiloff Test No. 1 during Cryo-Unlatch Test No.1	Calculated from Boil-off Test No. 1 during LH_2/LN_2 Tanking and Forward Seal Release
Forward Bulkhead (Q_{FB})	9,400	19,500	10,000
Stub Adapter (Q_{SA})	11,500	14,800	11,000
Forward Seal (Q_{FS})	9,000	10,600	3,600
Shroud Sidewall (Q_{SW})	42,000	52,900	32,800
Aft Seal (Q_{AS})	8,400	25,600	14,800
Helium Purge (Q_P)	34,000	40,900	40,800
LH_2 Tank Sump			
Intermediate Bulkhead	7,700	7,700	7,700
Fill/Drain Chute			
Cables and Penetrations			
Calculated Total	122,000	172,000	120,700
Measured Total	-	214,800	121,400

(1) Based on High Purge Flow Rate

TABLE VI-2 SUMMARY OF PURGES AND AMBIENT CONDITIONS DURING LH_2 BOILOFF TESTS - CSS CRYOGENIC UNLATCH TESTS

TEST	ANNULUS VENT in^2	SHROUD PURGES lb/hr GHe				SEAL PURGES lb/hr GN_2		BOAT TAIL PURGE	PAYLOAD PURGE	TANK/SHROUD ANNULUS PRESSURE	ANNULUS VENT FLOW	AMBIENT CONDITIONS				
		E/M	FWD	DEST	F/D	FWD	AFT	lb/hr GN_2	lb/hr GN_2	psig	lb/hr	T_a °R	T_w °R	P_b psia	W_d deg.	W_s mph
CRYO-UNLATCH NO. 1																
Boiloff Test No.1	0	36.3	36.3	29.8	4.2	150	150	N/A	N/A	.045 to .058	N/A	NAV	NAV	NAV	NAV	NAV
Boiloff Test No.2	0	36.3	36.3	29.8	4.2	150	150	N/A	N/A	.062 to .070	N/A	NAV	NAV	NAV	NAV	NAV
CRYO-UNLATCH NO. 2																
Boiloff Test No.1	0.15	4.0	25.1	29.9	4.2	150	150	200	N/A	.18 to .22	11.8-12.6	507	505	14.27	270	26
Boiloff Test No.2	0.15	4.0	25.0	29.8	4.2	0	0	0	N/A	.18 to .21	11.3-12.5	505	503	14.28	275	17
Boiloff Test No.3	0.15	12.3	62.6	29.9	4.2	150	150	200	N/A	.43 to .47	18.5	503	501	14.30	270	16
LH_2/LN_2 TANKING TEST																
Boiloff Test No.1	0.15	9.2	56.1	30.7	4.2	150	150	422	12.6	.23 to .25	NAV	495	493	14.31	260	20
Boiloff Test No.2	0.15	3.6	21.9	30.8	4.2	150	150	425	11.2	.10 to .106	NAV	494	491	14.33	260	20
Boiloff Test No.3	0.15	3.6	21.9	30.9	4.2	0	0	0	13.4	.077 to .096	NAV	492	490	14.36	260	20
Boiloff Test No.4	0.15	1.0	5.2	25.8	4.2	150	150	425	13.4	.044 to.049	NAV	491	490	14.37	260	20
CRYO-UNLATCH NO.3																
Boiloff Test No.1	0.15	3.5	21.6	30.3	4.2	150	150	430	10.8	.067 to .107	13.0-15.8	494	492	14.45	290	9-16
Boiloff Test No.2	0.15	3.6	21.9	30.9	4.2	150	150	475	12.0	.073 to.086	12.6-13.0	497	494	14.46	180	3-10

ABBREVIATIONS: E/M = Equipment Module; FWD = Forward Purge Ring; DEST = Destructor Housing; F/D = LH_2 Fill/Drain Chute; T_a = Dry Bulb Temperature; T_w = Wet Bulb Temperature; P_b = Barometric Pressure; W_s = Wind Speed; W_d = Wind Direction (0° = North = 270° on Shroud); N/A = Not Applicable; NAV = Not Available

TABLE VI-3 - COMPARISON OF LH_2 TANK BOILOFF TEST RESULTS FROM CRYO-UNLATCH TEST NO. 2

Boiloff Test Number	Helium Purge Rate--lb/hr	Forward & Aft Seal Conditioning Purges	Total Heat Rate for Full LH_2 Tank BTU/hr
1	59.0	On	162,000
2	58.8	Off	158,500
3	104.8	On	167,100

TABLE VI-4 - SUMMARY OF BOILOFF TEST RESULTS FROM THE LH_2/LN_2 TANKING AND FORWARD SEAL RELEASE TEST AND ESTIMATED FLIGHT VEHICLE LH_2 TANK HEATING RATES AT ETR

Boiloff Test No.	Helium Purge Rate lb/hr	Forward and Aft Seal Conditioning Purges	Tank/Shroud Annulus Weighted Helium Gas Temperature ^{o}R	Measured Total LH_2 Tank Heat Rate for Full Tank BTU/hr	Estimated LH_2 Tank Heat Rate for ETR Conditions BTU/hr
1	96.0	On	126	121,400	148,000
2	56.3	On	122	100,300	122,000
3	56.4	Off	120	96,000	-
4	32.0	On	120	91,000	-

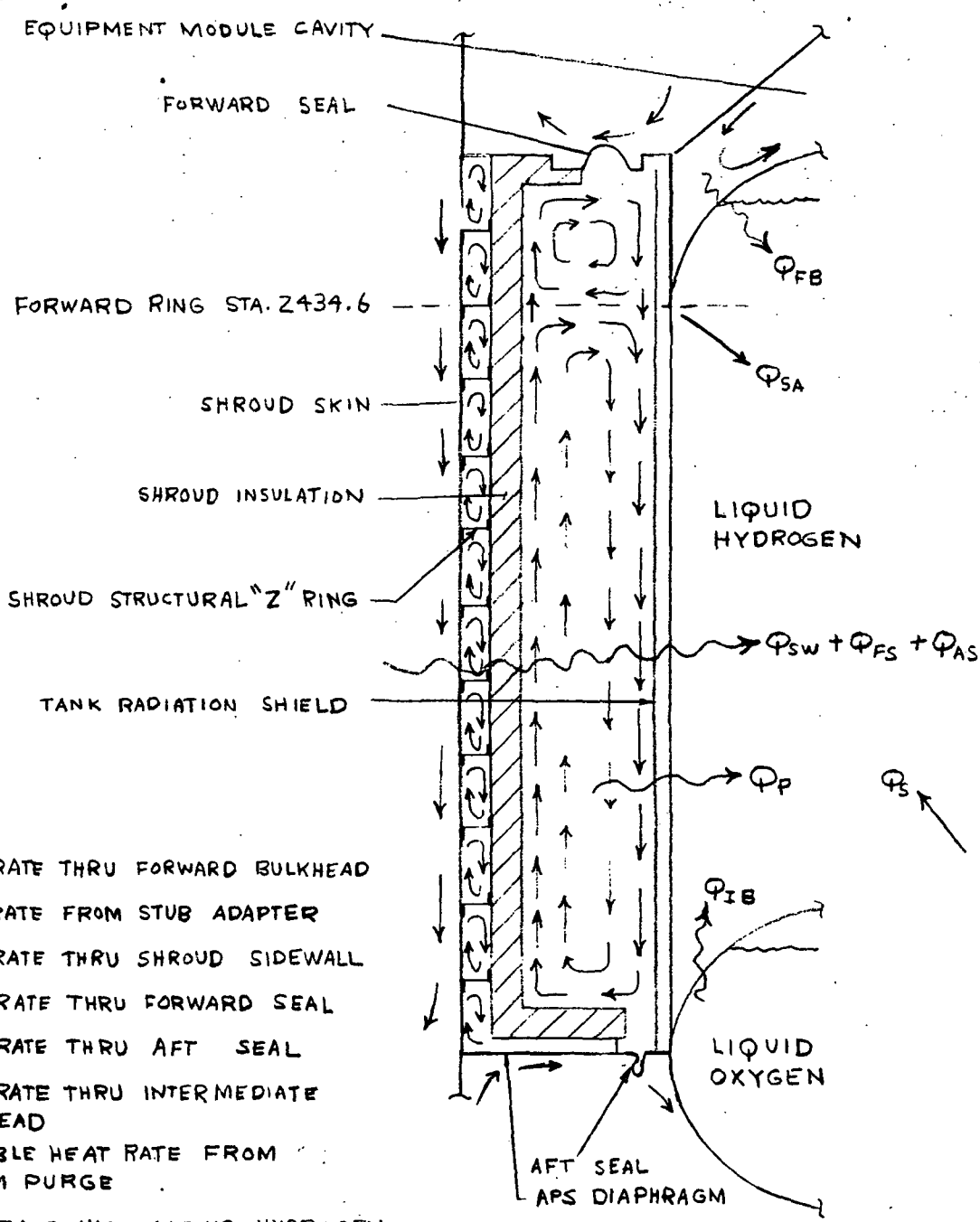

Φ_{FB} = HEAT RATE THRU FORWARD BULKHEAD

Φ_{SA} = HEAT RATE FROM STUB ADAPTER

Φ_{SW} = HEAT RATE THRU SHROUD SIDEWALL

Φ_{FS} = HEAT RATE THRU FORWARD SEAL

Φ_{AS} = HEAT RATE THRU AFT SEAL

Φ_{IB} = HEAT RATE THRU INTERMEDIATE BULKHEAD

Φ_P = SENSIBLE HEAT RATE FROM HELIUM PURGE

Φ_S = HEAT RATE INTO LIQUID HYDROGEN TANK SUMP

FIGURE VI-1 HEAT TRANSFER CONVECTIVE FLOW MODEL AND HEAT SOURCES USED FOR PRE-TEST ANALYSES

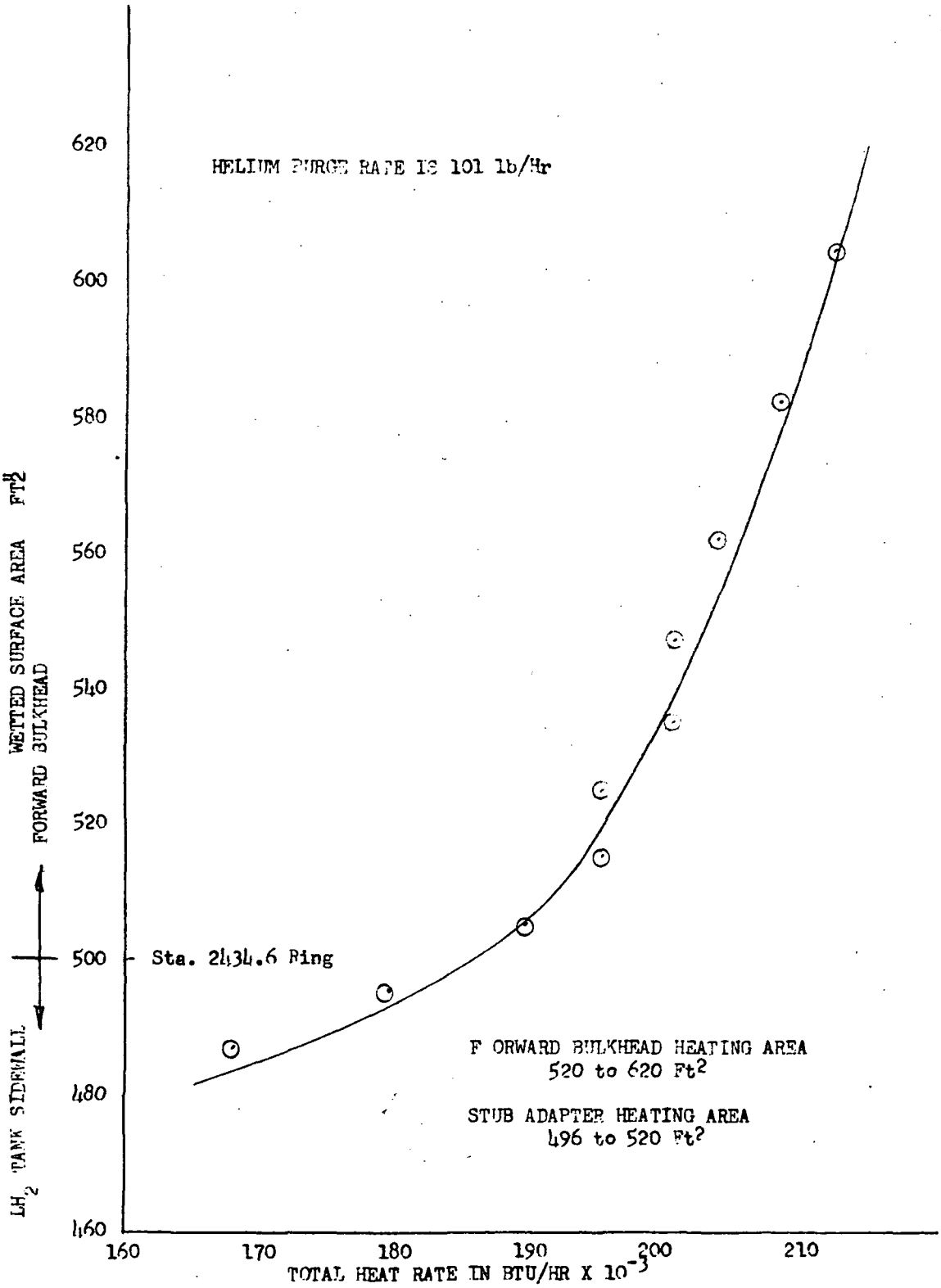

FIGURE VI-2 LH_2 TANK TOTAL HEAT RATE DATA FROM BOILOFF TEST NO.1 DURING CRYOUNLATCH TEST NO. 1

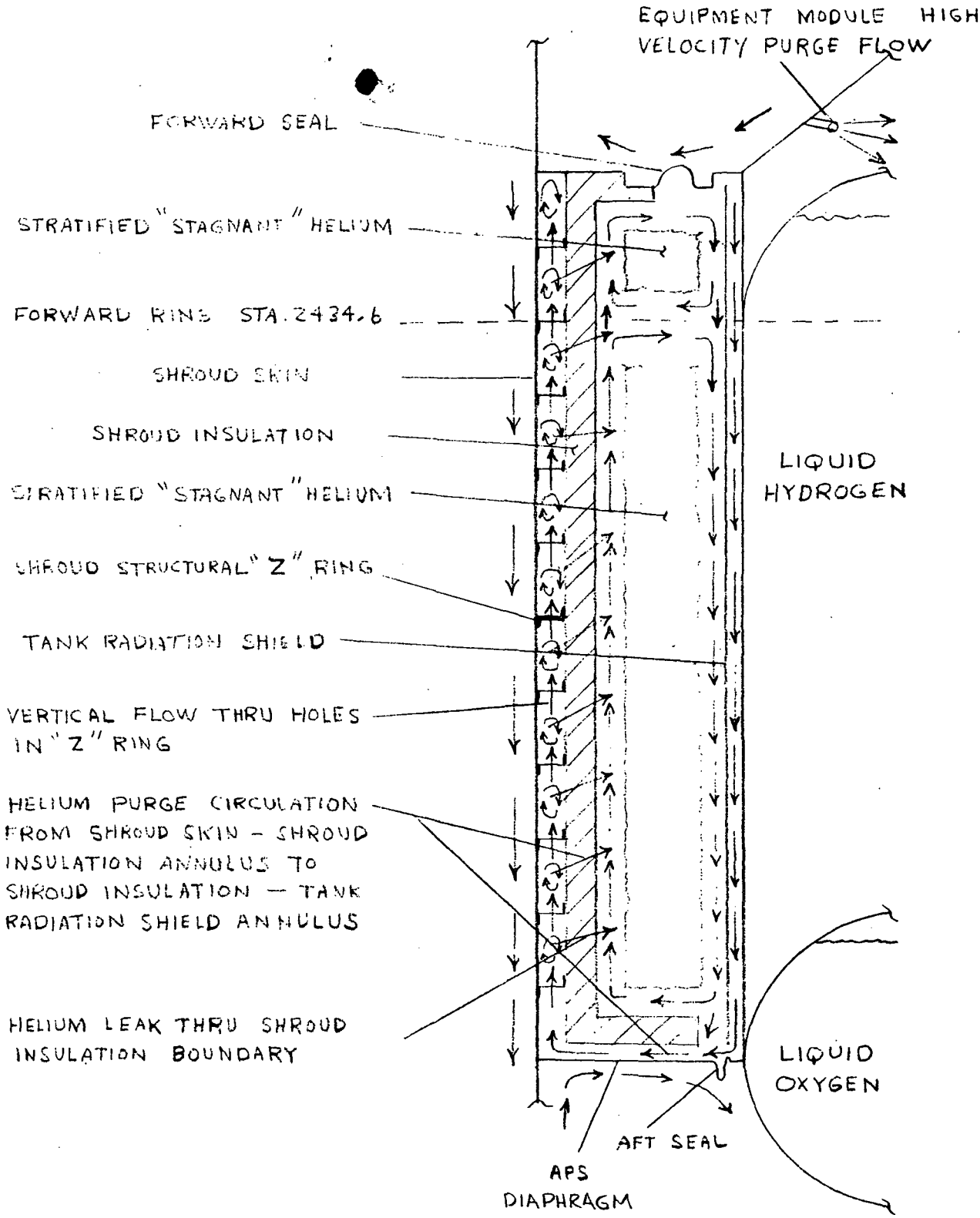

FIGURE VI-3 HEAT TRANSFER CONVECTIVE FLOW MODEL BASED ON DATA EVALUATION FROM CRYOUNLATCH TEST NO. 1

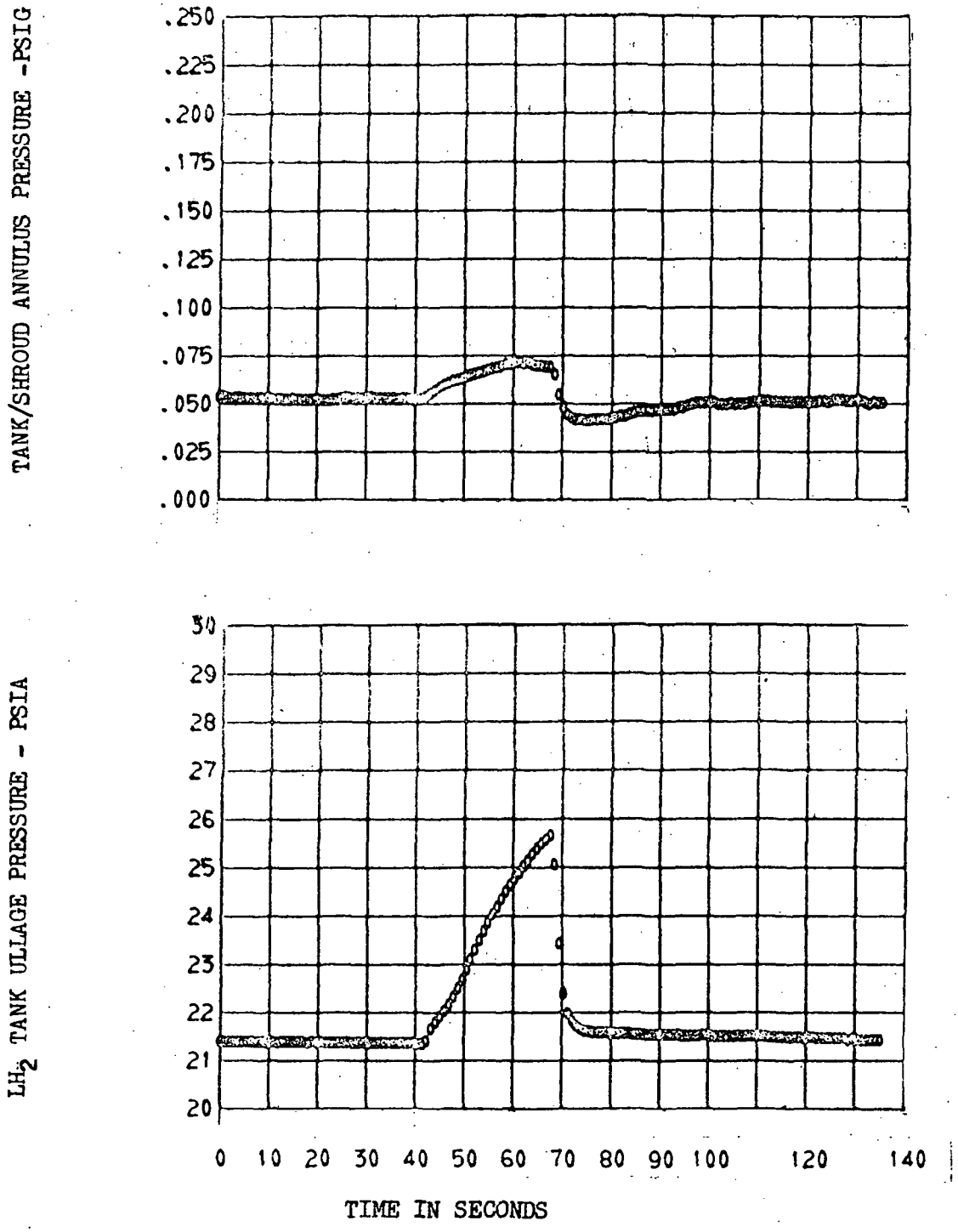

FIGURE VI-4 TANK/SHROUD ANNULUS PRESSURE INCREASE DURING LH_2 TANK SELF PRESSURIZATION . DATA FROM CRYO-UNLATCH TEST NO.1

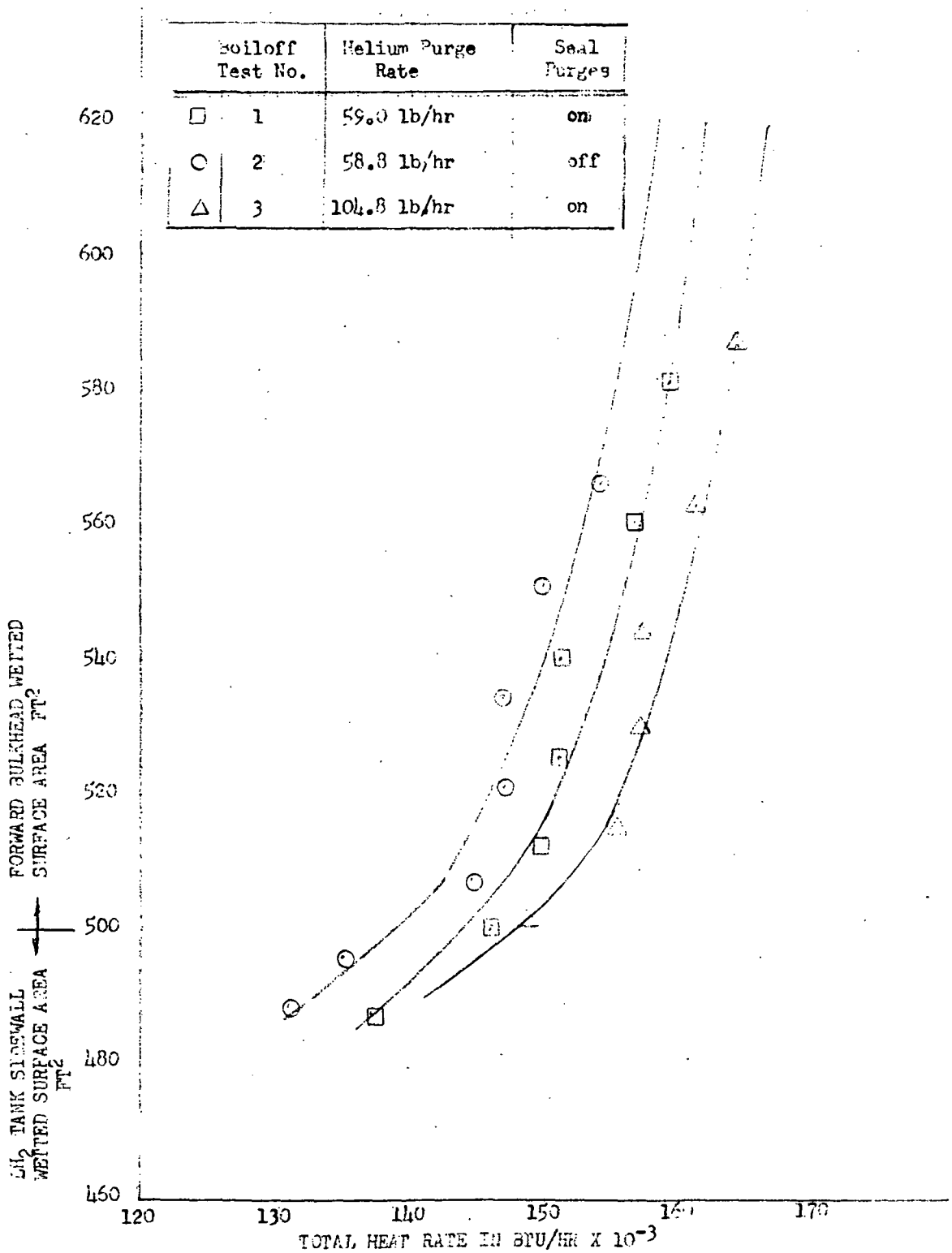

FIGURE VI-5 LH_2 TANK TOTAL HEAT RATE DATA FROM BOILOFF TESTS DURING CRYOUNLATCH TEST NO. 2

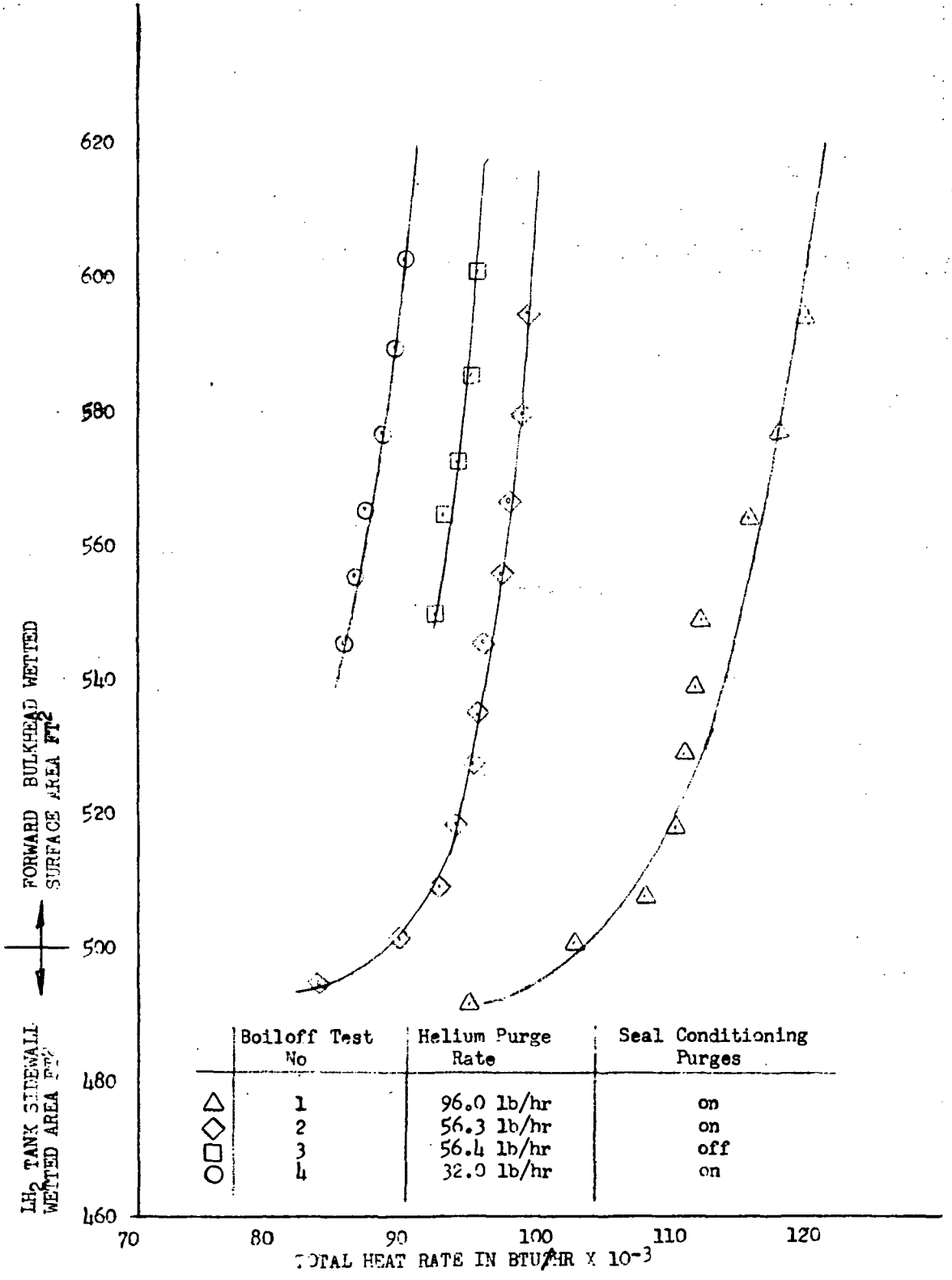

FIGURE VI-6 TOTAL HEAT RATE TO LH_2 TANK FROM BOILOFF TESTS DURING LH_2/LN_2 TANKING AND FORWARD SEAL RELEASE TESTS

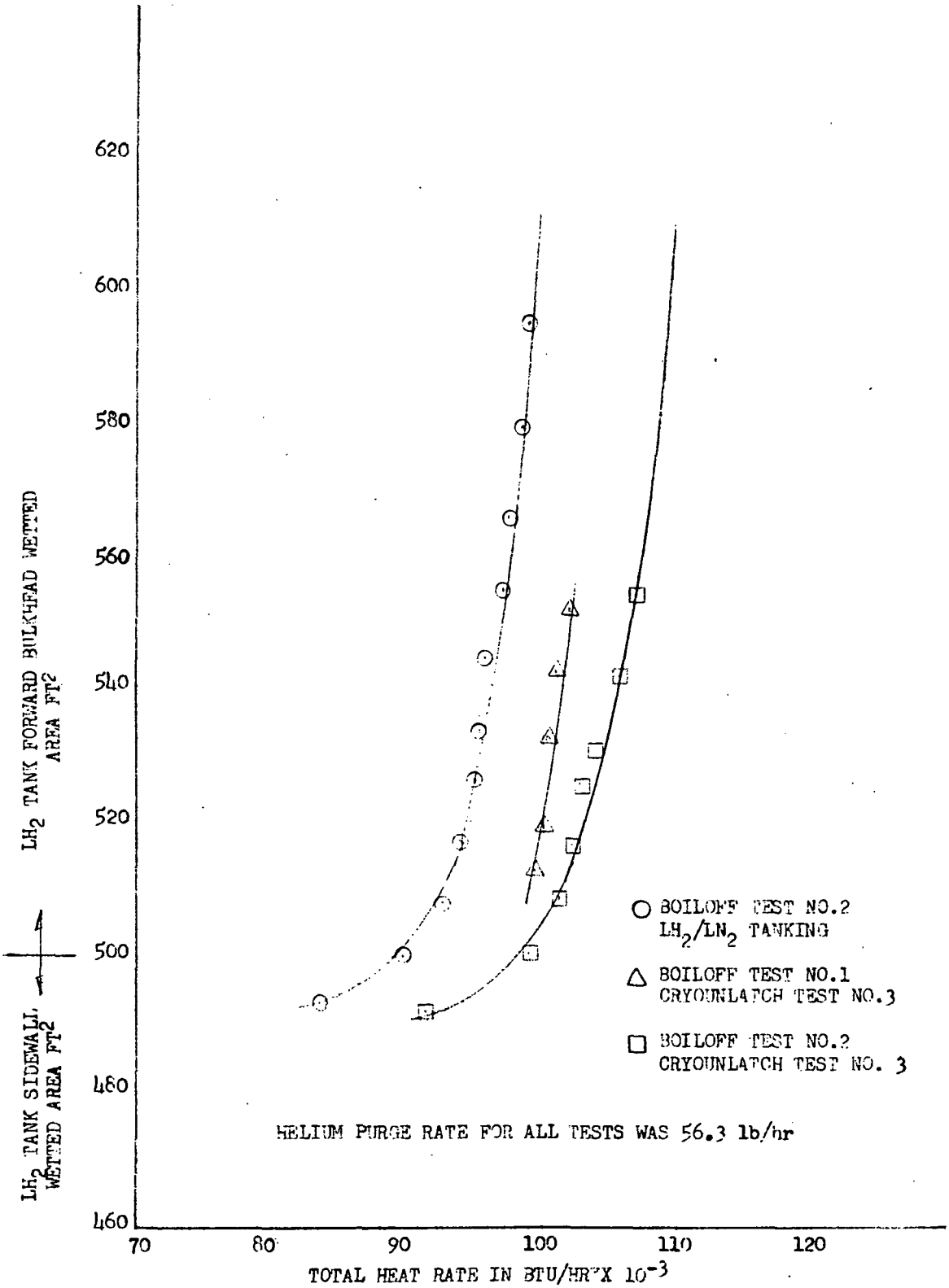

FIGURE VI-7 A COMPARISON OF THREE LH_2 TANK BOILOFF TESTS

VII. PYROTECHNIC SYSTEMS

by B. L. Beaton, T. L. Seeholzer, and J. L. Swavely

SUMMARY

The primary function of all pyrotechnic systems related to the CSS was successfully demonstrated in the three cyro-unlatch tests. Several anomalies relative to the secondary Super-Zip separation system occurred which did not compromise the primary separation system, but could produce undesirable contamination in the event of secondary system activation.

SYSTEM DESCRIPTIONS

Forward Bearing Reaction Separation System

The Forward Bearing Reaction (FBR) struts are each separated by a pyrotechnically actuated explosive bolt, as shown in Figure VII-1. (See Section VIII for forward bearing reactor description.) Bolt separation is accomplished by either of two electro-explosive detonators. The pressure produced by the detonator is transferred into a force by means of two pistons and a silicone force amplifier. The resultant force fractures the bolt in the groove area. This bolt has been successfully employed on the Atlas/Centaur nose fairing for fairing separation. Following bolt separation, the FBR strut halves are retracted against the CSS and the stub adapter by springs.

Forward Seal Release System

This system, incorporated after cryo-unlatch test no. 2, consists of a cable release by means of an explosive bolt. This bolt is the same as that used in the forward bearing reactor separation described above. See Section III for details of the seal release system and operation.

Forward Bearing Reaction and Forward Seal Release Electrical Actuation System

The functional schematic diagram of the squib firing system for both the forward bearing reaction and the forward seal release system is shown in Figure VII-2. A 400 amp direct current power supply simulated the flight battery and provided the power to the pyrotechnic control units (PYC) located on the Centaur equipment module. There is one PYC for the forward bearing reaction system and one for the forward seal release system. Within the PYC are EMI filters, redundant firing relays, and current limiting circuits which include series resistances to balance and limit current magnitude, and thermal relays to isolate shorted bridgewires. A control signal to the relays actuates the firing system. The functioning of each relay is monitored by use of auxiliary contacts.

For each test, the total current and power supply voltage were recorded along with firing commands and microswitch closures to indicate strut separation and retraction. In all tests, the current magnitudes, which vary as a function of the number of squibs being fired, were as expected. Time from the firing signal to microswitch closure ranged from 20 to 150 milliseconds.

Super-Zip Separation System

(Mechanical Description)

The Super-Zip separation systems, both primary and secondary, are shown in Figures VII-3 and VII-4. The systems incorporate a longitudinal and circumferential joint consisting of two explosive cords in a stainless steel tube as shown in Figures VII-5 and VII-6. When either cord is ignited, the resultant pressure expands the tube and fractures the frangible doublers.

The secondary system is fired only in the event the primary system fails to separate the shroud. Each joint is redundantly actuated by electric detonators as shown in Figures VII-7 and VII-8. At the payload section, there are detonation transfer lines which bridge the field joint and fire the cord by means of non-electric detonators (reference Figure VII-4).

Jettison of the CSS following joint separation is accomplished by eight jettison springs located at the base of the CSS and four helper springs on the split lines as shown in Figure VII-9.

Super-Zip Separation System

(Electrical Description)

The electrical system for initiation of the Super-Zip for these tests, is shown in Figure VII-10. A remotely controlled 400 amp direct current power supply was used to supply the necessary power for the Super-Zip detonators.

The squib fire circuits (SFC's) were supplied with 28 VDC power. The SFC's turned on and allowed current to flow to the detonators when a control signal was applied. This control signal was applied through contacts of a programmer controlled firing relay. Power was routed from the SFC's through resistor packages to the detonators and returned through current shunts. The resistor packages were designed to provide the proper amount of current, and to limit the current in the event of a shorted detonator or short circuit. The SFC's and current shunts are Titan flight type hardware.

Each SFC supplies power to four detonators in the primary system. The secondary system was initiated on tests nos. 2 and 3 when the CSS had been jettisoned and in the nets by means of adapter cables at the Titan/CSS interface, and by inserting test cables between the in-flight disconnects.

Outputs of the two current shunts and power supply voltage were recorded on oscillograph recorders.

SYSTEM OPERATION

Forward Bearing Reactor Separation System

Movie data and post-test inspection verified that the Forward Bearing Reaction (FBR) struts all successfully separated and retracted in all three cryo-unlatch tests. Post-test inspection revealed one significant problem relative to the explosive bolt cartridge electrical connector. Several connectors and backshells failed structurally after being subjected to two or more firings. The cause of the failure was that the cast aluminum of which the connector and backshell were made could not withstand the impact loads imparted at bolt separation. The material has been changed to a 2024-T851 aluminum alloy for increased structural capability and will be incorporated on the flight vehicles.

Forward Seal Releaser System

The explosive bolt actuated system operated successfully during the following tests:

1. Ambient temperature seal release
2. LN_2/LN_2 tanking and seal release
3. LN_2/LH_2 tanking and seal release
4. Cryo-unlatch test no. 3

The same problem with the FBR connectors occurred in the forward seal release connectors. (See Section III for details of the seal release operation.)

Super-Zip Separation System

(Mechanical Operation)

The Super-Zip system successfully separated the CSS in all three cyro-unlatch tests. The jettison springs rotated the CSS following separation. However, there were significant anoamlies which occurred during each test. These are summarized as follows:

Cryo-unlatch test no. 1: Post test inspection revealed the following:

a. Both primary and secondary systems fired in the longitudinal system. Only the primary should have fired.

b. The longitudinal Super-Zip tube was ruptured in five areas in the payload and tank sections. See Figure VII-11 for a typical rupture.

After further inspection, it was determined that the secondary system detonator at station 2514 on the 180° axis had fired, but the primary had not.

Inspection of connectors at this point revealed that the primary and secondary connectors were wired backwards, i.e., primary connector to secondary detonator and secondary connector to primary detonator.

Corrective action to prevent this from occurring again was:

a. Color code the detonators, detonator blocks, connectors, and shroud. White for primary, red for secondary. Revise installation procedures.

b. For future tests and flight, in addition to item (a) above, use a different type connector on the primary harness.

Cryo-unlatch test no. 2: During this test, the primary system successfully separated the CSS without any anomalies. After the CSS was in the nets, the secondary system was fired. The Super-Zip tube ruptured in three places in the longitudinal joint producing contamination as occurred in the first cryo-unlatch test. This test verified that although the system is redundant, it may produce contamination in the event the secondary system is actuated after any part of the tube has been expanded by the primary system.

Cryo-unlatch test no. 3: The primary system again separated the CSS successfully. Firing of the secondary system did not rupture the tube as occurred on previous tests. During firing of the primary system, the change of direction plates at the $15^{o}/25^{o}$ cone intersection were ripped. This was not detrimental to the CSS separation. However, the plates have been revised by addition of a more generous radius at the plate lip. This design will be used on future tests and for flight.

Super-Zip Separation System

(Electrical Operation)

Data were recorded for five electrical system firings of the Super-Zip system. The primary system was initiated for cryo-unlatch test no. 1 and both primary and secondary systems were initated for tests nos. 2 and 3.

The open circuit voltage for the five tests varied from 32.2 to 33.5 volts dc. The current shunts indicated a range from 30.0 amps to 34.0 amps. Each shunt measures the current to four detonators. Assuming an equal division of current to each detonator, the lowest value was 8.5 amps. The average value of detonator current for the five tests was 8.1 amps. The detonator firing times for the group of four detonators ranged from 1.4 milliseconds to 3.6 milliseconds.

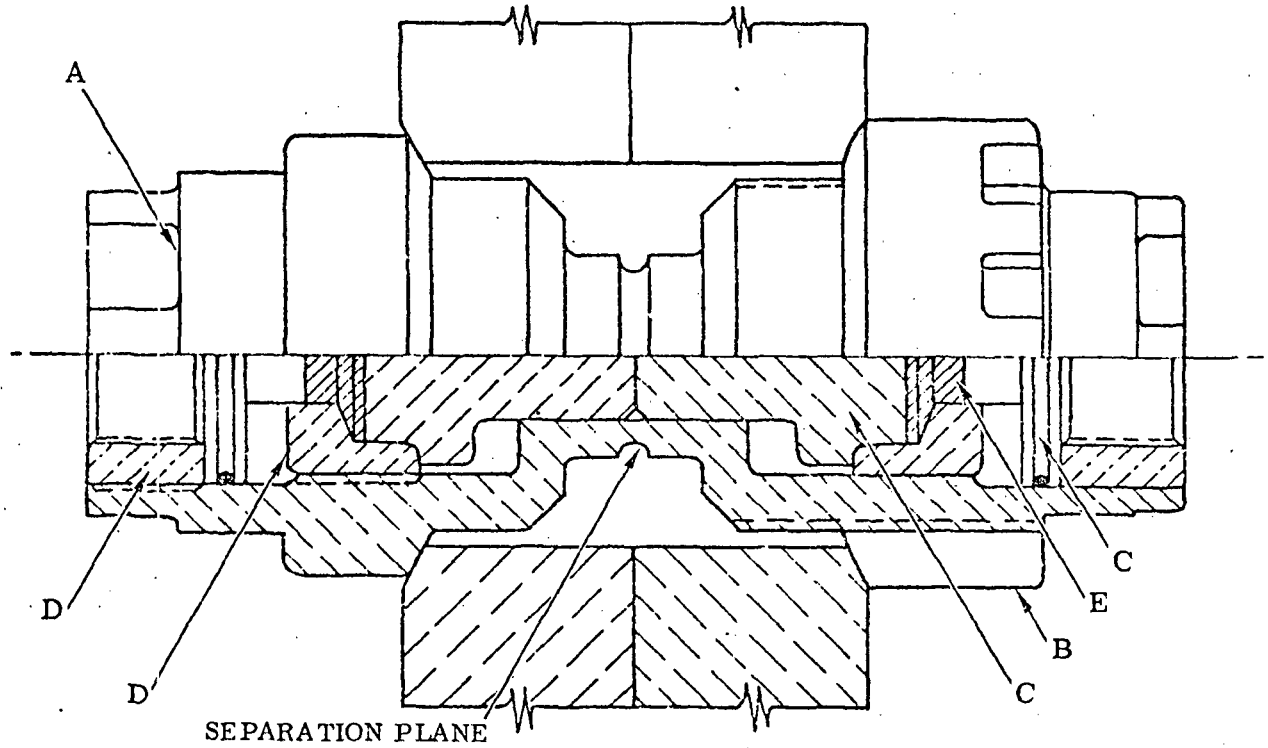

PART
A. BOLT BODY
B. NUT
C. PISTONS
D. RETAINER/INSERT
E. FORCE AMPLIFIER
F. ASSY

FIGURE VII-1 PYROTECHNICALLY ACTUATED EXPLOSIVE BOLT

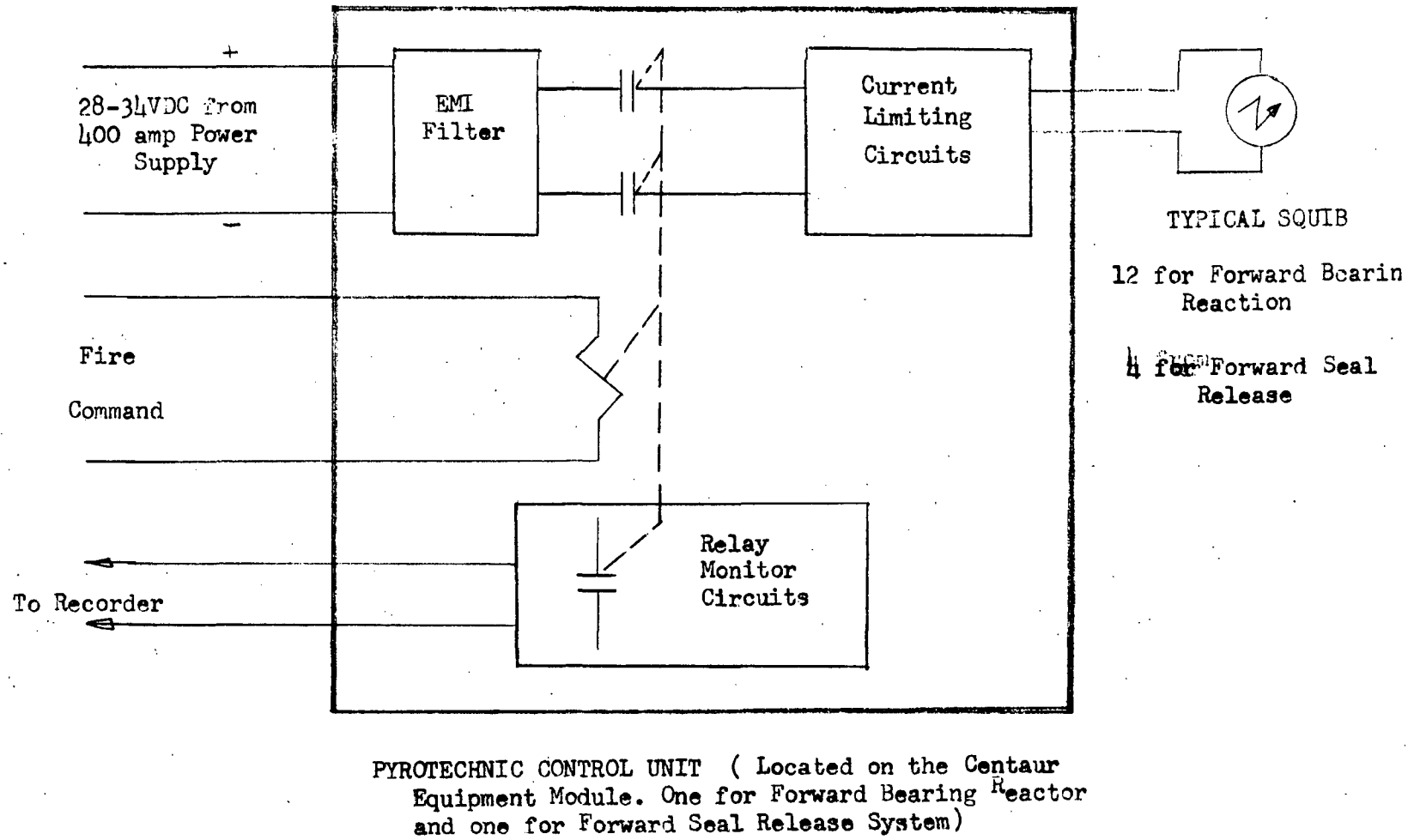

FIGURE VII-2 FUNCTIONAL SCHEMATIC FOR FORWARD BEARING REACTION AND FORWARD SEAL RELEASE PYROTECHNIC ELECTRICAL ACTUATION SYSTEM

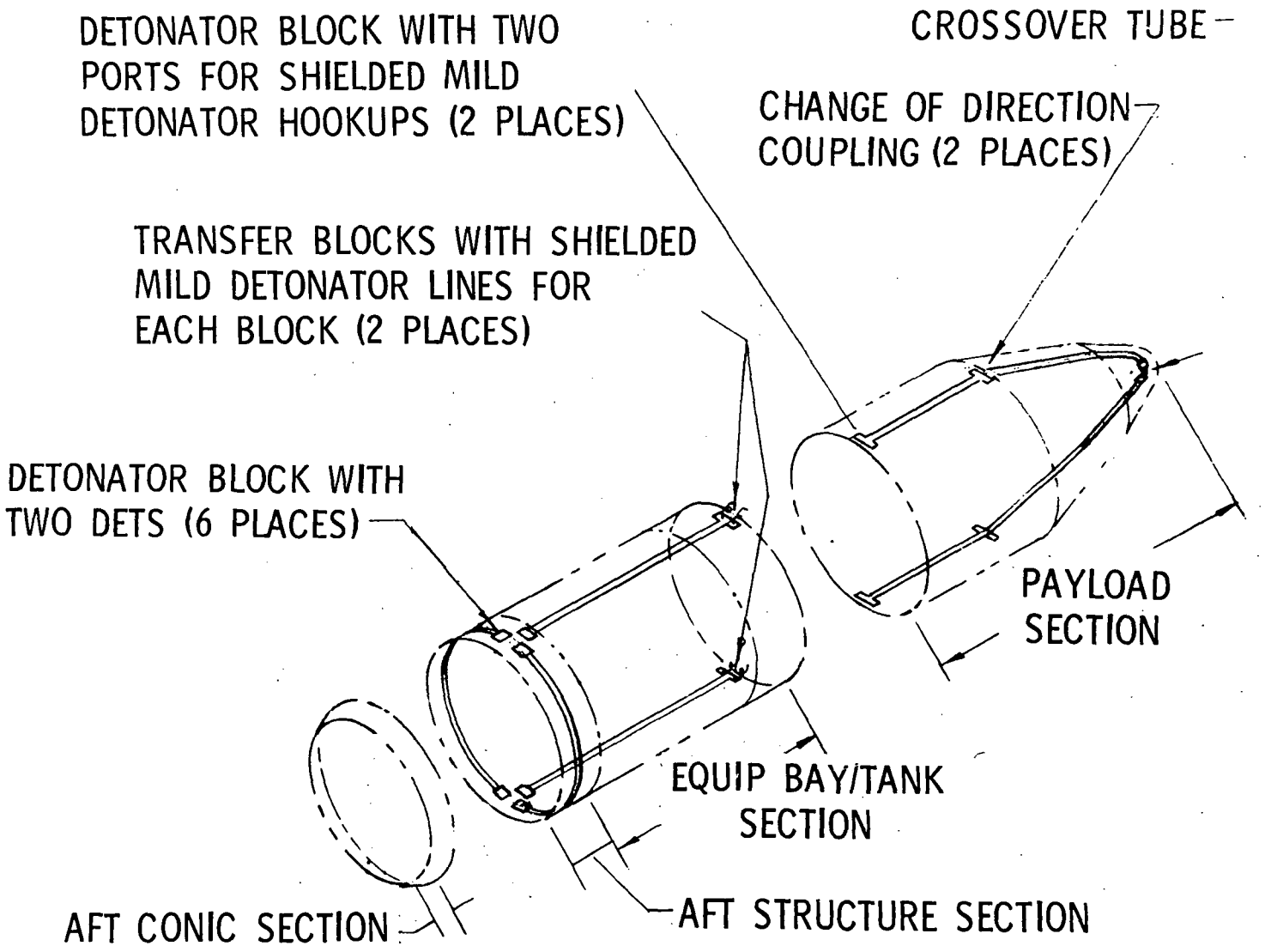

CS-59376

FIGURE VII-3 CSS SUPER-ZIP SEPERATION JOINT ARRANGEMENT

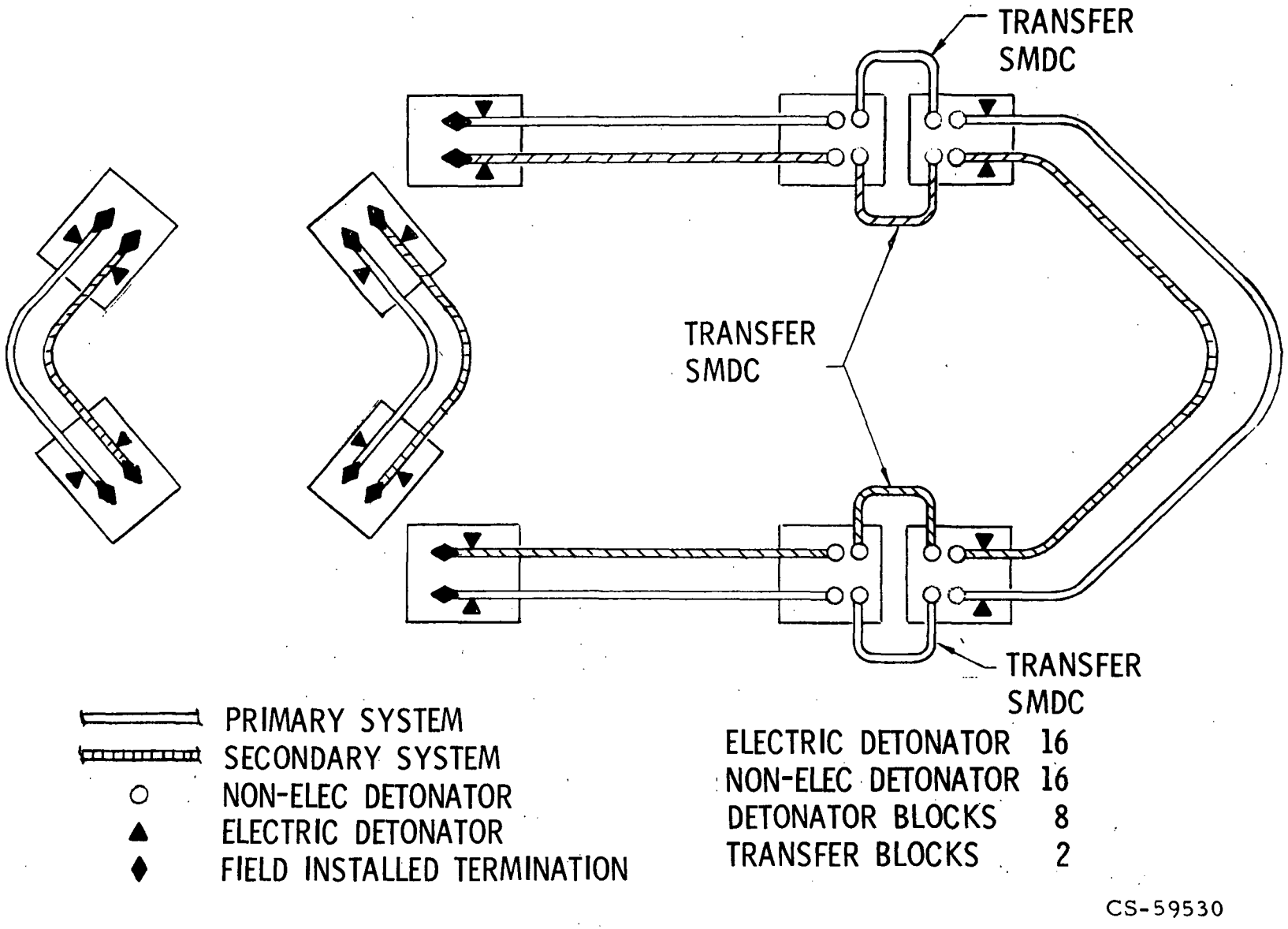

FIGURE VII-4 SUPER-ZIP SYSTEM SCHEMATIC

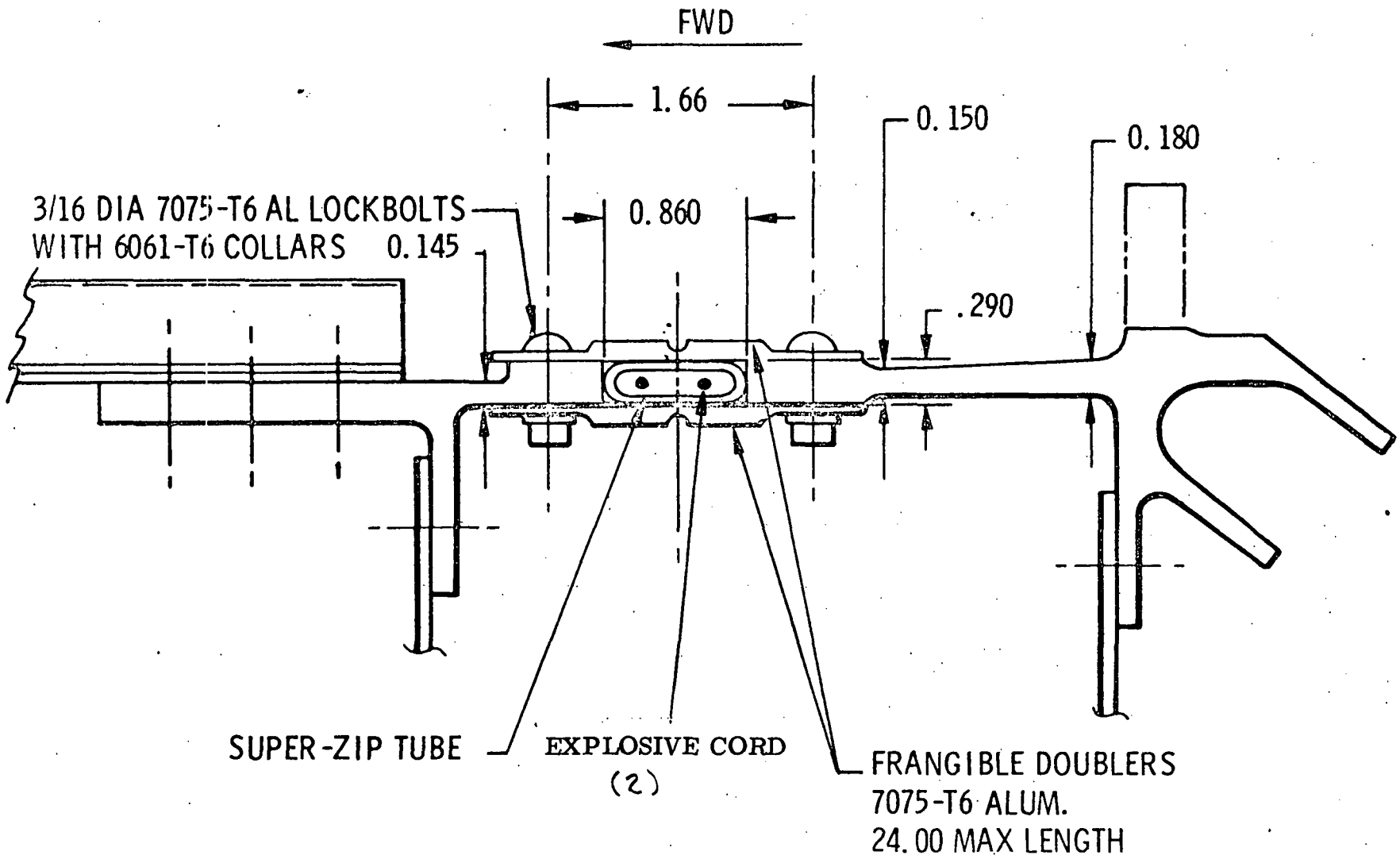

FIGURE VII-5 CROSS SECTION THROUGH SUPER-ZIP CIRCUMFERENTIAL SEPERATION JOINT

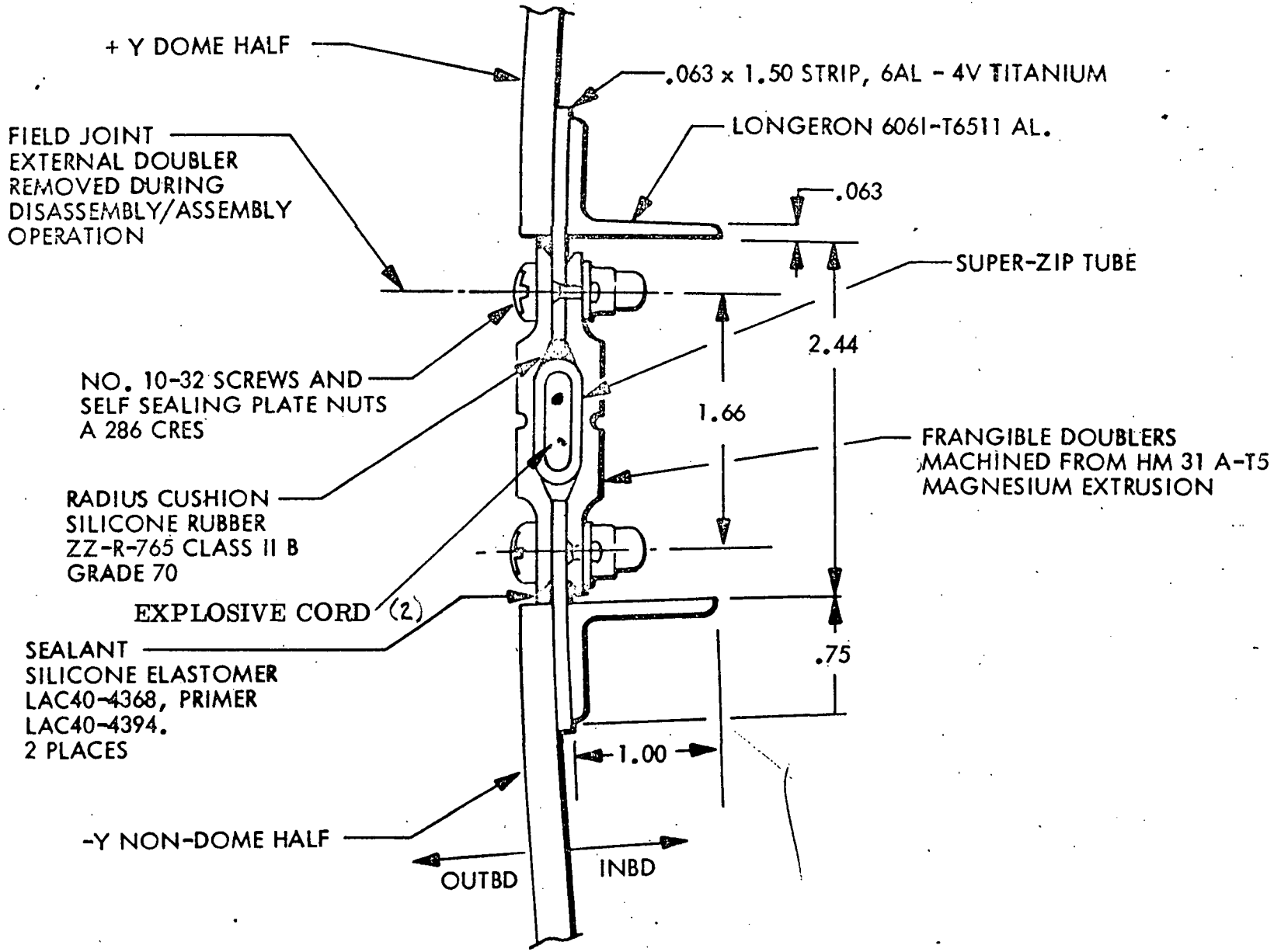

FIGURE VII-6 CROSS SECTION THROUGH SUPER-ZIP LONGITUDINAL SEPERATION JOINT

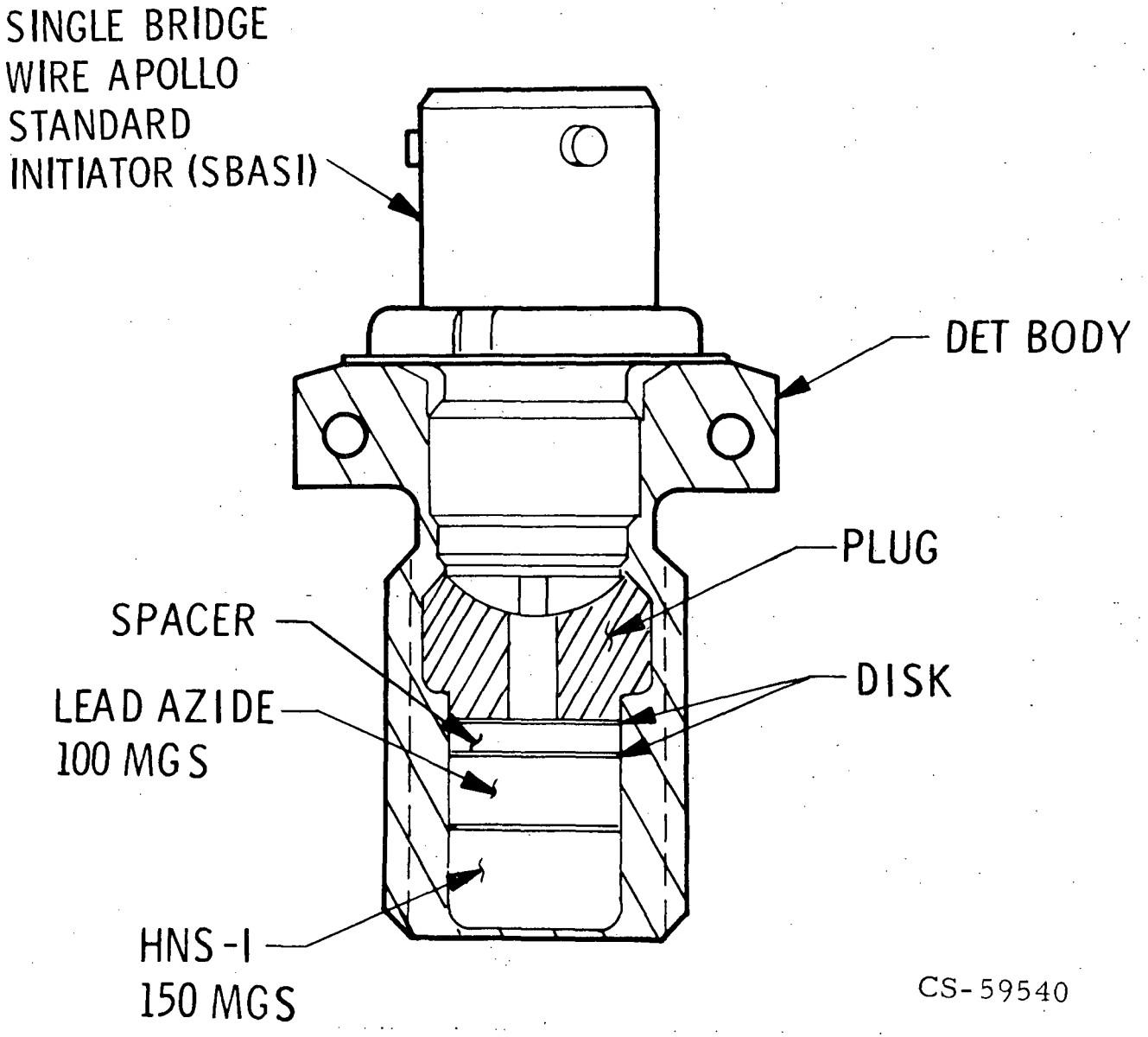

FIGURE VII-7 SUPER-ZIP DETONATOR CONFIGURATION

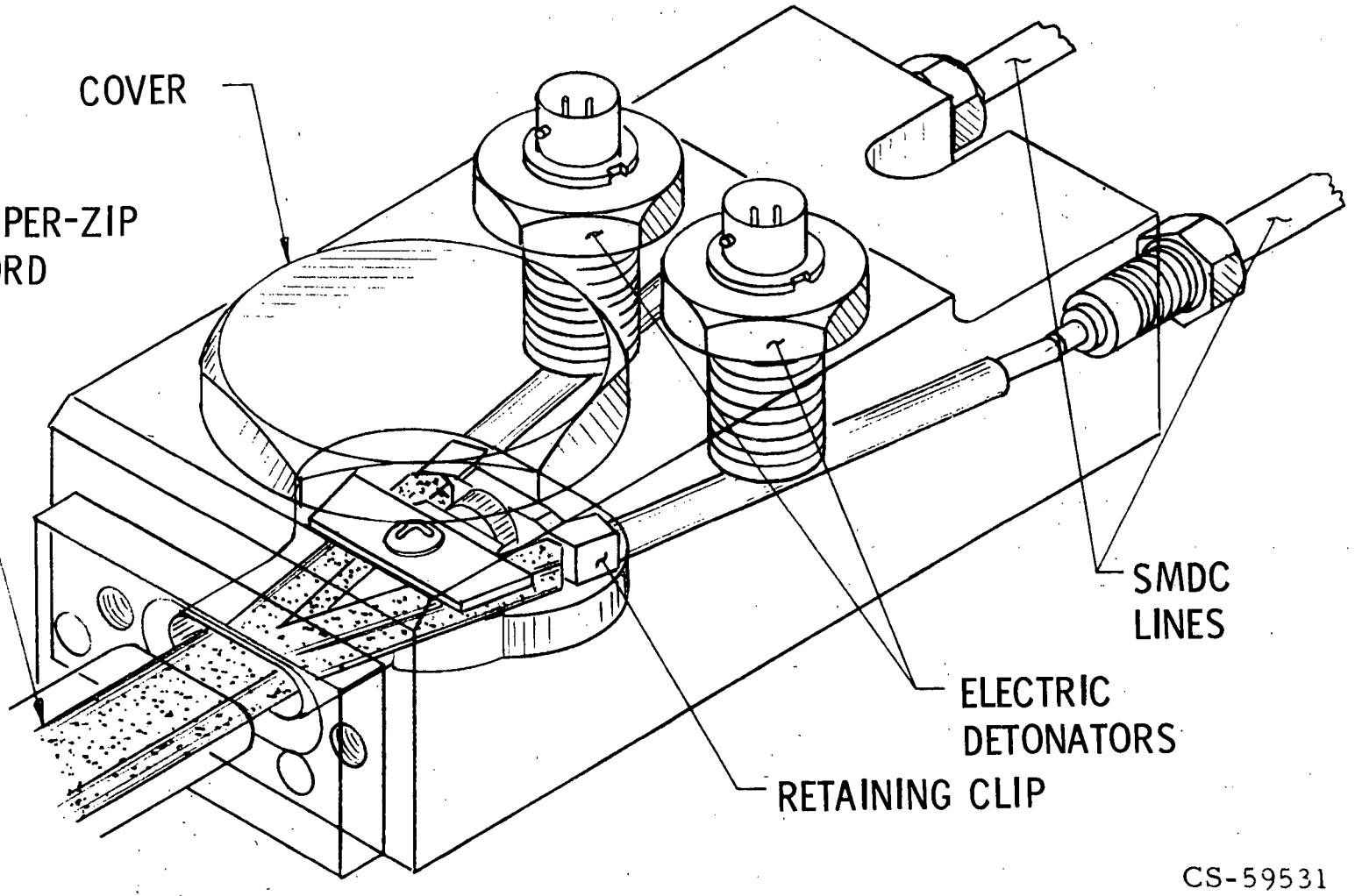

FIGURE VII-8 SUPER-ZIP DETONATOR BLOCK DETAILS

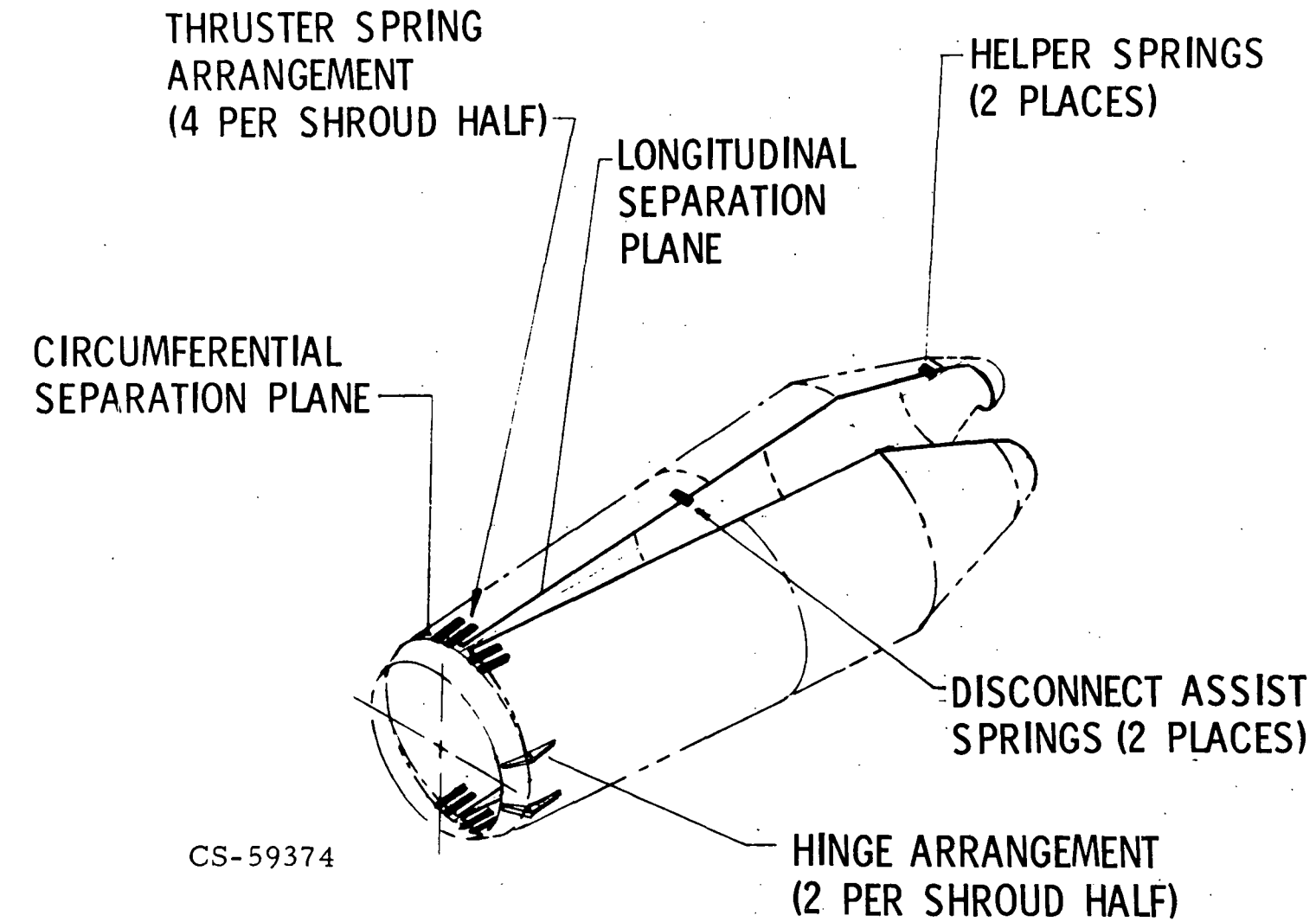

FIGURE VII-9 CSS JETTISON THRUSTER SPRING AND HINGE ARRANGEMENT

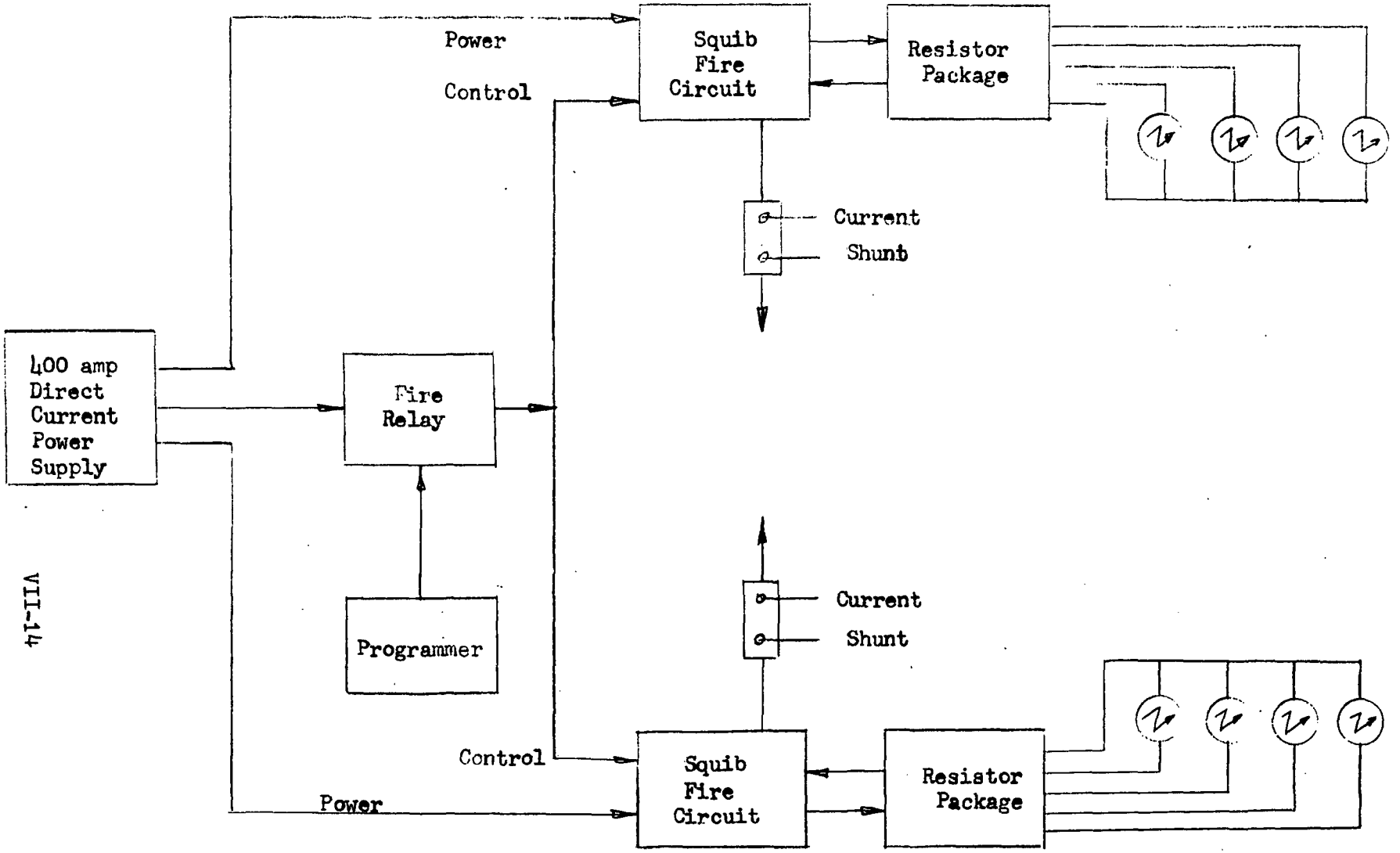

FIGURE VII - 10 SCHEMATIC OF SUPER-ZIP ELECTRICAL FIRING CIRCUIT USED DURING CSS CRYOUNLATCH TESTS

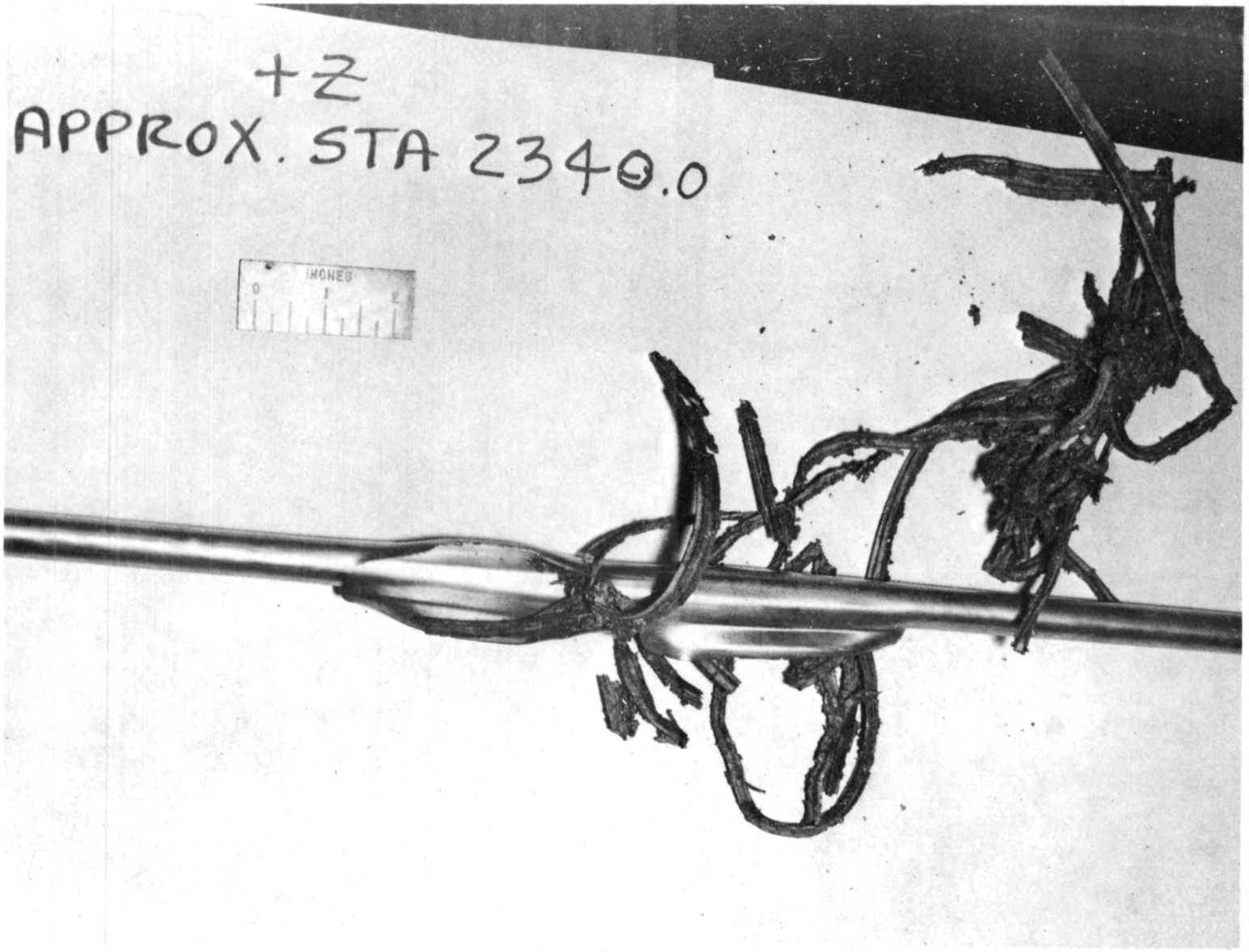

FIGURE VII-11 TYPICAL RUPTURE OF SUPER-ZIP TUBE DURING CRYOUNLATCH TEST NO 1 and 2

VIII. CENTAUR AND SUPPORTING STRUCTURES

by T. L. Seeholzer and R. T. Barrett

SUMMARY

The Centaur truss adapter, the equipment module, and the interstage adapter all were structurally adequate during the cryo-unlatch test program. The Centaur forward bearing reaction system struts separated and retracted properly during all tests, and showed no structural degradation.

HARDWARE DESCRIPTION AND RESULTS

Centaur Truss Adapter

The Centaur truss adapter, as shown in Figure VIII-1, supports the spacecraft on the Centaur. The adapter consists of 24 aluminum tube struts, mounted to the forward end of the Centaur stub adapter. Other than supporting the payload model used in the test program, the adapter was not loaded structurally. No problems were encountered.

Centaur Equipment Module

The Centaur equipment module is shown in Figure VIII-2. It is a truncated aluminum skin and stringer structure which supports the Centaur electronic equipment packages. More pertinent to these tests however, were the two electrical disconnect panels mounted at 66° and 252° at the base of the module as shown in Figure VIII-3. Electrical, instrumentation, and RF cables are connected from the Centaur to the CSS at these two points. At the time of CSS separation, these cables are disconnected by lanyards attached to connectors on the disconnect panel. Each connector/disconnect has a primary and secondary disconnect mode. The primary disconnect mode imposes a 30 pound load on the CSS, while the secondary disconnect mode imposes approximately a 300 pound load.

The electrical, instrumentation, and RF disconnects functioned properly in all three cyro-unlatch tests. On cryo-unlatch test no. 2, one electrical disconnect at 252° and one RF disconnect at 66° were purposely assembled to function in the secondary modes. Both disconnected satisfactorily.

Forward Bearing Reaction System

The Centaur Forward Bearing Reaction (FBR) system consists of six spring loaded struts between the Centaur and the CSS at station 2460, as shown in Figure VIII-4. Strut details are shown in Figure VIII-5. This system provides load sharing, and limits the relative deflection between the CSS

and Centaur. These struts are separated by redundant explosive bolts as described in Section VII. Retraction of the strut halves is accomplished by springs attached to the CSS and the Centaur stub adapter.

The FBR struts were successfully separated and retracted on all cryo-unlatch tests. Post test inspection revealed no functional or structural problems in the struts or attaching hardware.

Centaur Interstage Adapter

The Centaur interstage adapter is shown in Figure VIII-6. It provides the transition from the Titan skirt to the Centaur stage. It also provides the bottom attach point for the CSS on a ring located midway up the adapter. The adapter is of aluminum skin and stringer riveted construction.

The cryo-unlatch test loading conditions were, in general, non-critical for the interstage adapter. As a result, only a few strain gages were monitored. Of the gages monitored, only three indicated stresses above "noise levels" of the instruments. One gage (no. 4157) located on the outboard flange of the boattail support ring gave instantaneous readings up to 36,000 psi (versus a yield stress of 42,000 psi). However, averaged readings were in the order of 14,000 psi. The second highest instantaneous gage reading was 20,900 psi, this too also in the boattail. In summary, the stresses on the interstage adapter were not critical, and no apparent yielding occurred.

SUPPORT PAYLOADS ~12 000 LB; WILL BE STRUCTURALLY TESTED

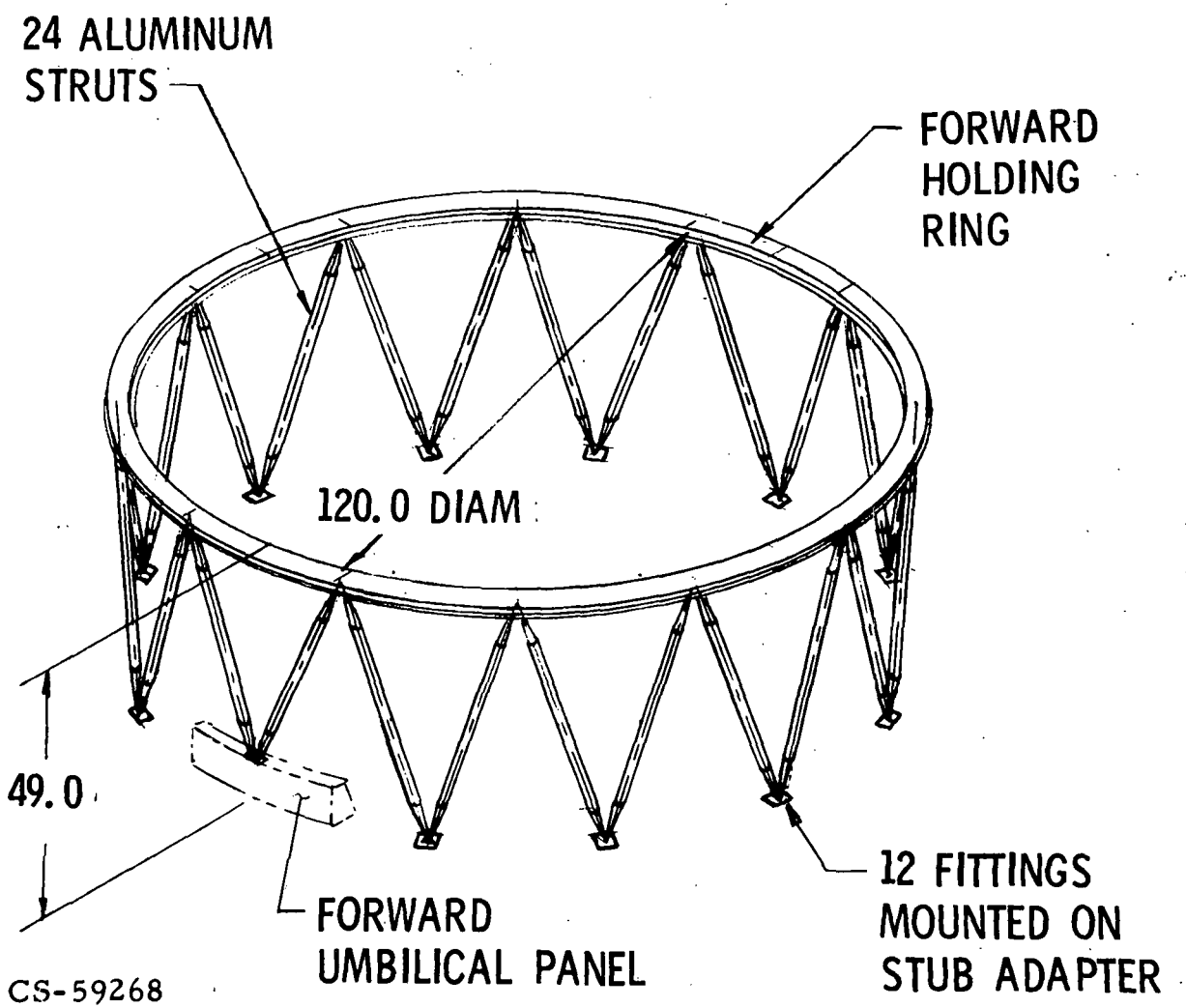

FIGURE VIII-1 CENTAUR TRUSS ADAPTER

ALUMINUM RING, SKIN, AND STRINGER CONSTURCTION;
SUPPORTS PAYLOADS 500 TO 4 000 LB; IDENTICAL TO D-1A

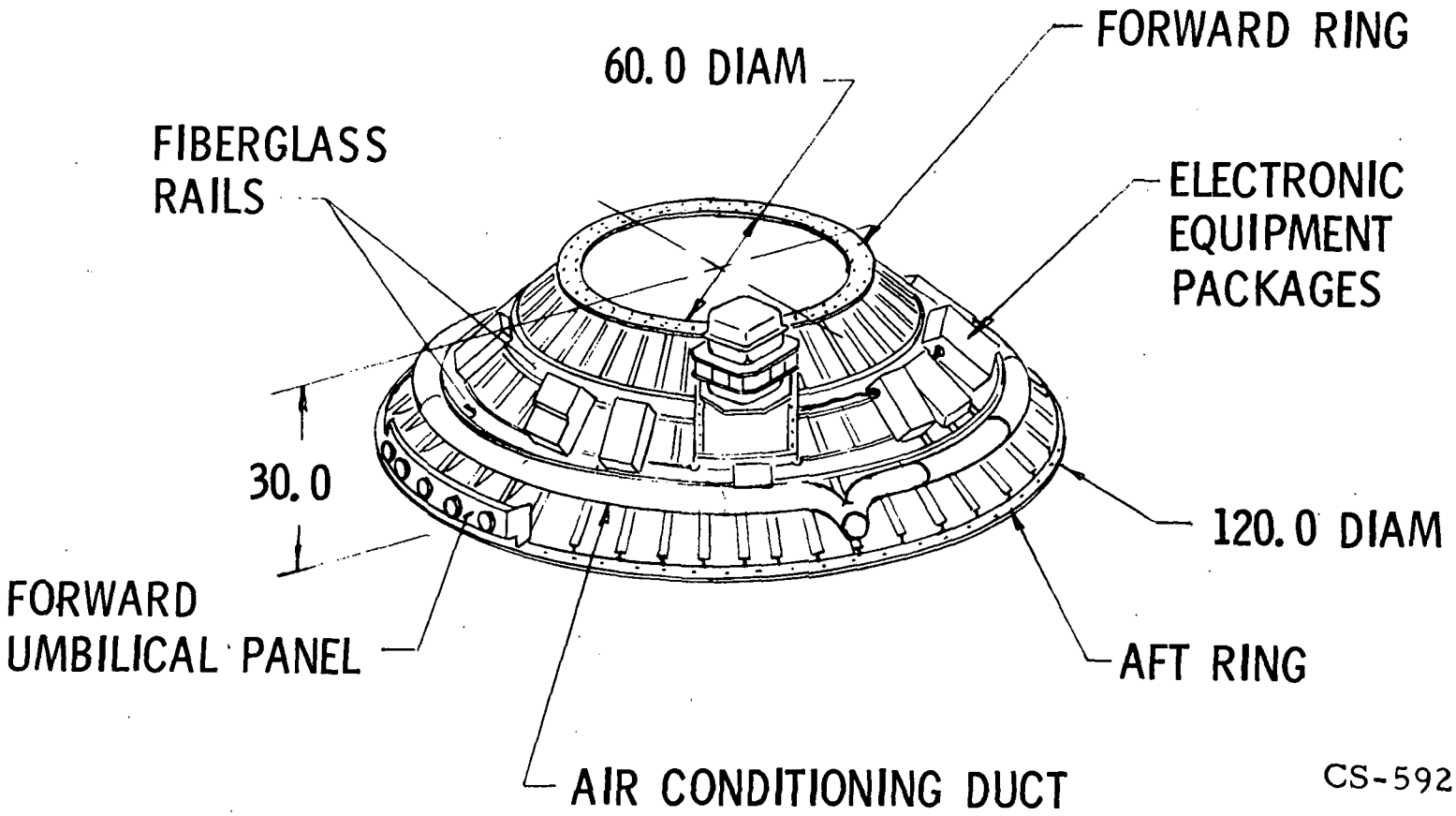

FIGURE VIII-2 CENTAUR EQUIPMENT MODULE

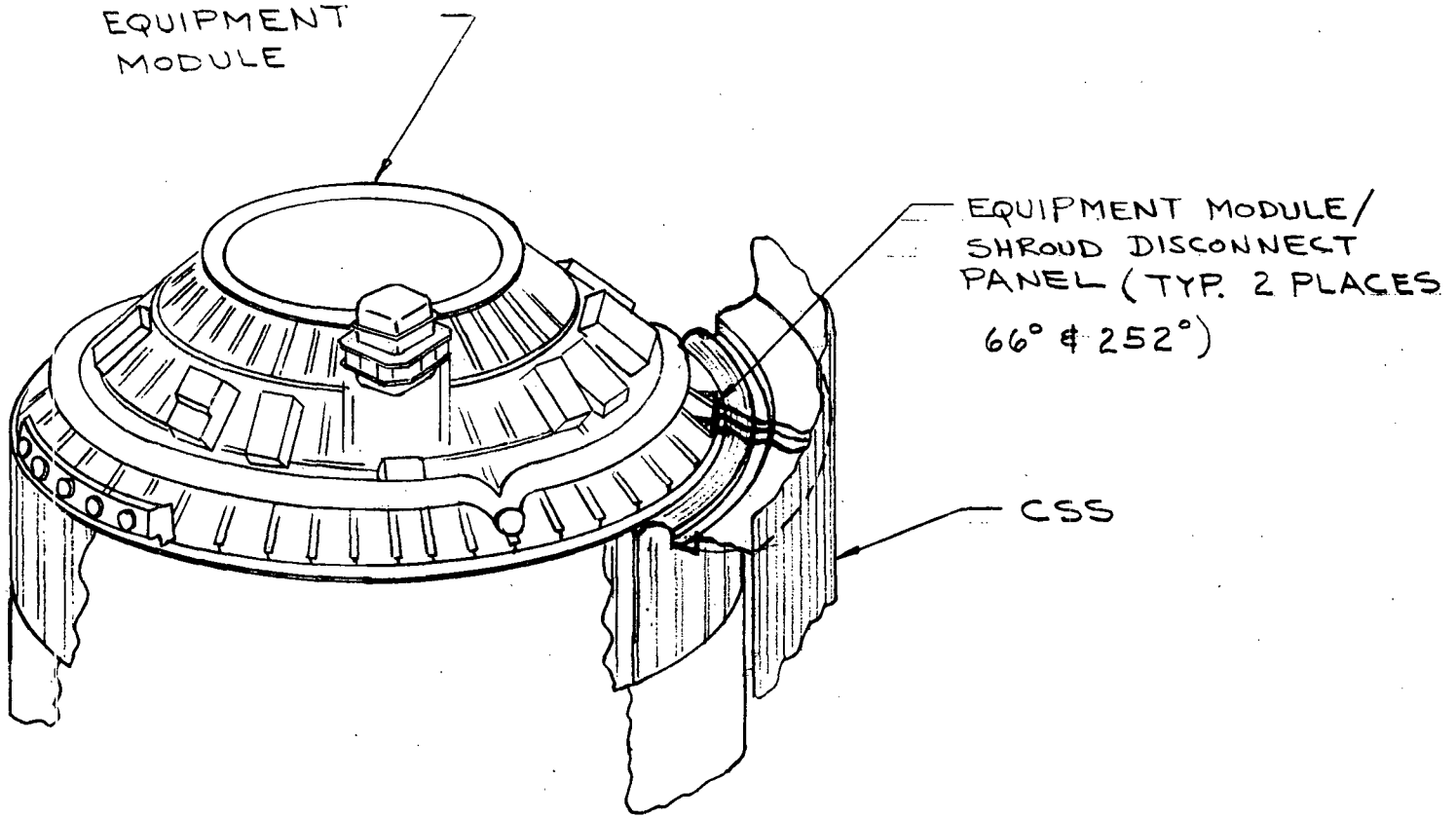

FIGURE VIII-3 CENTAUR EQUIPMENT MODULE ELECTRICAL DISCONNECT LOCATIONS.

PERMITS LATERAL LOAD SHARING; LIMITS DIFFERENTIAL DEFLECTIONS; STRUCTURALLY TESTED AT PLUM BROOK

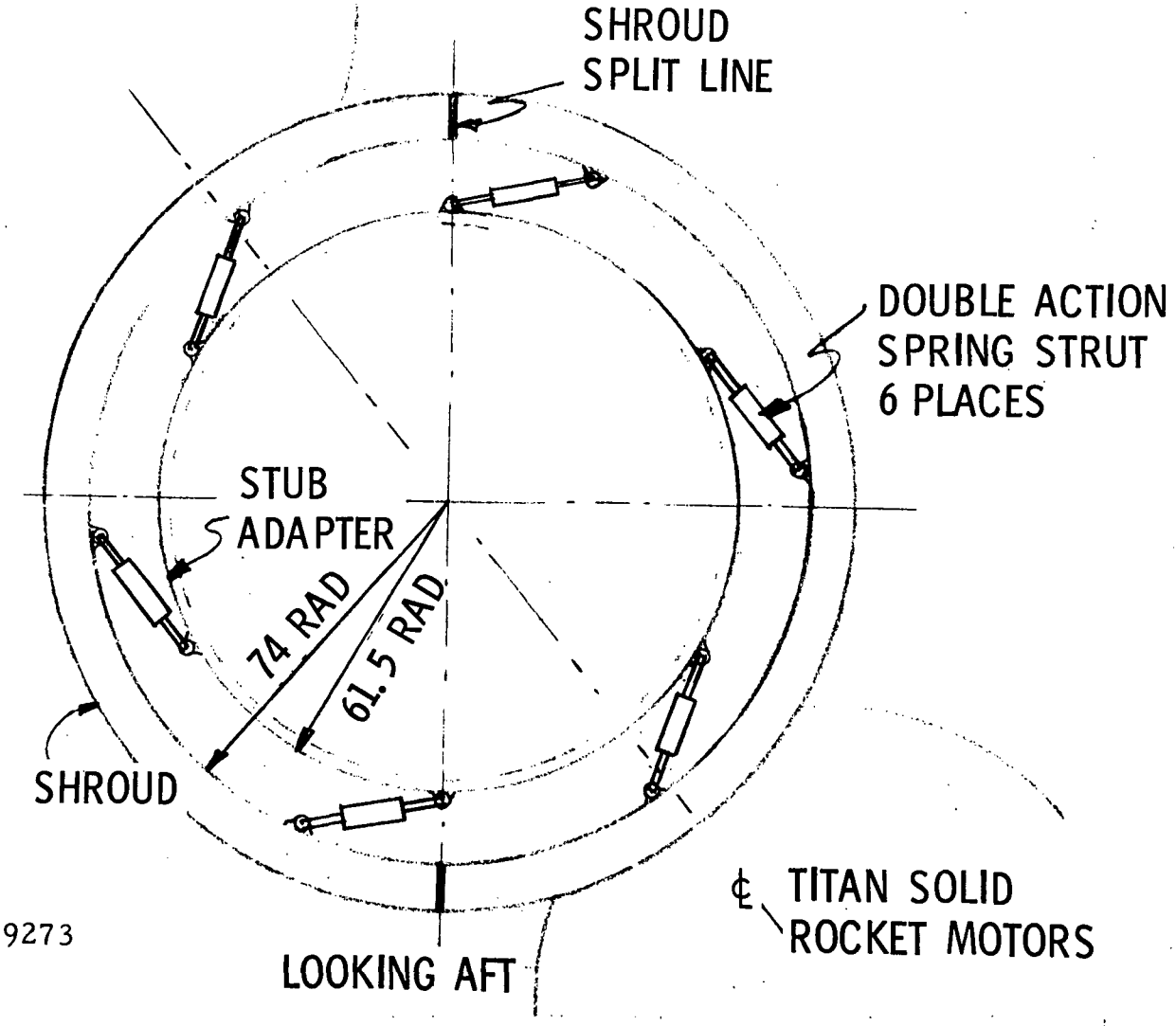

FIGURE VIII-4 CENTAUR FORWARD BEARING REACTOR STRUT LOCATIONS

DESIGN QUALIFIED BY STRUCTURAL AND SEPARATION TESTING

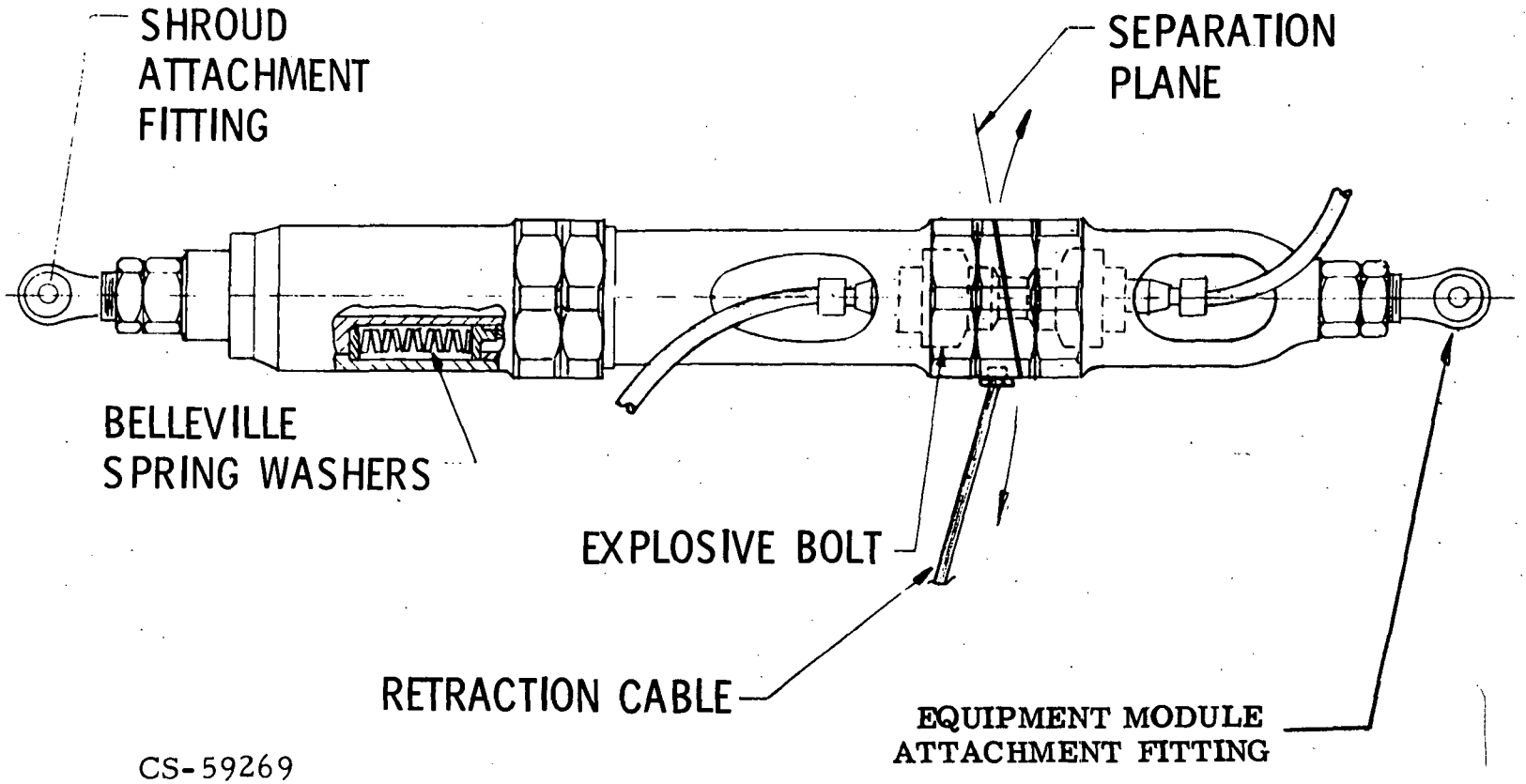

FIGURE VIII-5 CENTAUR FORWARD BEARING REACTOR STRUT CONFIGURATION

ALUMINUM RING, SKIN, AND STRINGER RIVETED CONSTRUCTION;
STRUCTURALLY TESTED AT PLUM BROOK

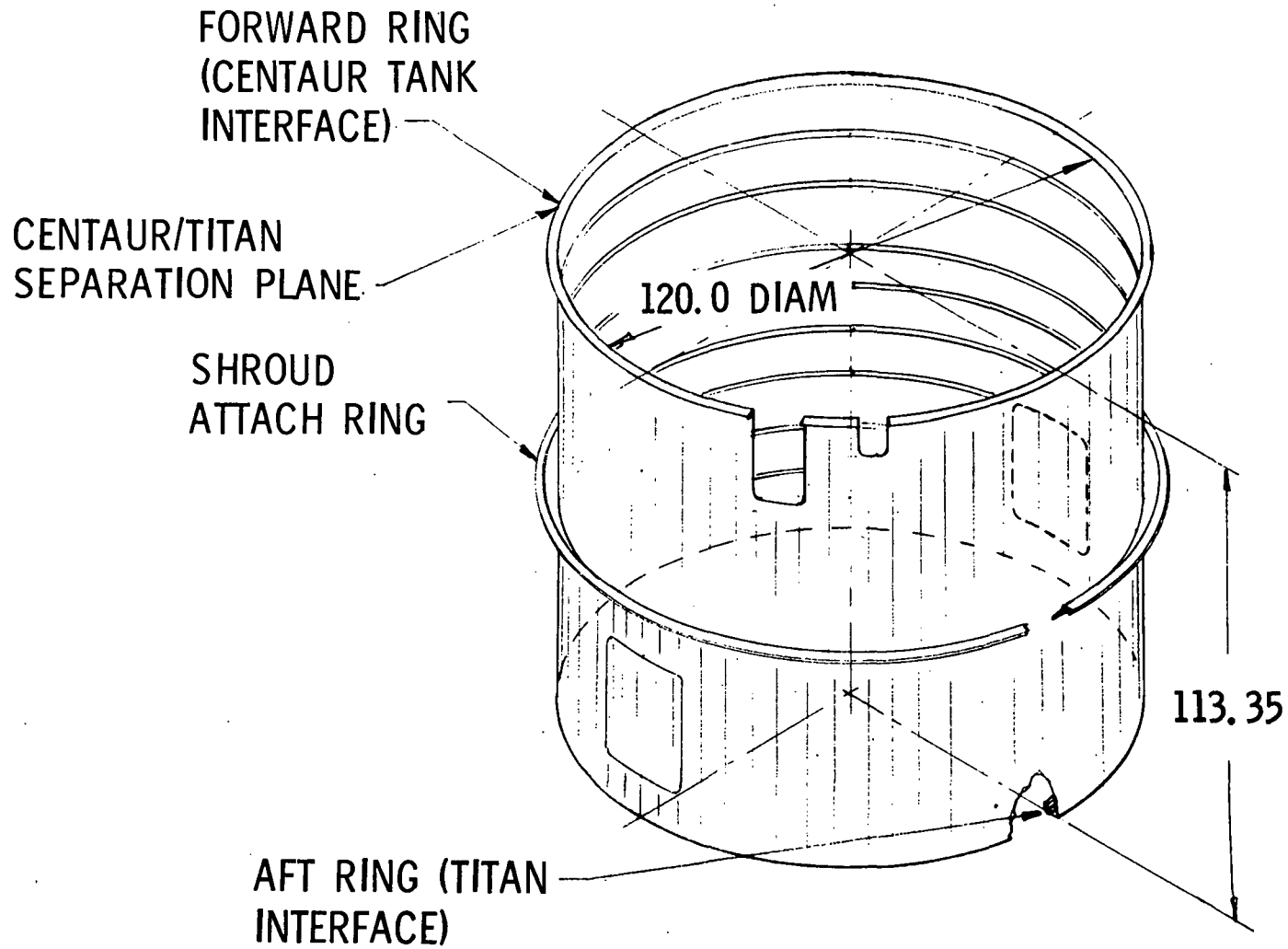

FIGURE VIII-6 CENTAUR INTERSTAGE ADAPTER

IX. SHROUD STRUCTURES

By G. S. Sarvay

SUMMARY

The three cryo-unlatch tests performed indicated that from a structural standpoint, the CSS has successfully demonstrated the ability to separate and partially jettison under a cryogenic environment with no observed structural degradation. The hinge loads for cryo-unlatch tests nos. 1 and 2 were affected by a problem in the separation of the forward seal from the shroud. The "hang-up" of the forward seal caused large radial displacement of the shroud split lines which resulted in larger than expected unsymmetric hinge loads. A redesigned forward seal release mechanism was utilized during test no. 3 and significantly improved the seal separation from the shroud. Since the test configuration for test no. 3 is representative of the flight article, data obtained from the test should be considered as the basis of comparison with heated jettison tests and flight vehicle performance.

HARDWARE DESCRIPTIONS

The Centaur Standard Shroud (CSS) structural system configuration is shown in figure IX-1. The metal clam shell structure encloses the entire Centaur vehicle and is mounted at its aft end (station 2180.48) to the General Dynamics' Convair Aerospace Division interstage adapter structure. The overall height of the shroud structure is approximately 687 inches, while its major diameter is 168 inches. The nose cone section is a biconic configuration with a 25 degree forward cone and a 15 degree aft cone. The 24 inch radius stainless steel nose cone dome was not used during the tests. The biconic skins are made from magnesium-thorium sheets which are strengthened by internal rings. The 168 inch diameter cylindrical portion of the shroud is constructed of an aluminum skin which is stiffened by external corrugated stiffeners and internal aluminum rings. The cylindrical portion of the shroud is mated to the 120 inch diameter interstage adapter by a conical transition boattail section which has a reentrance angle of approximately 37.4 degrees. The construction in this region of the shroud is a ring-stringer stiffened aluminum skin.

After the shroud has been severed circumferentially and longitudinally, each half is separately ejected from the vehicle. The thruster springs and hinge system arrangement is schematically illustrated in figure IX-2. The eight longitudinal thruster springs located at the base of the shroud are designed to provide the main jettison force. The structural arrangement of the pair of hinge brackets mounted at the base of each shell half is shown in figures IX-2 and IX-3. The forward hinge fitting is attached to the jettisonable portion of the shroud. The aft hinge fitting and support structure remain with the vehicle. The functions of the hinges are to control the pivot action and release of the shroud halves.

The sequence of events during the jettison of the shroud halves is shown in figure IX-4. The left sketch shows the pre-separated configuration of the aft separation joint and hinge mechanism. Upon severing of the shroud into half shells, the longitudinal thruster springs push the shroud forward until the upper pin contacts the cam surface of the fixed lower fitting as shown in the center sketch. The springs continue to apply their stored force until the center of gravity of the shroud is approximately over the lower pin. At this time the force is transferred to the lower pin for approximately 60 degrees of shroud rotation before separating from the vehicle. During the cryo-unlatch tests the total shroud rotation was limited to approximately 8 degrees by the catcher system.

RESULTS AND DISCUSSION

One of the primary structural objectives of the tests was to determine the hinge loads experienced during the jettison event. Strain gages were mounted on the aft hinges and support structure in order to predict the loads during jettison. Figures IX-5 and IX-6 display the arrangement of the strain gages and deflectometers which were used during the third cryogenic unlatch test. The Test Requirements Document (reference 2) should be referred to for test requirement or instrumentation details. The gages (A) located on the forward surface (tension hooks) of the aft hinges provide the most direct method for estimating axial tension loads.

Figure IX-7 delineates the approximate correlation between measured stress levels and applied loads during the initial application of tension loads. The relationship is:

$$P_x = -0.513 f_A$$

A comparison of the initial hinge tension loads for each of the three cryo-unlatch tests is shown in Table IX-1. The anomalous behavior in the hinge load data for tests nos. 1 and 2 can be directly attributed to the conditions which resulted from the forward seal "hang-up" during the jettison event. The maximum test loads in each of tests nos. 2 and 3 are approximately uniform for all hinges except for the 77 degree hinge. The deviation in the test results for the 77 degree hinge could have been introduced by poor surface contact, misalignment or improper calibration of the strain gage (A).

All the maximum stress and deflection results from the third test are tabulated in Table IX-2. The time of maximum tension loads occurred approximately 60 milliseconds after initiation of shroud separation. A majority of the maximum recorded axial deflections occurred later in time and ranged between 30 to 240 milliseconds after separation.

Figures IX-8 through IX-11 present plots of the aft hinge upper surface stresses, (gage (A), figure IX-4), during the first three seconds of shroud motion. The initiation of shroud separation is time zero on the figures. Also, during the same time sequence the stresses (gage D, figure IX-4) for the hinge support brackets are shown in figures IX-12 through IX-15. The plots indicate that the hinge loads consist of a damped response about a steady state rigid body tension load. The rigid body hinge loads result from the reaction loads at the hinges due to the rigid body rotation of the shroud shells.

CONCLUSIONS

1. From a structural standpoint, the CSS successfully demonstrated the ability to separate and jettison from a cryogenic vehicle configuration under atmospheric conditions.

2. Test data results and visual inspection from the three CSS cryo-unlatch tests indicate that no structural degradation or anomalies occurred as a result of the cryogenic environment, the separation and jettison sequences, and subsequent restraint by the catcher net system.

3. The hinge loads measured during CSS jettison were significantly less than design loads. Flight vehicle hinge loads can be determined by correlating the stress data between the aft hinge and hinge support bracket.

TABLE IX-1 MAXIMUM AXIAL TENSION LOADS ON HINGES AT TIME 0+

(INITIATION OF SHROUD SEPARATION)

HINGE LOCATION	TENSION LOAD P_X LBS.		
	TEST 1	TEST 2	TEST 3
77°	7800	3820	2680
103°	11000	6150	6350
257°	5290	5440	5900
283°	6050	5480	5150

TABLE IX-2 MAXIMUM STRESSES AND DEFLECTIONS FOR TEST NO. 3

INSTRUMENT NUMBER	PRE-TEST VALUE	TEST VALUE	TOTAL VALUE
4601S	84	-12,297	-12,381 PSI
4602S	169	- 6,402	- 6,571 PSI
4603S	42	6,718	6,676 PSI
4647S	- 84	- 5,307	- 5,223 PSI
4648S	INOPERATIVE		
4649S	211	4,660	4,450 PSI
4652S	211	- 9,813	-10,025 PSI
4653S	211	- 4,507	- 4,719 PSI
4654S	338	4,072	3,734 PSI
4657S	297	-11,202	-11,500 PSI
4658S	211	- 5,012	- 5,223 PSI
4659S	296	6,382	6,086 PSI
4695S	81	2,314	2,233 PSI
4696S	142	2,133	1,990 PSI
4697S	101	3,522	3,421 PSI
4698S	20	1,811	1,791 PSI
5009D	-.0035	.1435	.147 INCHES
5010D	.0050	-.1220	-.127 INCHES
5011D	.0025	.2160	.213 INCHES
5012D	-.0025	-.2640	-.266 INCHES
5017D	.0003	-.0508	-.051 INCHES
5018D	.0015	-.0680	-.069 INCHES
5061D	.0035	.240	.237 INCHES
5062D	.0045	.2815	.277 INCHES
5063D	INOPERATIVE		
5064D	-.0050	.2085	.203 INCHES
5069D	0	.2065	.206 INCHES
5070D	.0035	.3125	.309 INCHES
5071D	-.0045	.5715	.576 INCHES
5072D	-.0030	.5260	.529 INCHES

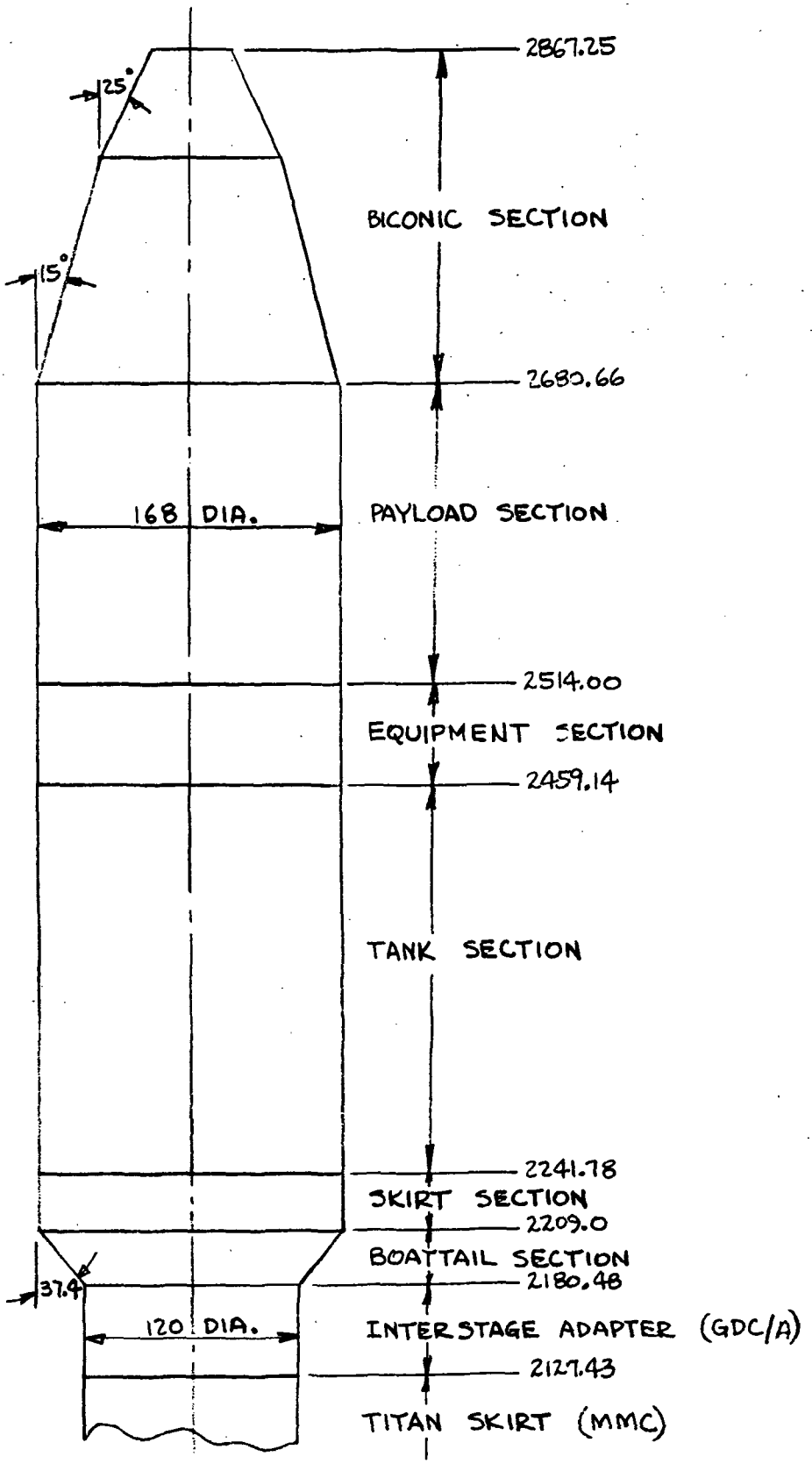

FIGURE IX-1 STRUCTURAL CONFIGURATION

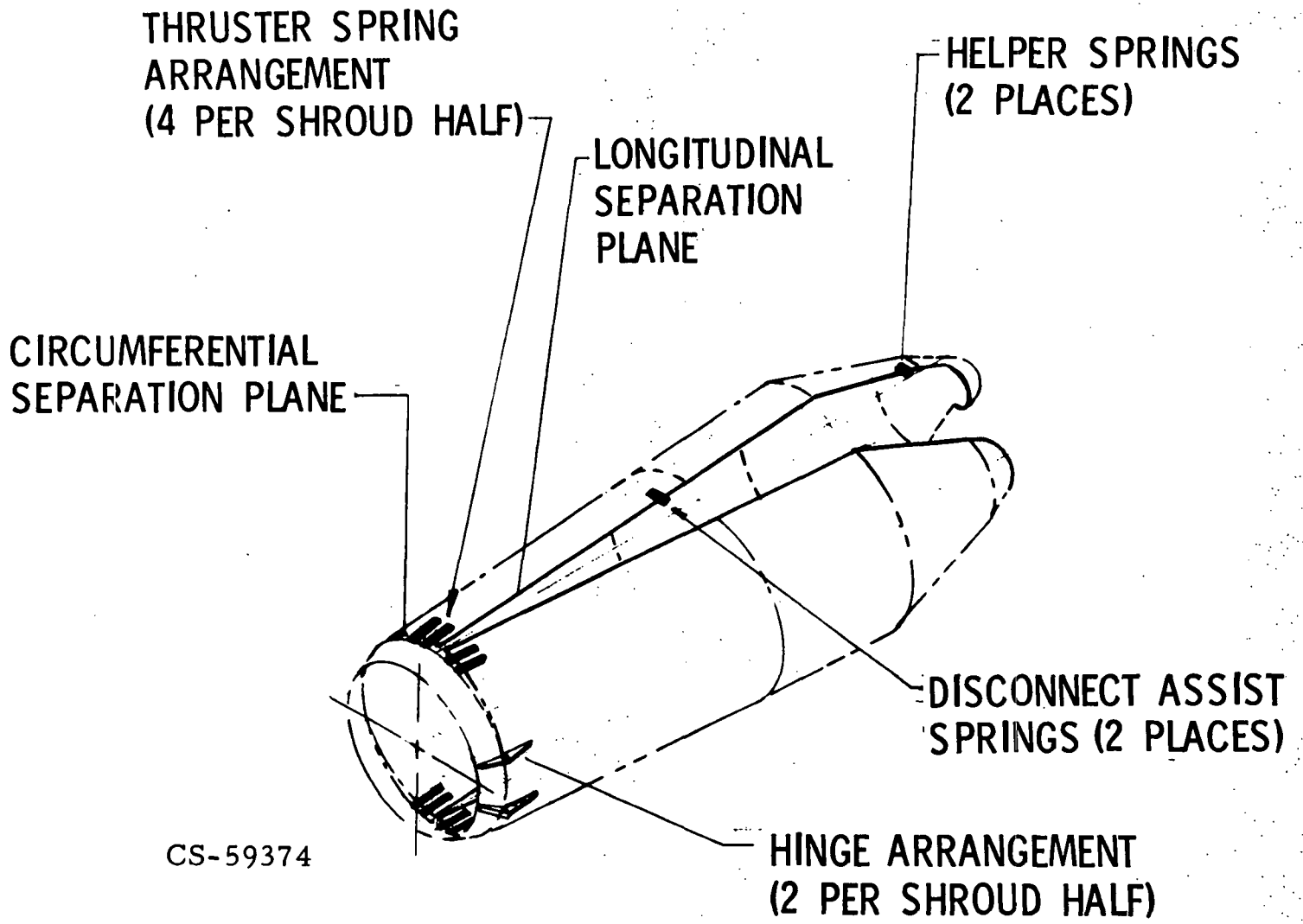

Figure IX-2 Thruster Spring/Hinge Arrangement

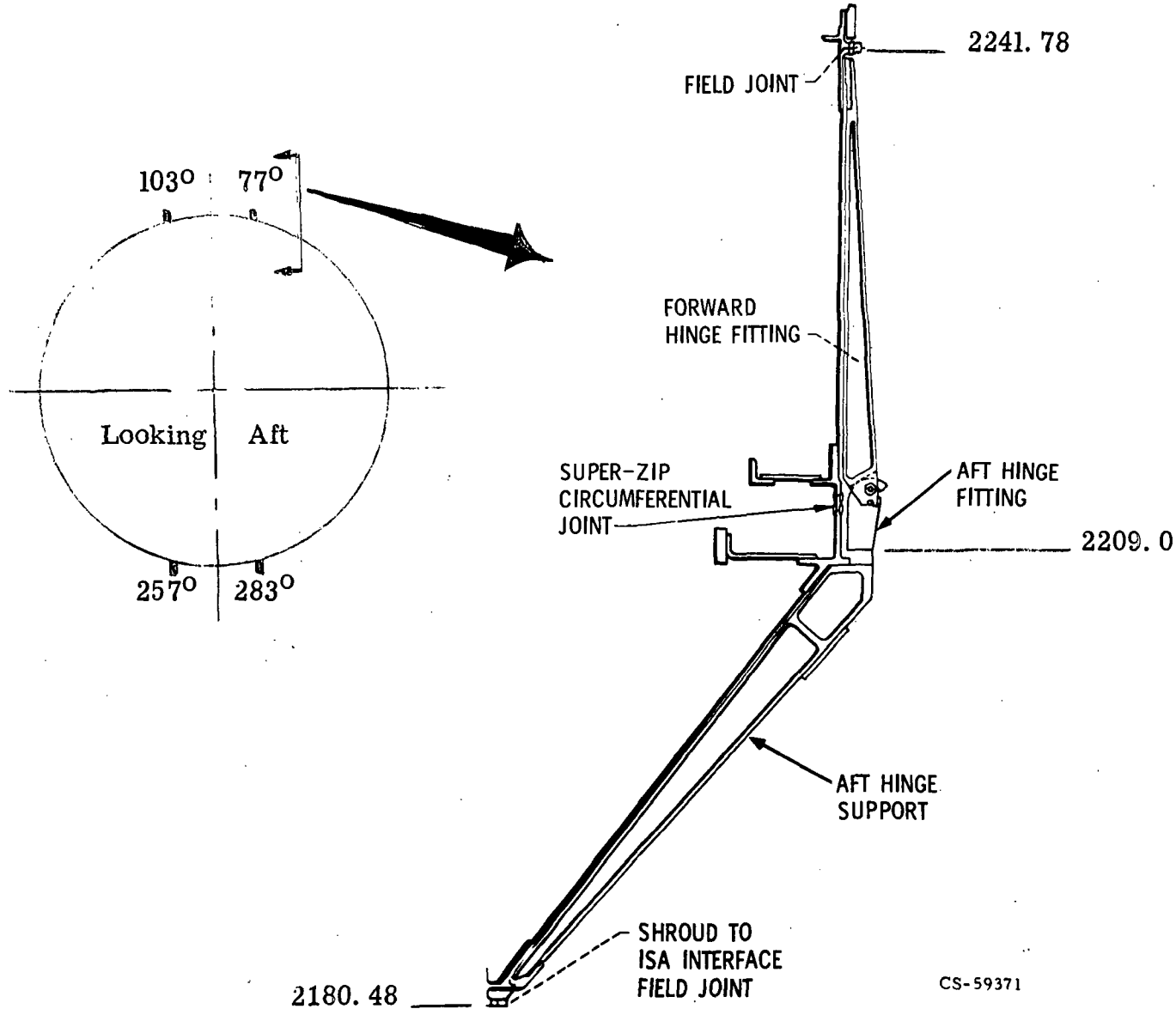

Figure IX-3 Hinge Structure Arrangement

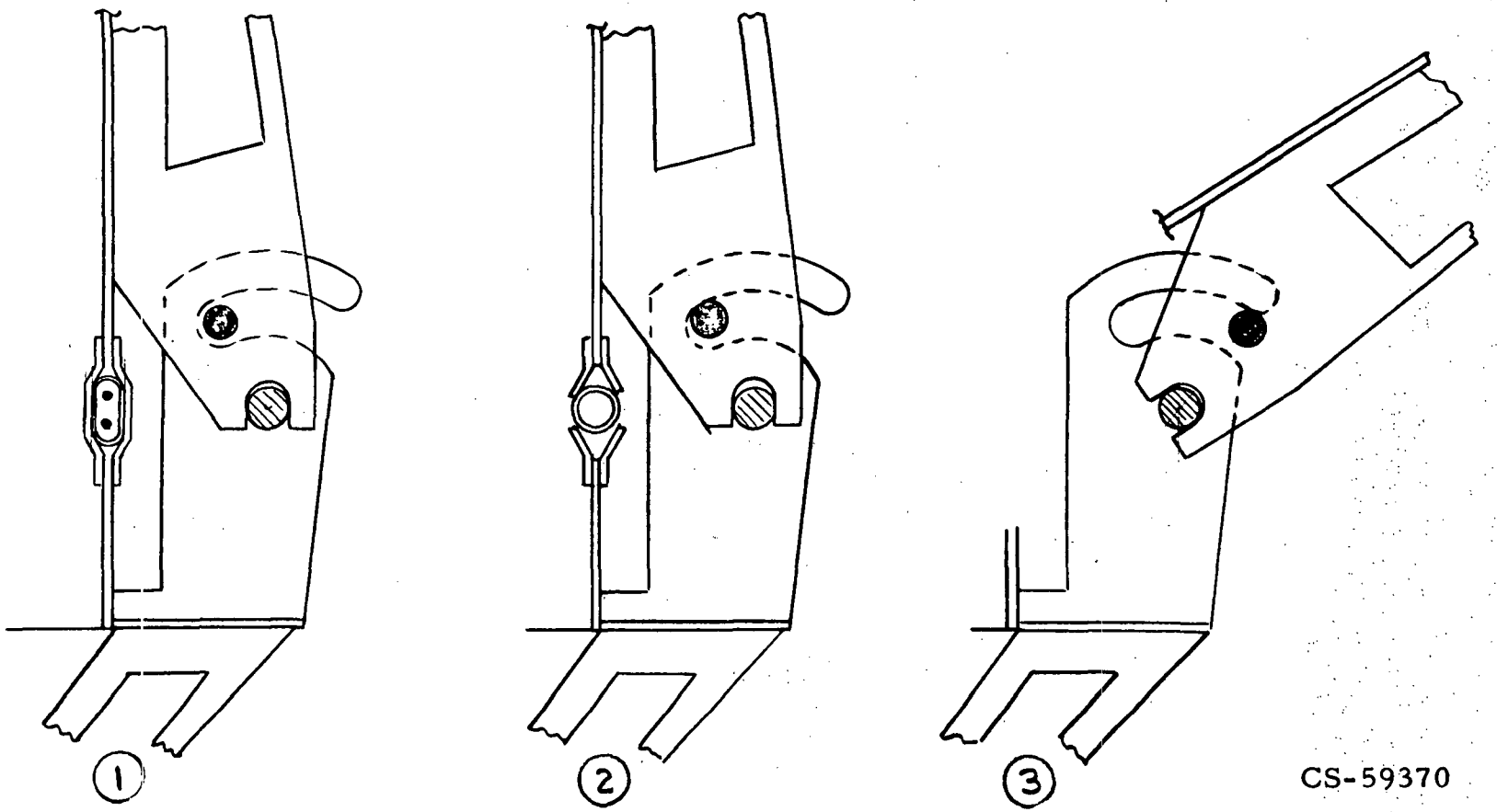

Figure IX-4 Jettison System Control

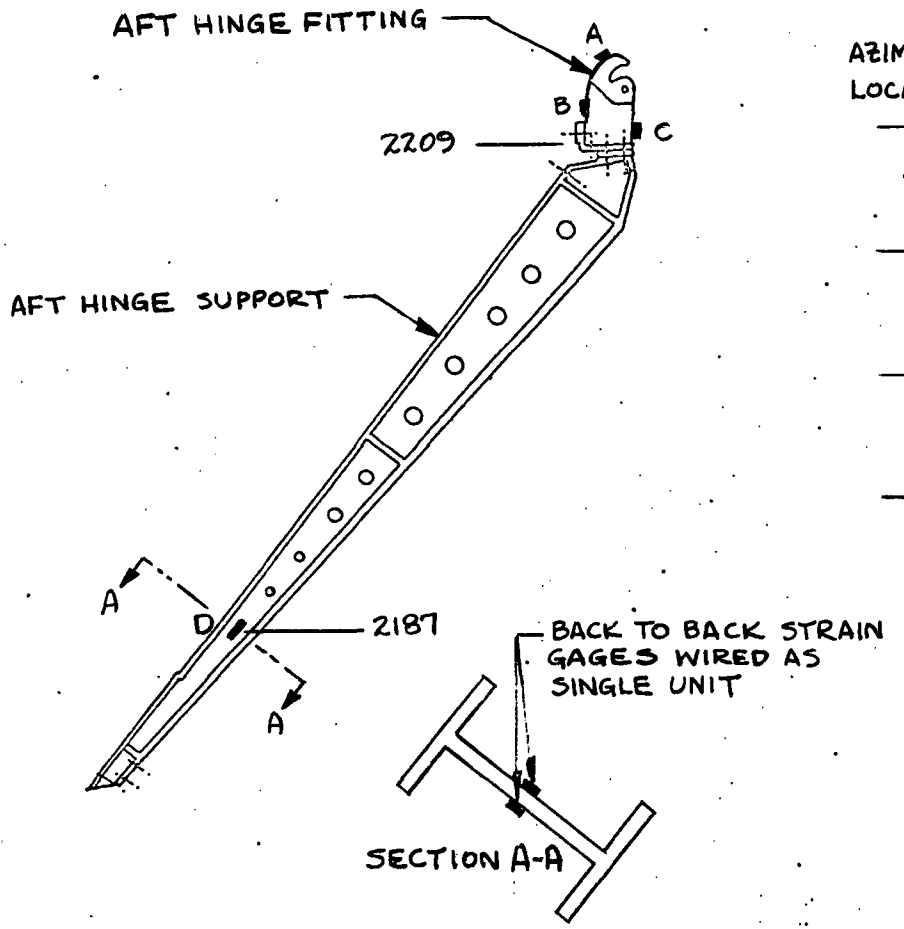

AZIMUTH LOCATION	GAGE LOCATION A	B	C	D
77°	4647S	4648S	4649S	4695S
103°	4601S	4602S	4603S	4698S
257°	4657S	4658S	4659S	4696S
283°	4652S	4653S	4654S	4697S

FIGURE IX-5 STRAIN GAGE LOCATIONS (TEST 3)

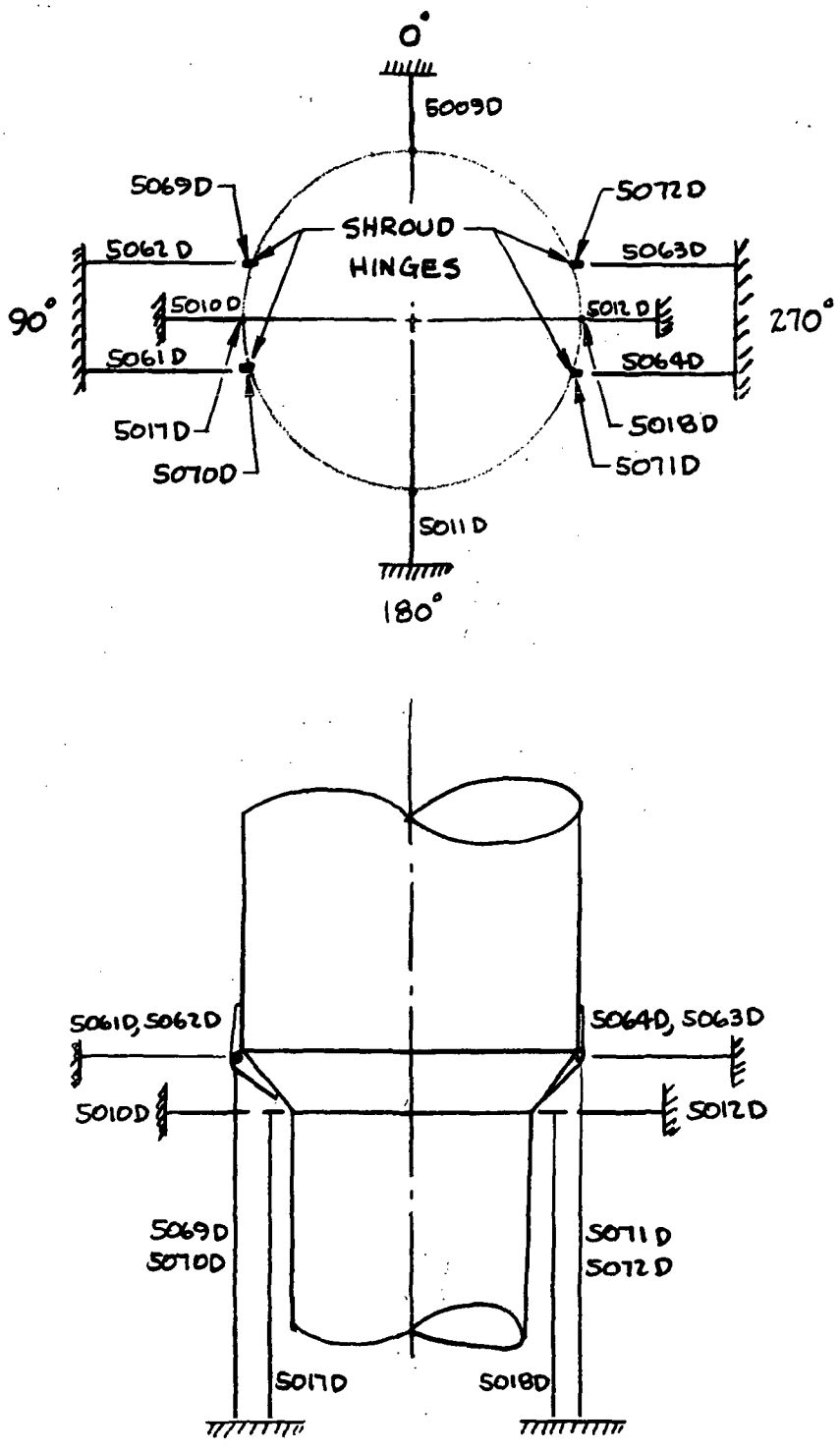

FIGURE IX-6 DEFLECTOMETER LOCATIONS (TEST3)

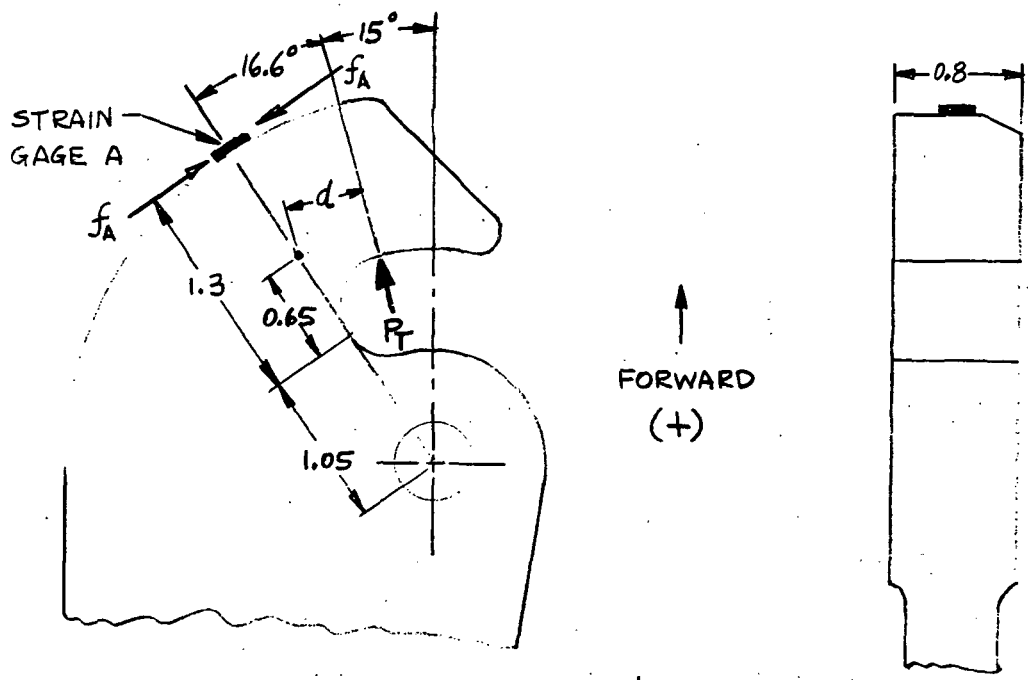

$$f_A = \frac{P_T \sin 16.6^\circ}{b\,h} - \frac{P_T\, d\left(\frac{h}{2}\right)}{\frac{b\,h^3}{12}}$$

Where :

P_T = Pin reaction at time 0^+
b = Thickness of hinge ~ 0.8 inches
h = Height of cross section ~ 1.3 inches
d = Moment arm ~ 0.486 inches

Therefore :

$$f_A = \frac{P_T \sin 16.6^\circ}{(.8)(1.3)} - \frac{6\,P_T(.486)}{(.8)(1.3)^2}$$

$$f_A = -1.885\,P_T$$

Axial Load:

$$P_X = P_T \cos 15^\circ = -\frac{f_A \cos 15^\circ}{1.885}$$

$$P_X = -0.513\,f_A$$

FIGURE IX-7 HINGE TENSION LOADS

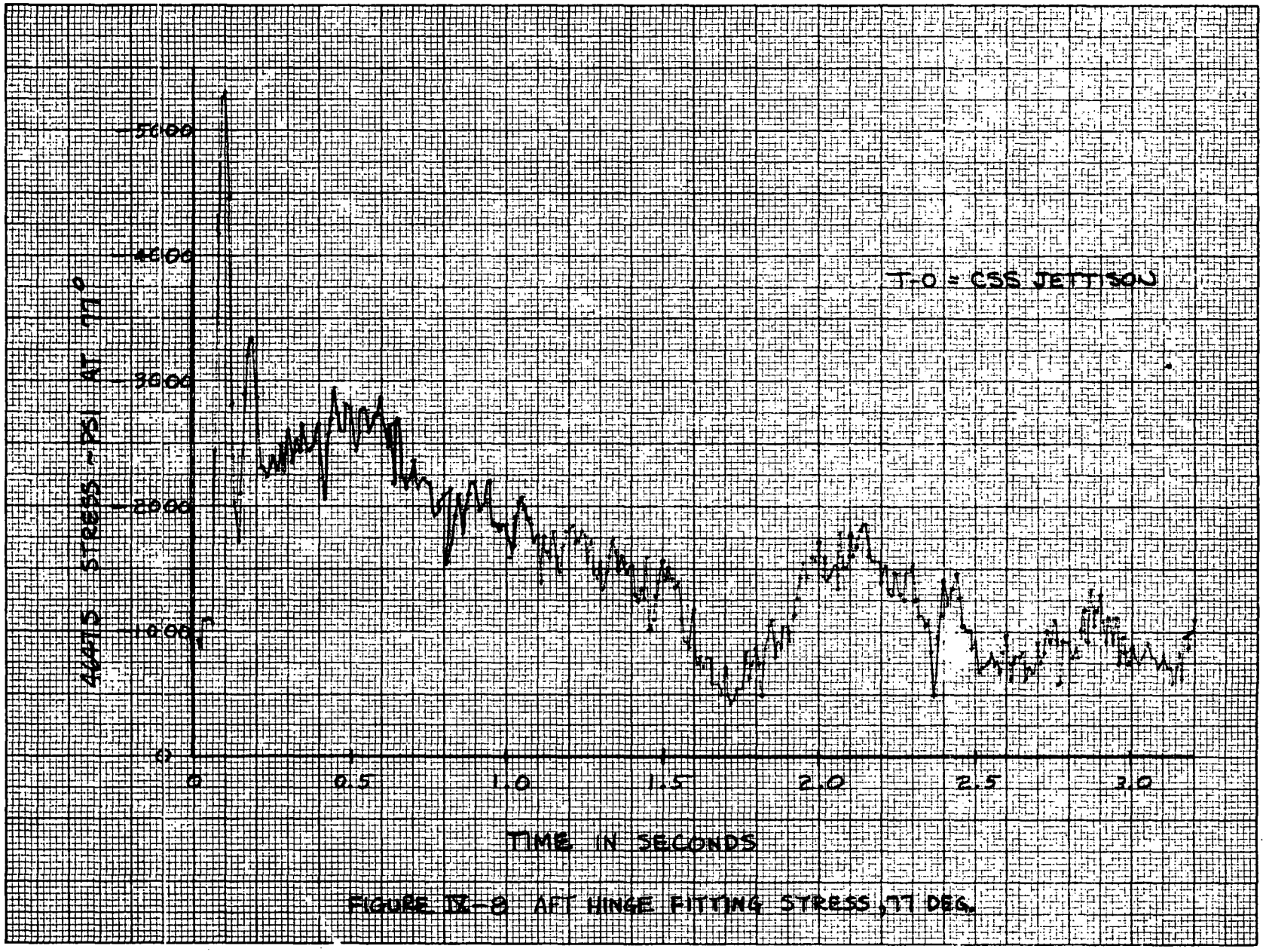

FIGURE IX-8 AFT HINGE FITTING STRESS, 77 DEG.

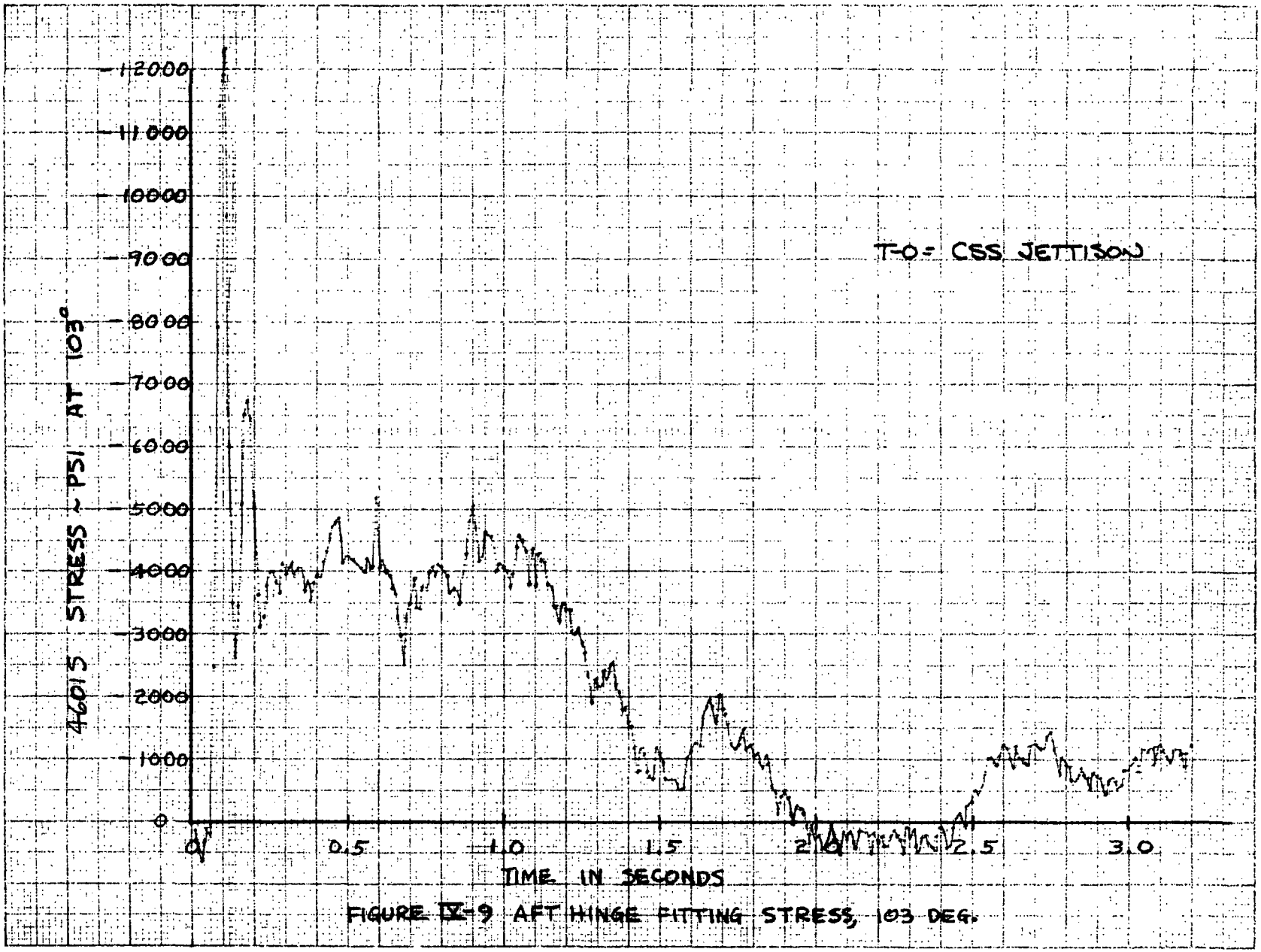

FIGURE IX-9 AFT HINGE FITTING STRESS, 103 DEG.

4657

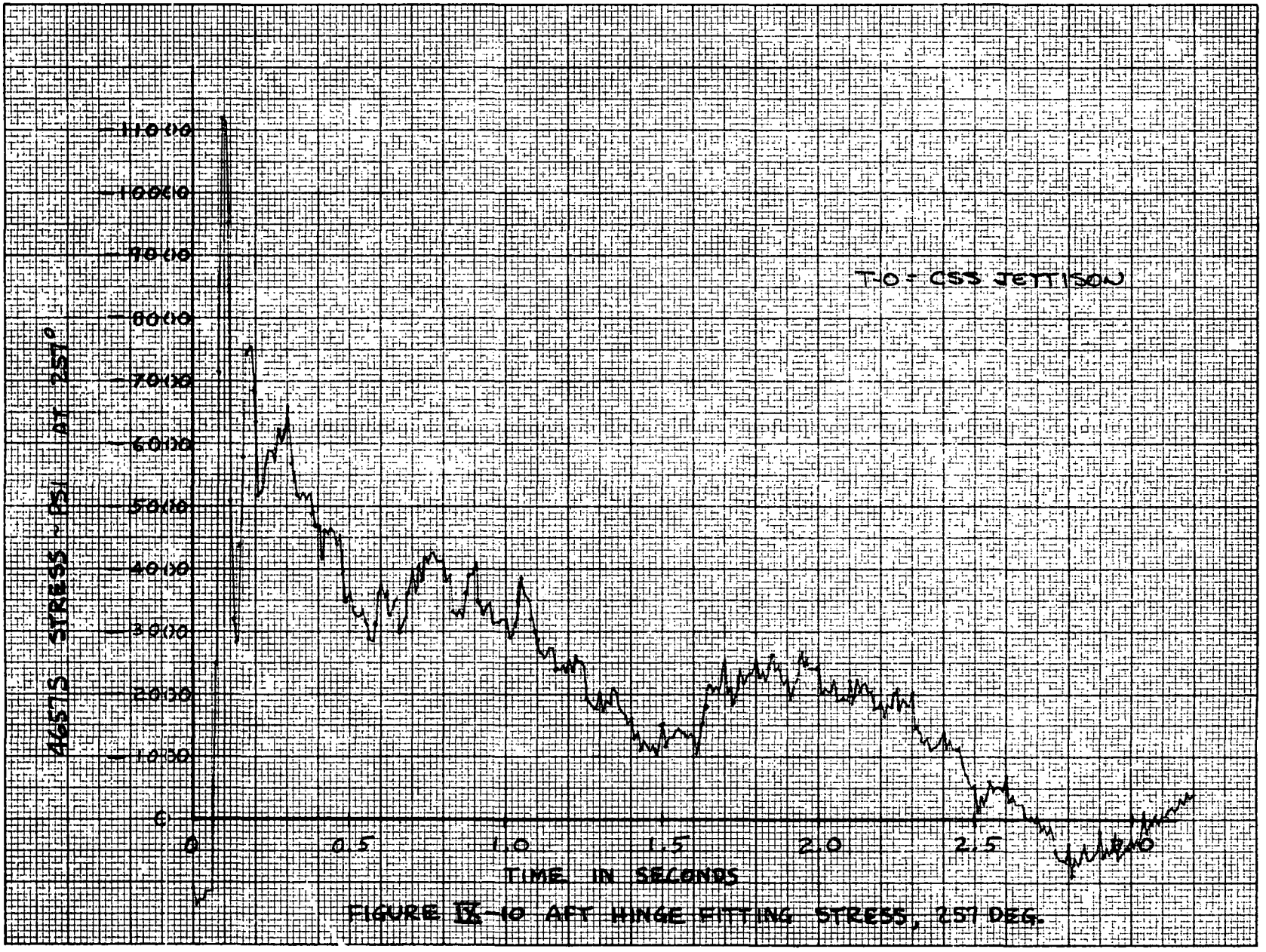

FIGURE IX-10 AFT HINGE FITTING STRESS, 257 DEG.

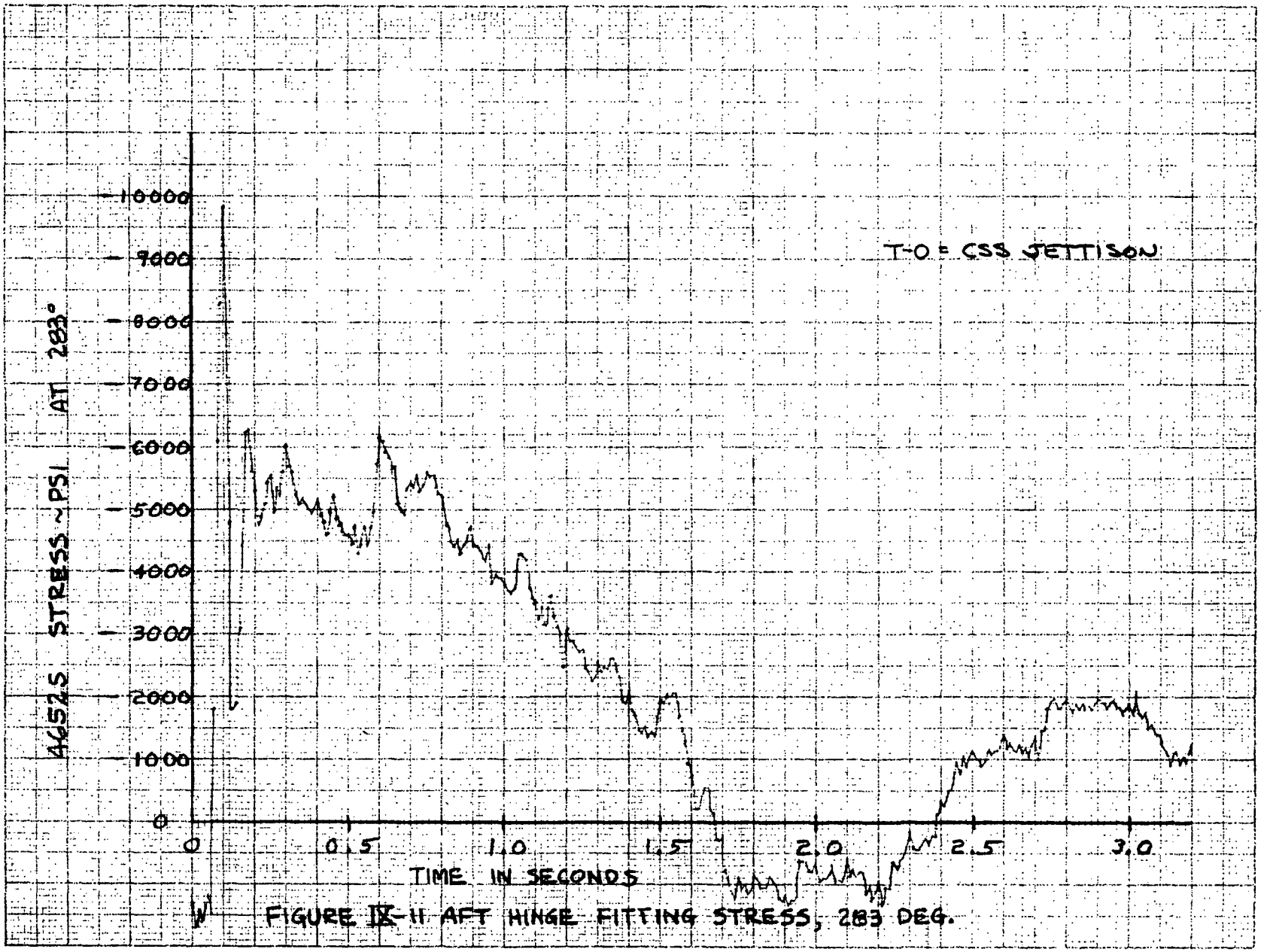

FIGURE IX-11 AFT HINGE FITTING STRESS, 283 DEG.

4695

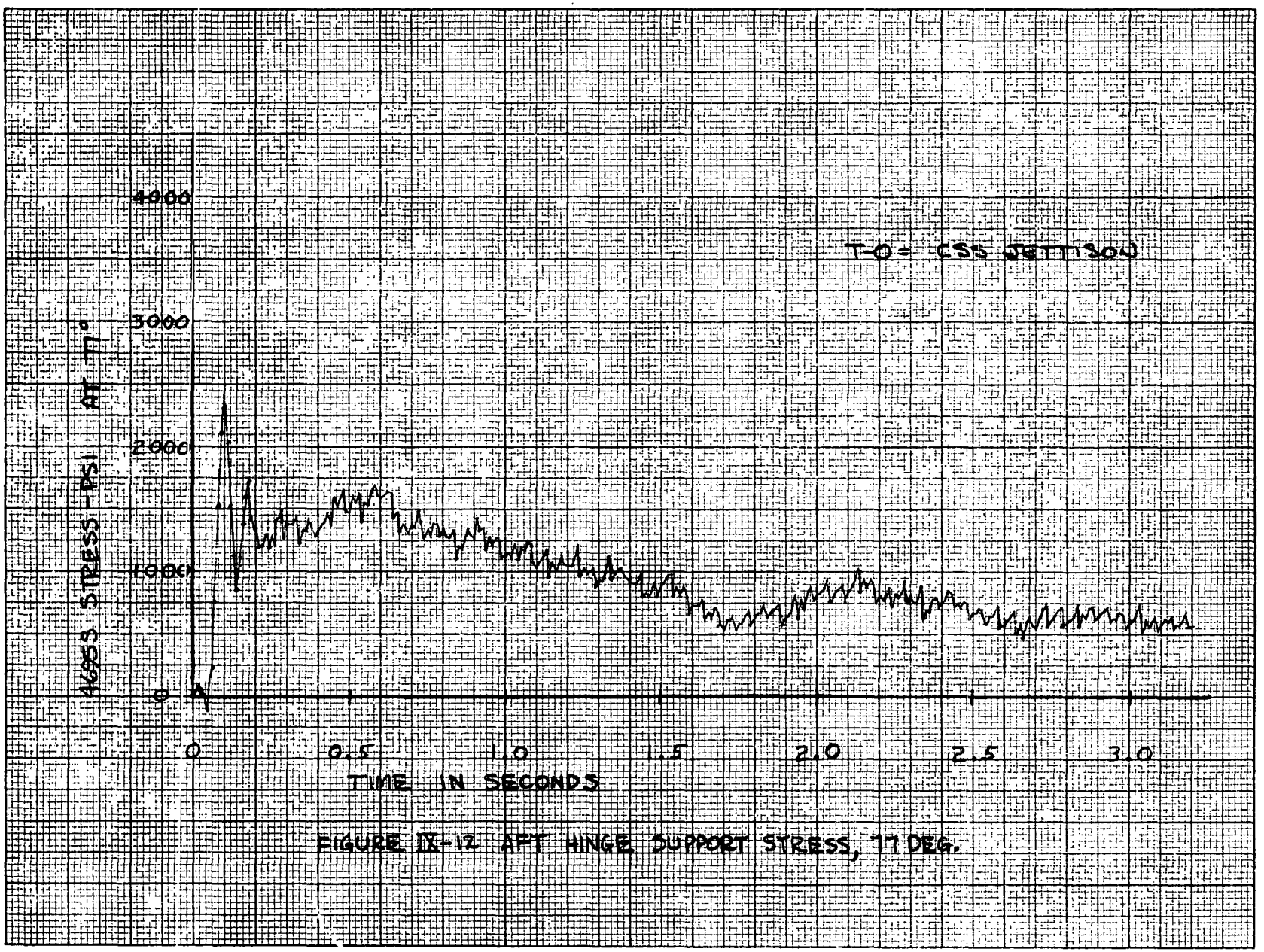

FIGURE IX-12 AFT HINGE SUPPORT STRESS, 11 DEG.

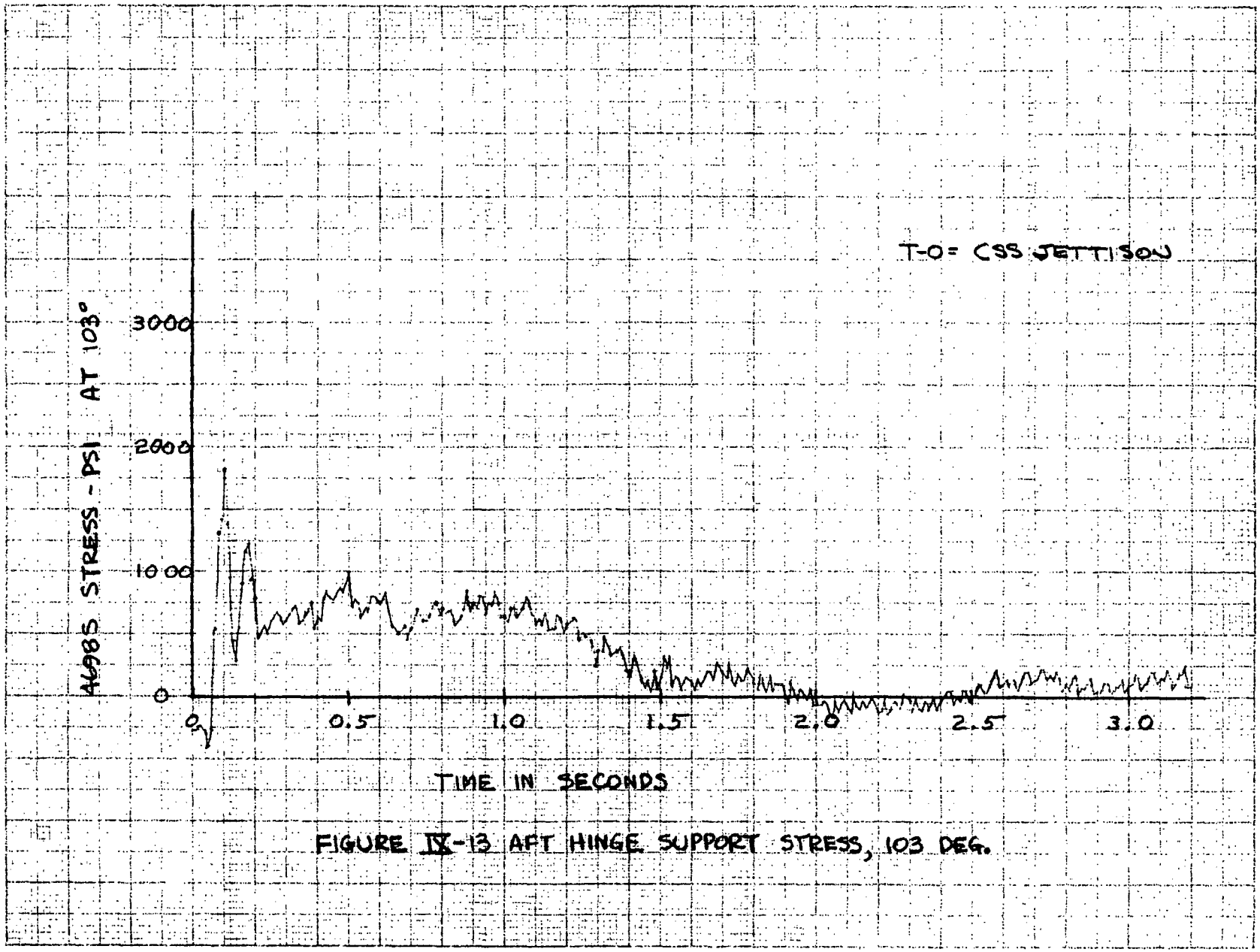

FIGURE IX-13 AFT HINGE SUPPORT STRESS, 103 DEG.

4676

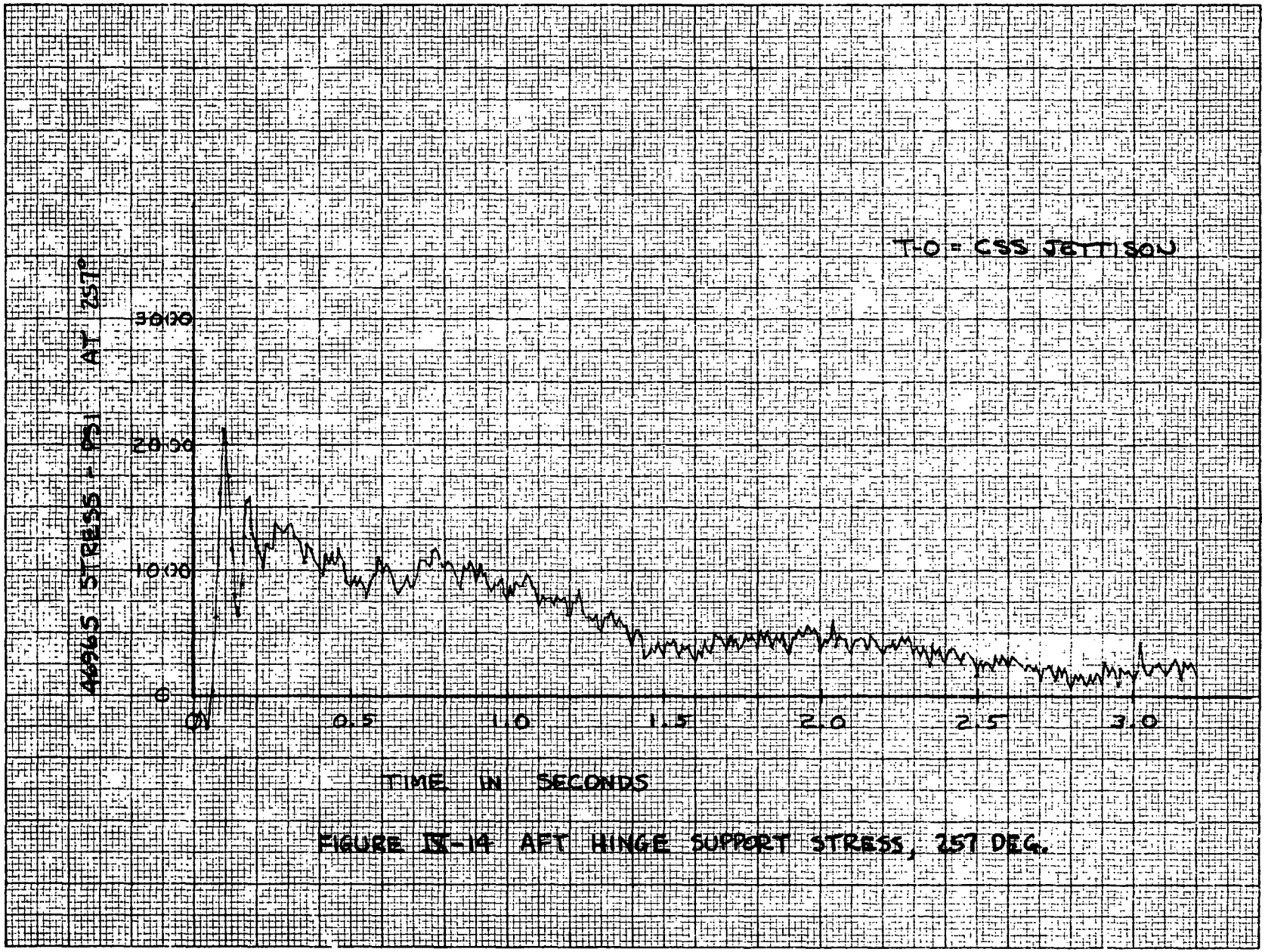

FIGURE IX-14 AFT HINGE SUPPORT STRESS, 257 DEG.

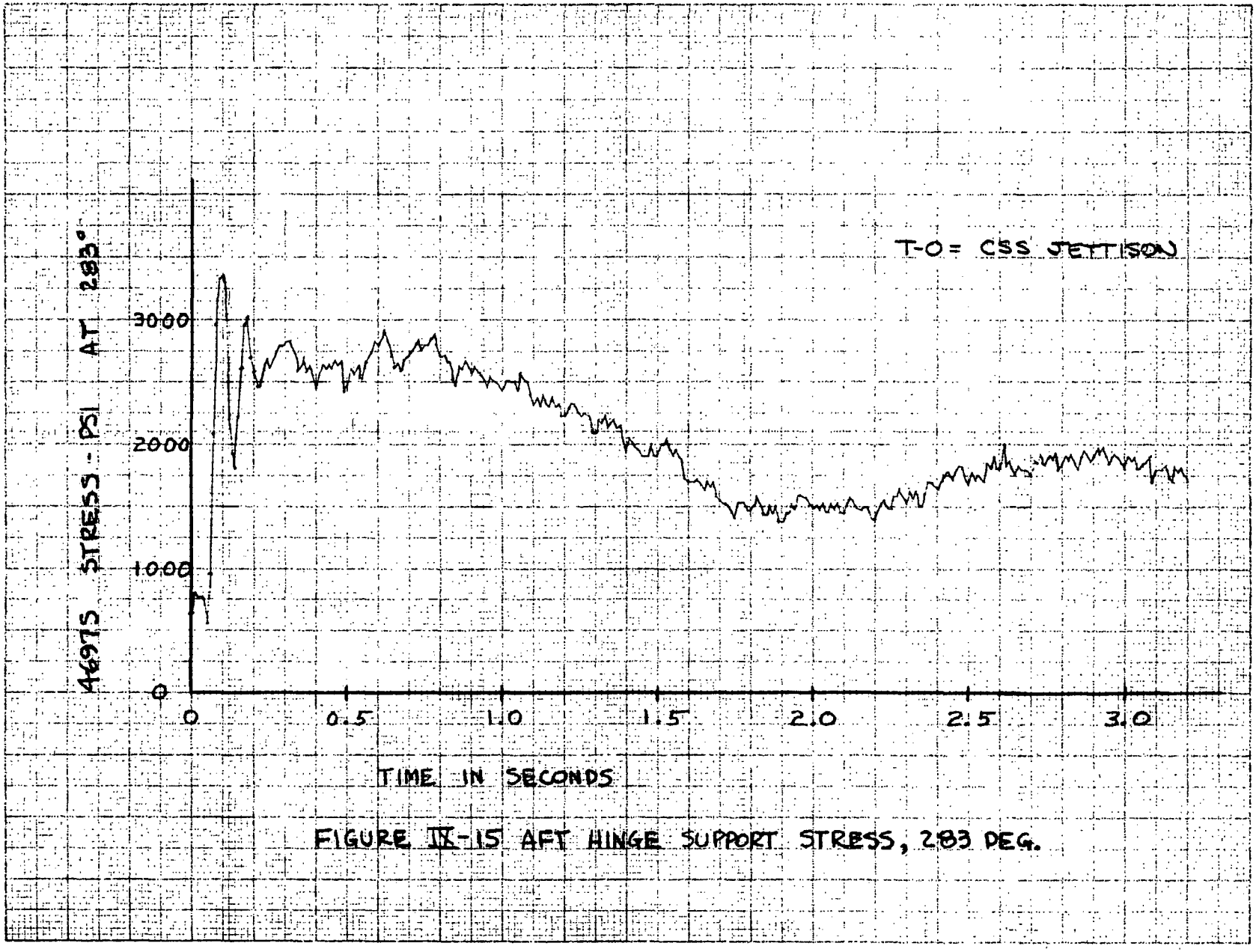

FIGURE IX-15 AFT HINGE SUPPORT STRESS, 283 DEG.

X. SHROUD JETTISON MOTION

by E. J. Cieslewicz

SUMMARY

The high speed movie camera system worked well and provided valuable data for all three cryogenic unlatch tests. Shroud jettison motions were recorded on film which aided in the corrective redesigns which took place between tests. The dynamic response of the shroud throughout jettison was obtained from the film and is part of this report.

On cryogenic unlatch test one, the +Z (East) side split line remained essentially closed for 0.6 seconds longer than the -Z (West) side. For cryogenic test two the same reaction took place but for opposite sides and for a 1.0 second time duration. The third cryogenic unlatch worked perfectly and no sign of any delayed action was apparent.

Peak angular velocities for all three tests were approximately 50 percent lower than expected. Measured values were in the order of six to nine degrees per second compared to the 16 degrees per second expected. Shroud breathing, the vibratory motion of the shroud half edges, through jettison was in the order of five to six cycles per second. There is evidence on some of the breathing motion data taken at midsection of the shroud (stations 2456 and 2511) of frequencies of about 15 cycles per second.

CAMERA LOCATIONS AND DESCRIPTIONS

The high speed movie cameras were strategically installed in the test site, figure X-1, to provide film data along the entire longitudinal length of Super-Zip. The layout was changed between the first and second test to avoid loss of camera data by falling frost. This change was necessary because cameras 8 and 9 were aimed upward and were immediately showered with frost particles when the Super-Zip system was fired. All other data cameras remained the same throughout the three test series. Table X-1 lists all the pertinent data regarding camera lenses and locations. Table X-2 lists the information on the locations of all targets used for the three tests.

Cameras 1 and 13 shown in the layout were mounted on the catwalk of the traveling crane. These were redundant to assure overall coverage from above. The even numbered cameras, namely cameras 2, 4, 6, and 8 were located on the +Z side or East side of the shroud (0^{o} split line) as installed in B-3 test site. Odd numbered cameras 3, 5, 7, and 9 were located on the -Z side or West side of the shroud (180^{o} split line).

The data cameras were operated at a rate of 500 frames per second and used Kodak type RAR black and white film with an estar base. This film was used to provide a minimum of film breakage problems since it is stronger than the more conventional acetate based films.

Other cameras used to monitor forward bearing reaction link separations and seal separation were operated at 400 frames per second with the same type film used for the data cameras. These cameras were mounted internal to the shroud. Overall viewing cameras were operated at 128 frames per second and with color film to provide qualitative observation of the jettison operation.

CAMERA PERFORMANCE

The cameras performed well, with few exceptions, for all three of the cryogenic unlatch tests. On the first test problems were experienced with film timing marks but fortunately camera speed calibrations were made just prior to the tests and the nominal film rates were used for the data reduction. Two of the five internally mounted cameras failed to operate for test two because of mechanical and film jamming failures. All cameras except camera number 3 operated for the third test.

CSS JETTISON MOTION DATA

Cryo-Unlatch Test No. 1

Figures X-2 and X-3 are plots of the shroud half positions as they varied with time. Both halves edge motions are plotted on the curves to illustrate more effectively the relative motion that one half had to the other. A significant fact that becomes obvious when both of these figures are studied is that the split line on the +Z or East side of the shroud remained essentially closed for 0.6 seconds before starting to open. The opposite split line on the -Z or West side started to open immediately and when the rotation of 1^{o} was achieved the rate of change of opening slowed down. This occurred also at 0.6 seconds. Just after 0.6 seconds two events occurred. The +Z side starts to open and the rate of change of opening on the -Z side starts to increase. It is obvious that something was retarding the jettisoning action on the +Z or East split line for cryogenic test No. 1.

Figure X-4 of cryogenic test one shows the breathing action which both shroud halves go through after Super-Zip firing. The plot is arranged such that the lines show the paths that the four targets at station 2654 go through when observed from above. (See figure X-1 for camera layout.) It should be noted that the four targets move in the -Z or West direction and at 0.6 seconds the shroud has traveled toward the opening split line approximately 3 inches. This figure also shows the breathing frequency to be in the order of 5 to 6 cycles per second.

Figure X-5 is a plot of angular position versus time of both shroud halves as observed from camera number 7, (See figure X-1 for camera location) located at the base of shroud on the -Z side (West). This plot shows a sign of the reluctance of the shroud to accelerate at 0.6 seconds. The jagged effect of this curve is due to the fact that the vertical (+X) component of target movement was used to determine position on an arc and the shroud's vertical oscillations give an erroneous position along the circular path. The horizontal component of target movement could be used to eliminate this effect in future tests.

Cryo-Unlatch Test No. 2

Figures X-6 and X-7 are plots of the shroud half positions as they varied with time. Both halves' edge motions are plotted on the curves to illustrate more effectively the motion of one half to the other. Comparison of these figures indicates that the split line on the -Z or West side of the shroud remained essentially closed for 1.0 seconds before starting to open. The opposite split line on the +Z or East side started to open immediately and when the rotation of 2 to 2½ degrees was achieved the rate of change of opening slowed down. This also occurred at 1.0 seconds. Just following 1.0 seconds two things happen. The -Z side starts to open and the rate of change of opening of the +Z side starts to increase. Again, it is obvious that something was retarding the jettisoning action on the -Z or West split line for cryogenic test two just by studying these motion curves.

Figure X-8 of cryogenic test two shows the breathing action which both shroud halves go through after Super-Zip firing. The plot is arranged such that the lines show the paths that the four targets at station 2654 go through when observed from above. (See figure X-1 for camera layout.) It should be noted that the four targets move in the +Z or East direction and at 1.0 seconds the shroud has traveled toward the opening split line approximately 4½ inches. This figure also shows the breathing frequency to be in the order of 6 cycles per second.

Cryo-Unlatch Test No. 3

Unfortunately camera 3 failed to operate for this test and a comparative angular position versus time at station 2654 cannot be made. Figure X-9 shows the +Z or East side split line and neither the flat bottomed delay or the corresponding rotational rate change is apparent as for tests one and two.

Figures X-10 and X-11 show the two split lines at station 2456 as their open angle varies with time. Except for peak angular displacements shown on these plots, they are almost identical. Essentially no leading or lagging took place for this jettison test.

The above can also be said of figures X-12 and X-13 which show the angular position versus time plots taken from targets located at station 2511.

Figure X-14 shows the shroud position versus time from the camera number 2 position. The displacement shown on this curve and other displacement curves to follow gives the actual distance displaced horizontally from the targets original position. Camera number 3 did not run for this test and a comparison of both split lines of the shroud at station does not exist. However, if shroud motions like those shown in figures X-15 and X-16 for station 2456 and again in figures X-17 and X-18 for stations 2511 are typical then a very smooth and uniform separation was achieved for test number three.

Figures X-19, X-20, and X-21 utilize data from cameras 2, 4, and 5 to show the breathing action which both shroud halves go through after the Super-Zip firing. The plots are arranged such that the lines show the paths that the targets traveled as observed from above. The lower frequency breathing observed on test one and two are not evident on plots X-20 and X-21 but rather a higher frequency component of about 15 cycles per second.

For reference only, figure X-22 shows a predicted CSS rotation angle versus time. The curves were generated assuming vacuum conditions and a 1 g field for 100 percent efficient springs and 80 percent efficient springs. The prediction of CSS responses under the assumed conditions were used to design the catch system, therefore, all dispersions on parameters which influenced response were in a direction to increase system energy. All data from the tests indicated that net contact did not occur until 1.3 to 1.8 seconds after unlatch. The large mis-match between test data and analytical predictions cannot be accounted for by dispersions in system hardware parameters. The predominant force restraining motion during the tests appears to be aerodynamics as opposed to other restraining forces such as friction, binding, and nominal disconnect forces, although these type forces were prevalant on tests No. 1 and 2.

CONCLUSIONS

Cryogenic unlatch tests numbers one and two showed signs of a faltering split line motion in the earlier portions of the jettison. Test number one was sluggish in opening on the +Z split line side and actually lagged in opening by 0.6 seconds. Test number two was also sluggish and showed the same type of delayed opening by 1.0 seconds, but on the -Z split line side.

Attempts to exclude further, the moisture suspected of causing the sluggish jettison in test two was successful based on the performance of test number three. No signs of sluggish response were observed.

Peak jettison rates were found to be lower in magnitude than the predicted 16 degrees per second at 5 degree rotation. Rates were in the order of 6 to 9 degrees per second. Breathing rates for the tests were 5 to 6 cycles per second. High harmonics of about 15 cycles per second were visible especially on the third test. Total excusions in breathing were within two inches for the third test which seemed to be most representative of a good jettison.

TABLE X-1 MOVIE CAMERA FILM PLANE COORDINATES FOR

CRYO-UNLATCH TEST NOS. 1, 2, AND 3

CAMERA NO.	LENS FOCAL LENGTH	POSITION OF FILM PLANE		
		X-DIRECTION (SHROUD STA. NO.)	Y-DIRECTION (INCHES)	Z-DIRECTION (INCHES)
1	12	3152.1	-12.3	52.1
2	10	2773.7	0.3	103.8
3	10	2774.7	2.6	-105.4
4	16	2673.6	0.4	104.3
5	16	2671.4	0.1	-105.3
6	10	2254.8	39.9	-219.1
7	10	2255.9	-40.5	219.7
8	10* (16)	2183.1 (2401.7)	-0.9 (0.3)	87.0 (104.1)
9	10 (16)	2183.6 (2402.3)	0.8 (1.3)	-87.1 (105.3)
13	10	3149.0	5.8	52.1

*Numbers in parenthesis are values for tests nos. 2 and 3

TABLE X-2 TARGET CENTERLINE LOCATIONS

TARGET NO.	STATION CENTERLINE	AZIMUTH CENTERLINE (DEGREES)	RADIAL OFFSET CENTERLINE (INCHES)
1-A	2867	5.3	3.7
1-B	2867	174.7	3.7
1-C	2867	185.3	3.7
1-D	2867	354.7	3.7
2-A	2654	174.7	3.6
2-B	2654	185.3	3.6
3-A	2654	5.3	3.6
3-B	2654	354.7	3.6
4-A	2511	174.7	3.6
4-B	2511	185.3	3.6
4-C	2456	174.7	3.6
4-D	2456	185.3	3.6
5-A	2511	5.3	3.6
5-B	2511	354.7	3.6
5-C	2456	5.3	3.6
5-D	2456	354.7	3.6
6-A	2275	174.7	1.3
6-B	2275	185.3	1.3
6-C	2231	174.7	1.3
6-D	2231	185.3	1.3
7-A	2275	5.3	1.3
7-B	2275	354.7	1.3
7-C	2231	5.3	1.3
7-D	2231	354.7	1.3
8-A	2265* (2269)	174.7 (174.3)	3.6 (3.7)
8-B	2265* (2269)	185.3 (185.7)	3.6 (3.7)
8-C	2222 (2226)	174.7 (175.3)	3.6 (3.7)
8-D	2222 (2226)	185.3 (184.7)	3.6 (3.7)
9-A	2265 (2269)	5.3 (5.7)	3.6 (3.7)
9-B	2265 (2269)	354.7 (354.3)	3.6 (3.7)
9-C	2222 (2226)	5.3 (4.7)	3.6 (3.7)
9-D	2222 (2226)	354.7 (355.3)	3.6 (3.7)

*Numbers in parenthesis are the values for test nos. 2 and 3

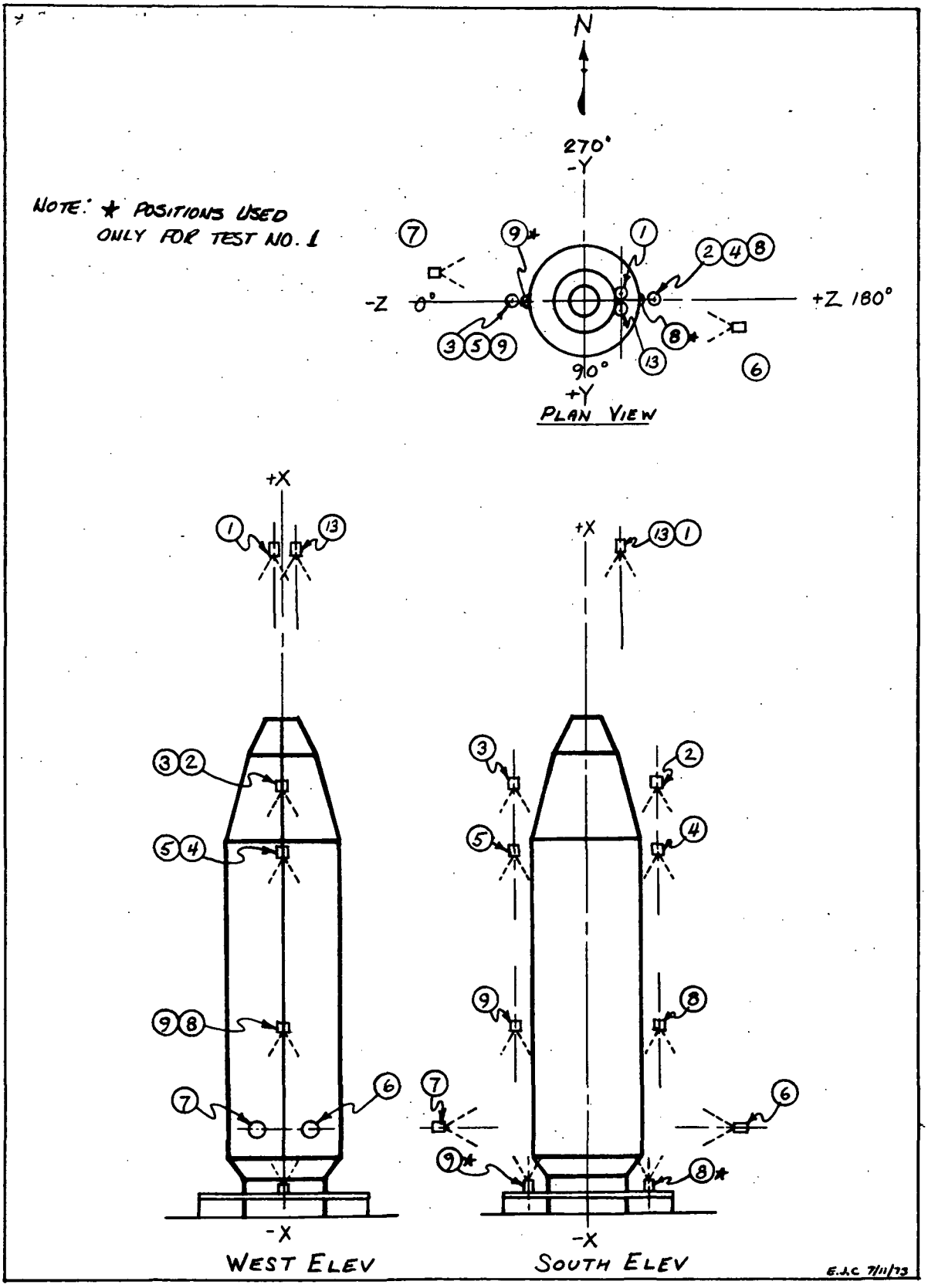

FIGURE X-1 MOVIE CAMERA LAYOUT FOR CRYOGENIC TESTS 1, 2, & 3

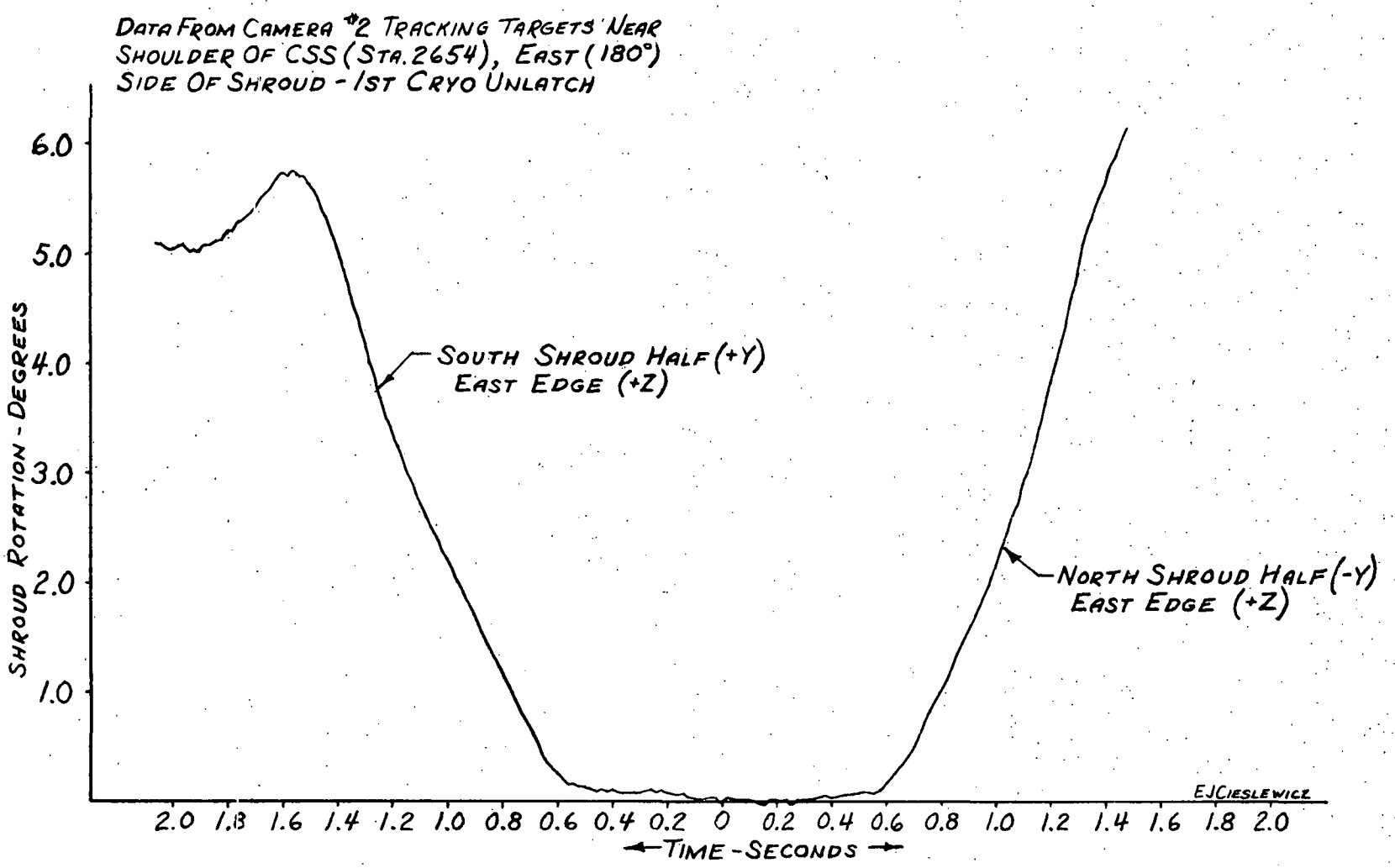

FIGURE X-2 NORTH & SOUTH SHROUD HALF ROTATION VS. TIME 1ST CRYO UNLATCH

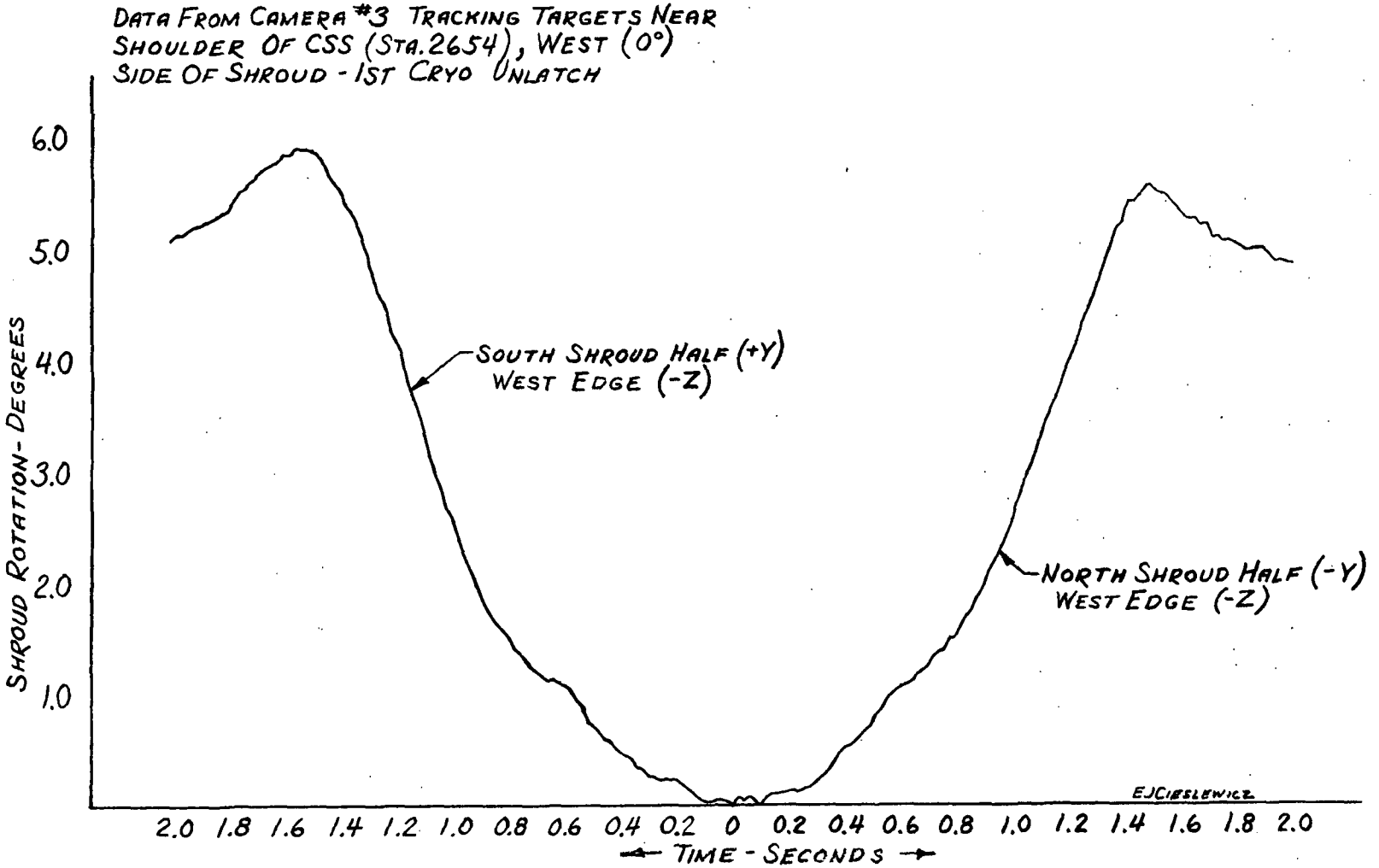

FIGURE X-3 NORTH & SOUTH SHROUD HALF ROTATION VS. TIME 1ST CRYO UNLATCH

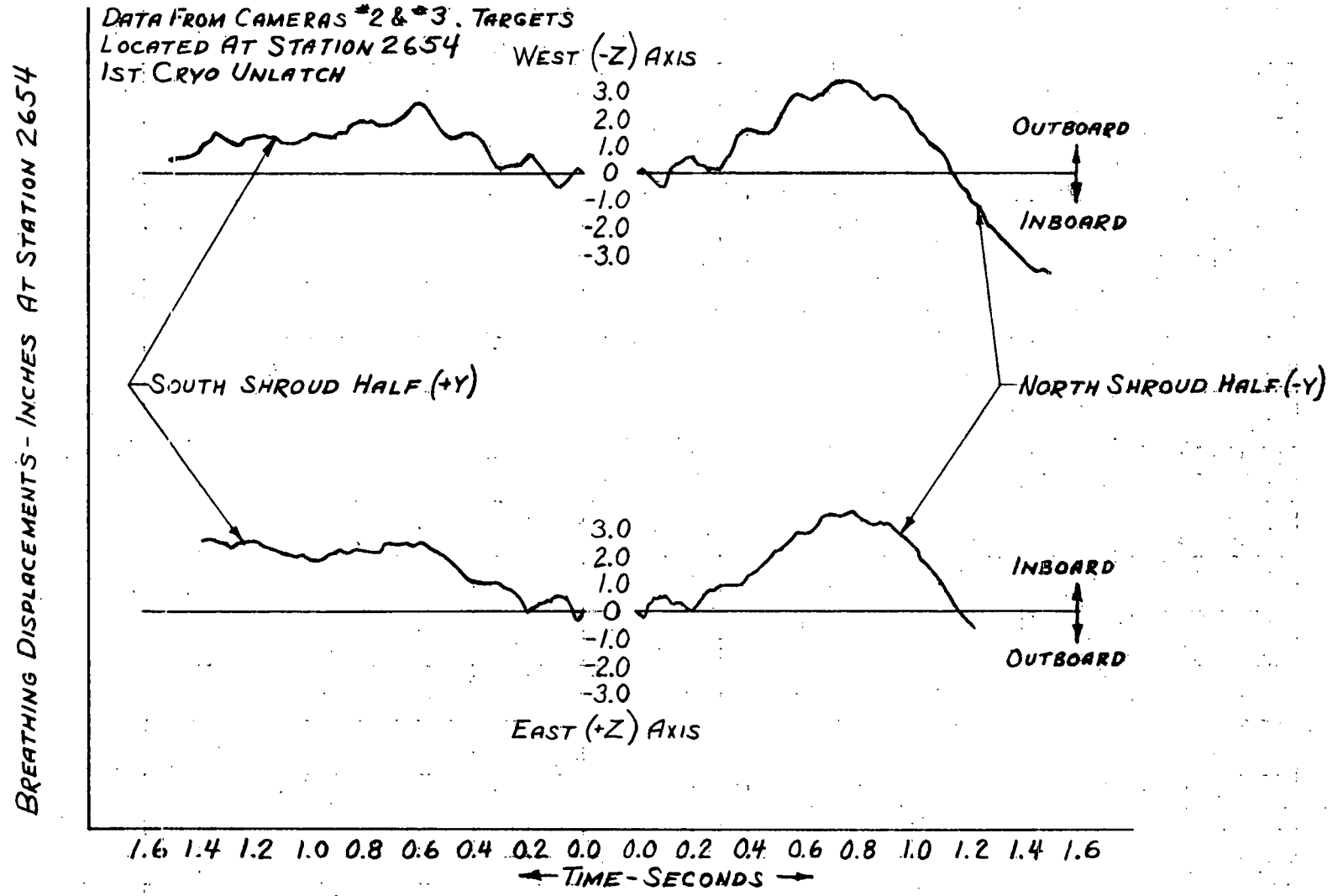

FIGURE X-4 NORTH & SOUTH SHROUD HALF BREATHING MOTIONS VS. TIME 1ST CRYO-UNLATCH

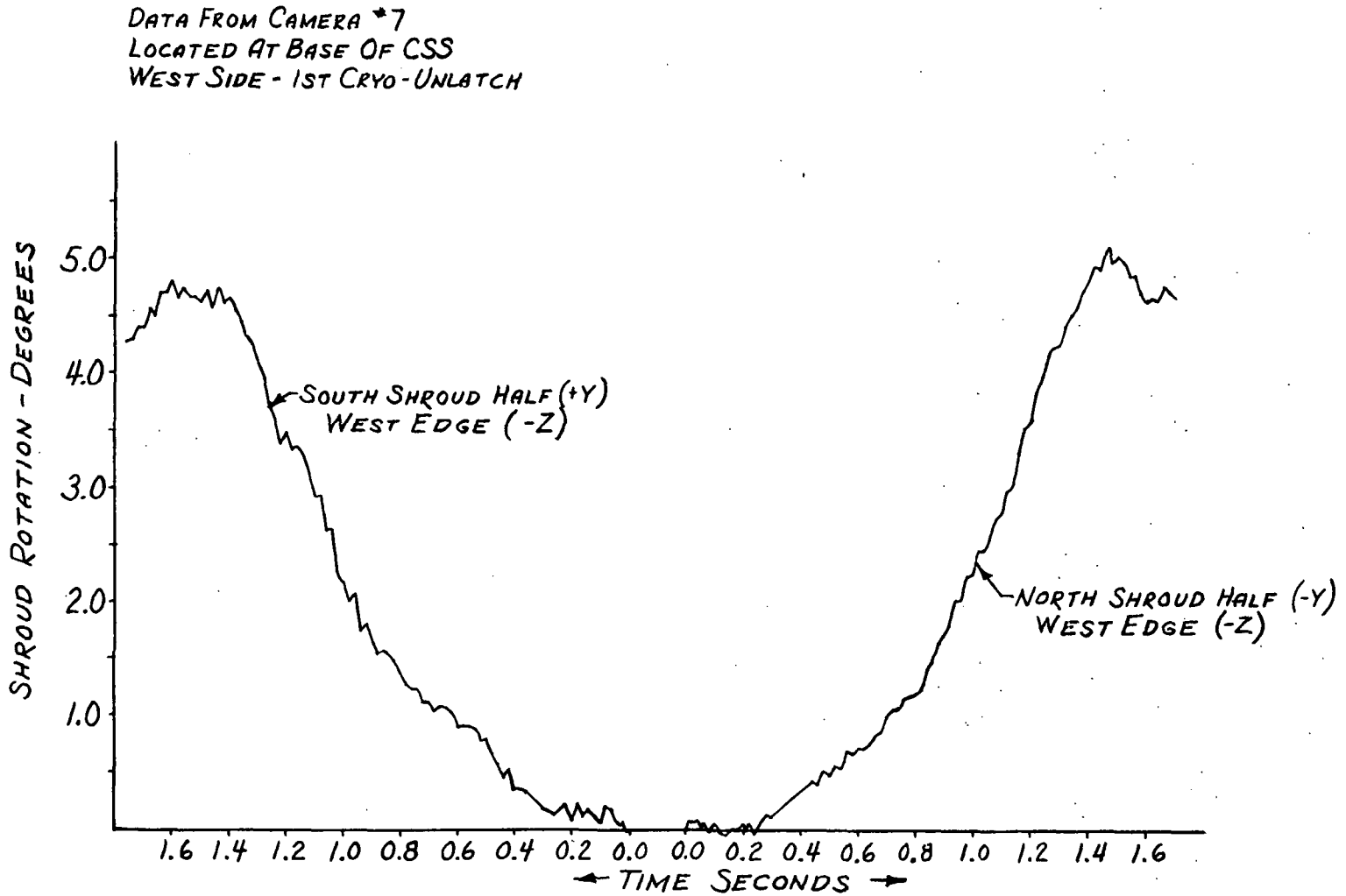

FIGURE X-5.- NORTH & SOUTH SHROUD HALF ROTATION VS. TIME 1ST CRYO-UNLATCH.

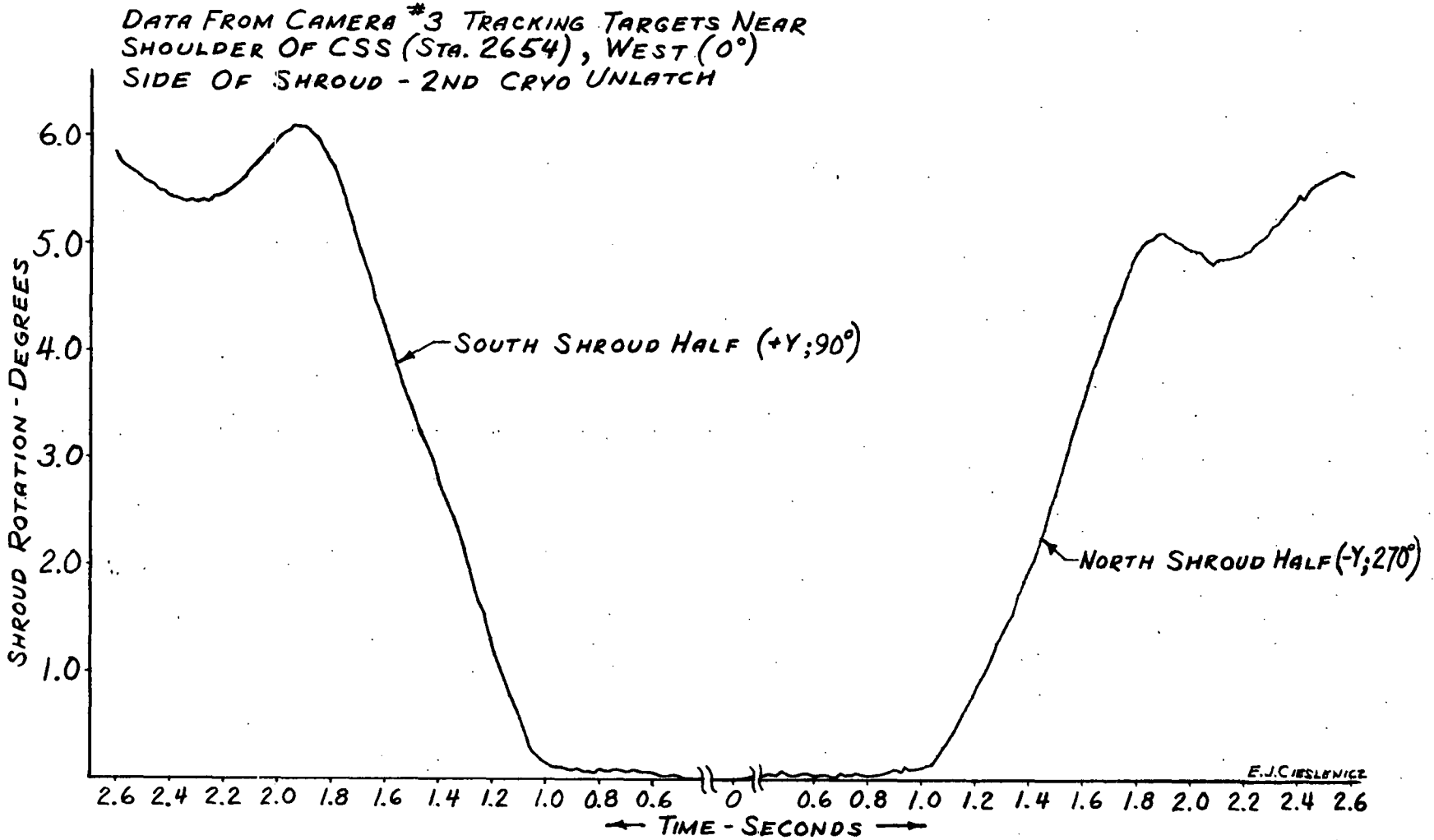

FIGURE V-6 NORTH & SOUTH SHROUD HALF ROTATION VS. TIME 2ND CRYO UNLATCH

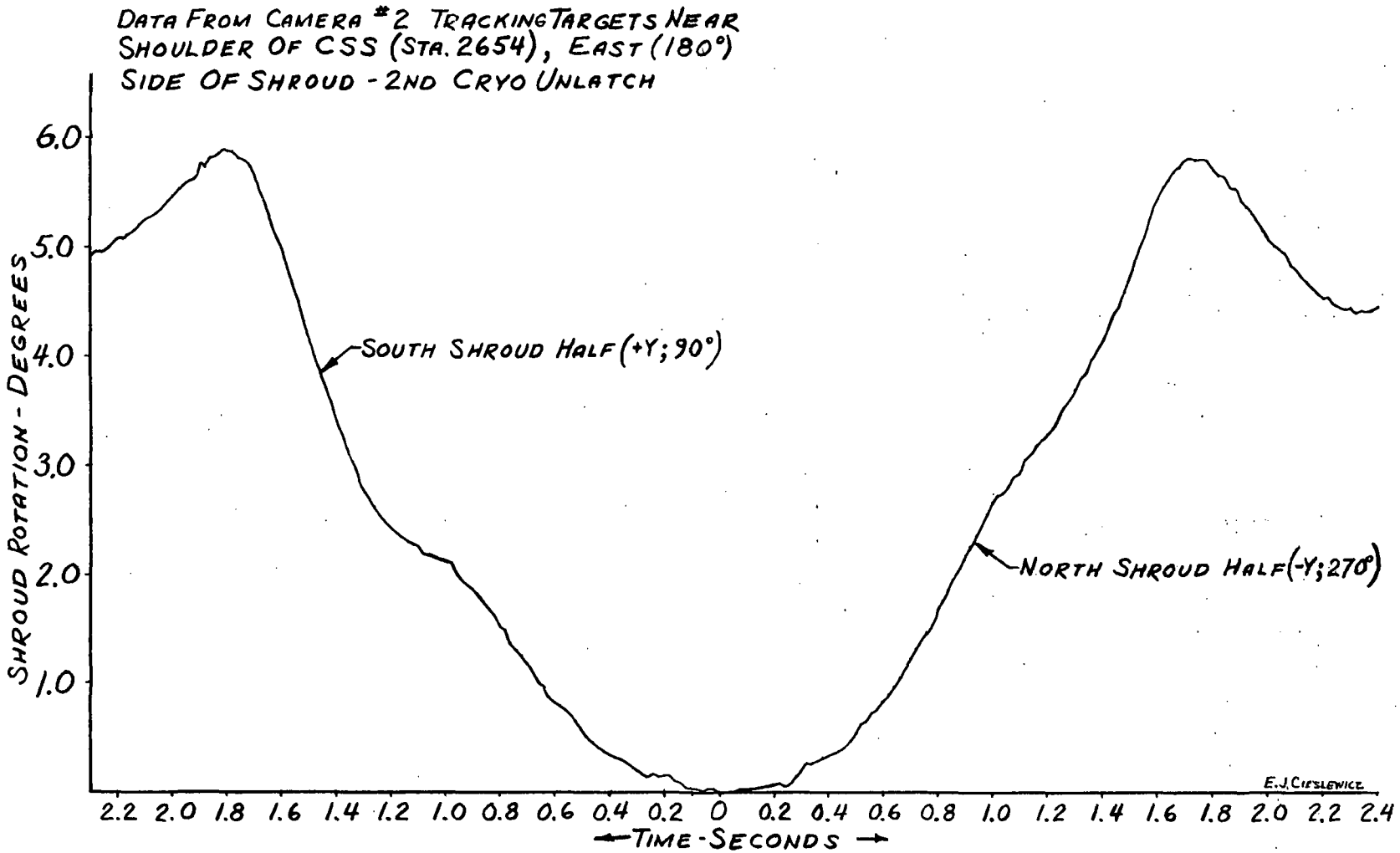

FIGURE X-7 NORTH & SOUTH SHROUD HALF ROTATION VS. TIME 2ND CRYO-UNLATCH

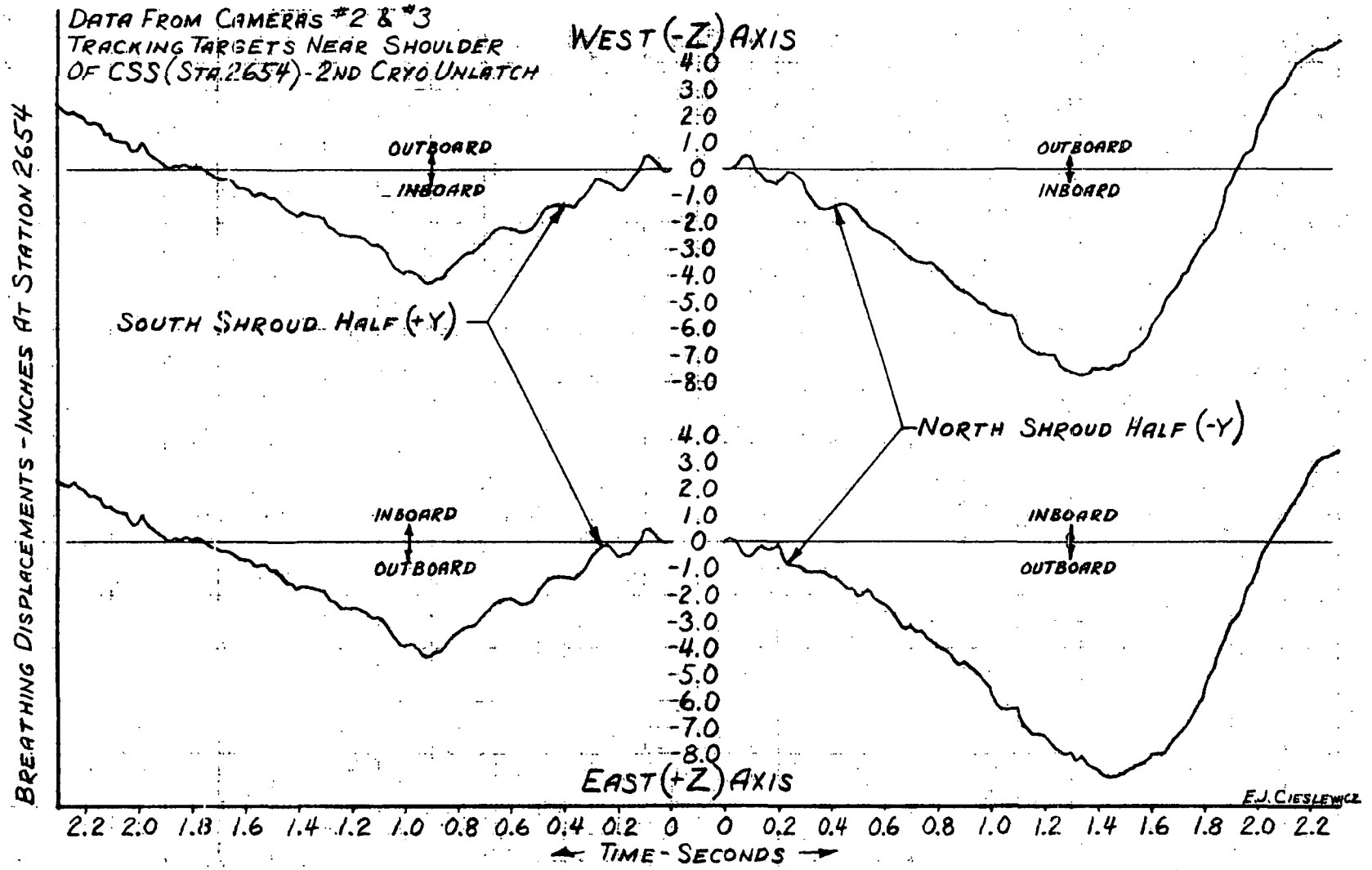

FIGURE X-8 NORTH & SOUTH SHROUD HALF BREATHING MOTIONS VS. TIME
2ND CRYO UNLATCH

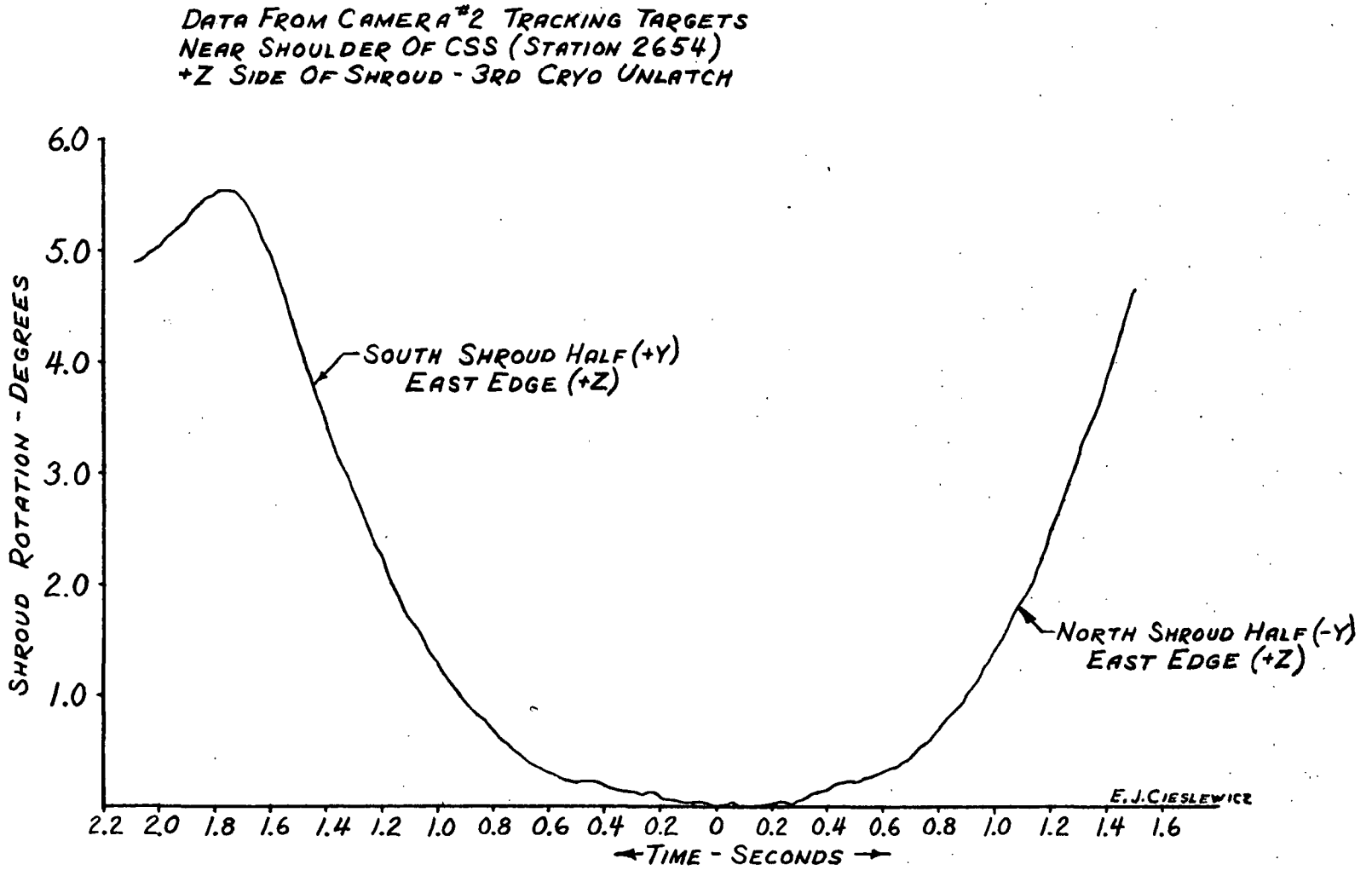

FIGURE X-9 NORTH & SOUTH SHROUD HALF ROTATION VS. TIME, 3RD CRYO UNLATCH

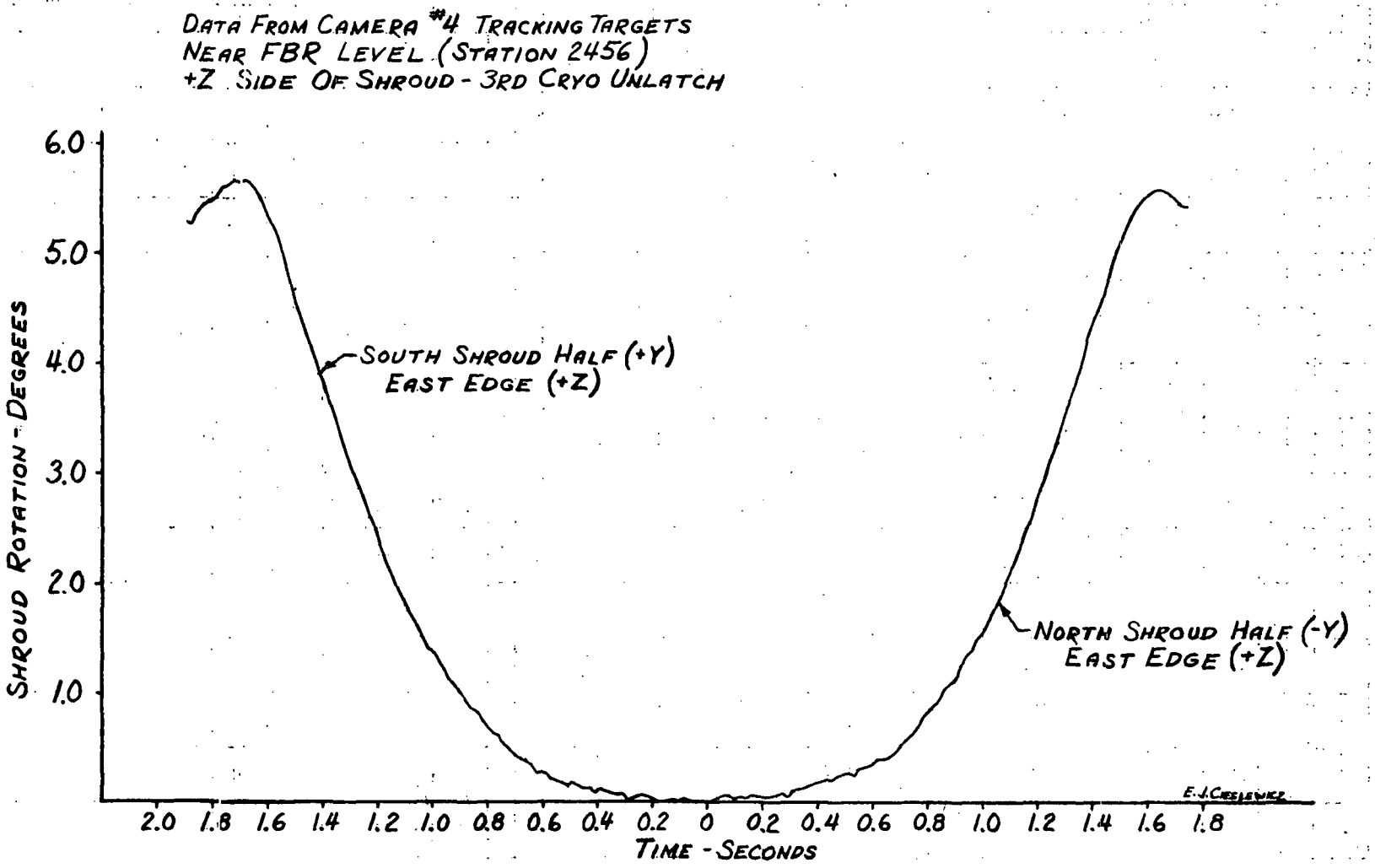

FIGURE X-10 NORTH & SOUTH SHROUD HALF ROTATION VS. TIME, 3RD CRYO UNLATCH

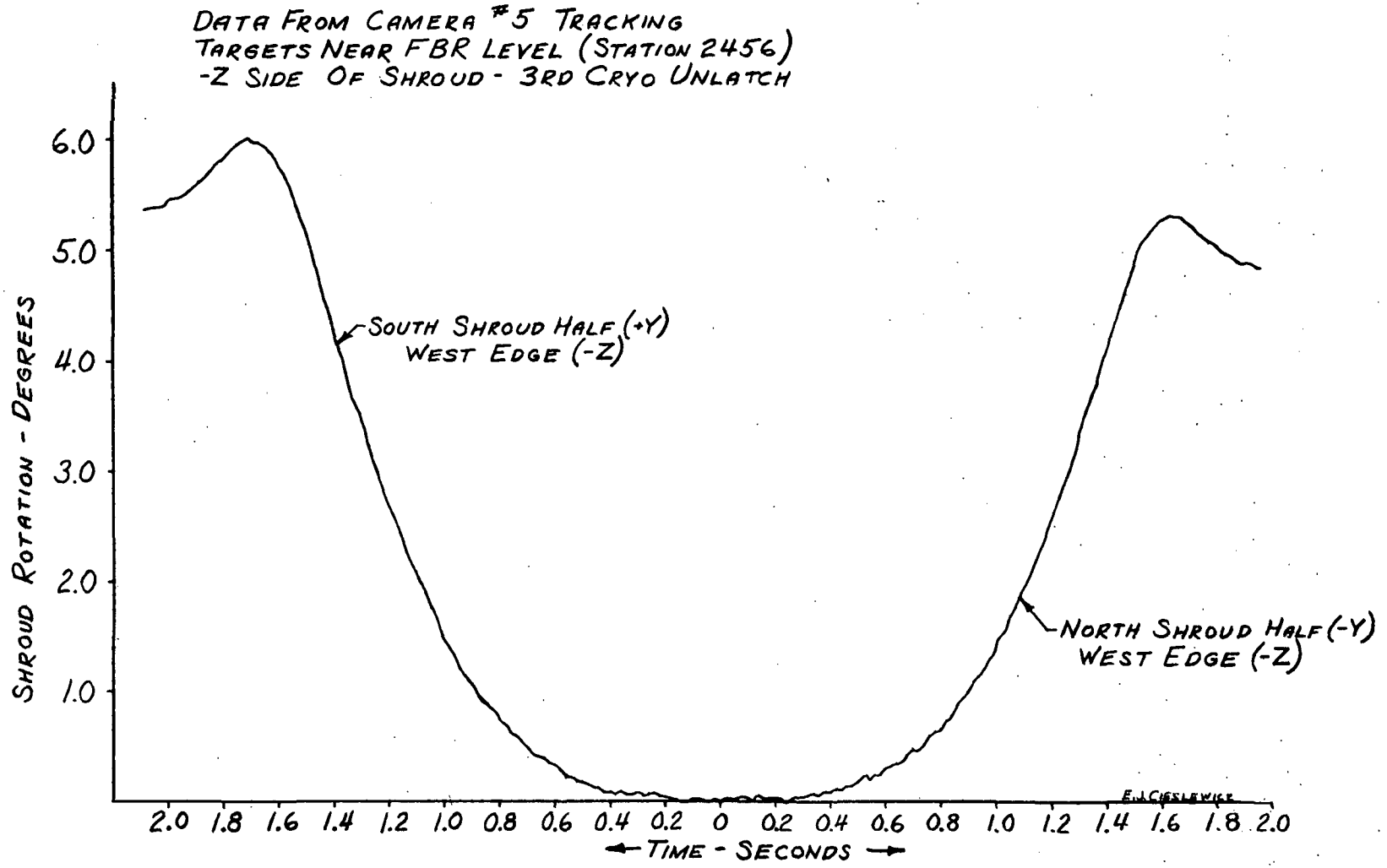

FIGURE X-11 NORTH & SOUTH SHROUD HALF ROTATION VS. TIME, 3RD CRYO UNLATCH

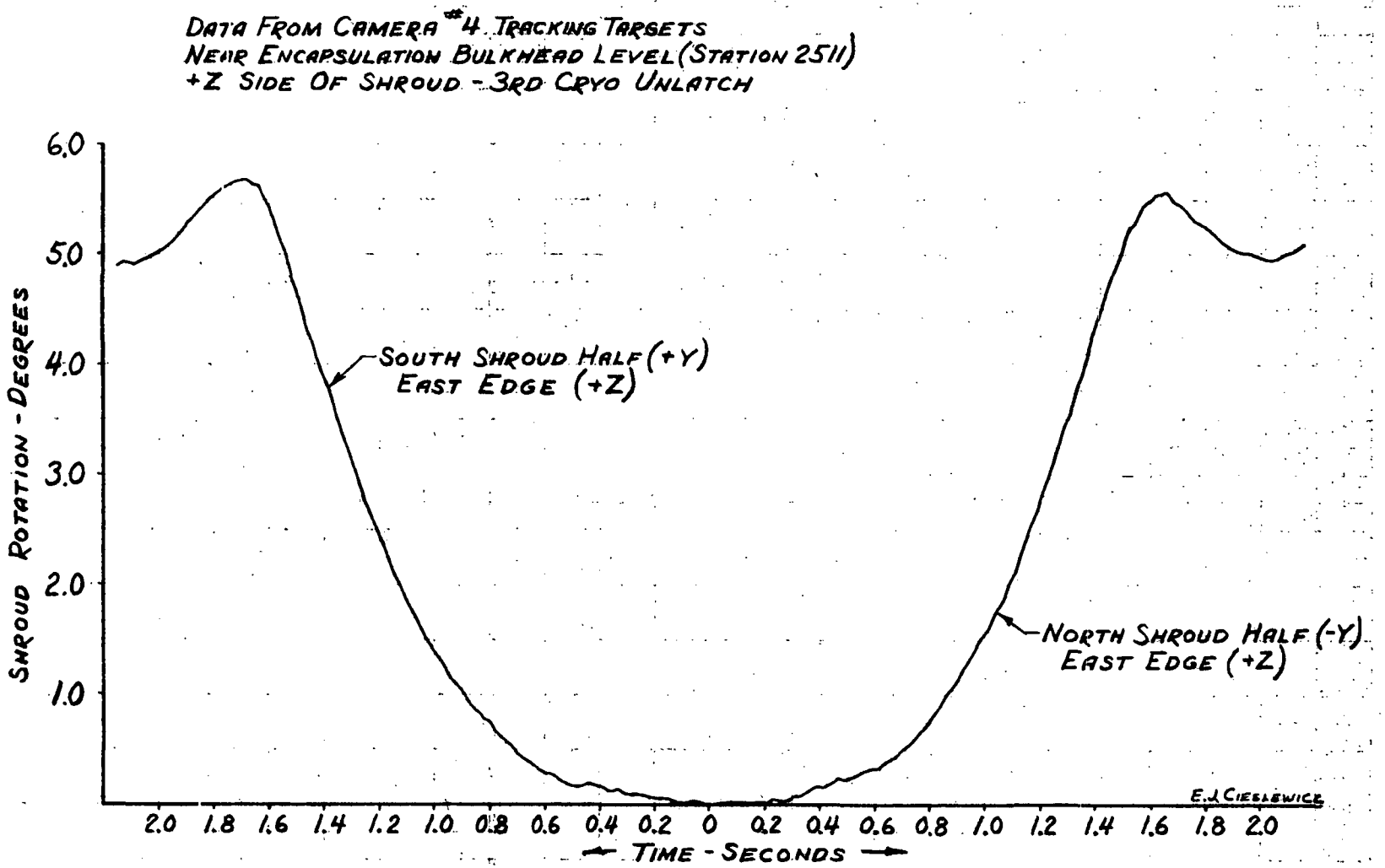

FIGURE X-12 NORTH & SOUTH SHROUD HALF ROTATION VS. TIME, 3RD CRYO UNLATCH

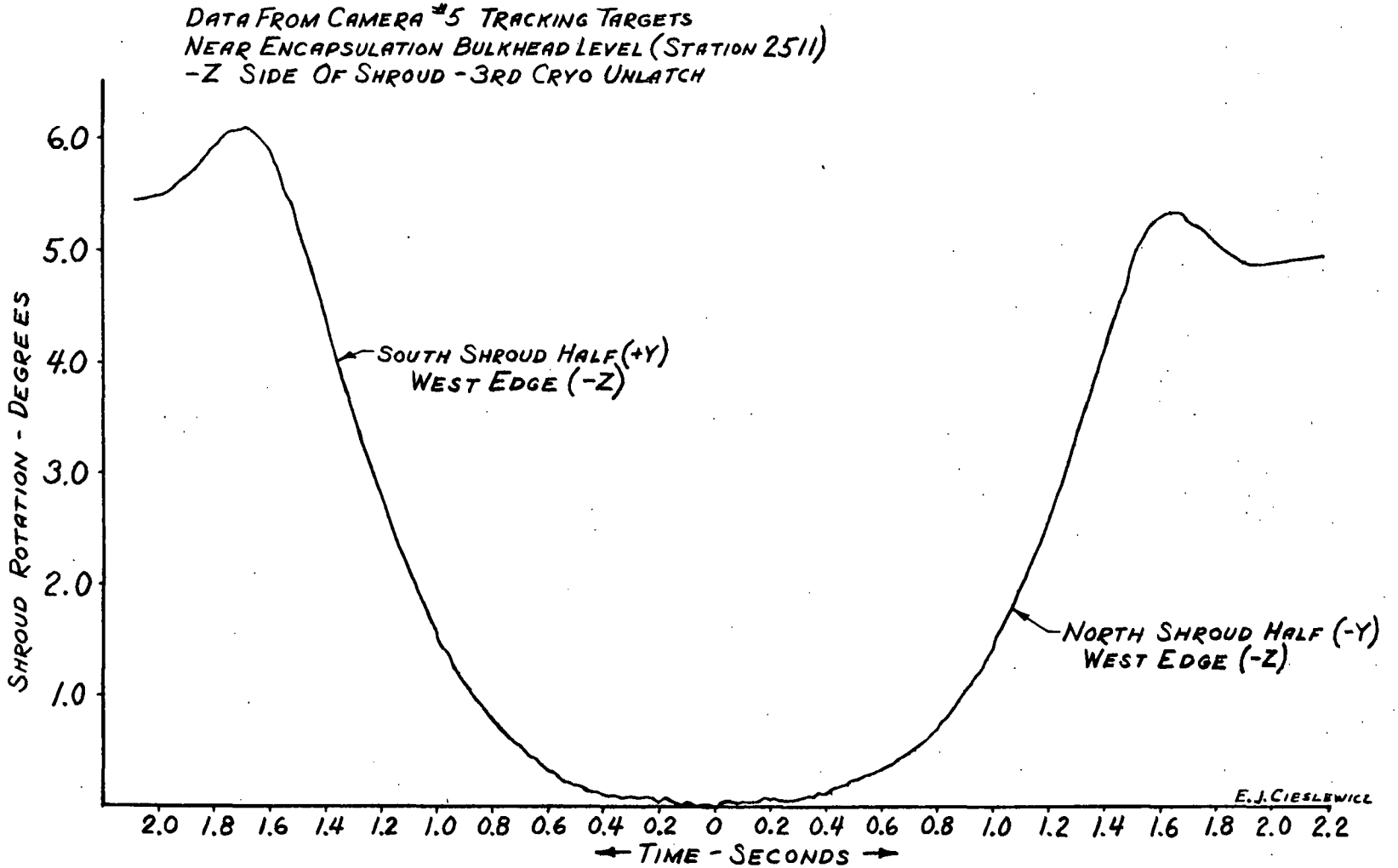

FIGURE X-13 NORTH & SOUTH SHROUD HALF ROTATION VS. TIME, 3RD CRYO UNLATCH

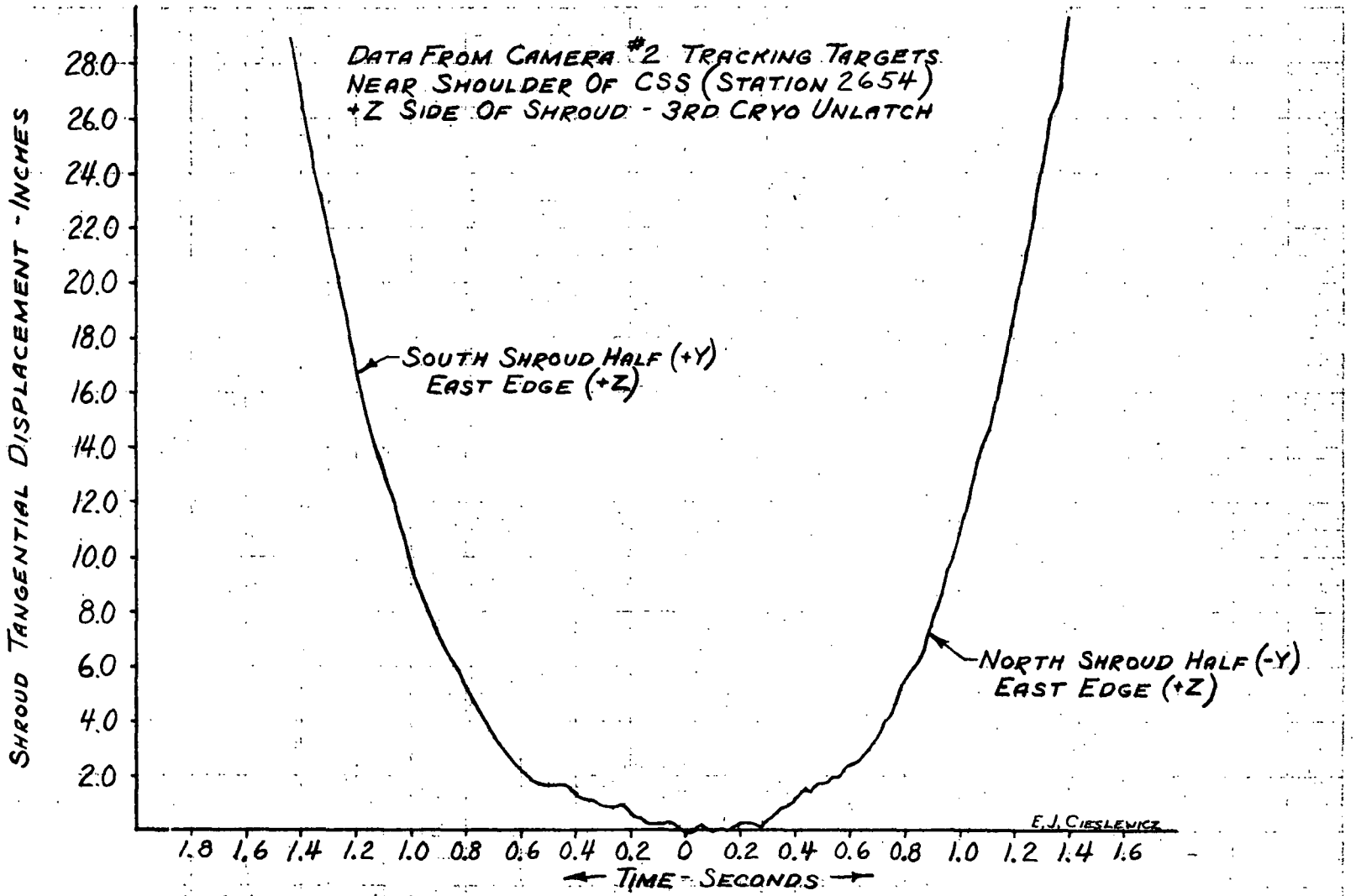

FIGURE X-14 NORTH & SOUTH SHROUD HALF DISPLACEMENT VS. TIME, 3RD CRYO UNLATCH

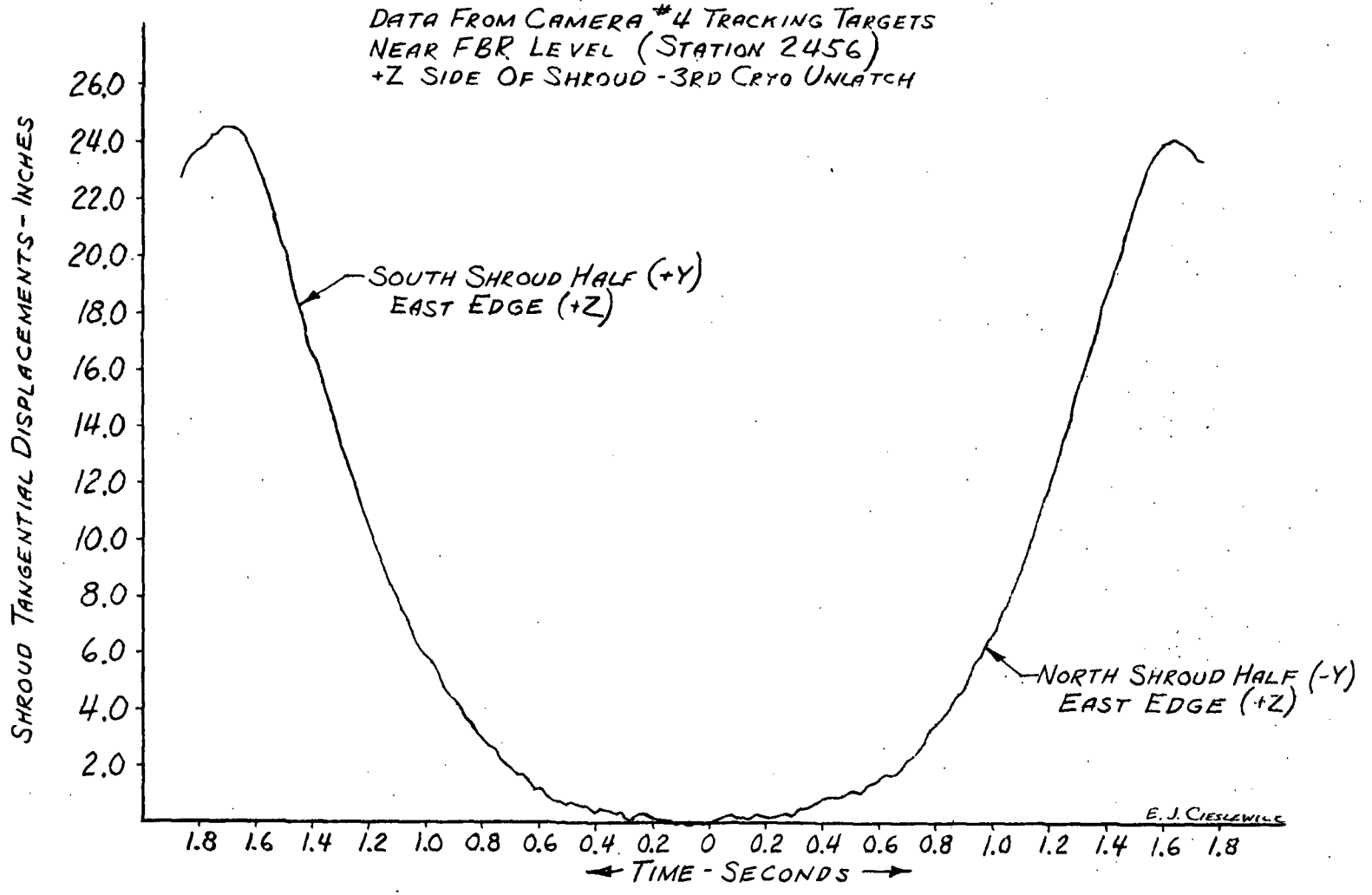

FIGURE X-15 NORTH & SOUTH SHROUD HALF DISPLACEMENT VS. TIME, 3RD CRYO UNLATCH

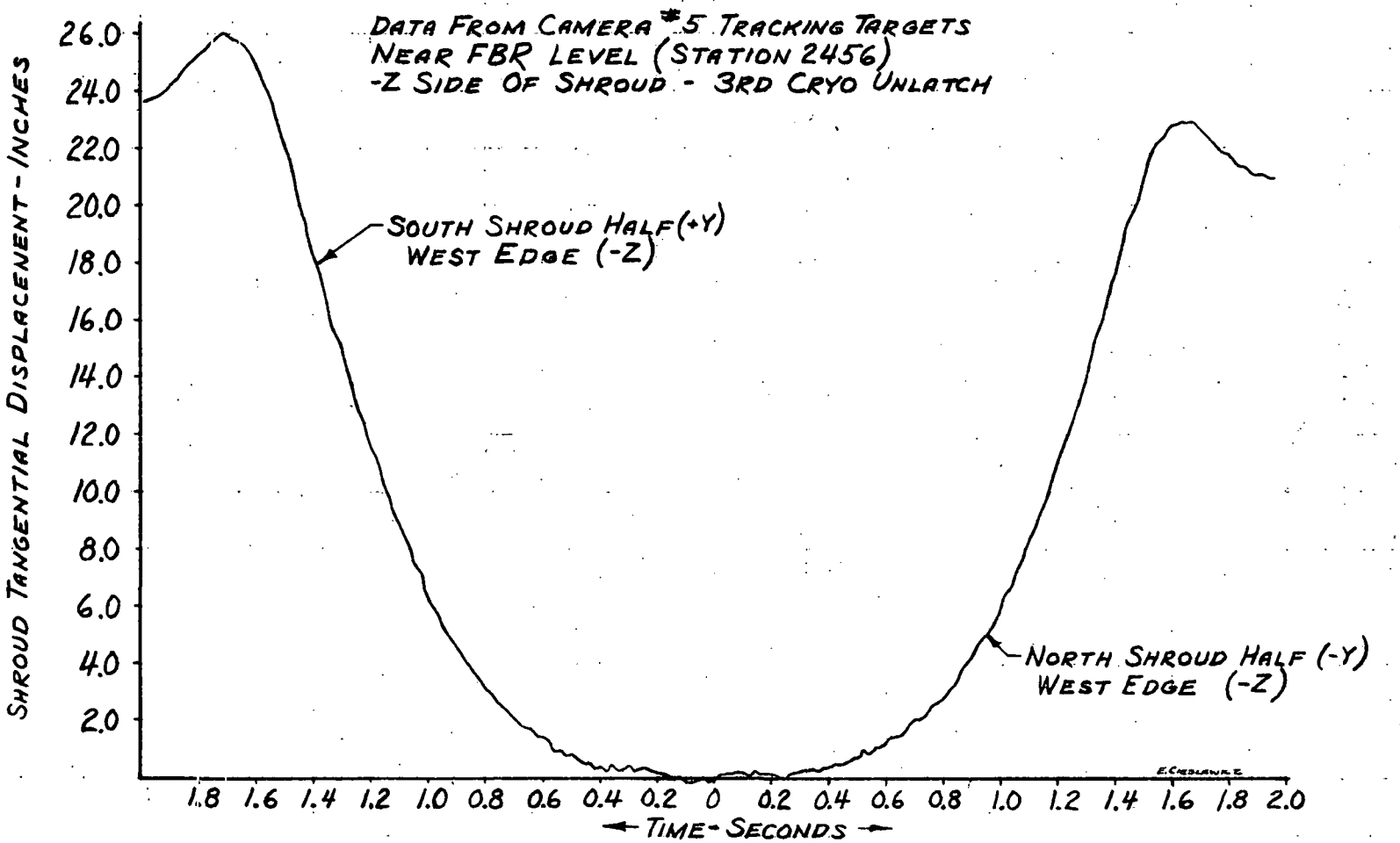

FIGURE V-16 NORTH & SHROUD HALF DISPLACEMENT VS. TIME, 3RD CRYO UNLATCH

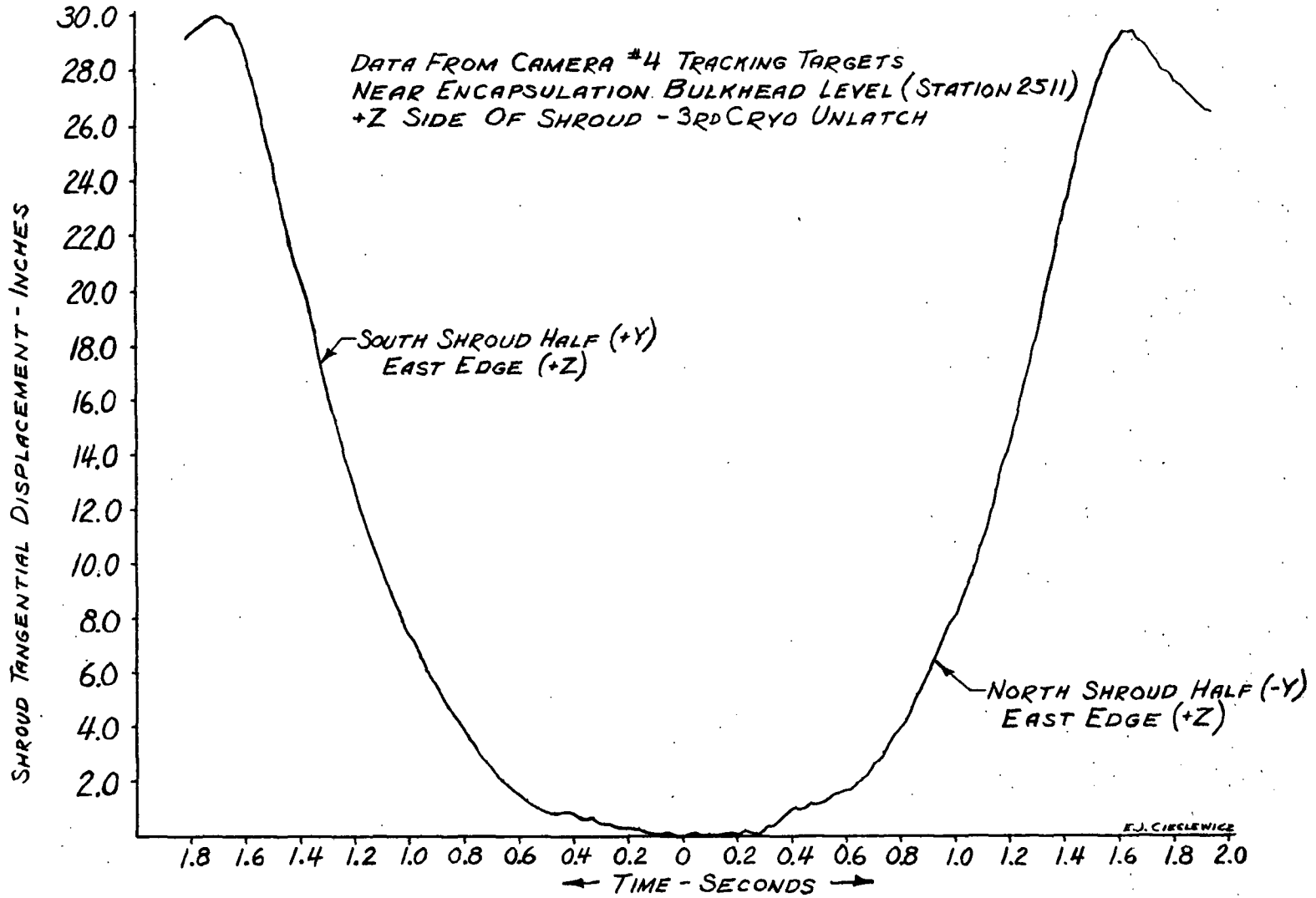

FIGURE XII7 NORTH & SOUTH SHROUD HALF DISPLACEMENT VS. TIME, 3RD CRYO UNLATCH

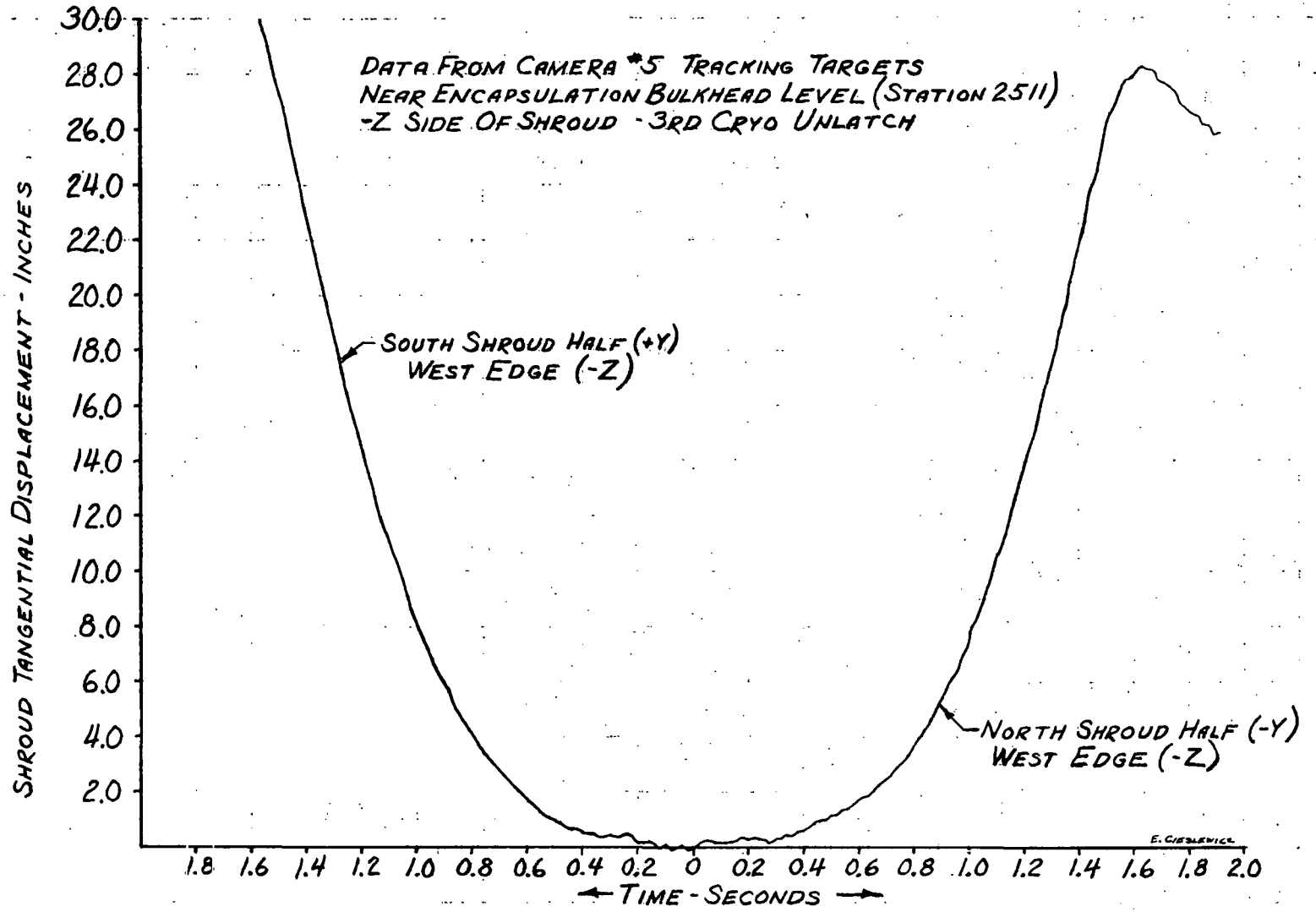

FIGURE X-18 NORTH & SOUTH SHROUD HALF DISPLACEMENT VS. TIME, 3RD CRYO UNLATCH

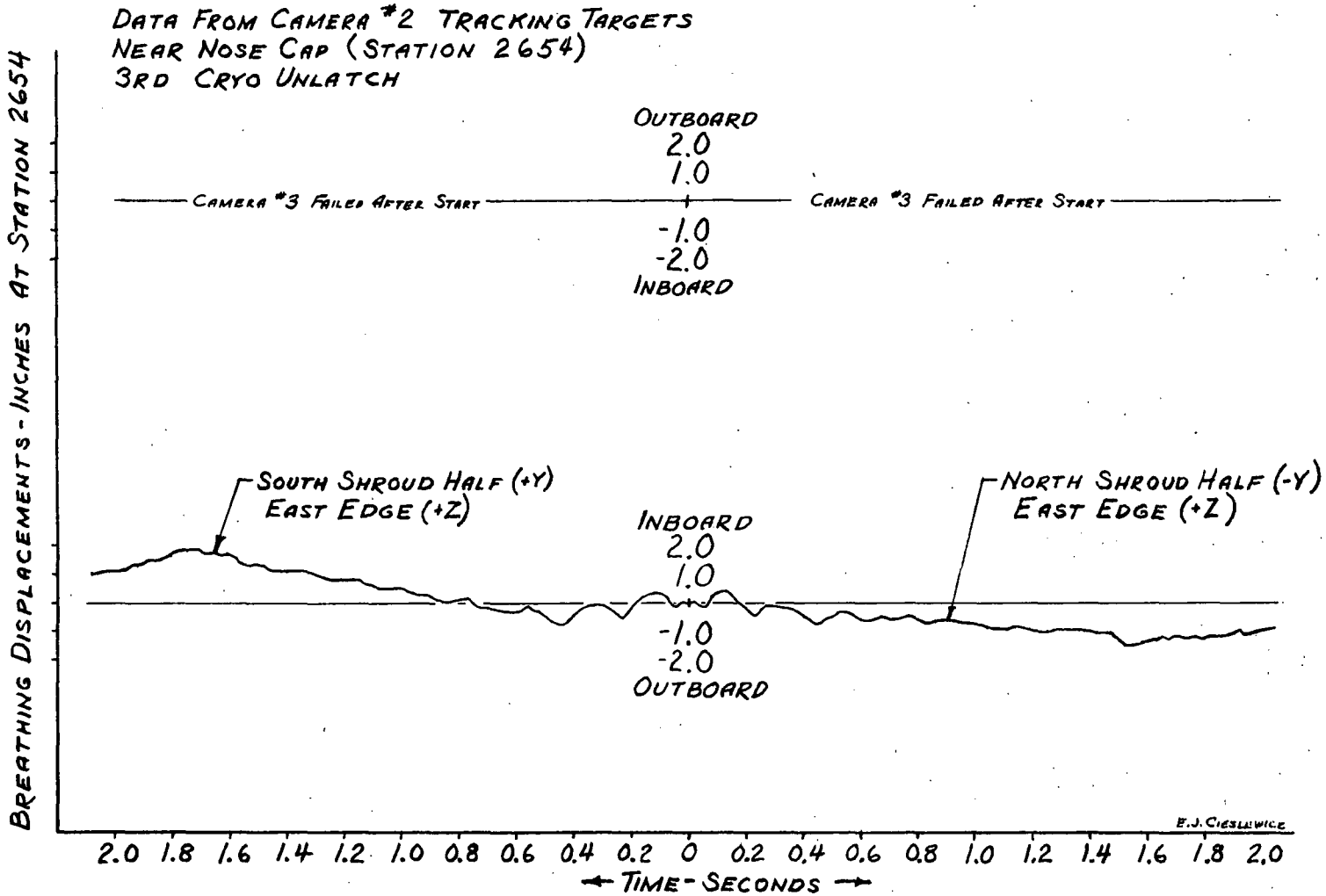

FIGURE X-19 NORTH & SOUTH SHROUD HALF BREATHING MOTIONS VS. TIME, 3RD CRYO UNLATCH

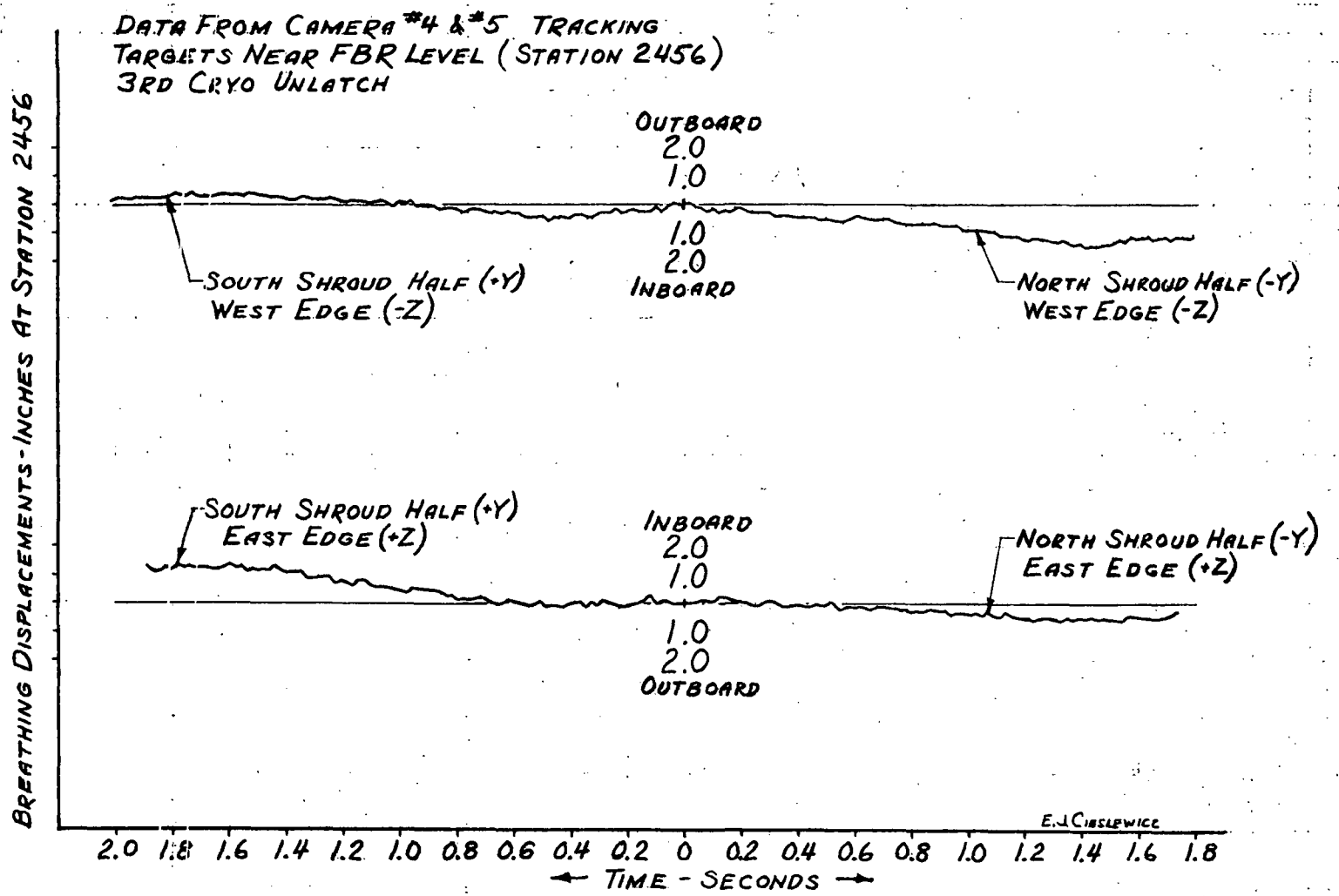

FIGURE I-20 NORTH & SOUTH SHROUD HALF BREATHING MOTIONS VS TIME, 3RD CRYO UNLATCH

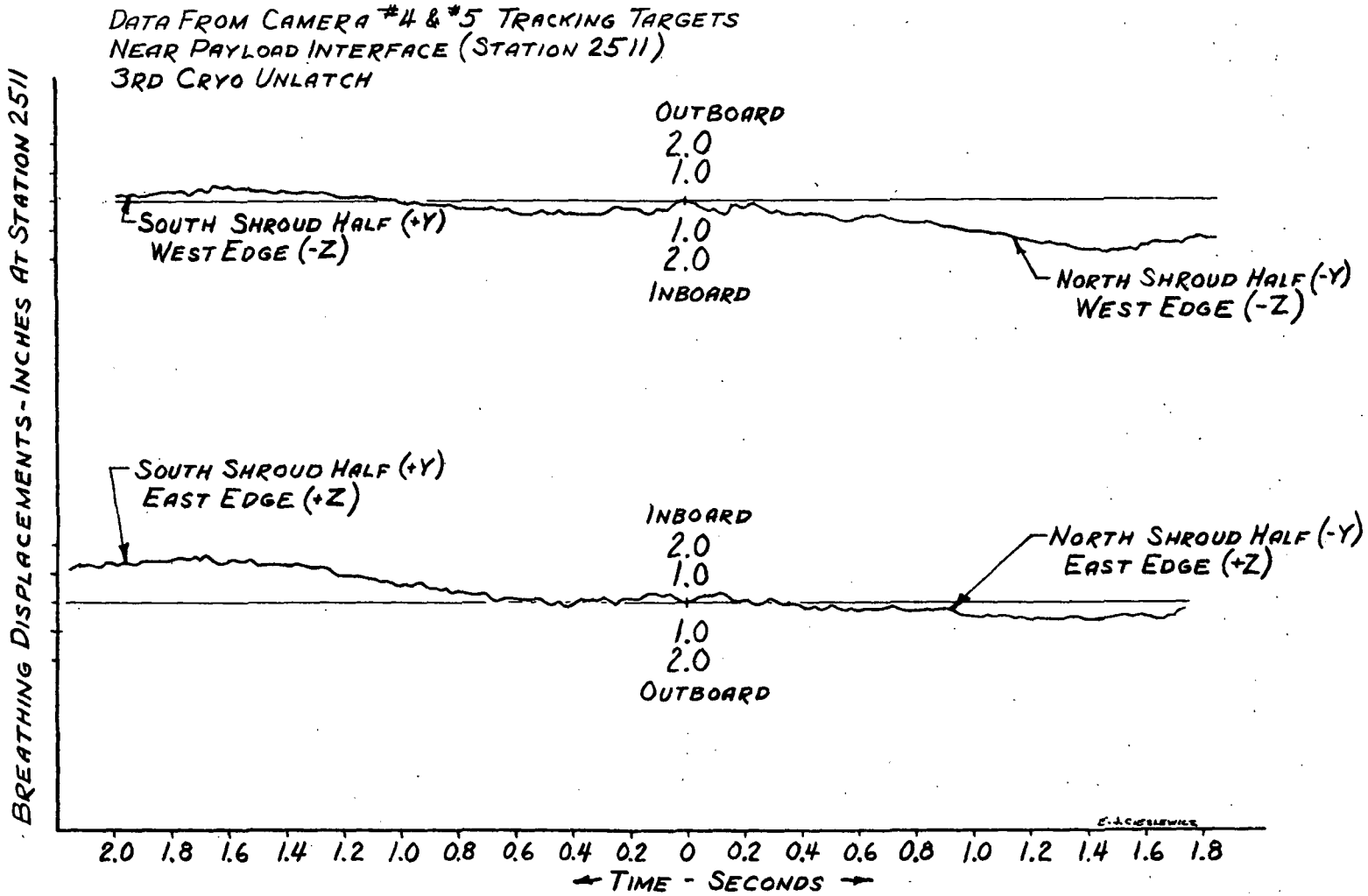

FIGURE X-21 NORTH & SOUTH SHROUD HALF BREATHING MOTIONS VS. TIME, 3RD CRYO UNLATCH

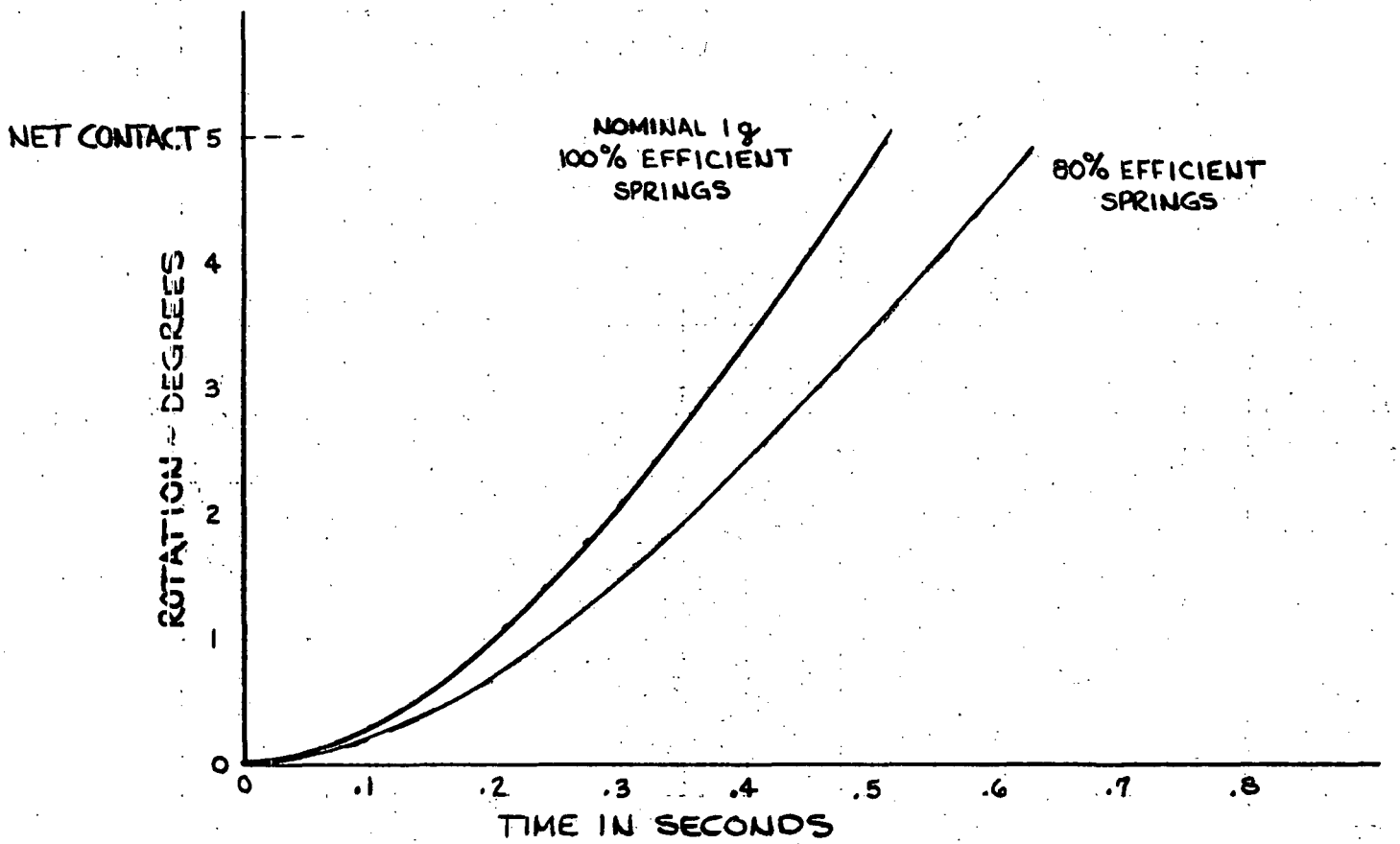

FIGURE X-22 PREDICTED CSS ROTATION HISTORY TO NET CONTACT

XI. SHROUD DYNAMICS/SHOCK LOADS/VIBRATION

by H. M. Tang

SUMMARY

Shock data were obtained during the three Centaur Standard Shroud cryo-unlatch tests. Each test consisted of three events: forward bearing reaction strut disconnect, shroud Super-Zip joint firing, and forward seal release. The forward seal was released by a mechanical device for the first two tests and the third one was by a pyrotechnic device. Since the seal released by mechanical means would create much less shock than by pyrotechnic means, the shock spectral analysis presented herein includes (a) forward bearing reaction strut disconnect and Super-Zip joint firing for three tests and (b) forward seal release for the third test.

CENTAUR EQUIPMENT MODULE AND ELECTRONICS PACKAGES

Figure XI-1 shows the locations of the accelerometers and electronic packages for three tests. The packages are dummy units with weights closely simulating the flight hardware. Table XI-1 shows the accelerometer locations and axes orientations at certain packages which were used for each test. Figure XI-2 shows the qualification levels for the packages. Figures XI-3 through XI-9 are the plots of the envelopes of the package responses for each event of each test. These figures show that the forward bearing reaction strut separation yields maximum shock response for the packages. A comparison of figures XI-3 to XI-9 with figure XI-2 shows that the test results are well below the qualification level.

TITAN SKIRT

Figure XI-10 shows the locations of the accelerometers for the tests. Figure XI-11 shows the Titan skirt pyrotechnic shock spectral response qualification levels. Figures XI-12 through XI-18 are the plots of the envelopes of the acceleration responses for the tests. These plots show that the shroud Super-Zip joint firing yields the maximum shock responses. A comparison of these plots with figure XI-3 shows that the test results are well below the qualification level.

TITAN TRUSS

Figure XI-19 shows the locations of the accelerometers for the tests. Figures XI-20 and XI-21 are the plots of the envelopes of the acceler-

ation responses for the first test, since there was no instrumentation at this region for the second and third tests. These plots show that the Super-Zip joint firing yields the maximum shock responses. A comparison of these plots with figure XI-3 shows that the test results are well below the qualification level.

STATION 2204 RING

Figure XI-19 shows the locations of the accelerometers for the tests. Figures XI-22 through XI-26 are the plots of the envelopes of the acceleration responses for the second and third tests, since there was no instrumentation at this region for the first test. These plots show that the shroud Super-Zip joint firing yields the maximum shock responses. No comparison of these plots with qualification levels can be made since there was no general specification available.

INTERSTAGE ADAPTER

Figure XI-19 shows the locations of the accelerometers for the tests. Figures XI-27 through XI-31 are the plots of the envelopes of the acceleration responses for the second and third tests, since there was no instrumentation at this region for the first test. These plots show that the shroud Super-Zip joint firing yields the maximum shock responses. No comparison of these plots with qualification levels can be made since there was no general specification available.

TABLE XI-1

ACCELEROMETER LOCATION FOR PACKAGES MOUNTED ON CENTAUR EQUIPMENT MODULE

TEST NO. 1 (9/28/72)			TEST NO. 2 (11/8/72)			TEST NO. 3 (2/7/73)		
MEAS. NO.	HARDWARE	DIRECTION	MEAS. NO.	HARDWARE	DIRECTION	MEAS. NO.	HARDWARE	DIRECTION
903	SIU	M	903	SIU	M	906	IRU	-X
904	SIU	-N	904	SIU	-N	907	IRU	Y
905	SIU	L	905	SIU	L	908	IRU	-Z
906	IRU	-X	912	DCU	-M	909	RMU	M
907	IRU	Y	913	DCU	-N	910	RMU	-N
908	IRU	-Z	914	DCU	-L	911	RMU	-L
909	RMU	M	948	SCU	M	948	SCU	M
910	RMU	-N	949	SCU	N	949	SCU	N
911	RMU	-L	950	SCU	L	950	SCU	L
912	DCU	-M	951	SC-1	M	951	SC-1	M
913	DCU	-N	952	SC-1	N	952	SC-1	N
914	DCU	-L	953	SC-1	L	953	SC-1	L

Note: M is Parallel to Surface L is Lateral to Surface N is Normal to Surface

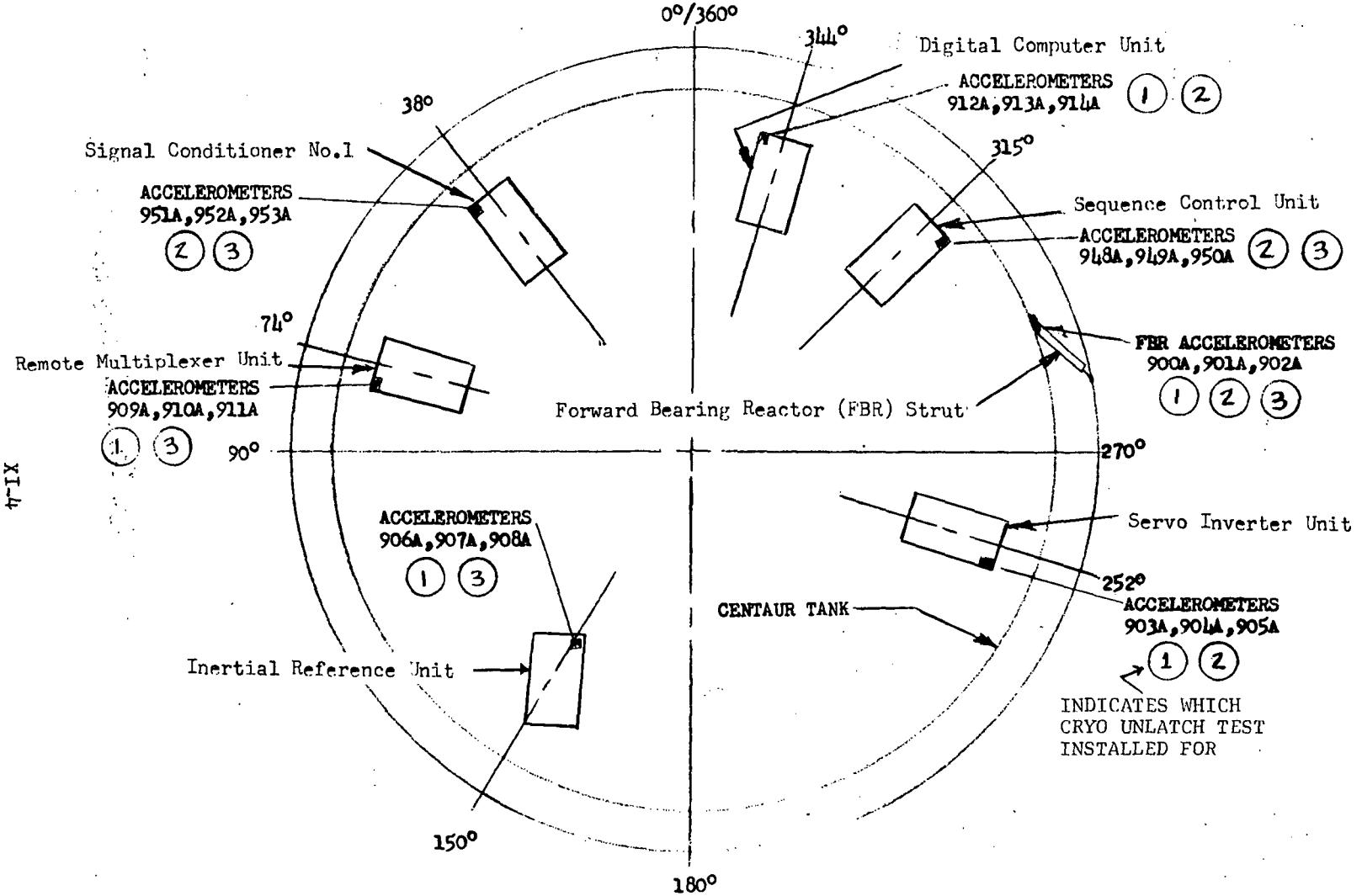

FIGURE XI-1 LOCATION OF ACCELEROMETERS ON THE EQUIPMENT MODULE AND FBR STRUT
CSS CRYOGENIC UNLATCH TESTS - PLUM BROOK - B-3 FACILITY

Page Intentionally Left Blank

FIGURE XI-2 SHOCK QUALIFICATION SPECIFICATION FOR PACKAGES MOUNTED ON THE CENTAUR EQUIPMENT MODULE

PRELIMINARY DATA - SUBJECT TO CHANGE

FIGURE XI-3 FBR STRUT DISCONNECT. CRYOUNLATCH TEST NO.1. PACKAGES MOUNTED ON THE CENTAUR EQUIPMENT MODULE

PRELIMINARY DATA - SUBJECT TO CHANGE

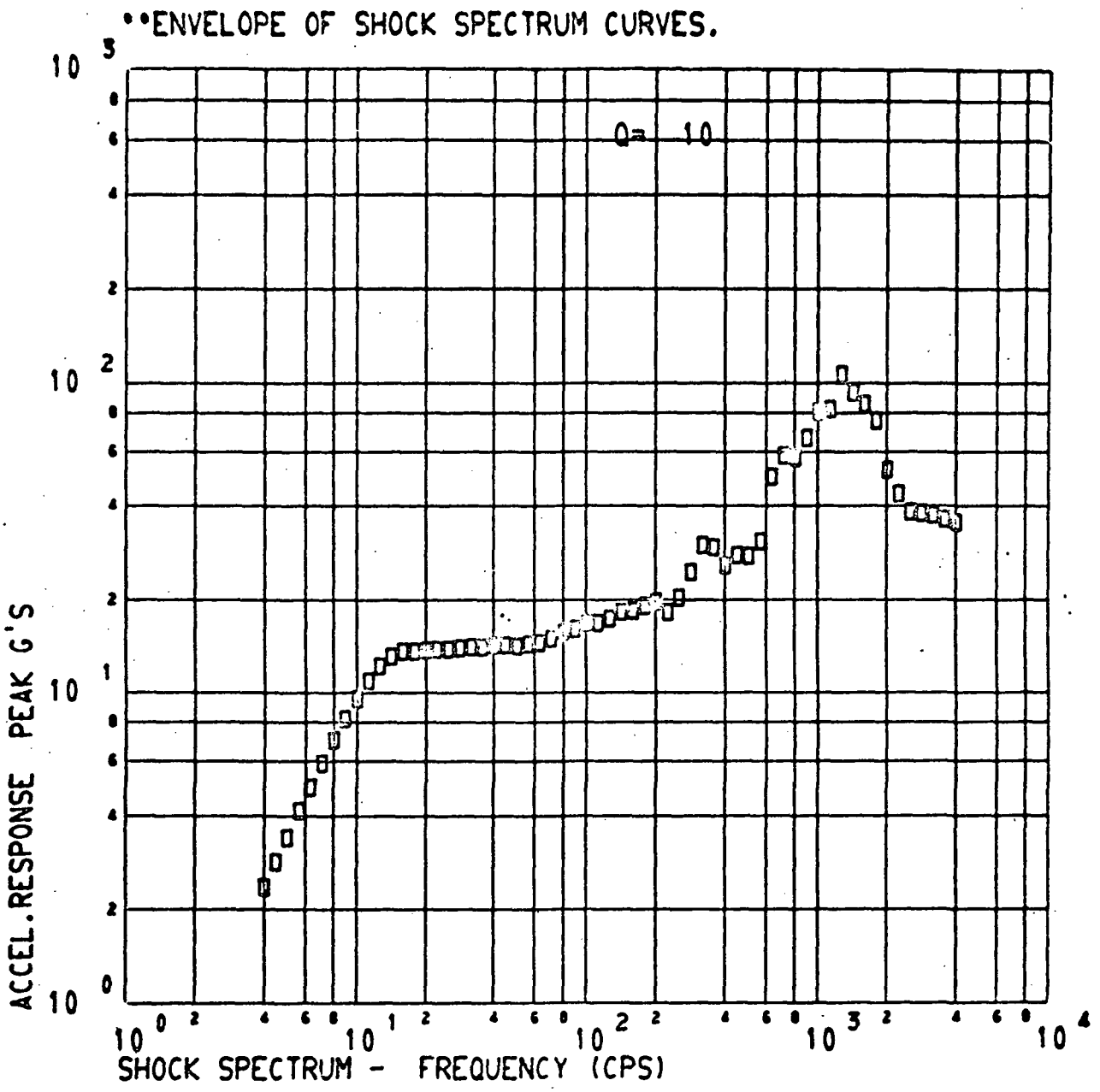

FIGURE XI-4 FBR STRUT DISCONNECT. CRYOUNLATCH TEST NO.2. PACKAGES MOUNTED ON THE CENTAUR EQUIPMENT MODULE

PRELIMINARY DATA - SUBJECT TO CHANGE

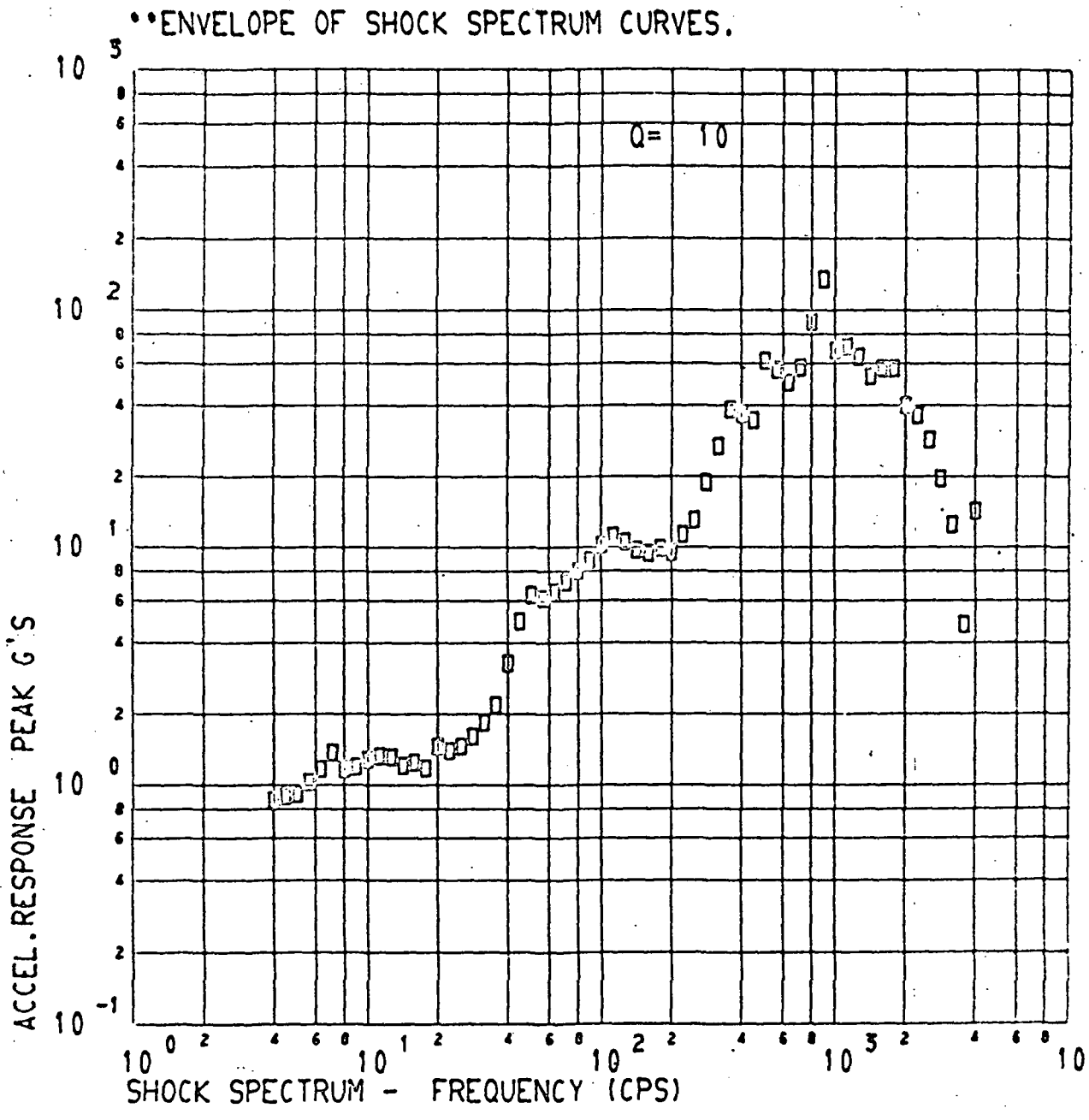

FIGURE XI - 5 FBR STRUT DISCONNECT. CRYOUNLATCH TEST NO. 3. PACKAGES MOUNTED ON THE CENTAUR EQUIPMENT MODULE

PRELIMINARY DATA - SUBJECT TO CHANGE

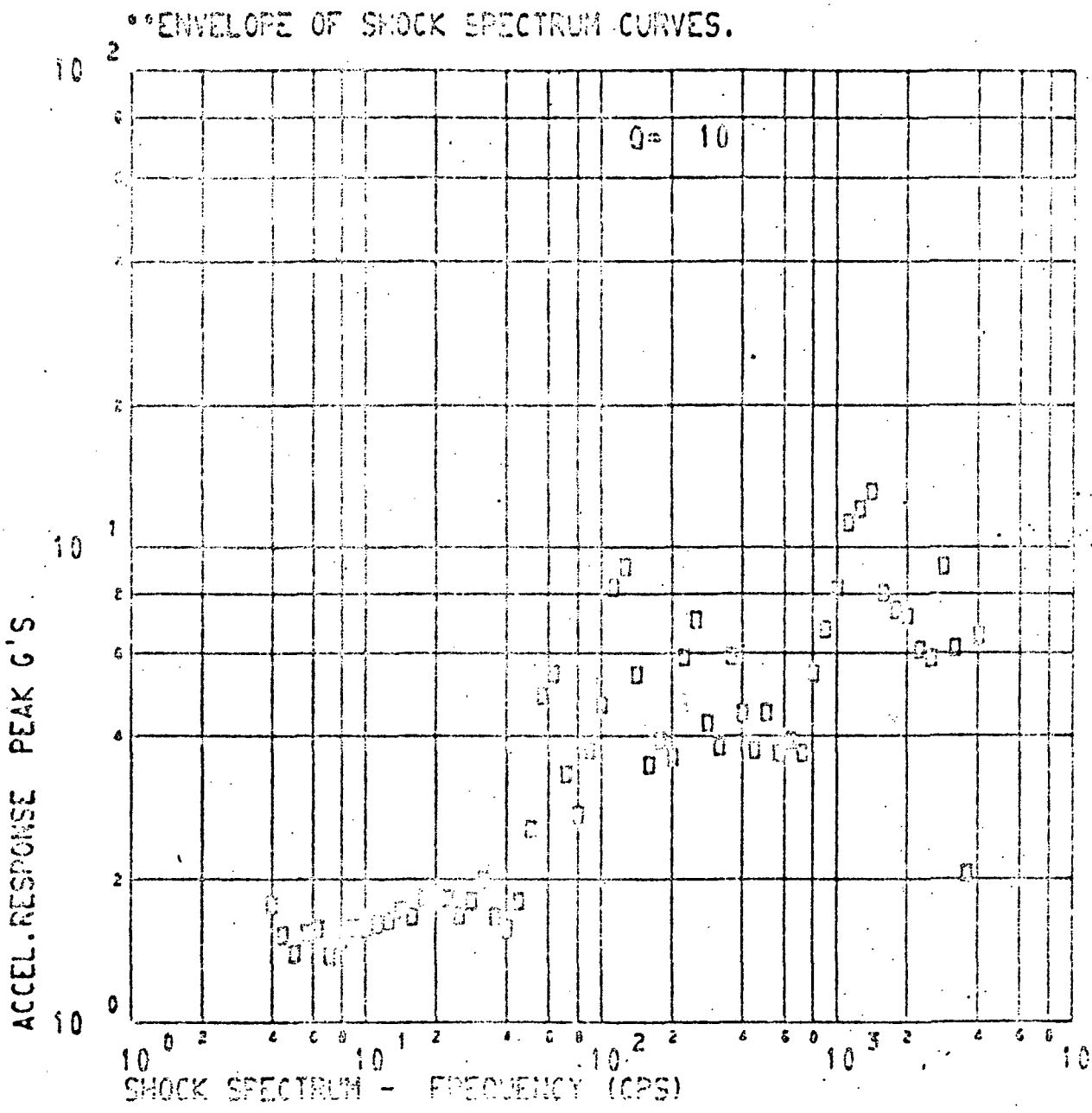

FIGURE XI-6 FORWARD SEAL RELEASE. CRYOUNLATCH TEST NO. 3. PACKAGES MOUNTED ON THE CENTAUR EQUIPMENT MODULE

PRELIMINARY DATA - SUBJECT TO CHANGE

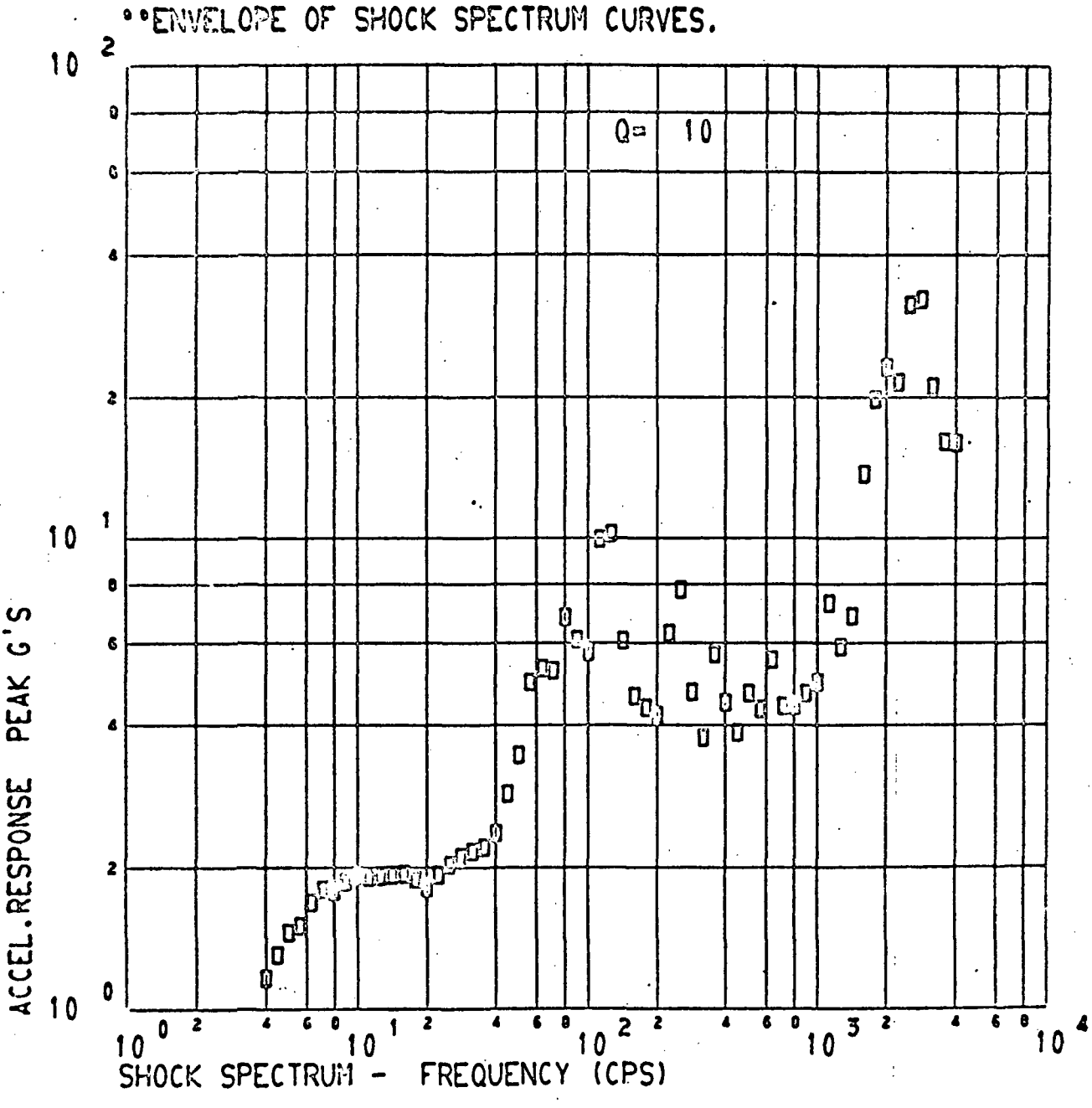

FIGURE XI-7 SUPER*ZIP FIRING. CRYOUNLATCH TEST NO.1. PACKAGES MOUNTED ON THE CENTAUR EQUIPMENT MODULE

PRELIMINARY DATA - SUBJECT TO CHANGE

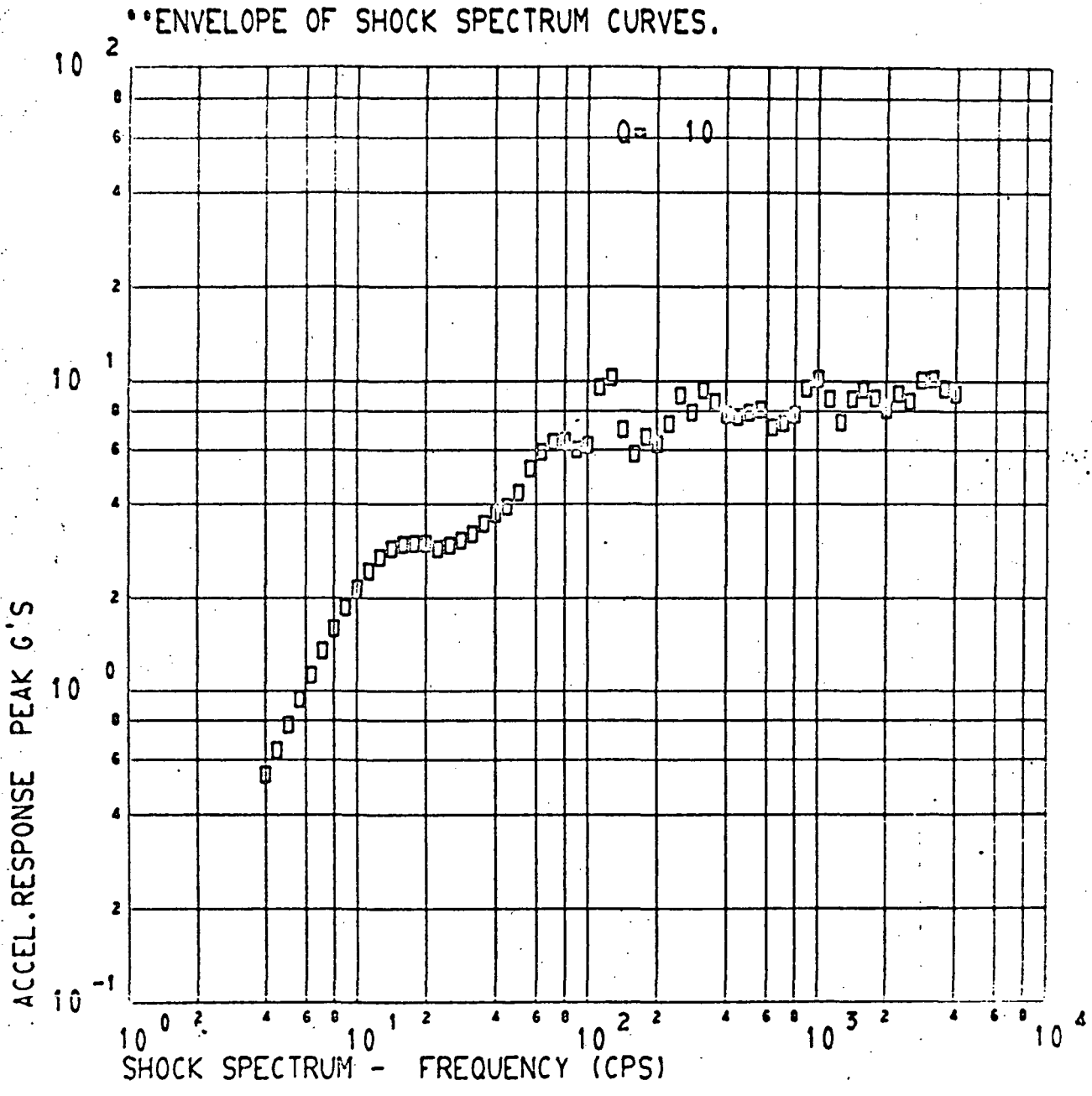

FIGURE XI-8 SUPER*ZIP FIRING. CRYOUNLATCH TEST NO. 2. PACKAGES MOUNTED ON THE CENTAUR EQUIPMENT MODULE

PRELIMINARY DATA - SUBJECT TO CHANGE

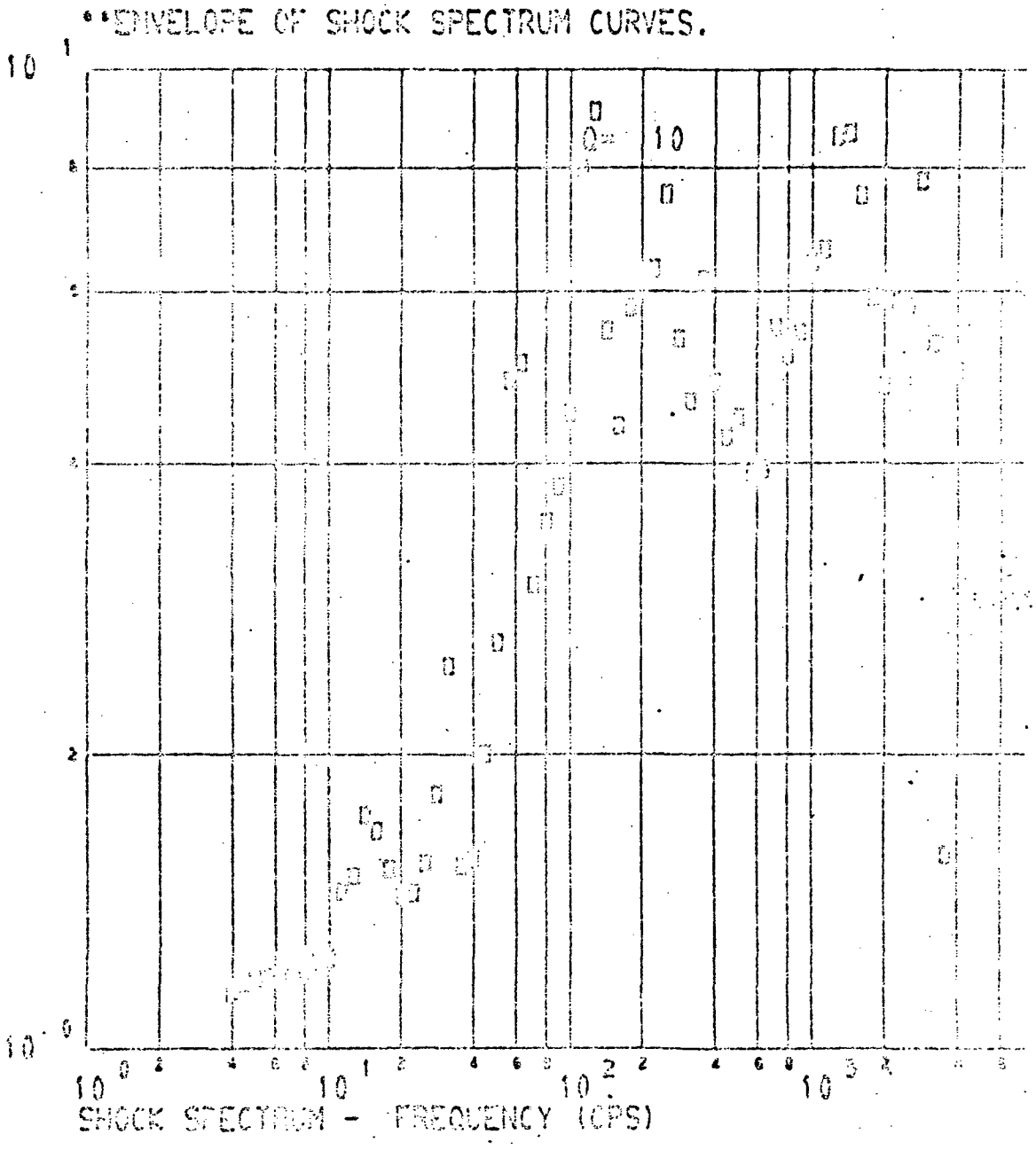

FIGURE XI-9 SUPER*ZIP FIRING CRYOUNLATCH TEST NO. 3 PACKAGES MOUNTED ON THE CENTAUR EQUIPMENT MODULE

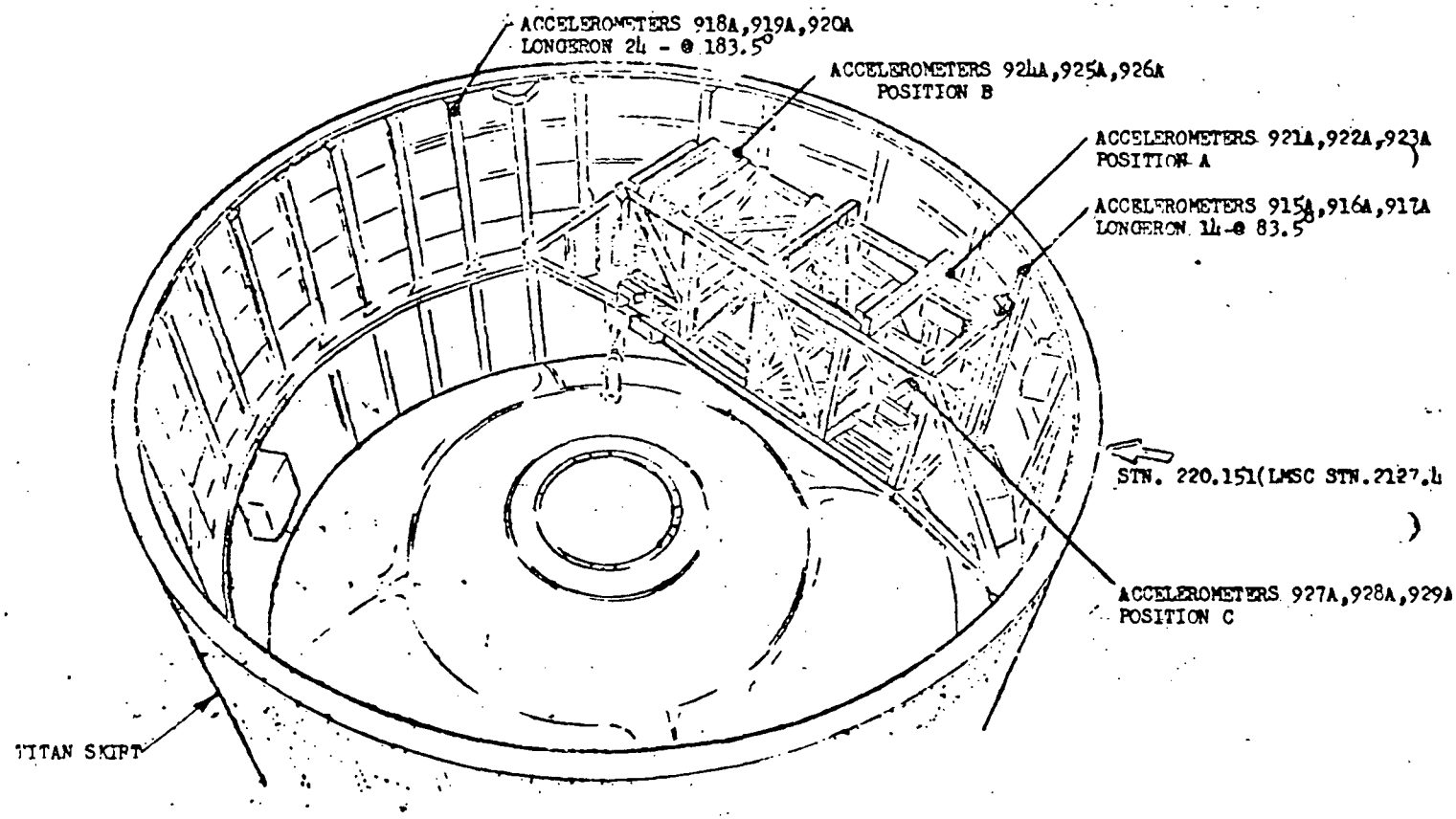

FIGURE XI - 10 LOCATION OF ACCELEROMETERS ON THE TITAN SKIRT - CSS CRYO-UNLATCH TESTS - B-3 FACILITY - PLUM BROOK

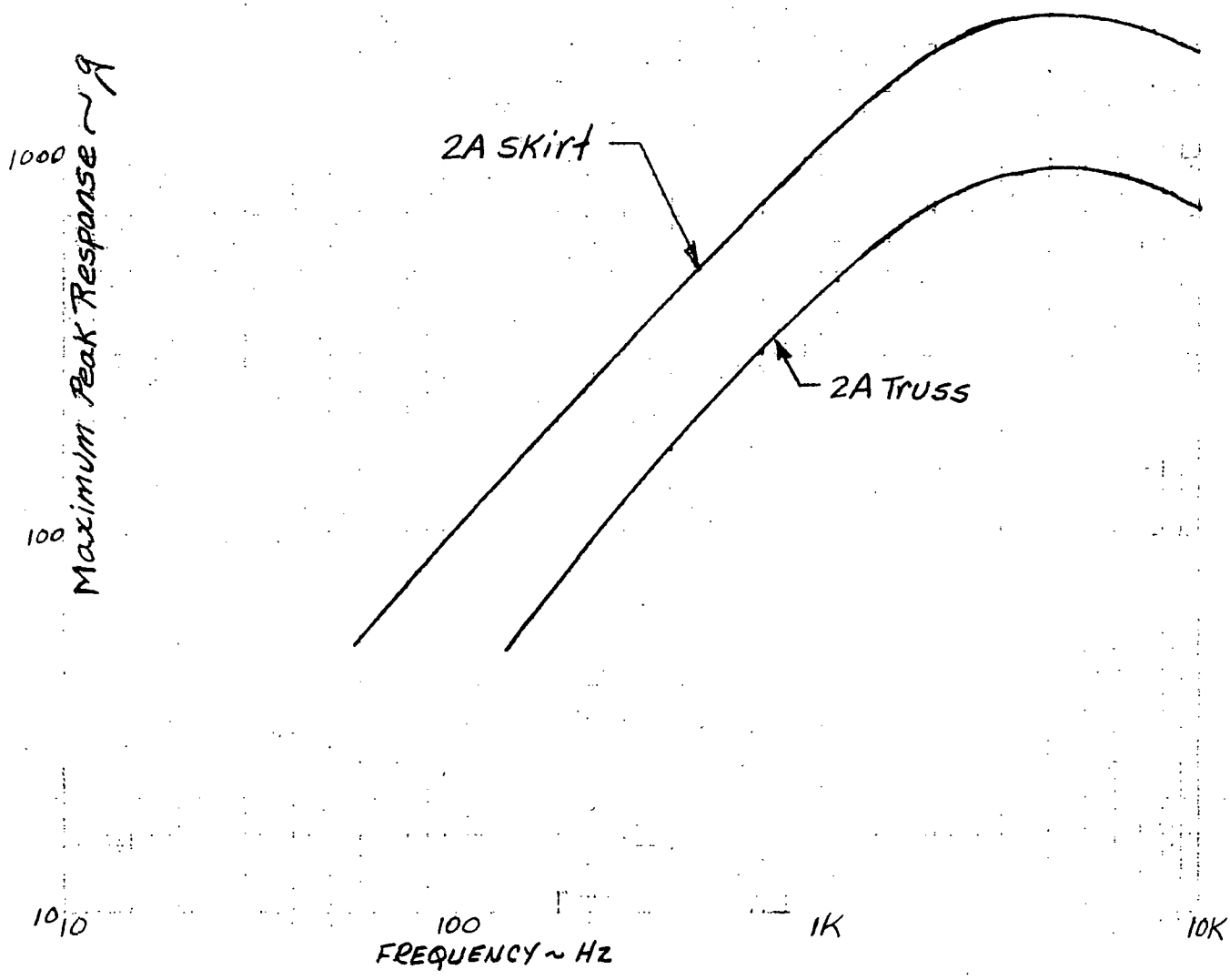

FIGURE XI-11 TITAN COMPARTMENT 2A PYROTECHNIC SHOCK SPECTRAL RESPONSE

QUALIFICATION LEVELS

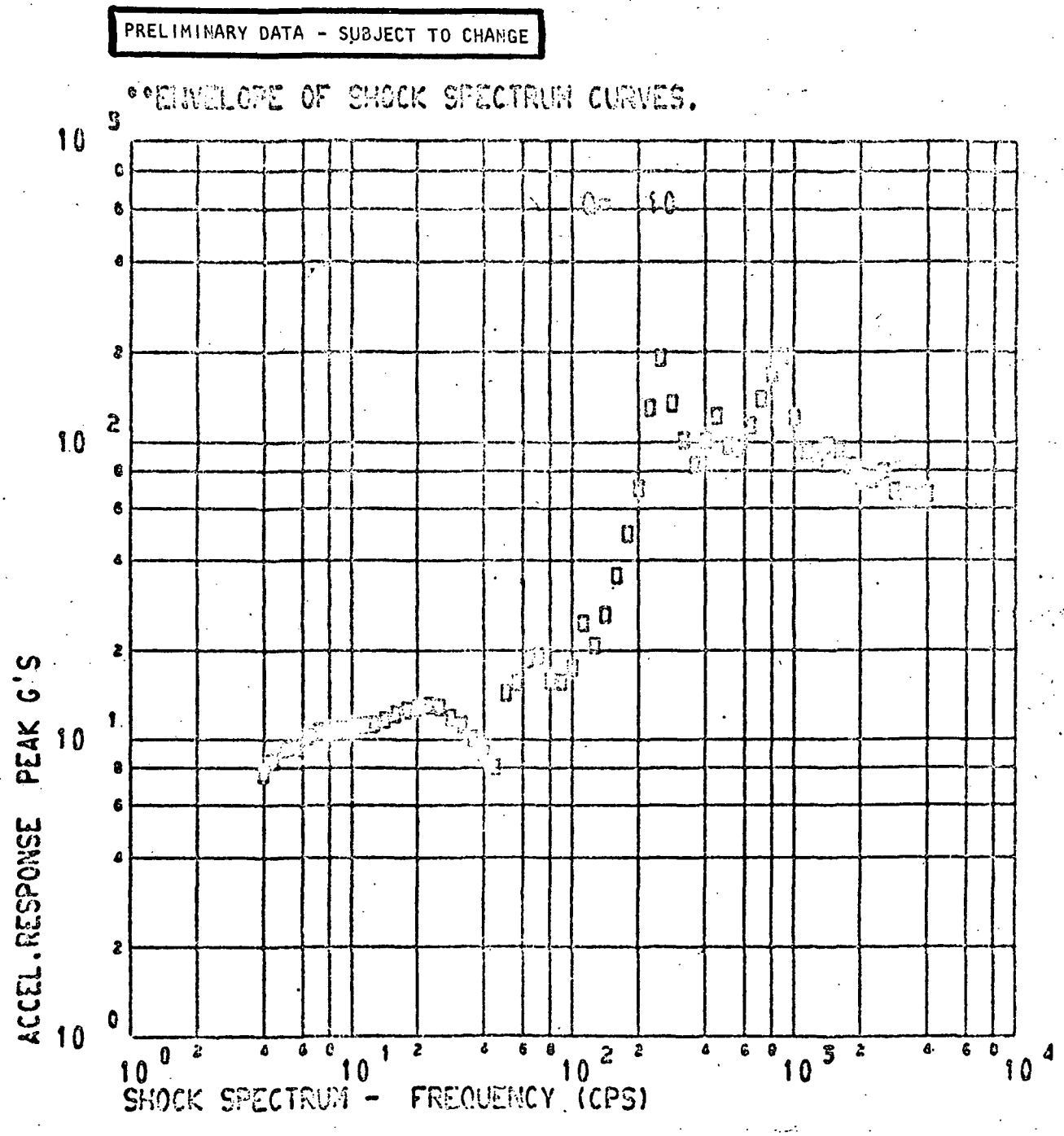

FIGURE XI-12 FBR STRUT DISCONNECT. CRYOUNLATCH TEST NO. 1

TITAN SKIRT AREA 2A

PRELIMINARY DATA - SUBJECT TO CHANGE

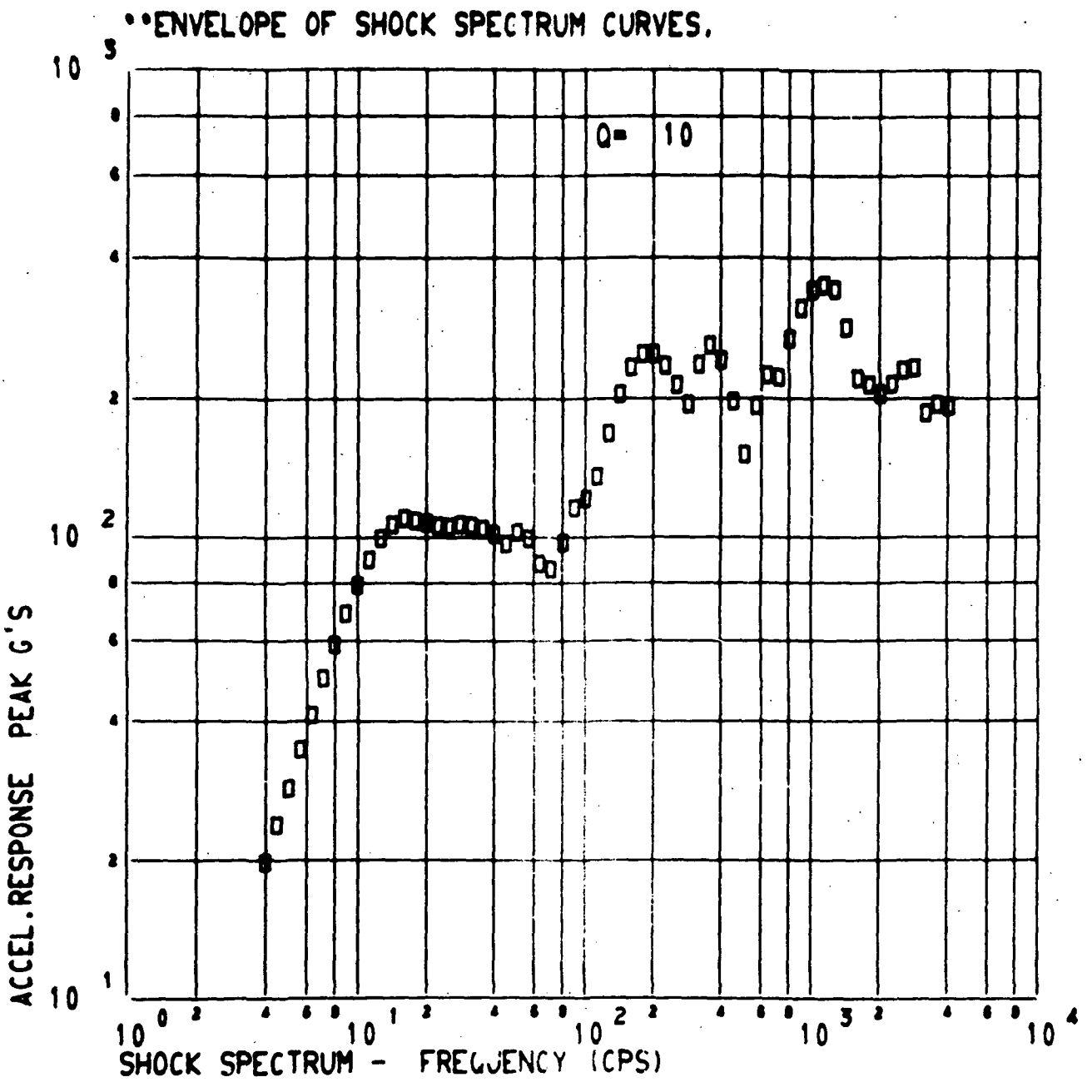

FIGURE X - 13 FBR STRUT DISCONNECT. CRYOUNLATCH TEST NO. 2. TITAN SKIRT AREA 2A

PRELIMINARY DATA - SUBJECT TO CHANGE

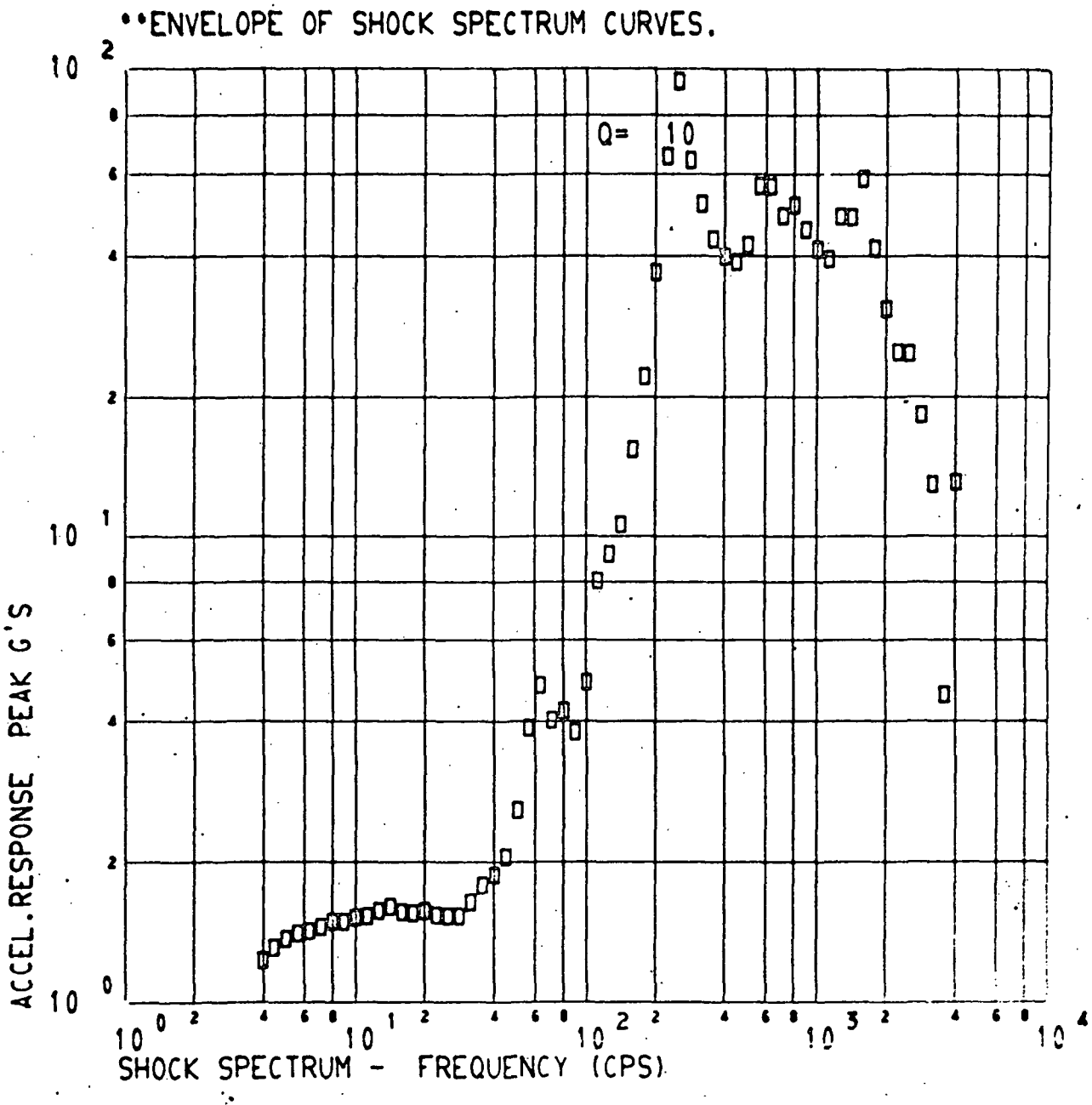

FIGURE XI-14 FBR STRUT DISCONNECT. CRYOUNLATCH TEST NO. 2. TITAN SKIRT AREA 2A

PRELIMINARY DATA - SUBJECT TO CHANGE

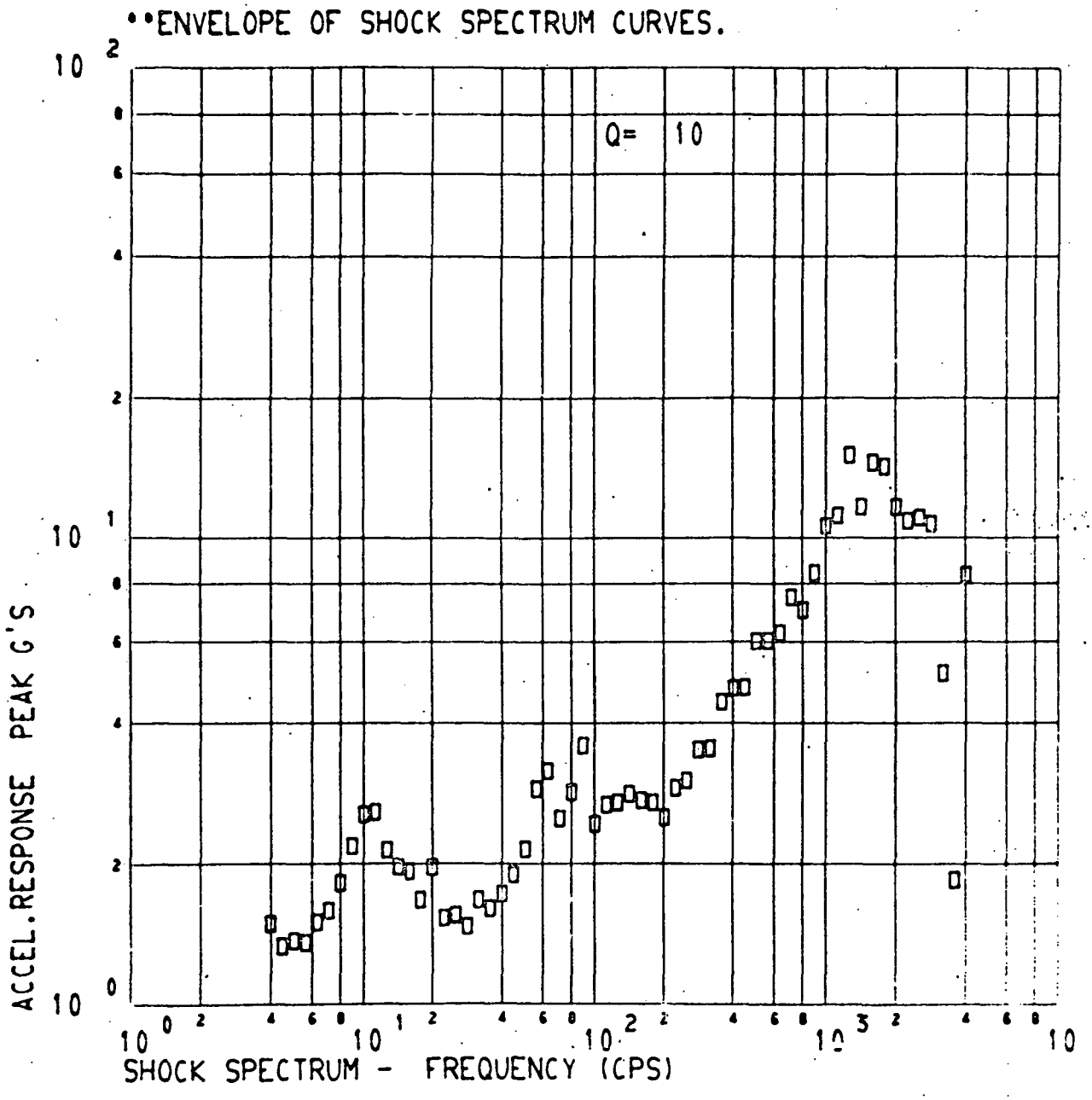

FIGURE XI-15 FORWARD SEAL RELEASE. CRYOUNLATCH TEST NO. 3. TITAN SKIRT AREA 2A

PRELIMINARY DATA SUBJECT TO CHANGE

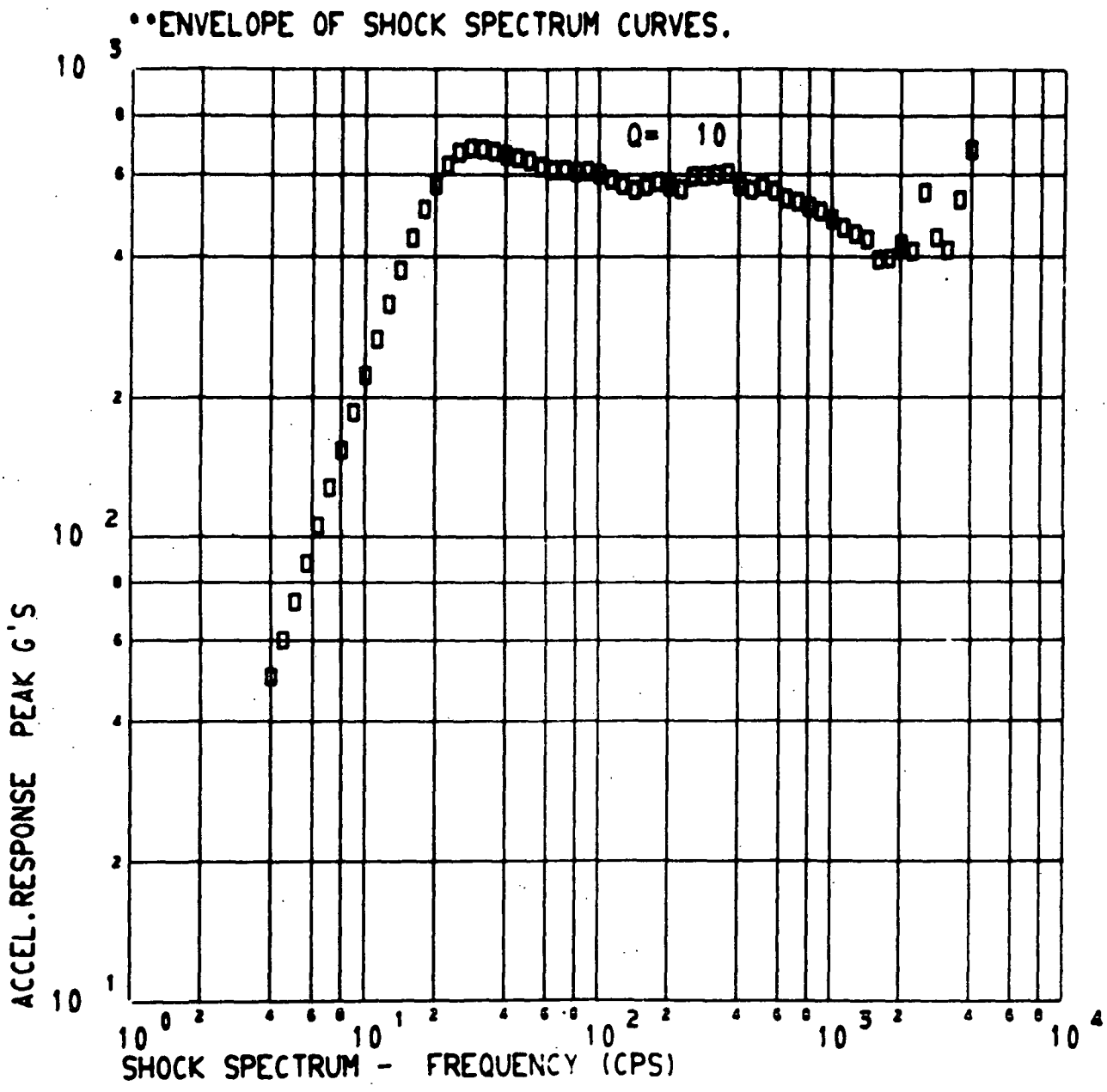

FIGURE XI-16 SUPER*ZIP FIRING. CRYOUNLATCH TEST NO.1. TITAN SKIRT

AREA 2A

PRELIMINARY DATA - SUBJECT TO CHANGE

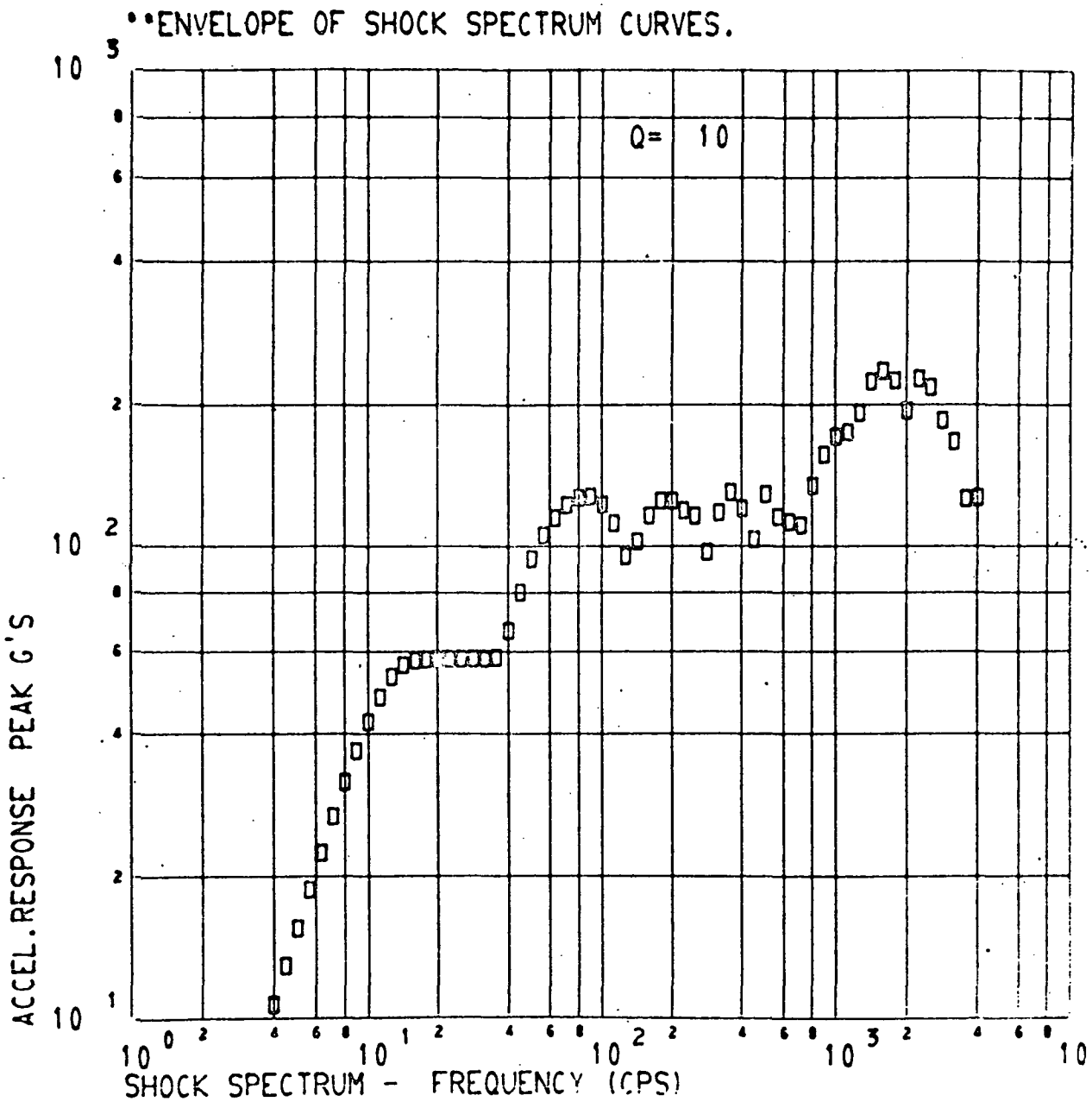

FIGURE XI-17 SUPER*ZIP FIRING. CRYOUNLATCH TEST NO.2. TITAN SKIRT AREA 2A

PRELIMINARY DATA - SUBJECT TO CHANGE

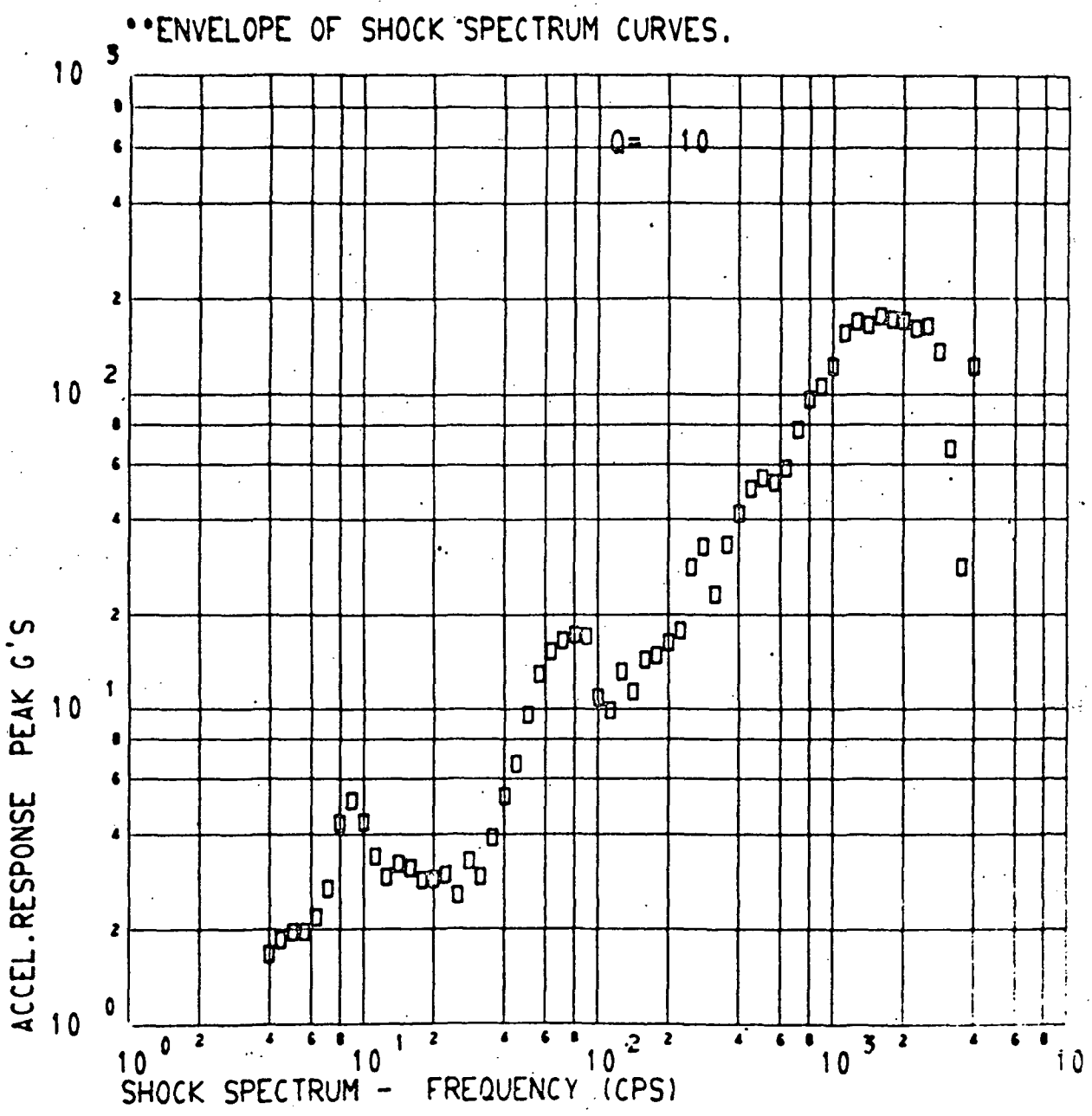

FIGURE XI-18 SUPER*ZIP FIRING. CRYOUNLATCH TEST NO.3: TITAN SKIRT AREA 2A

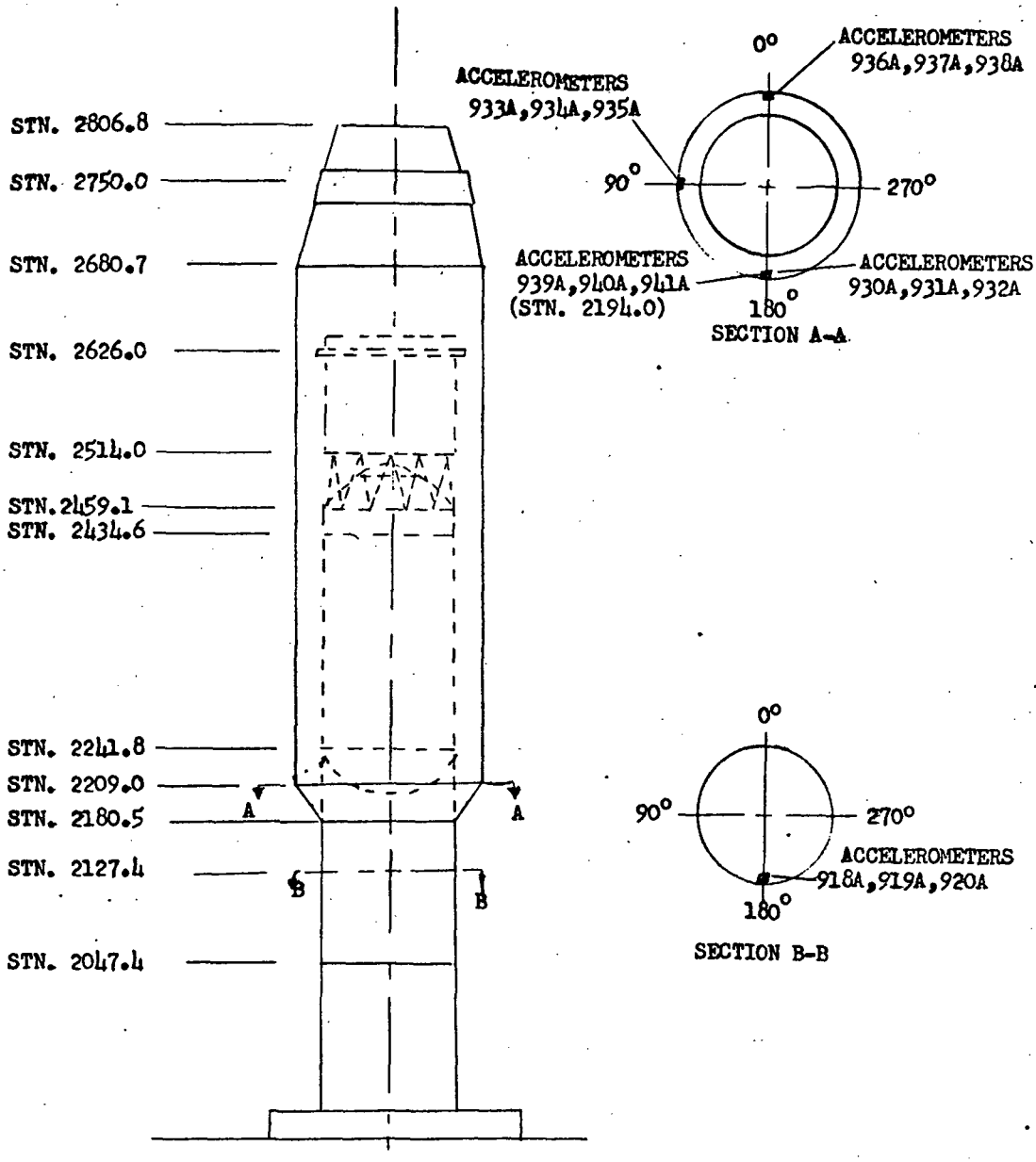

FIGURE XI-19 LOCATION OF ACCELEROMETERS ON THE BOATTAIL AND THE ISA - CSS CRYO-UNLATCH TESTS - B-3 FACILITY PLUM BROOK

PRELIMINARY DATA SUBJECT TO CHANGE

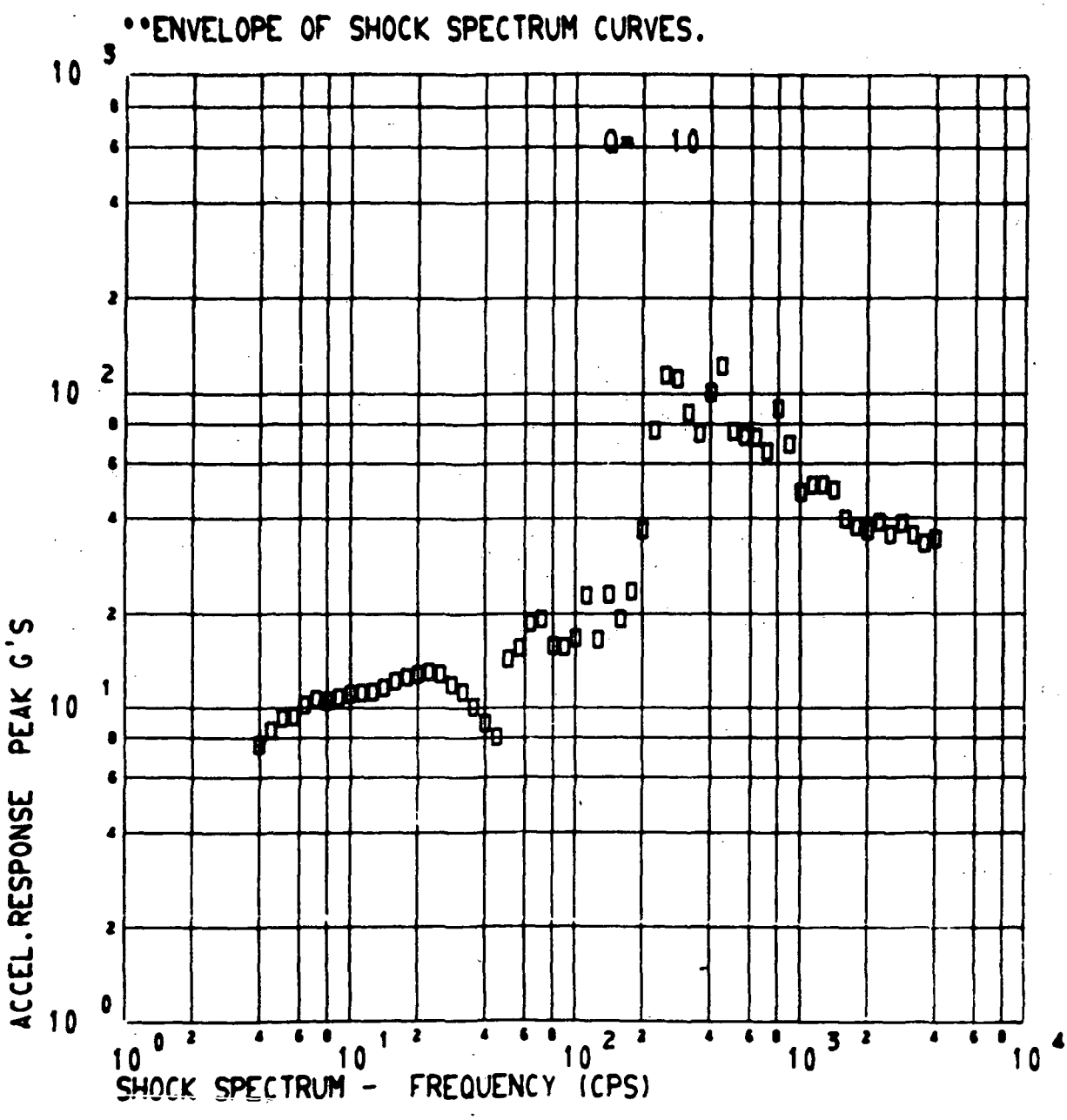

FIGURE XI - 20 FBR STRUT DISCONNECT. CRYOUNLATCH TEST NO. 1 TITAN SKIRT

PRELIMINARY DATA SUBJECT TO CHANGE

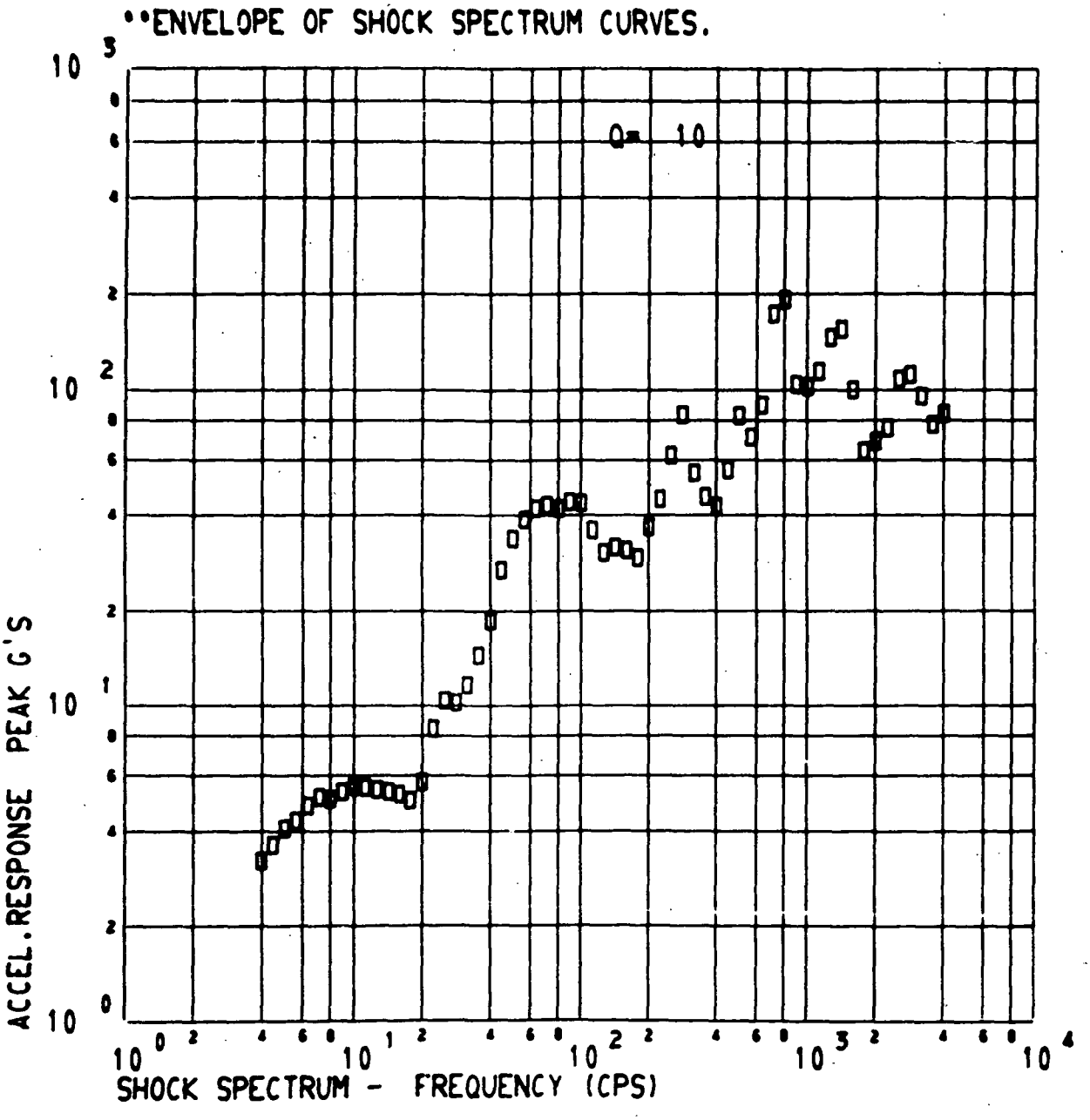

FIGURE XI - 21 SUPER*ZIP FIRING. CRYOUNLATCH TEST NO,.1 TITAN SKIRT

PRELIMINARY DATA SUBJECT TO CHANGE

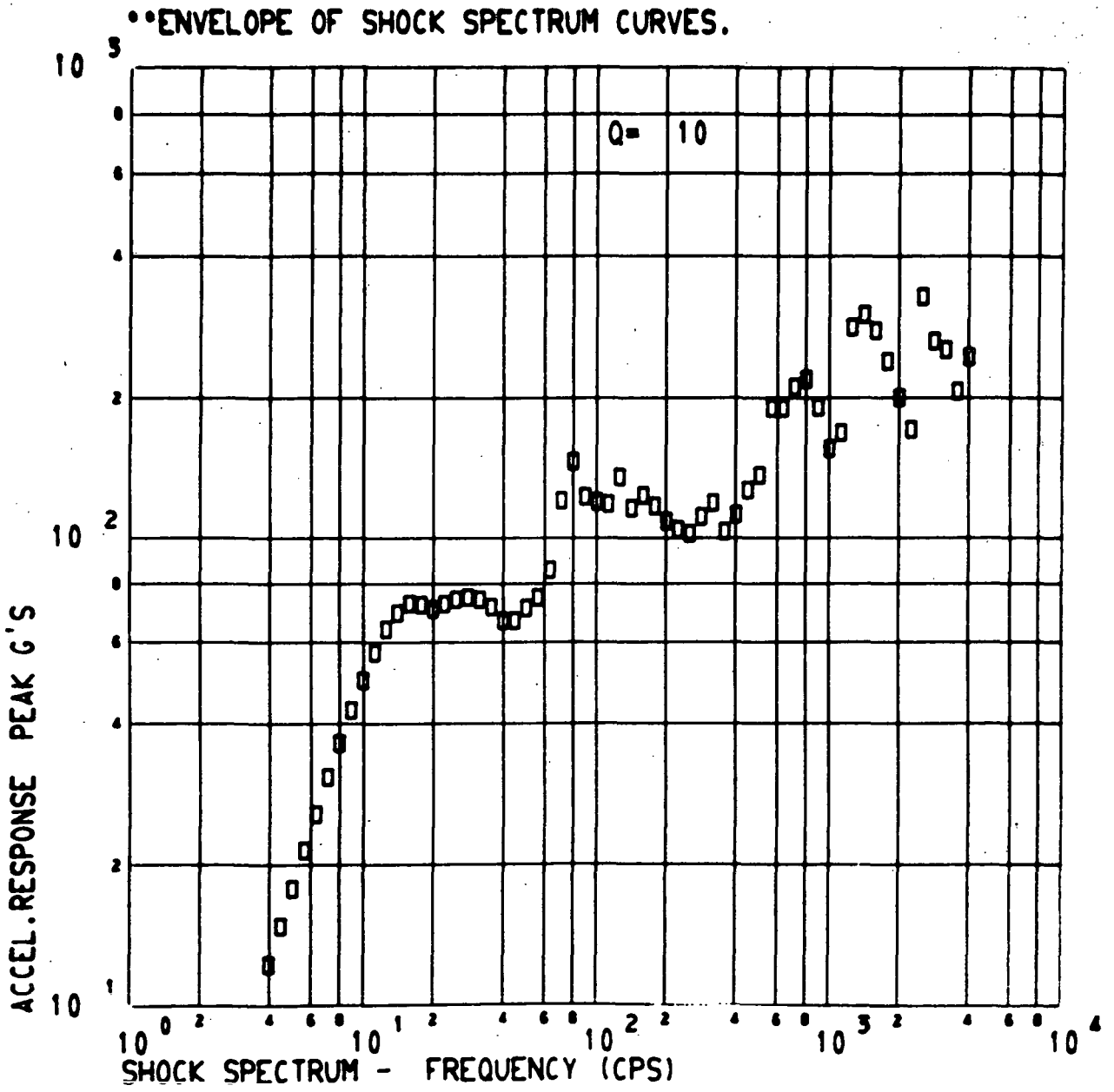

FIGURE XI-22 FBR STRUT DISCONNECT. CRYOUNLATCH TEST NO.2. STATION NUMBER 2204 RING

PRELIMINARY DATA - SUBJECT TO CHANGE

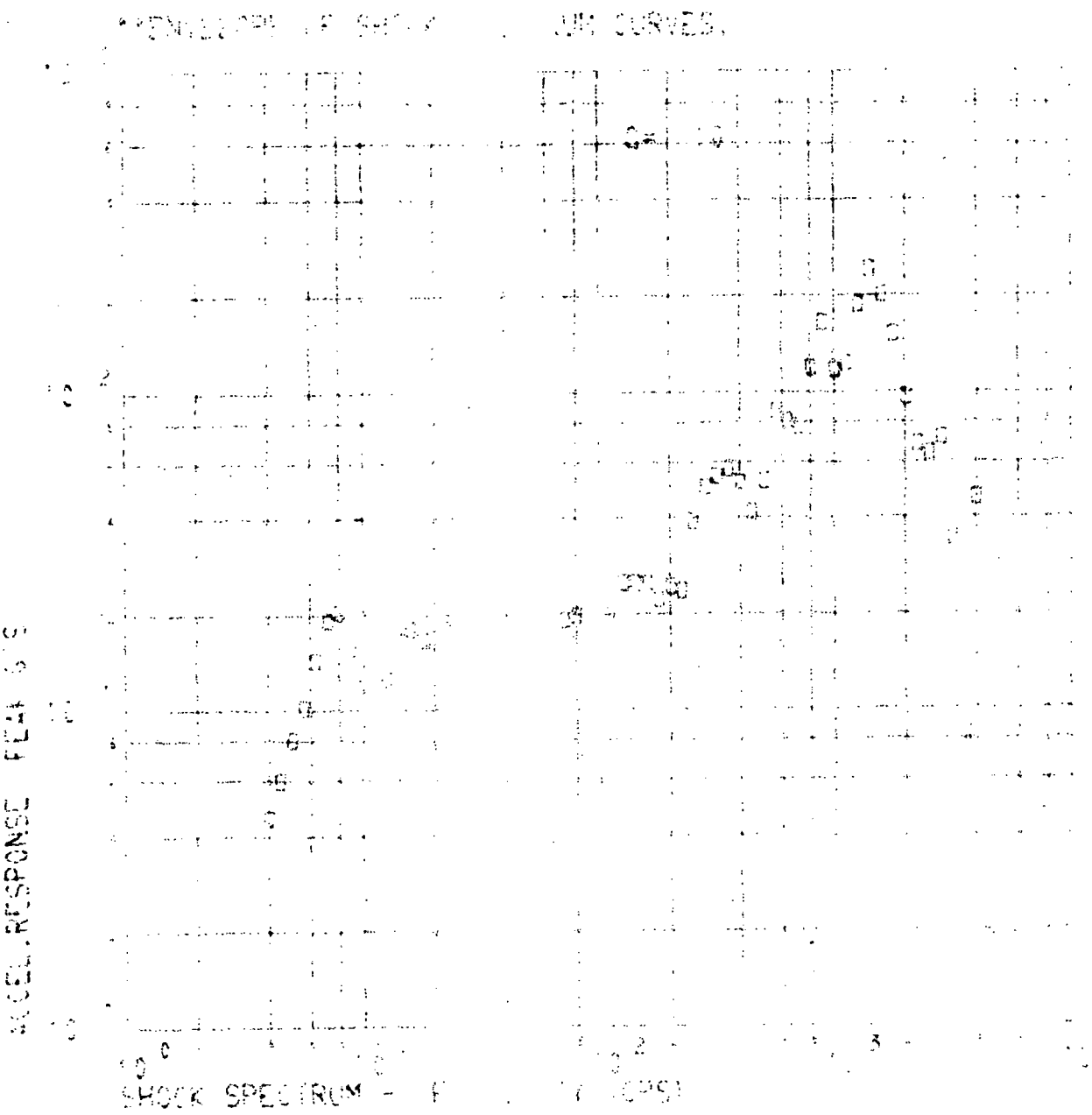

FIGURE XI - 23 FBR STRUT DISCONNECT. CRYOUNLATCH TEST NO. 3 STATION 2204 RING

PRELIMINARY DATA - SUBJECT TO CHANGE

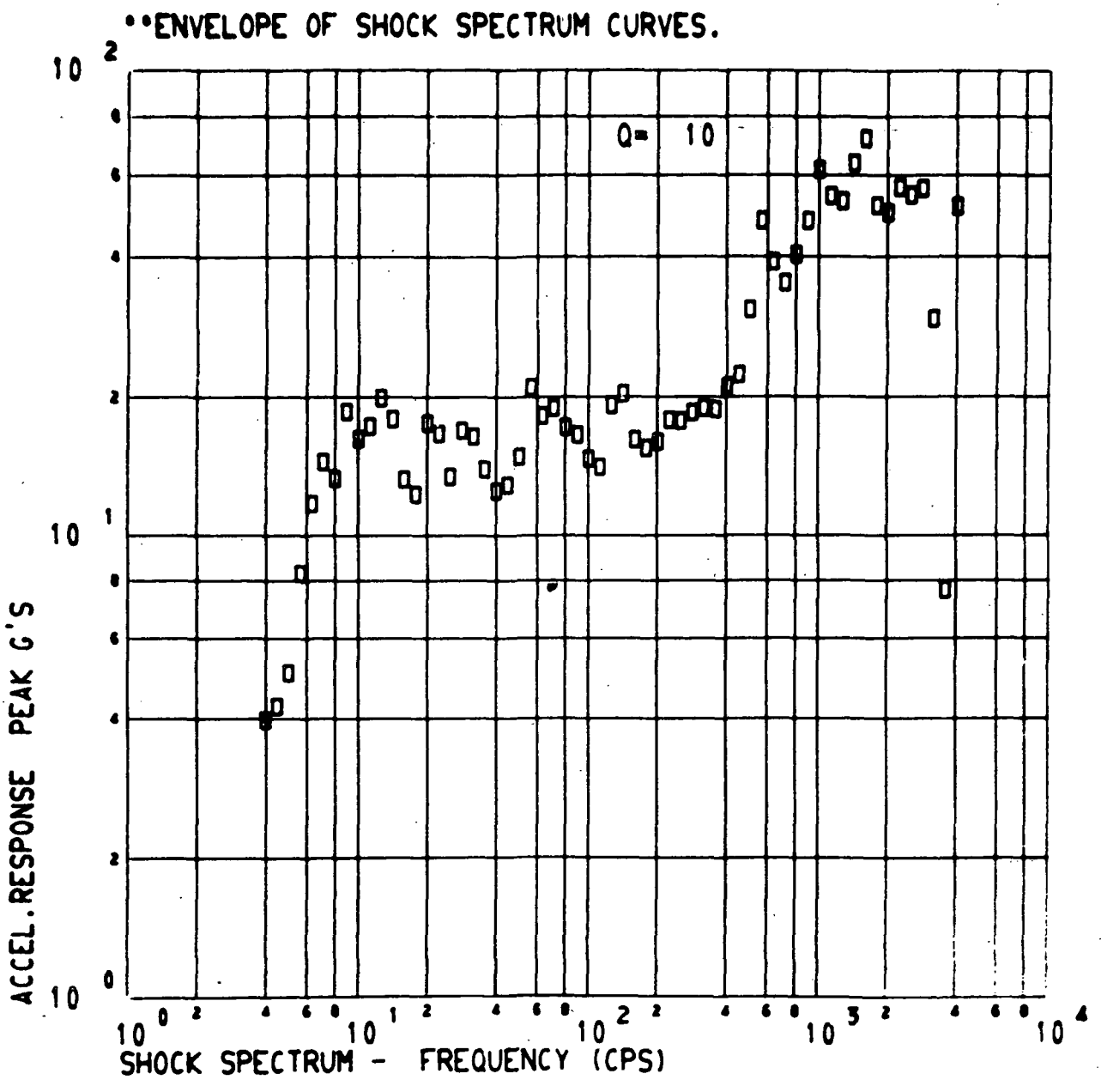

FIGURE XI-24 FORWARD SEAL RELEASE. CRYOUNLATCH TEST NO.3. STATION NUMBER 2204 RING

PRELIMINARY DATA - SUBJECT TO CHANGE

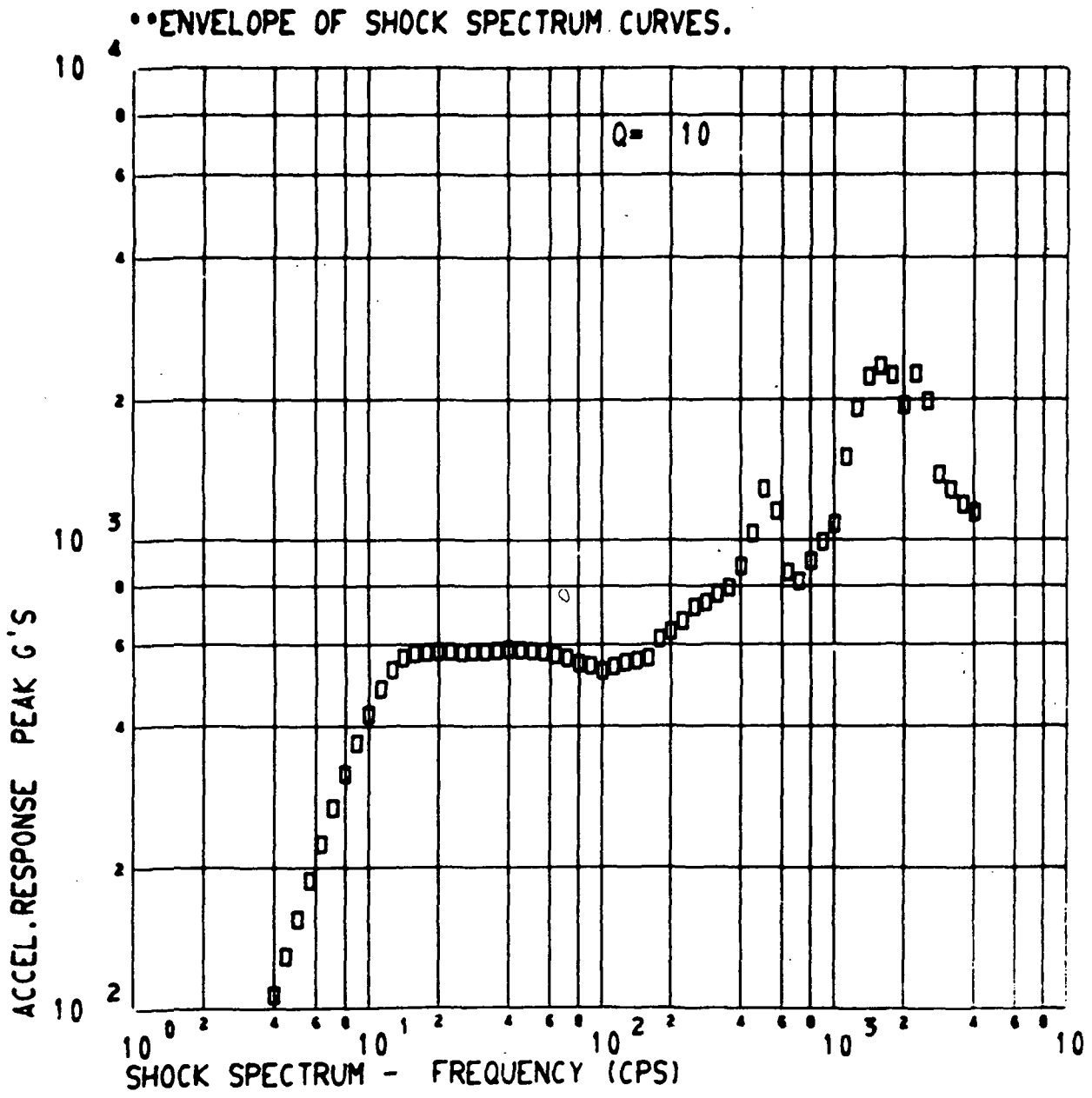

FIGURE XI-25 SUPER*ZIP FIRING. CRYOUNLATCH TEST NO. 2 STATION NUMBER 2204 RING

PRELIMINARY DATA - SUBJECT TO CHANGE

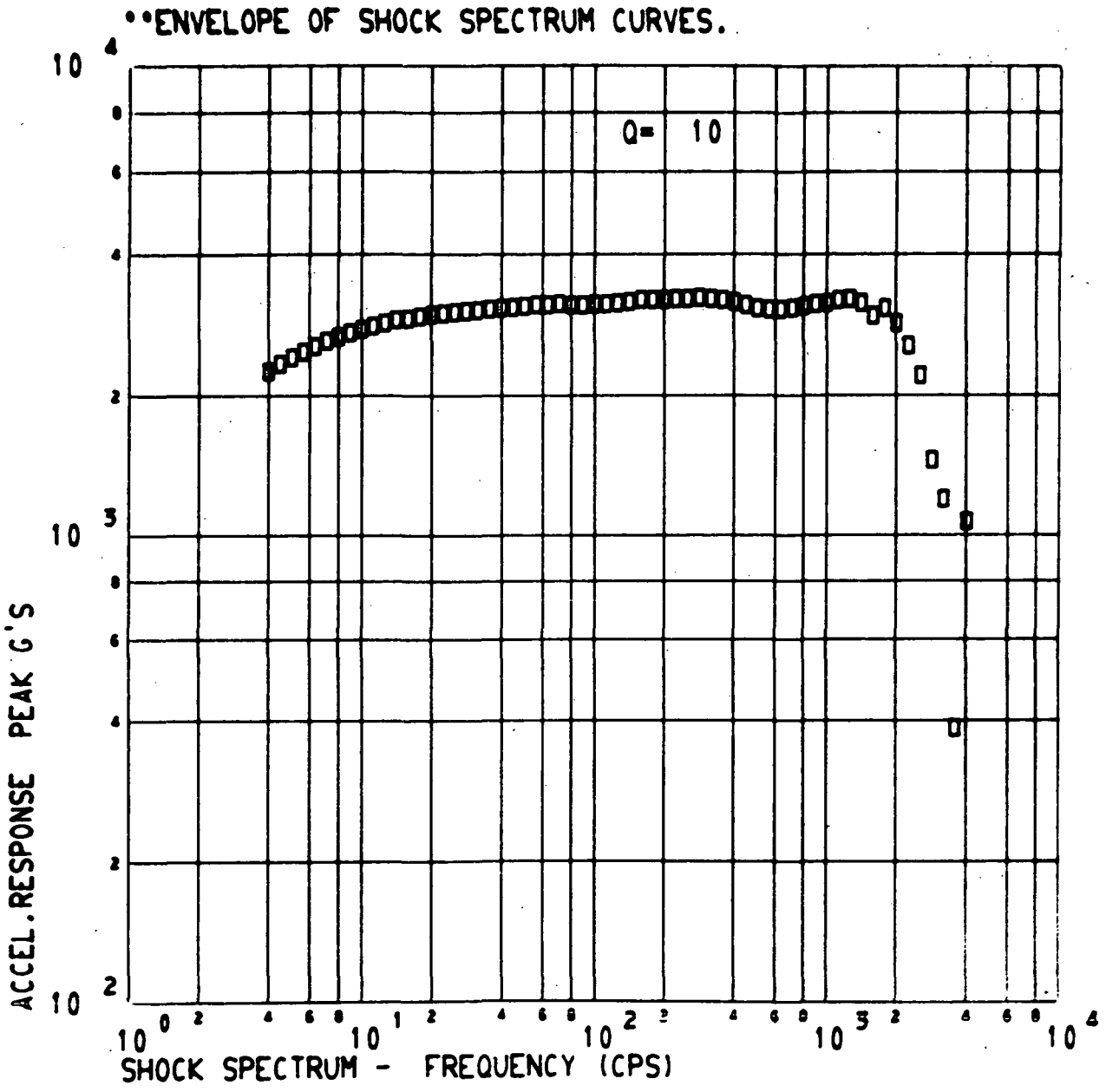

FIGURE XI-26 SUPER*ZIP FIRING. CRYOUNLATCH TEST NO.3. STATION NUMBER 2204 RING

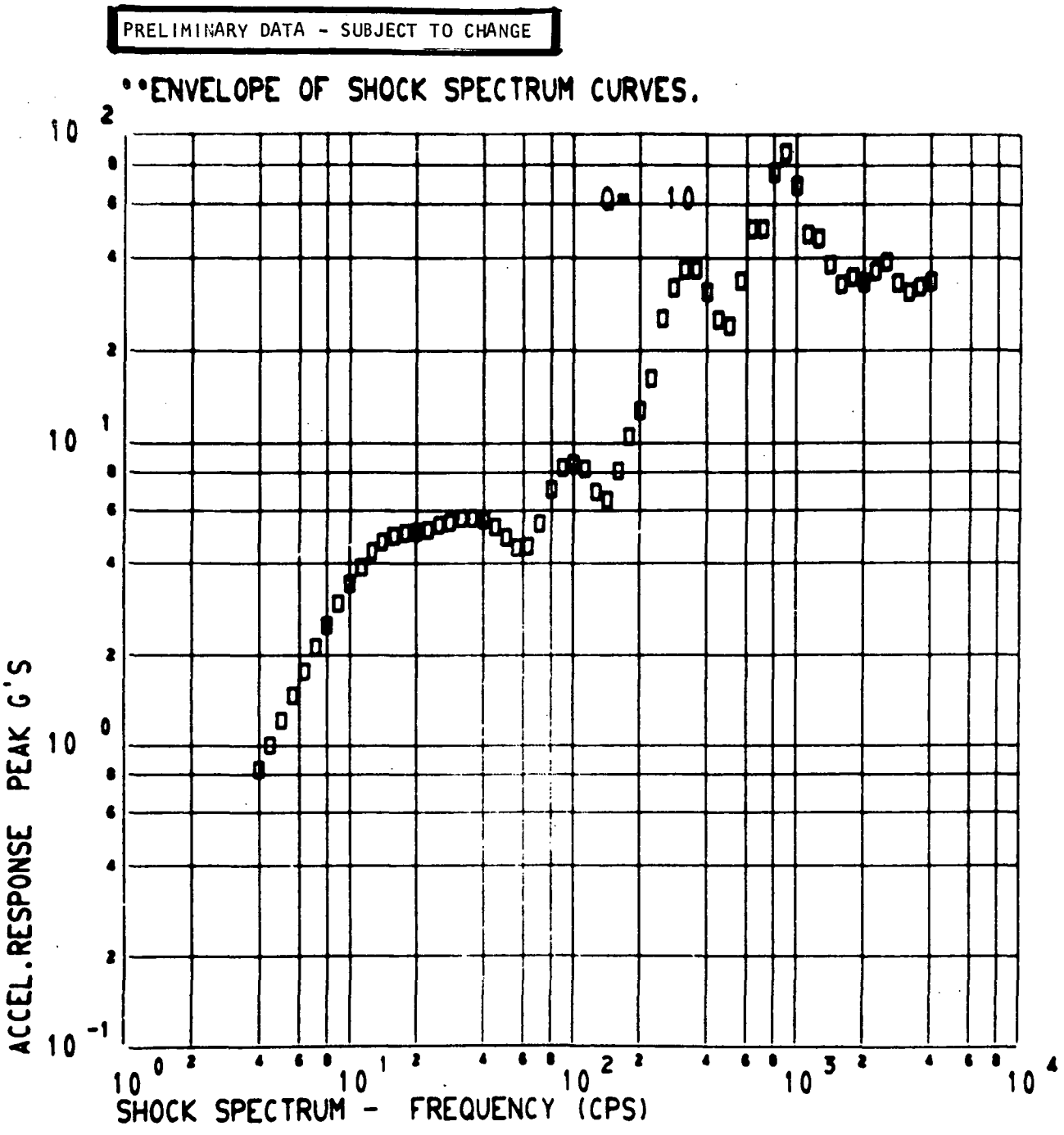

FIGURE XI-27 FBR STRUT DISCONNECT. CRYOUNLATCH TEST NO. 2. INTERSTAGE ADAPTER

PRELIMINARY DATA SUBJECT TO CHANGE

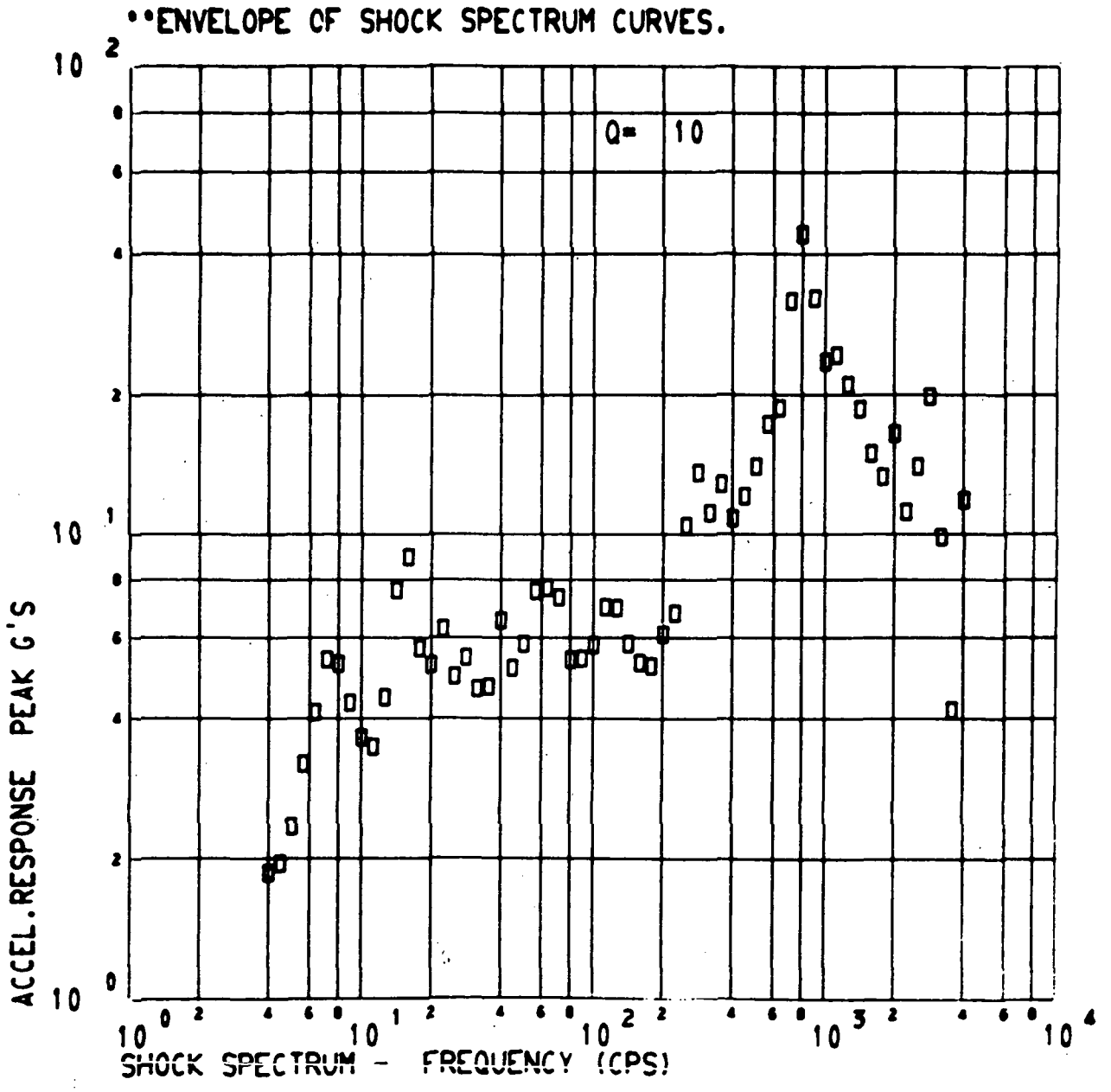

FIGURE XI-28 FBR STRUT DISCONNECT. CRYOUNLATCH TEST NO.3. INTERSTAGE ADAPTER

PRELIMINARY DATA - SUBJECT TO CHANGE

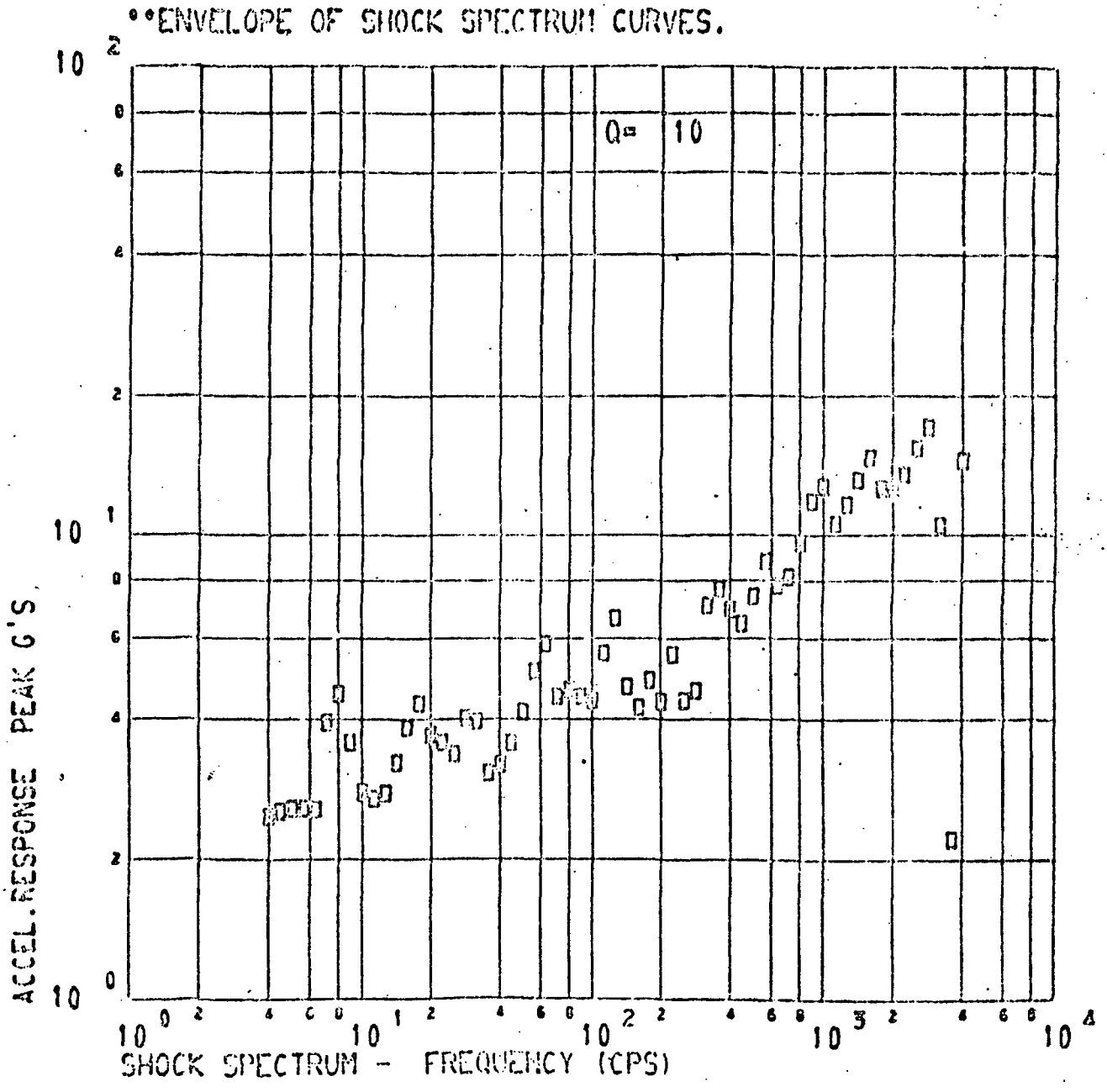

FIGURE XI-29 FORWARD SEAL RELEASE. CRYOUNLATCH TEST NO.3. INTERSTAGE ADAPTER

PRELIMINARY DATA - SUBJECT TO CHANGE

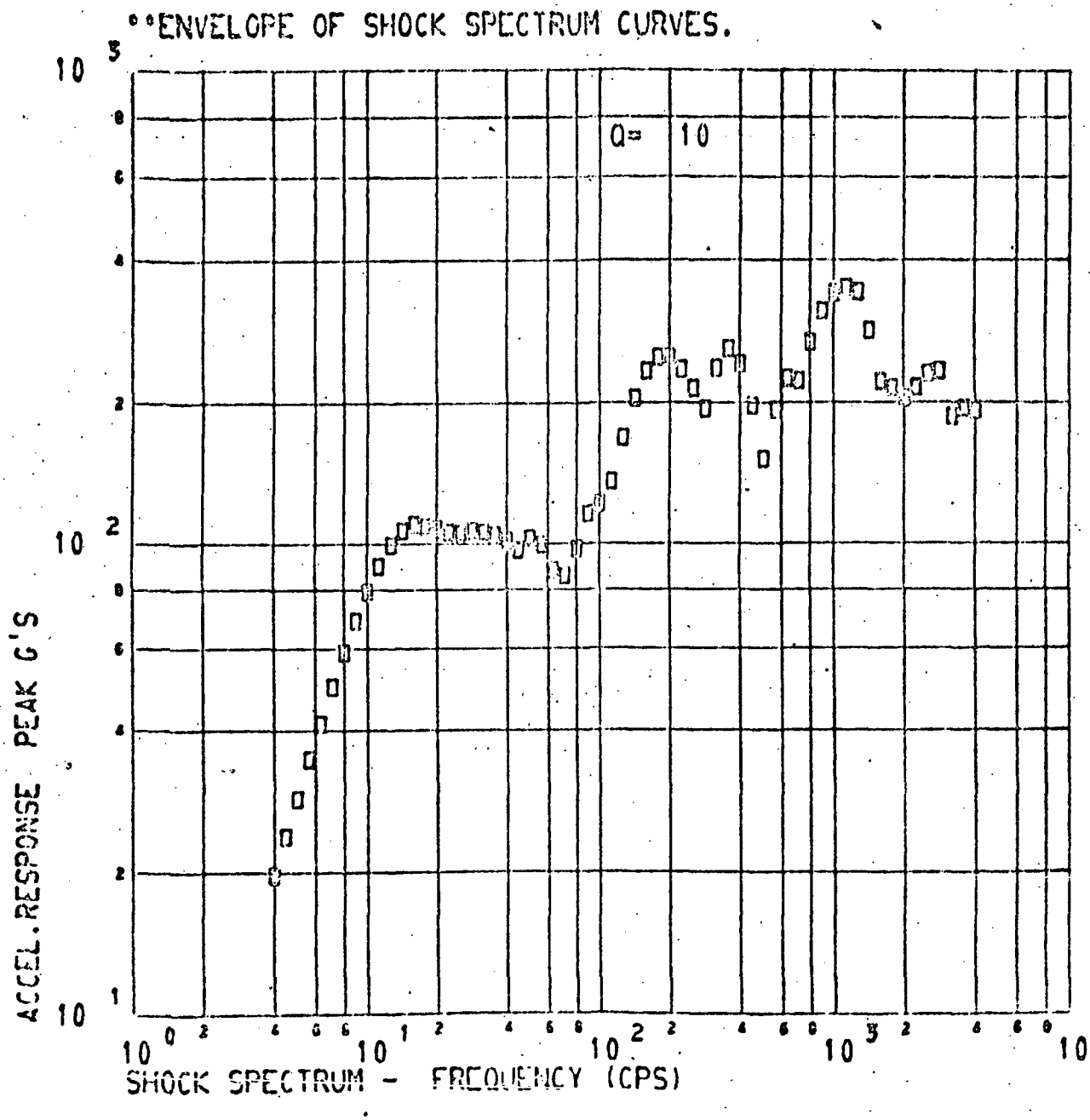

FIGURE XI-30 SUPER*ZIP FIRING. CRYOUNLATCH TEST NO. 2. INTERSTAGE ADAPTER

PRELIMINARY DATA - SUBJECT TO CHANGE

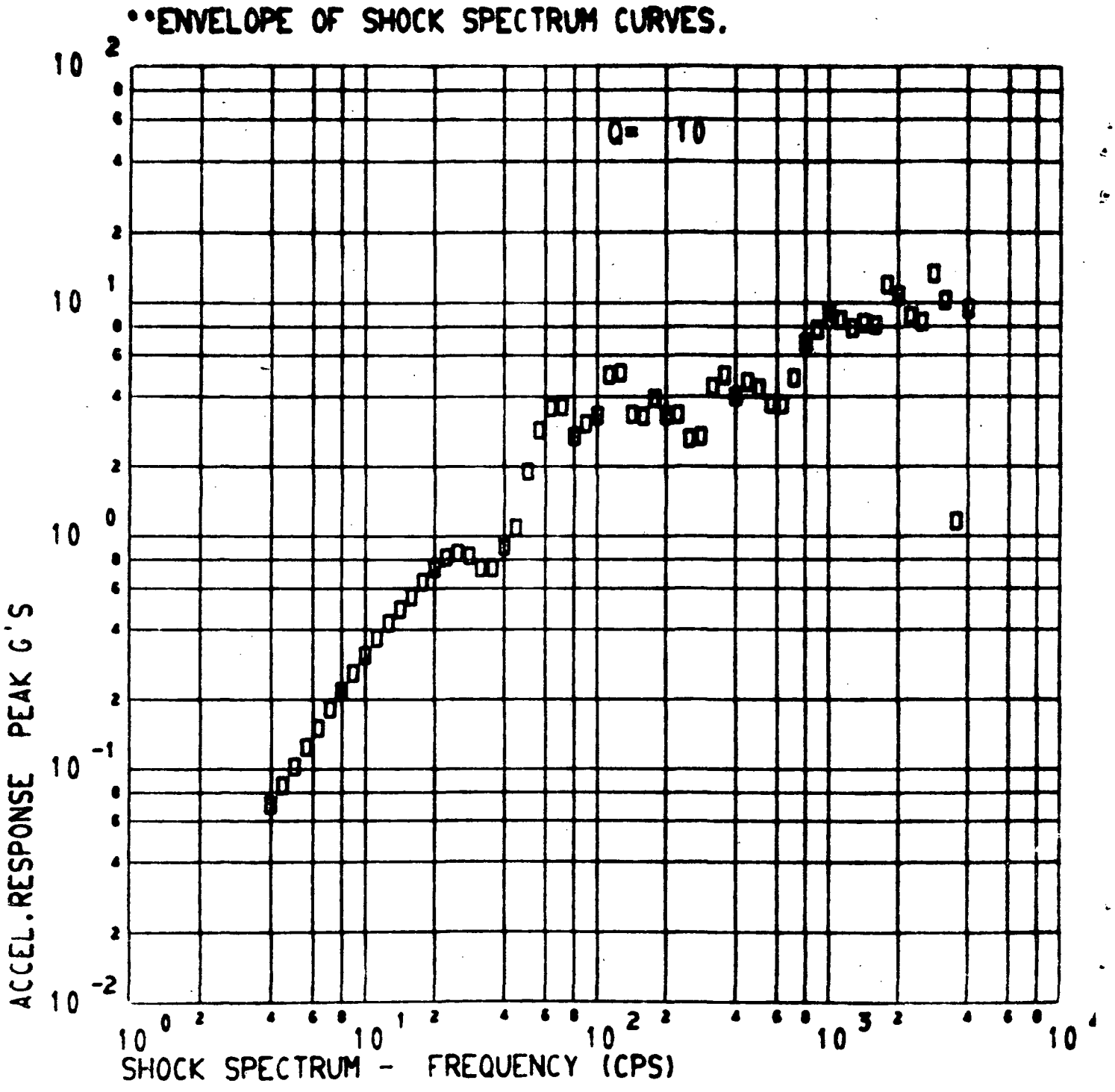

FIGURE XI-31 SUPER*ZIP FIRING. CRYOUNLATCH TEST NO. 3. INTERSTAGE ADAPTER

REFERENCES

1. Test Engineering Section, Launch Vehicles Directorate, Lewis Research Center: Cryogenic and Structural Qualification Test Plan for Centaur Standard Shroud, LeRC/TCPO-8 (formerly LeRC Test Plan 10770), Revision II, March 6, 1972.

2. Test Engineering Section, Launch Vehicles Directorate, Lewis Research Center: Test Requirements Document, Centaur Standard Shroud Cryogenic Unlatch Tests, LeRC/TCPO-16, August 11, 1972.

3. Pre-Launch Purging, Pressurization, and Venting Design Requirements for Centaur D-1T Shroud/Tank Compartment. General Dynamics' Convair Aerospace Division Report 988-3-71-114, Revision B, July 18, 1972.

APPENDIX A

CONTROL AND ABORT SYSTEMS

by E. J. Cieslewicz

SUMMARY

The Xerox Data Systems XDS-910 digital computer at the B-3 test facility provided control for the facility and vehicle systems. A specially designed output command system and an abort monitor system were used in conjunction with the computer as shown in Figure A-1. Three automatic sequences were performed for shroud jettison tests. All three tests were highly successful and yielded data for evaluation and improvements of the CSS jettison and insulation systems.

CONTROL AND ABORT REQUIREMENTS

Each test conducted had slightly different control and abort requirements. A representative sequence, which was used for the third cryogenic unlatch test, is used here for discussion.

Control Requirements for Automatic Sequence

An illustration of the autosequence control requirements is shown in Figure A-2. This figure lists all relays to be operated by the computer throughout the test. Each relay has its status represented in bar chart format. One start of the relay is shown as a single line and its opposite state is shown as a bar. The relay identification shown conforms to the bar state only (see Figure A-2). Status changes from autosequence start take place in the figure from left to right as time varies. The time scale shown is in seconds. It should be noted that certain sequence holds are shown taking place during the test. The computer program essentially commands relays in an open-loop control fashion until a hold period is reached. Further sequencing of the relays does not take place during a hold until the computer has received an indication through the abort monitor of an occurrence of a desired event. Consequently, the holds shown are variable in time duration and dependent on the test configuration. The hold events and their identification are as labeled in the figure.

Abort Requirements for Automatic Sequence

An illustration of the autosequence abort requirements and how they varied with time is also shown in Figure A-2. This figure lists all the data that were specifically examined by the abort monitor for the computer. Each of

the channels listed has its required armed-disarmed status, as shown in the bar chart format. The bars indicate the period of time an abort channel was to be armed and the digital notation of "one" or "zero" within them designates the desired response throughout that interval. Further identification of the abort channels and the significance of the one-zero notation is shown in Table A-1.

The time-scale identification and program-hold identification are the same as those used to explain the control requirements sequencing.

TABLE A-1 ABORT CHANNEL, IDENTIFICATION, INPUT, NOTATION, AND CONDITION LISTING

ABORT CHANNEL	ABORT NAME	USE FEATURE	SIGNAL INPUT FOR DETECTION AT ABORT MON.	DIGITAL NOTATION OF "1" DENOTES	NOTATION FOR ABORT
24	Manual Push Button	Real Time Data Look	Normally Open	Button Not Pushed	0
61-66	Forward Bearing Reaction Struts	FBR Separation and Retraction	Normally Open Limit Switch	FBR Not Fired or Retracted	0, 1
67, 68	High Disc Brake Pressure	Shroud Catch System	Analog Voltage	Greater Than 330 PSIA	1
69, 70	Low Disc Brake Pressure	Shroud Catch System	Analog Voltage	Greater Than 300 PSIA	0
71, 72	FBR and Super-Zip Firing Voltage	Low Voltage	Analog Voltage	Greater Than 32 Volts	0
79	Abort Monitor Power Supply	Low Voltage	Analog Voltage	Greater Than 3.0 Volts	0
80	Test Conductor Abort	Button Switch	Normally Open Switch	Button Not Pushed	0
81	Data Record Failure	Recording Indication	Normally Closed Relay Contact	Data Not Being Recorded	1
83	Programmed Valve Permissive	Computer Control of Programmed Functions	Programmed Item Switch Contacts	Item Not In Program Mode	1
84	Tank Protection Abort	Proper LO_2 and LH_2 and CSS Pressures	Analog Voltages to Comparator Contacts	Tank Pressures or CSS Pressure Marginal	1

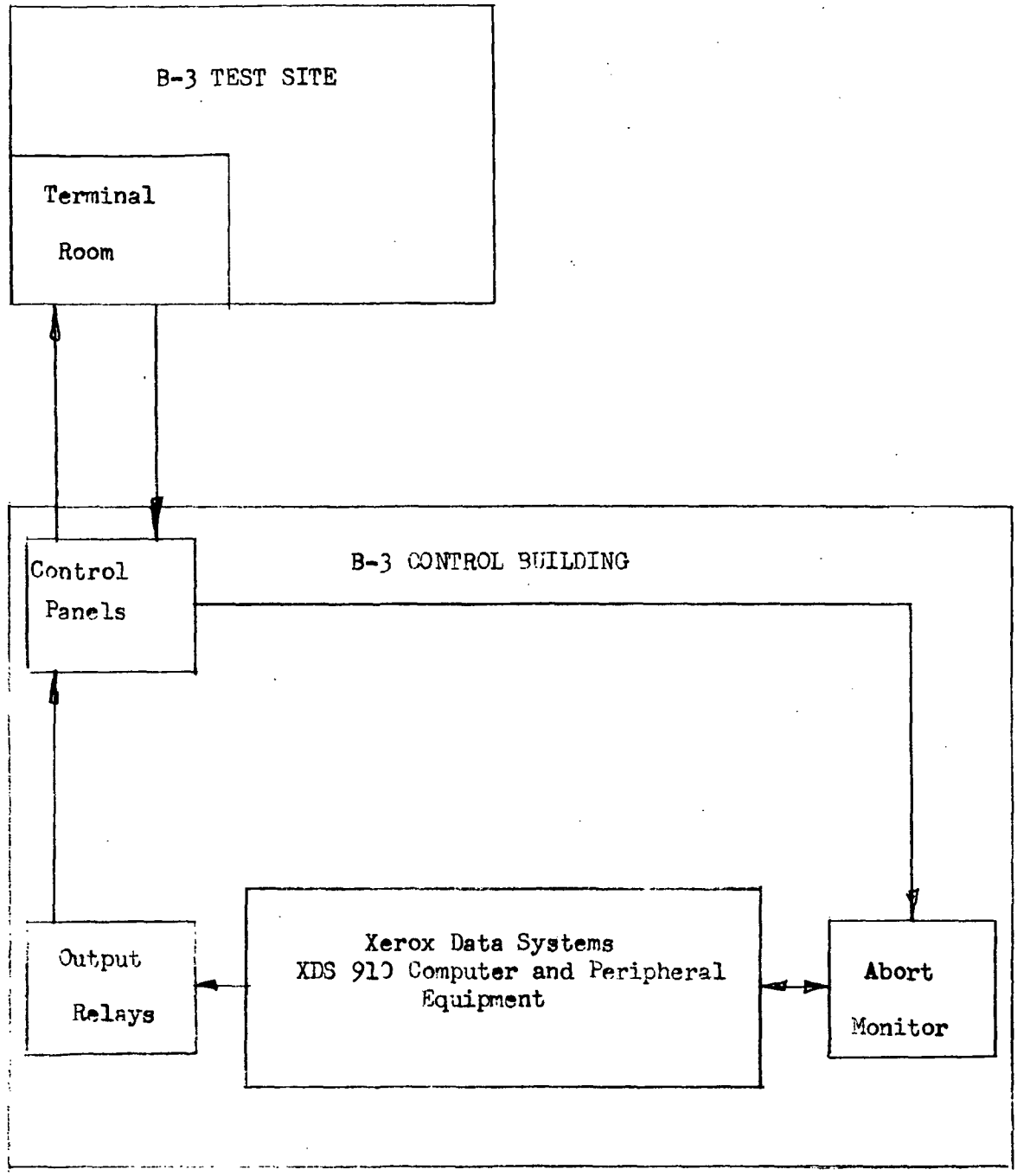

FIGURE A - 1 B-3 CONTROL AND ABORT SYSTEM LAYOUT

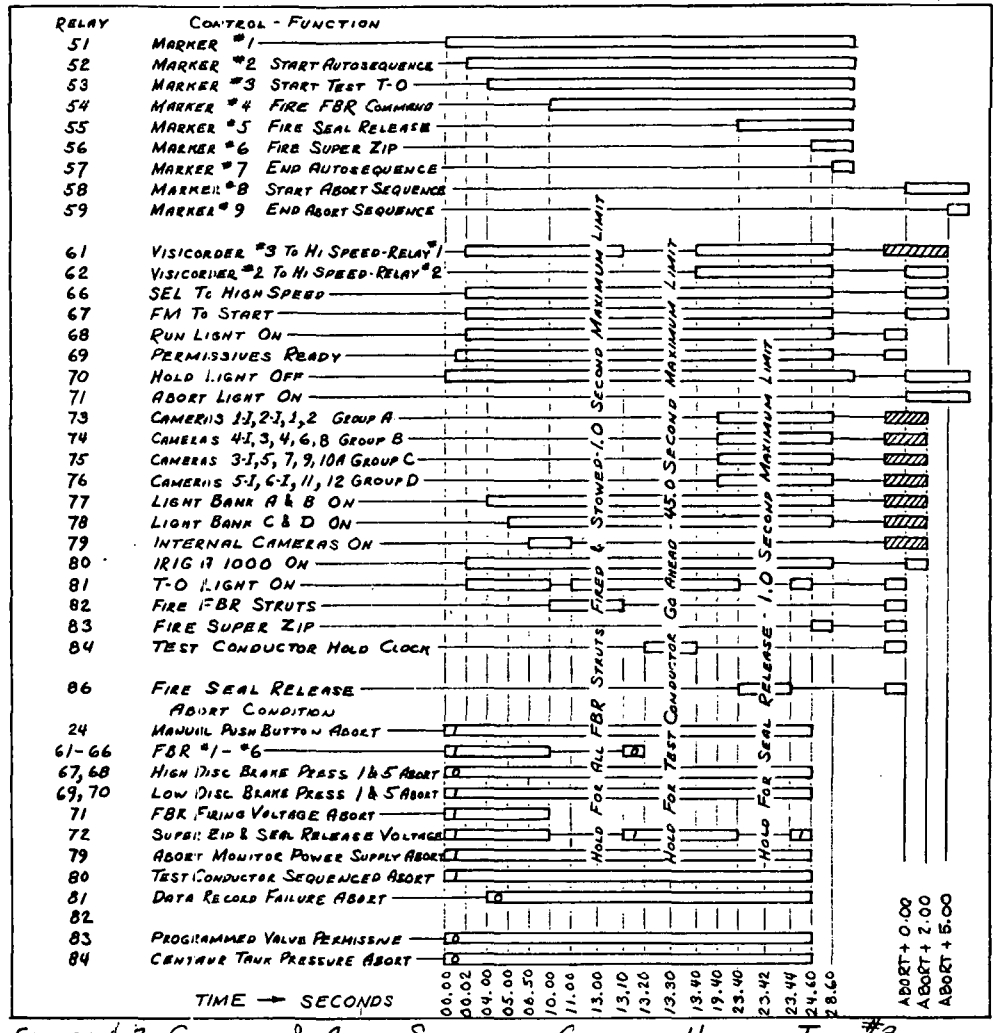

FIGURE A-2 CONTROL & ABORT SEQUENCE - CRYOGENIC UNLATCH TEST #3

ABORT CHANNELS & LIMITS	
CHANNEL	ABORT LIMIT
24	CONTACT CLOSURE BY DATA OBSERVER
61 - 66	CONTACT OPENING BEFORE FIRING & CONTACT CLOSURE AFTER FIRING
67,68	PRESSURE > 330 PSIA (151P & 155P)
69,70	PRESSURE < 300 PSIA (151P & 155P)
71,72	VOLTAGE < 32 VOLTS (255V & 251V)
79	VOLTAGE < 3.0 VOLTS
80	CONTACT CLOSURE BY DATA OBSERVER
81	CONTACT OPENING BY DATA RECORD SYSTEM
83	CONTACT OPENING FUNCTION OUT OF PROGRAM
84	CONTACT OPENING PRESSURIZATION SYSTEM ERROR OUTPUT BULKHEAD ΔP < 2.5 OR > 22 PSID (54P) HIGH LOX PRESSURE > 37.5 PSIA (503P) HIGH LH_2 PRESSURE > 27.5 PSIA (501P) LH_2 - EQUIP. MOD < 2.0 PSID (408P)

APPENDIX B

INSTRUMENTATION AND DATA SYSTEMS

by F. L. Manning

SUMMARY

The instrumentation and data systems used to support the Cryogenic Unlatch Tests of the Centaur Standard Shroud (CSS) in the Plum Brook B-3 facility generally performed as expected. Only the Forward Bearing Reaction (FBR) strain gages exhibited any significant data errors. The final results from the digital data reduction program were available for analysis within an average of 36 hours after completion of testing.

SYSTEM DESCRIPTIONS

Data Recording System

A schematic of the data recording systems used to support the Cryogenic Unlatch Tests is shown in figure B-1. Transducer signals originating from locations on the test hardware (CSS, Centaur, ISA or Titan Skirt) or from facility instrumentation were carried on cabling to interconnect boxes on levels 3 and 4 of the facility. From there the signals were routed down to the ground level instrument room and terminated in the facility patchboard. The instrument room also contained some of the signal conditioning equipment required. This included the balance panels for the pressure transducers and the platinum resistance thermometer signal conditioners. The power supplies and balance panels for the strain gages and deflectometers were located on levels 3 and 4.

From the facility patchboard, the signals were patched into the digital multiplexer patchboard. Signals were also paralleled at this point into amplifiers and the resulting signals sent to real time recorders (Brush and Visicorders) located in the J-bay of the B-Control building. The digitized, multiplexed signals were sent on above ground lines to H-building for recording on magnetic tape using the Central Recording System.

In addition to the real time recorders available in B-Control, a visual display using cathode ray tubes (CRT) was also available. The digitized transducer signals recorded in H-building were also available to a XDS-9300 computer in B-Control. This computer was programmed to calibrate these signals and display them in engineering units on the CRT's. The CRT displays were controlled by individual mini-computers (CF-16) and could be changed through the use

of a typewriter terminal interface. Thus, any instrument which was on the digital system could be displayed in engineering units in near real time on the CRT's. It was also possible to obtain a permanent record of the CRT face by using a facsimile recorder interfaced with the system.

Data recording: The primary experimental data for the Cryogenic Unlatch Tests were recorded in digital form on magnetic tape using the central recording system in the H-Control and Data Building. The basic sampling rates used were 2,000 data points per second and 20,000 data points per second. The data word block had a block length of 400 data channels.

The 20,000 points per second sampling rate was used only during the auto sequence portion of each test (i.e., FBR, FSR, and Super-Zip firing sequences). Other digital data recording required was recorded using the 2,000 points per second sampling rate.

As described above, real time monitoring for field data analysis and/or abort purposes was available on strip-chart recorders. Parameters chosen for the strip-chart recorders included tank pressures, critical temperatures, purge and vent pressure, tank to shroud annulus pressure, pyrotechnic information, FBR breakwires and aft seal split line deflections.

Data reduction: Selected data were recorded in real time on strip charts and using the CRT printer interface to allow a preliminary evaluation of each test. The primary data magnetic tapes from each test were copied and edited at H-Control and Data Building immediately after completion of each test. The copy was retained at Plum Brook and not erased until it was determined that successful data retrieval and reduction had been accomplished.

The data tapes returned to LeRC, were processed by retrieving selected data from the tapes using a computer retrieval program and storing these data in the IBM 360. The data reduction program then processed these data by converting the recorded millivolt signals into temperatures, pressures, strains or stresses, deflections, and propellant levels. Random noise effects were reduced by using a five (5) point smoothing routine on the data.

Final display of the data was in the form of both column tabular arrays and plots. The reduced data was sent to a microfilm machine for final processing. The results of this processing consisted of a roll of microfilm, each frame of which contained each a page of tabular data or a selected plot. The film was then sent to an outside contractor for printing. Copies were returned within 24 hours. On the average the entire data reduction procedure took 36 hours from the completion of testing to the receipt of final reduced data.

In addition, a special data display program was available for selected parameters used during the jettison portion of the autosequence. This program did not average the data but rather displayed it in an unsmoothed

or "raw" format. This enabled some parameters to be sampled as many as 100 times per second (when sampled twice within any one data block length).

INSTRUMENTATION

Parameters measured during the Cryogenic Unlatch Tests included pressures (absolute, gage, and differential), temperatures, liquid levels, strains, deflections, and vibration or acceleration levels. A brief description of each type of transducer used to measure these parameters is given in this section. Also included are descriptions of unique or unusual instrumentation installations used on these tests.

Pressure: Most of the pressure measurements were made using strain gage type pressure transducers which were evacuated and hermetically sealed. These transducers were compensated for a temperature range of between 77.7 and 327.7K (140^{o}R and 590^{o}R). In addition, each pressure transducer was calibrated at three different temperatures, 297.2, 200, and 77.7K (535, 360, and 140^{o}R) in order to obtain an accurate temperature related calibration resistance to be used in the signal conditioning bridge circuitry.

It was then possible to standardize the full scale output of each pressure transducer to 20 millivolts.

In addition to the above transducers, two special high accuracy, low range differential pressure transducers were also used. One was used to measure the tank-shroud annulus pressure (TSAP) and the other measured the pressure drop across the facility vent line venturi. These transducers were basically precision capacitive potentiometers with the variable member being a prestressed metal diaphragm. This diaphragm separated two gas tight enclosures and was positioned between fixed capacitor plates. Thus a change in total pressure in the enclosures caused the diaphragm to deflect, resulting in a change in the relative capacitance between the diaphragm and the capacitor plates. The signal conditioning associated with these transducers had the advantage of producing high voltage output plus automatic self-ranging. This multiple range feature enabled the transducer to have seven effective ranges of 1, .3, .1, .03, .01, .003, and .001 psi.

Temperature: Temperatures were measured with Chromel-Constantan junction thermocouples and platinum resistance thermometers.

Thermocouples: The thermocouples used were made of high-grade Chromel-Constantan wires and were installed using a number of different methods. Two installations in particular were unique. The first was on the forward seal. The material of the forward seal did not lend itself to normal surface thermocouple installation methods (i.e., epoxying or taping the thermocouple junction in place). Therefore, a special installation consisting of a patch of seal mate-

rial and self-curing adhesive was devised. The fianl installation is whosn in figure B-2. The second method of thermocouple installation was used where surface temperatures of the aluminum shroud structure were desired. Basically, the method consisted of amking a small bead on each of the thermocouple wires and then installing each wire individually using a resistive welder. This method became known as the "electropeen" technique for thermocouple installation. The welder was equipped with a variable pressure switch and timer as well as variable power input to the electrodes. In this way it was possible to set up the equipment before working on the test article. The advantages in this method included ease and speed of installation, ruggedness, and good thermal surface contact.

In addition, by laying separate wires it was possible to determine a thermocouple failure since if one wire lifted from the surface an open circuit developed. A typical installation using this "electropeen" method is shown in figure B-3.

Platinum resistance thermometers (PRT): The platinum sensing elements used in the PRT's were commercially manufactured. However, the transducers using these elements were constructed and calibrated by NASA. Each PRT probe or patch and its signal conditioning unit was individually calibrated for a particular temperature sensing range. This individual calibration procedure meant that each PRT and its associated signal conditioner were considered to be a single instrument.

Stress: Stress and strain levels in the CSS and related hardware were measured using wire filament strain gages. Due to the large number of gages required and the limited amount of facility wiring available, a "Chevron" type of circuit was used. Basically, this circuit consisted of one power supply being used with up to 12 strain gage bridges. The active gages were installed on the test articles and the remainder of the bridge was located with the power supply in the cabinets on level 3. A circuit schematic is shown in figure B-4.

Two types of strain gage arrangements were installed on the test hardware. These consisted of a single element gage (Uniaxial) and a two element, 90 degree rosette gage (Poisson). The Uniaxial gages were used in areas where the major strain axis was well defined or where only the single strain component was required. Generally, these gages were mounted back to back in order to determine bending strains imposed in the test article. The Poisson gage was used in areas where the major strain axis was assumed known and additional output signal strength required. Typically, the Poisson gages produced a signal 1.33 times the signal of a Uniaxial gage. All gages were self-temperature compensated. Additional temperature compensation was achieved by installing dummy gages on non-stress members (see figure B-4).

Liquid level sensors: Continuous liquid level sensors were placed in the Centaur tanks as shown in figure B-5. These were basically variable capacitors consisting of coaxial electrode tubes using

cryogenic liquids or gases as the dielectric medium. The probes were calibrated in output versus station number. The volume of the tank at any station was known and therefore the mass of liquid in the tank at any station could be calculated. With the capacitance probe system, it was possible to calculate the station number of the liquid level within an error of better than ±1.27 cm (±.5 inches).

Deflection: Relative displacements or deflections were measured through the use of linear potentiometers. Typically the transducer was mounted to some "hard point" in the facility and a small line then attached from the potentiometer to some point on the test hardware. A circuit similar to the strain gage circuitry was used for the total number of wires and power supplies required.

During the jettison, the edge motion deflections were measured using a proximity device developed by Plum Brook personnel. The transducer consisted of basically two parts. One part was a field generating coil. This coil was a flat, one turn coil 1' X 4' in dimension mounted to a non-conductive material. The sensor consisted of a flat pancake 2.5" in diameter with a 1" hole in the center. A junction field effect transistor was connected to this coil as a source follower. The sensor signal was AC coupled into an amplifier in the instrument room. The output from the amplifier was then rectified and filtered in order to obtain a DC output signal. The output signal was calibrated for 0 - 5 volts DC full scale and 3.0" to 13.0" full scale. While the calibration was non-linear, it was repeatable and good results from the data were obtained.

Vibration: The shock and vibration measurements were obtained with both piezoelectric and piezo-resistive accelerometers. The results were recorded on FM analog tape in the H-Control and Data Building.

RESULTS AND DISCUSSION

The instrumentation and data systems supporting the cryogenic unlatch test in B-3 performed within specifications. Only the data from the FBR strut strain gages could not be used due to the excessive errors induced by a thermal shifting problem. Figure B-6 shows a comparison between a normal "Chevron" strain gage circuit and the one that was inadvertently used on the FBR strain gages. It can be seen that while the circuit can be balanced at ambient temperatures, an unbalance in the lines occurs if the temperature of the power lines decreases significantly. Since these lines were routed down the side of the Centaur hydrogen tank, a large decrease in temperature was experienced when the propellants were loaded. The resulting unbalance in the power lines caused an apparent strain equivalent to as much as 2,000 microstrain or 50 percent error.

Other than the FBR strain gages, the instrumentation and data systems had a failure rate of less than 5 percent for the entire test program. This meant that out of a total of 400 available instruments less than

20 were inoperative on any test. This included instruments known inoperative prior to starting the test.

CONCLUSIONS

1. The data and instrumentation systems associated with the cryogenic unlatch tests in B-3 performed within specifications and with an overall reliability of better than 95 percent.

2. The FBR strain gage data could not be used for analysis due to large thermal drift errors.

3. The "Chevron" strain gage circuit can be used where a limitation on wiring and power supplies exists.

4. The "electropeen" method of installing thermocouples can be used on thin metal surfaces where speed of installation and high reliability is desired.

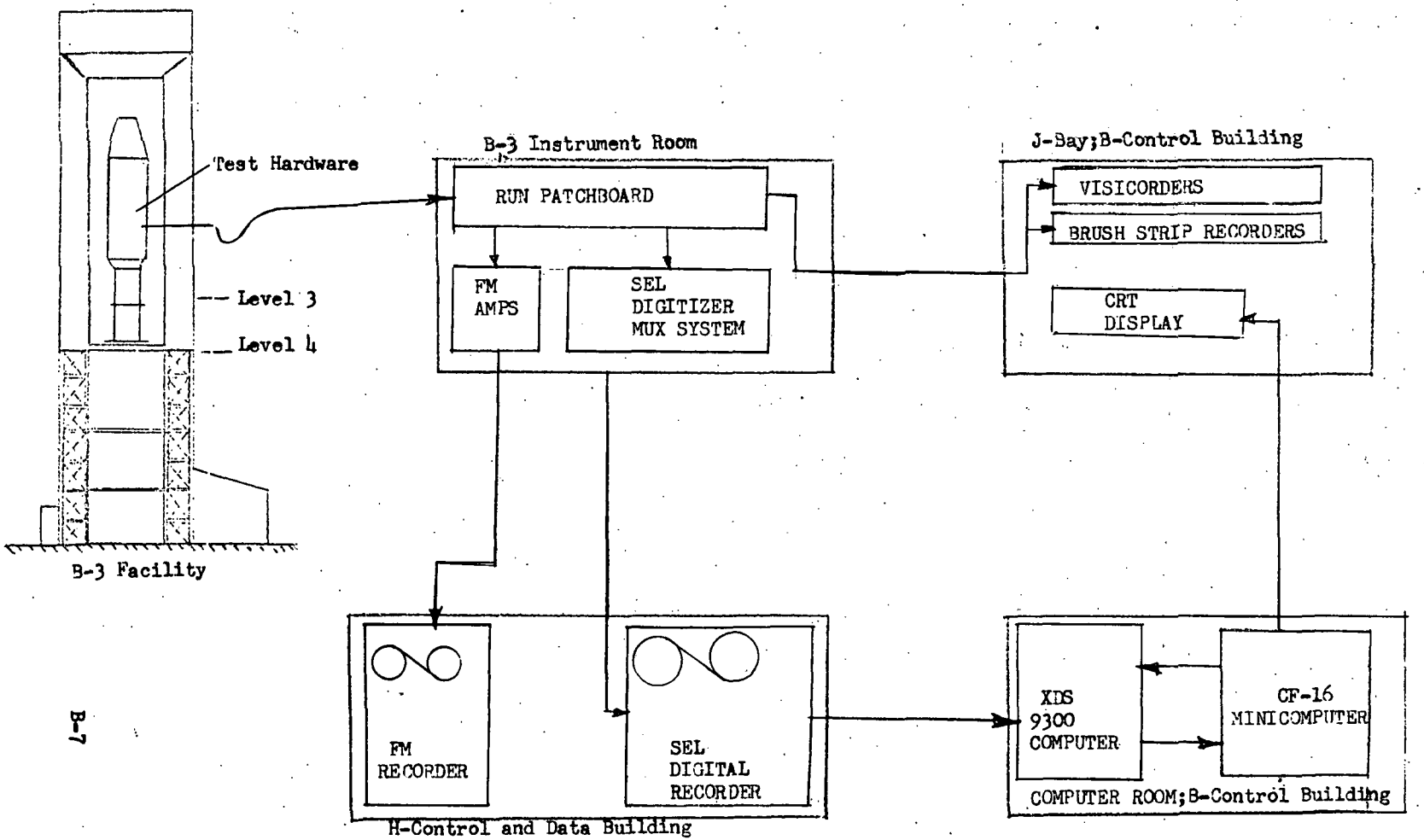

Figure B-1.-Instrumentation and data systems flow schematic for Cryogenic-Unlatch Tests at Plum Brook B-3 Facility.

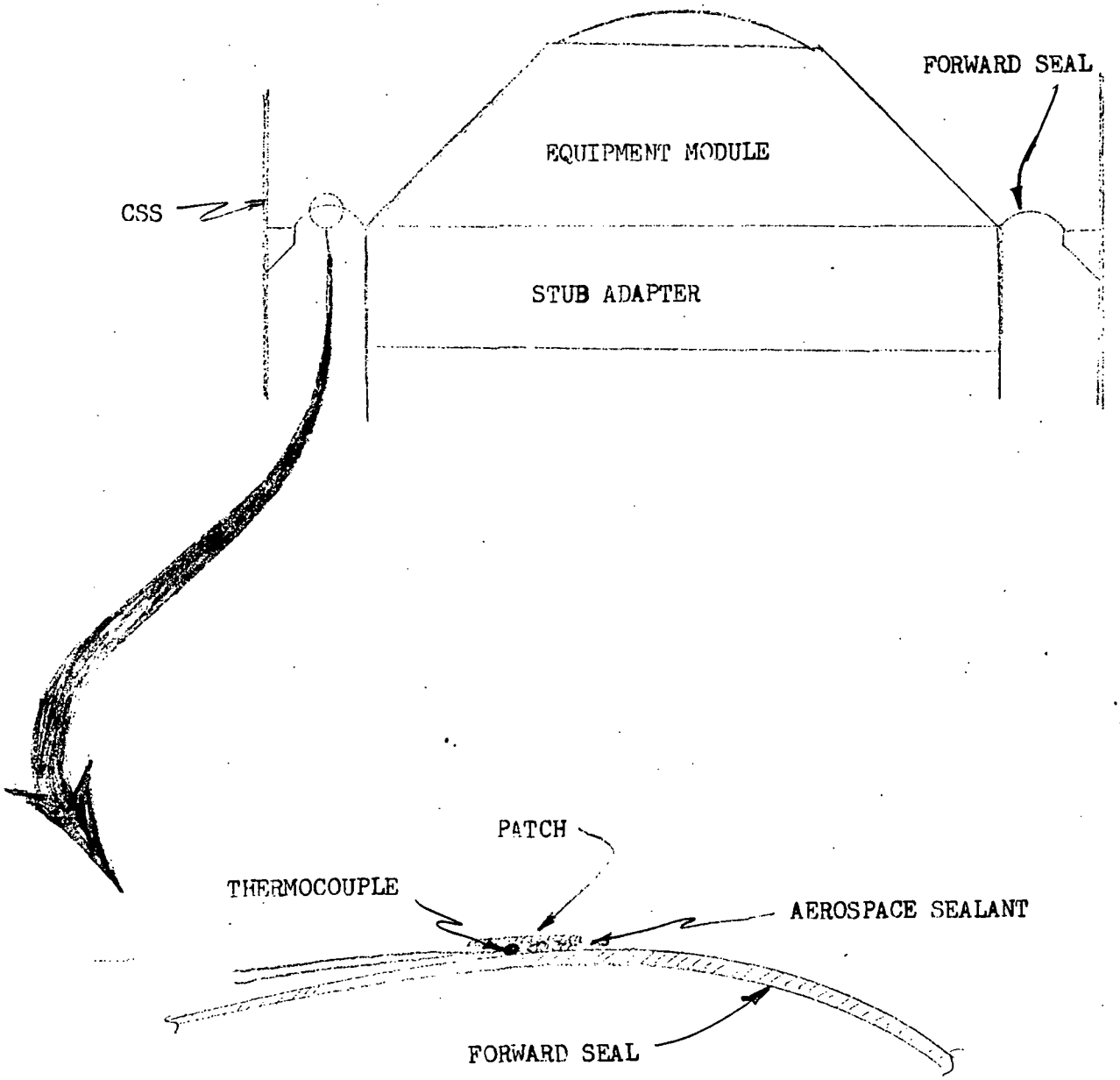

Figure B-2.-Thermocouple installation on the CSS forward seal

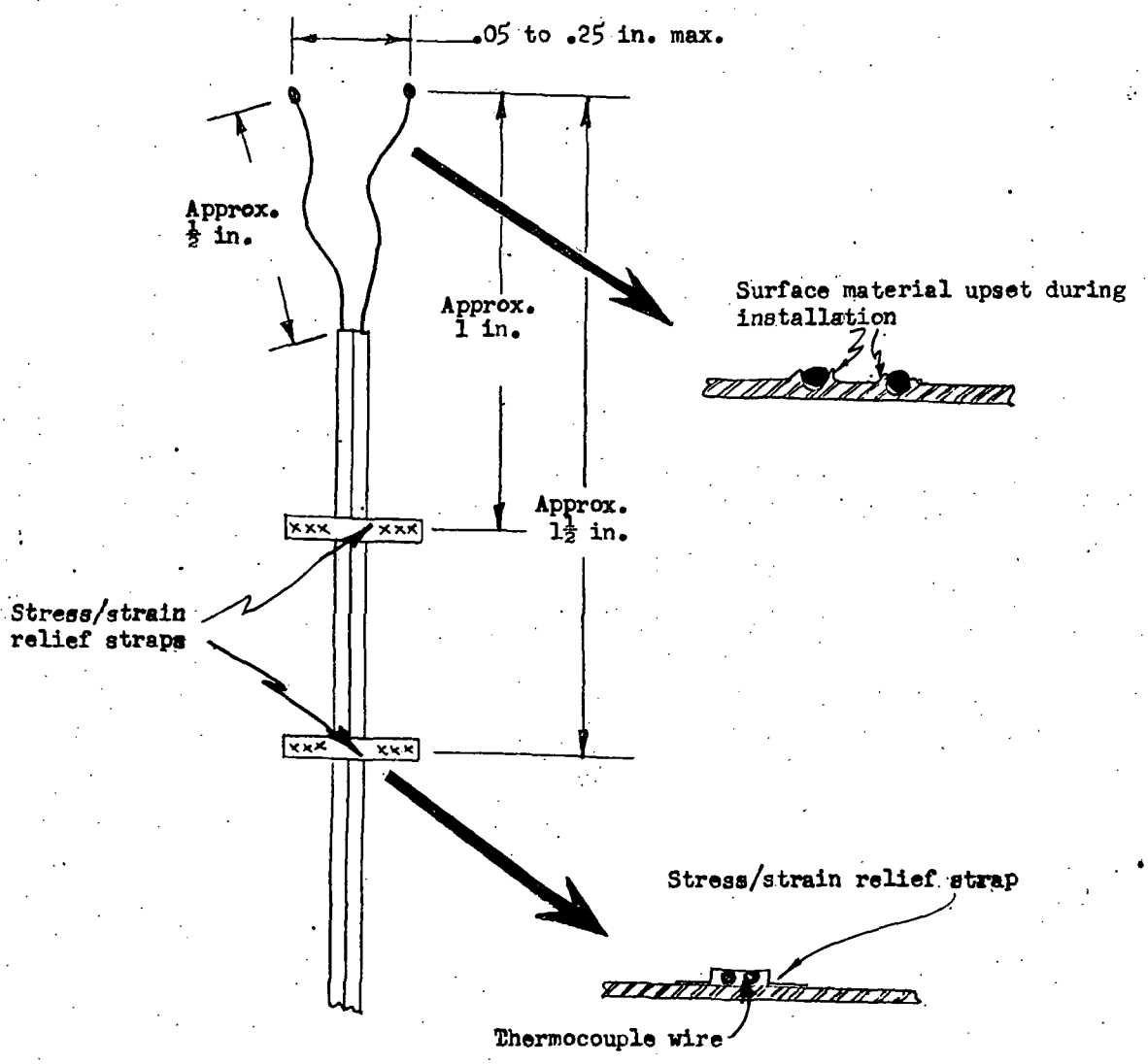

Figure B-3.-Typical "electropeen" thermocouple installation used during the Cryogenic-Unlatch Tests - Plum Brook B-3 Facility

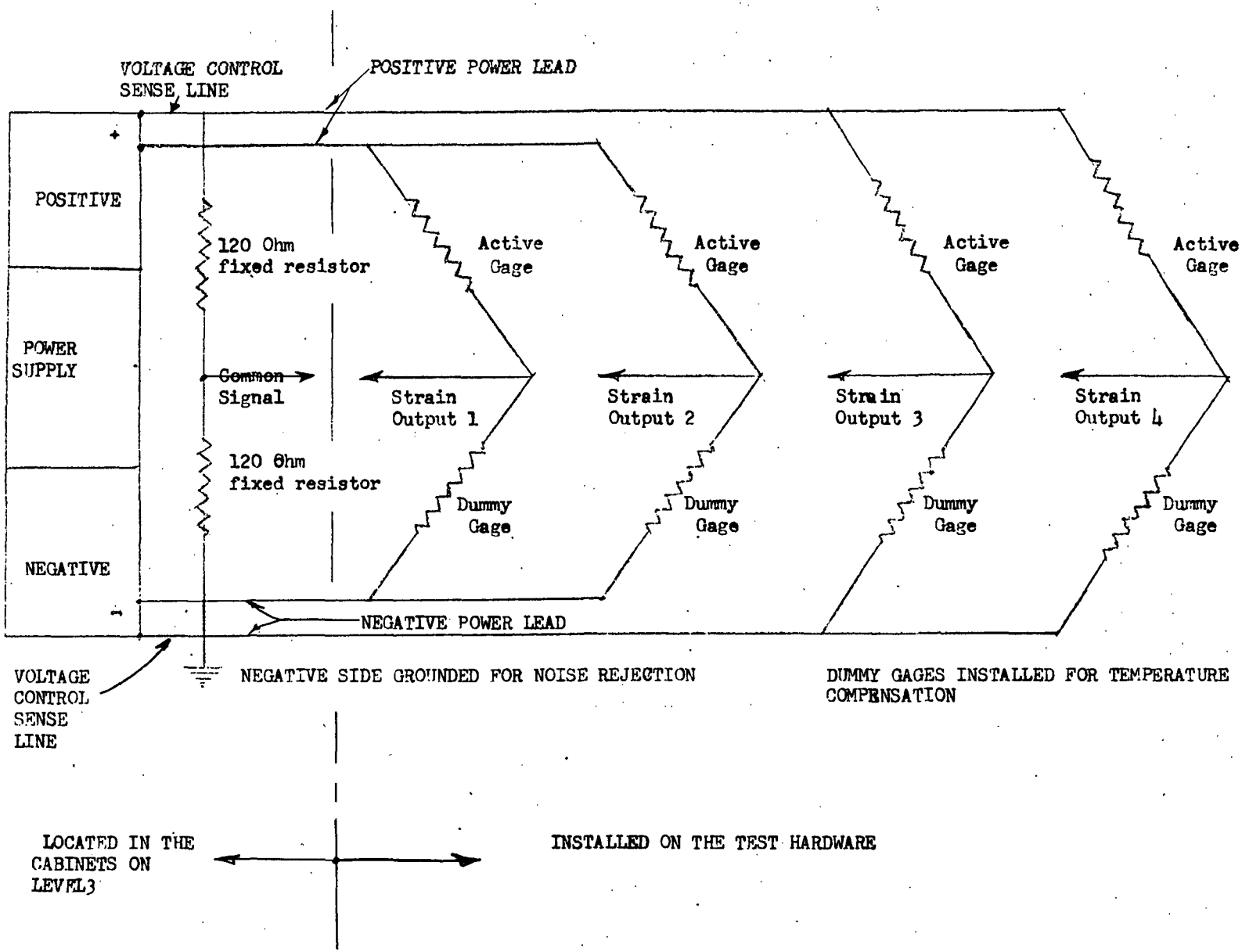

Figure B-4.-Schematic of the "chevron" circuit used with the strain gages installed for the Cryogenic-Unlatch Tests Plum Brook B-3 Facility

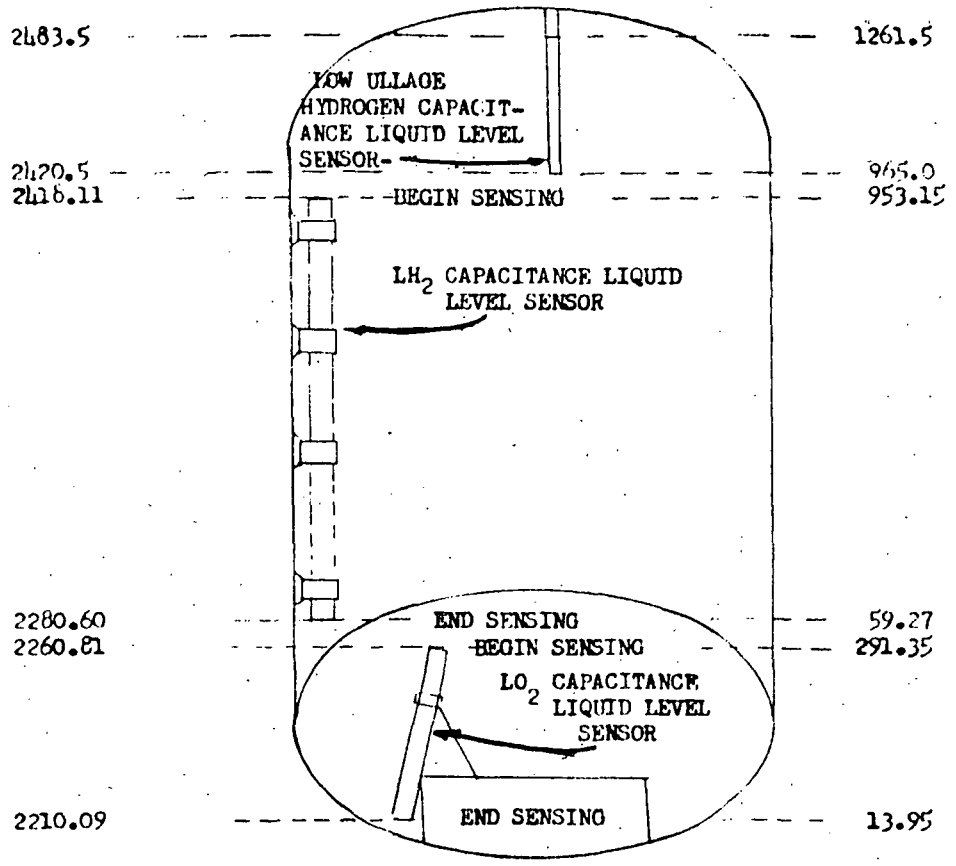

NOTE: LH_2 TANK VOLUME - 1265.4 FT.^{3}
LO_2 TANK VOLUME - 375.7 FT.^{3}

Figure B-5.-Locations of the liquid level capacitance probes installed for the Cryogenic-Unlacth Tests -Plum Brook B-3 Facility

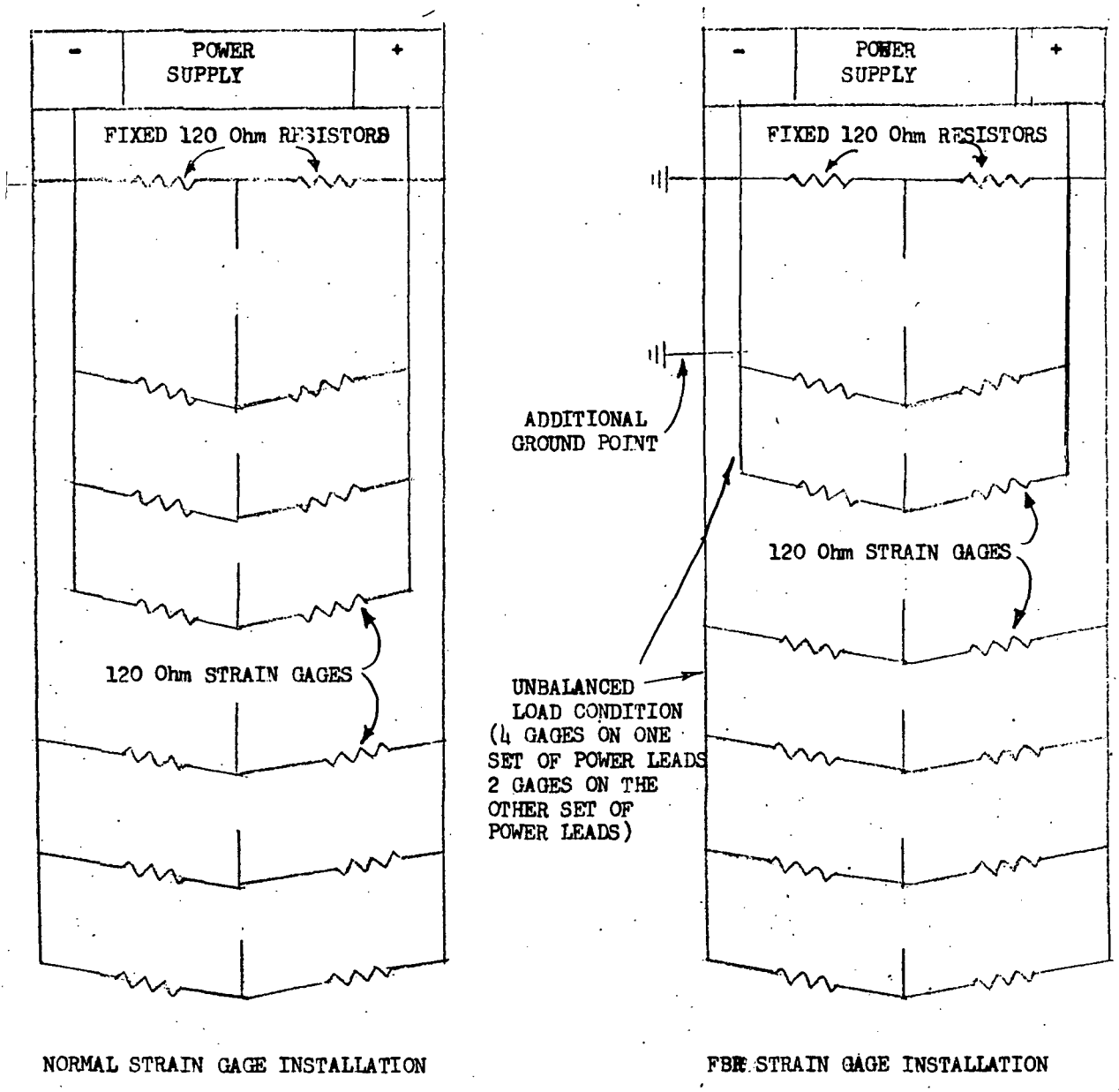

Figure B-6.-Schematics showing the comparison between the normal "chevron" strain gage circuit and the circuit installed for the FBR strain gages for the Cryogenic-Unlatch Tests -Plum Brook B-3 Facility

APPENDIX C

FACILITY AND SUPPORTING SYSTEMS

by W. E. Klein

The B-3 Facility, located at NASA Lewis Research Center's Plum Brook Station in Sandusky, Ohio, was used to conduct the Centaur Standard Shroud (CSS) Cryogenic Unlatch tests. Figure C-1 shows an overall view of the facility with the CSS installed.

The B-3 Facility is a tower structure 50 feet square by 200 feet high. The interior of the test stand was stripped of all hardware to give a clear working area of approximately 24 feet by 36 feet. The test area started at the first working level, 74 feet above ground level, and continued up to the bottom of the crane hook at 176 feet above ground level. The crane has a capacity of 65 tons and can travel from a point in the center of the building to a point over a railroad siding next to the building. Several sets of movable platforms were installed for access around the shroud. A 3-ton capacity elevator services the main working levels of the test stand. Roll doors on three sides of the building were raised for ventilation while hydrogen was in the building.

The following paragraphs give brief descriptions of the major facility systems and capabilities.

CRYOGENIC SYSTEMS

Liquid Hydrogen

The facility is connected to a 200,000 gallon, self-pressurizing, liquid hydrogen storage dewar. The dewar is located approximately 300 feet from the facility. Hydrogen can be transferred into the facility at a maximum flow rate of 800 gallons per minute through a 3-inch diameter vacuum jacketed line.

Liquid Nitrogen

The liquid nitrogen system has a manifold with connections for four liquid nitrogen roadable dewars. A liquid nitrogen pump, rated at 270 GPM at 140 psi, transfers nitrogen through a 2-1/2 inch diameter insulated copper line from ground level to the upper levels of the facility. Three 4500 gallon liquid nitrogen roadable dewars were connected to the manifold during the cryo-unlatch tests.

INERT GAS SYSTEMS

Nitrogen

The facility has a 2400 psig working pressure manifold and parking area for eight gaseous nitrogen tube trailers. In addition, two 5000 psig GN_2 railcar stations are connected to the GN_2 manifold through a pressure reducing station. Four tube trailers rated at 2400 psig and 70,000 standard cubic feet capacity, and two railcars rated at 5000 psig and 780,000 SCF capacity were used for each test. This system was used for LN_2 system purges, valve operator pressure, electrical equipment purges, and shroud payload area pressurization.

A gaseous nitrogen bottle farm is located at the southeast corner of the facility. The bottle farm consists of 200 nitrogen bottles with a total capacity of 300,000 SCF at 2400 psig. This farm can be made common with the 2400 psig GN_2 manifold. However, for these tests, this farm was used as a backup system for valve operator pressure.

Helium

The facility has a 2400 psig working pressure manifold and parking area for four gaseous helium tube trailers, each with a capacity of 70,000 SCF at 2400 psig. In addition, two 3500 psig GHe railcars were connected to the GHe manifold through a pressure reducing station. Each railcar is rated at 300,000 SCF at 3500 psig. This system was used for shroud tank section pressurization and LH_2 system inertion.

HYDRAULIC SYSTEM

Two identical hydraulic pump systems are located on the third level. Each system has a 60 gallon reservoir and a variable displacement pump rated at 30 gpm at 3000 psig. Both pumps are connected to a single distribution system that runs throughout the facility. If one pumping system fails, the other system can be started remotely from the control room. A small hydraulic pump rated at 5 gpm at 3000 psig is also connected to the distribution system for low flow operation. The hydraulic system was used as valve operator pressure for the Centaur tank pressure control valves and various flow control valves.

VACUUM SYSTEM

A single stage, 720 CFM mechanical vacuum pump was used for inerting the liquid hydrogen transfer and dump systems. The vacuum system has a capability of evacuating the hydrogen systems to less than one Torr. Alternate evacuation and helium gas purge cycles inert these systems prior to loading liquid hydrogen.

LH_2 BURNOFF SYSTEM

The B-3 Facility burnoff stack is located approximately 315 feet southeast of the test stand. This burnoff was used to dispose of the liquid hydrogen during the Centaur LH_2 tank fast dump. The burnoff line consists of 150 feet of 8 inch pipe and 300 feet of 14 inch pipe. None of the line is insulated. A natural gas flare is located on top of the burnoff stack. The burnoff has a capacity of 200 lb/sec. of hydrogen.

SAFETY SYSTEMS

Standard gas analyzer and fire detectors are used to detect hydrogen leaks at various locations throughout the facility. Upon the detection of any gaseous hydrogen or a fire, the location is displayed on the safety and annunciator panels in the control room.

CONTROL CENTER

Control of the B-3 Facility during all testing is from the B Control Building. This building is located approximately 2600 feet west of the facility. The B-3 control bay, the XDS 910 sequence and abort control computer, and the XDS 9300 computer and data display system are located in the building.

DATA ACQUISITION SYSTEM

The B-3 data acquisition system is a part of the Plum Brook 30 KC primary data system. All prime data is transmitted in multiplexed, digital form from the data sub-system in B-3 test stand to H Building for recording and processing. Analog FM signals are also recorded in H Building.

The data acquisition signal conditioning equipment is located in two basic areas. The instrument cabinets located on levels 3 and 4 contained the following signal conditioning equipment:

a. Thermocouple ovens - 288 channels

b. Deflectometers - 96 channels

c. 1/2 bridge type strain gage balance panels for strain measurements - 252 channels

d. Accelerometers, voltage generating type - 32 channels

e. He/N2 gas analyzer system - 5 channels

f. Liquid level measurement systems - 3 channels

Most of the remaining signal conditioning equipment is located in the Forward Instrument Room at ground level in the test stand. The Forward Instrument Room contained the following equipment:

a. Strain gage balance panels (pressures and accelerometers) - 64 channels

b. Platinum Resistance Thermometers - 24 channels

c. Scanner signal monitor, 400 channels, digital voltohm meter, printer, scope

d. Data sub-system multiplexer consisting of 400 channel multiplexer, analog to digital converter, transmission unit, decimal readout, digital to analog converter, and a memoscope display.

A number of analog signals are sent to B Control building for meter and strip chart displays for monitoring various parameters during the test.

CENTAUR TANK STRETCH AND STANDBY PRESSURIZATION SAFETY SYSTEMS

The walls of the Centaur tank are too thin to support the weight of the tank. Therefore, if the tanks are not continuously pressurized, a stretch system must be installed to keep the tank from collapsing. The stretch system in B-3 consisted of a Hydra-set, supported by the overhead crane, connected to the truss adapter through a sling. The Hydra-set supplied enough force to counterbalance the weight of all hardware on top of the Centaur tank and pull on the tank with 5000 pounds force.

The Hydra-set actuation pressure was sensed by a pressure switch. The contacts of the pressure switch were wired through Plum Brook's Emergency Communications Center (ECC). If the stretch pressure drifted out of limits, a crew was called to repair the problem.

The standby pressurization system consisted of a hand regulator and some isolation and vent valves for each tank. The oxygen tank was always kept pressurized. The hydrogen tank was normally vented to the atmosphere during standby. Whenever the crane was needed, the hydrogen tank was pressurized and stretch removed.

Both tank pressures were sensed by pressure transducers during standby. The transducer signals were fed to meter relays located near the tank standby pressure control panels. The meter relay contacts were wired to an alarm in the ECC. In addition, a differential pressure switch sensed the two tank pressures. In effect, this sensed the intermediate bulkhead differential pressure. If the LO_2 tank pressure

came within 3 psid of the LH_2 tank pressure, the pressure switch sent an alarm to the ECC.

CENTAUR TANK FILL, VENT, AND BULKHEAD DIFFERENTIAL PRESSURE PROTECTION SYSTEMS

The Centaur tanks were filled with cryogenics for the shroud heat leak and ground hold simulation tests. Liquid nitrogen was pumped from a dewar at ground level up to the Centaur oxygen tank. Liquid hydrogen was transferred to the Centaur hydrogen tank from the pressurized 200,000 gallon storage dewar. The oxygen tank was always filled first. The schematic for these lines is shown in Figure C-2.

After the liquid hydrogen transfer line was chilled, liquid hydrogen was introduced slowly into the tank to maintain a predetermined rate of temperature drop on the vehicle intermediate bulkhead. During this slow chilldown, the pressure in the intermediate bulkhead was monitored to determine that it dropped to a suitable vacuum due to the freezing of gaseous nitrogen in the intermediate bulkhead. Only after obtaining preset minimum temperatures at the inlet of the hydrogen tank and preset pressures in the intermediate bulkhead was the flow of hydrogen allowed to increase to fill the remainder of the tank to the desired level. The tank was filled at a rate of approximately 500 GPM, the fill rate used during prelaunch operations at the Eastern Test Range.

The hydrogen tank was normally dumped at a rate of approximately 1000 gpm into the burnoff line. However, it was also possible to back transfer the hydrogen into the 200,000 gallon storage dewar at a rate of approximately 100 gpm. It was possible to back transfer the liquid nitrogen into the LN_2 dewar. However, the LN_2 was normally dumped into the burnoff line or through a dump valve at ground level. These lines are shown in Figure C-2.

A system of servo-operated valves and pressure relief valves, as shown in Figure C-2, was connected to each of the Centaur tanks. These systems maintained the tank pressures at the desired levels throughout the tests. As shown in Figure C-2, there was one oxygen tank vent system that was used throughout the tests. There were two vent systems on the hydrogen tank. The flight vent system was connected to a 6-inch vent line in the facility. This vent was used during the initial tank fill operations and during the boiloff tests to simulate ground hold conditions. The 8-inch facility vent was connected to a flange in the forward door of the Centaur tank. This system was sized to handle the boiloff if the shroud should accidently separate with a full tank of hydrogen. The flight vent system could not handle the flow rate under this condition. The facility vent was used during shroud separation tests when the flight vent would have vented hydrogen gas into the facility.

The Centaur tank intermediate bulkhead can be reversed ("popped down") into the liquid oxygen tank if a higher pressure exists in the liquid hydrogen tank than in the liquid oxygen tank. Therefore, pressure

transducers sensing the pressure differential between the two tanks were monitored continuously by the bulkhead P protection system. If a differential pressure less than 2.0 psi occurred, the liquid hydrogen tank was vented. If a differential pressure greater than 23.0 psi occurred, the liquid oxygen tank gas was vented. Two additional pressure transducers sensed the difference in pressure between the Centaur hydrogen tank and the pressurized areas around the tank. If the pressure difference dropped below 2 psid, the hydrogen vent valve was closed and shroud vent valves were opened.

SHROUD INSTALLATION AND REMOVAL

Shroud assembly operations were very similar to those which will be used at the Eastern Test Range. The Centaur interstage adapter, boattail Centaur tank, and associated flight hardware were installed. These items were not part of the equipment which was separated with the shroud.

The remainder of the equipment had to be removed, refurbished, and re-installed after each separation test. The skirt section of the shroud was installed in halves. Then the hinges were installed and aligned. Next, the tank section of the shroud was installed in halves as shown in Figures C-3 and C-4. Once the tank section was installed, installation of the remainder of the tank associated equipment could start. This included the forward and aft seals, forward bearing reaction struts, hydrogen vent disconnects, hydrogen vent fin, and other flight type hardware.

At this point, the installation procedure deviated from that at the Eastern Test Range. At the ETR, the payload is encapsulated inside the cylindrical payload section and nosecone section of the shroud and installed as an assembly. At B-3, the payload model envelope simulator was installed (Figure C-5). Then the shroud cylindrical payload section is installed as a cylinder (Figure C-5) by lifting over the top of the payload model. The two halves of the nosecone are pre-assembled and then mounted on top of the cylindrical payload section (Figure C-6).

A wind restraint system was used for handling the shroud under certain wind conditions. This system consisted of a 16,000 pound ballast beam hanging from the shroud lifting fixture, as shown in Figures C-5 and C-6. Guides were attached at the top and bottom of each shroud section at each side. These guides were then attached to the cables supporting the ballast beam. This, in effect, adds sufficient mass to the shroud sections to keep them from swinging excessively in the wind. When the winds were below 12 MPH, the wind restraint system was not used (Figure C-4). When the winds were above 20 MPH, no shroud handling operations were attempted.

Three hinged work platforms were installed in the facility to provide access to the shroud near the field joints and at the top of the Centaur tank. When work was completed on the shroud before a test run, the plat-

forms were raised to the vertical position. This cleared the center of the test stand for shroud separation.

After the test the shroud was in two halves laying back in the nets. For this reason the assembly procedure could not be reversed for shroud removal. The handling fixtures were first installed on the +Y (90^{o}) half. After supporting the shroud half from the crane, the catch nets were removed. Then the hinges were disassembled and the shroud half lifted out of the test stand. The shroud half was rotated to a horizontal position on a railroad car (Figure C-7) and taken to the refurbishment area. The -Y half was removed in the same manner, except it had to be rotated around the Centaur tank to get it to the south door. Basically, the refurbishment consisted of replacing the spent Super*Zip joint. In addition, a number of instrumentation changes were made between runs.

CATCH NET SYSTEM

The catch net system consisted of a nylon strap net supported by a six inch aluminum pipe at each side. The net consisted of one inch wide nylon straps spaced approximately 10 inches apart vertically and horizontally. The 1-inch straps were all stitched into a 2-inch wide nylon strap around the outside edge of the net. The net started just below the nose cone and covered 150 inches of the cylindrical payload section. The net was fastened on each side to two disc brakes as shown in Figure C-8. The shroud energy was absorbed by pulling cables off drums attached to the disk brakes.

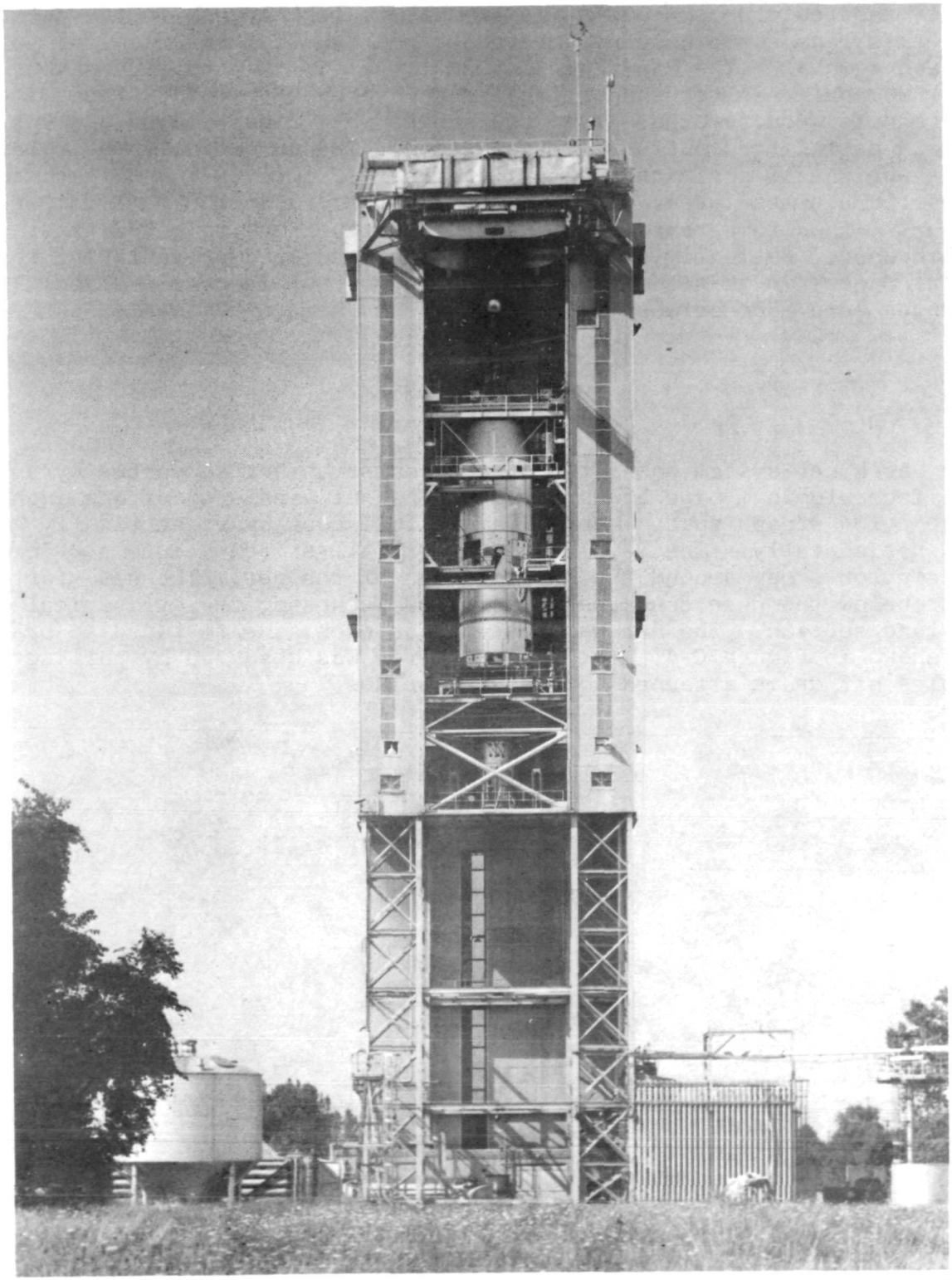

FIGURE C-1
"B-3" TEST STAND WITH CSS INSTALLED

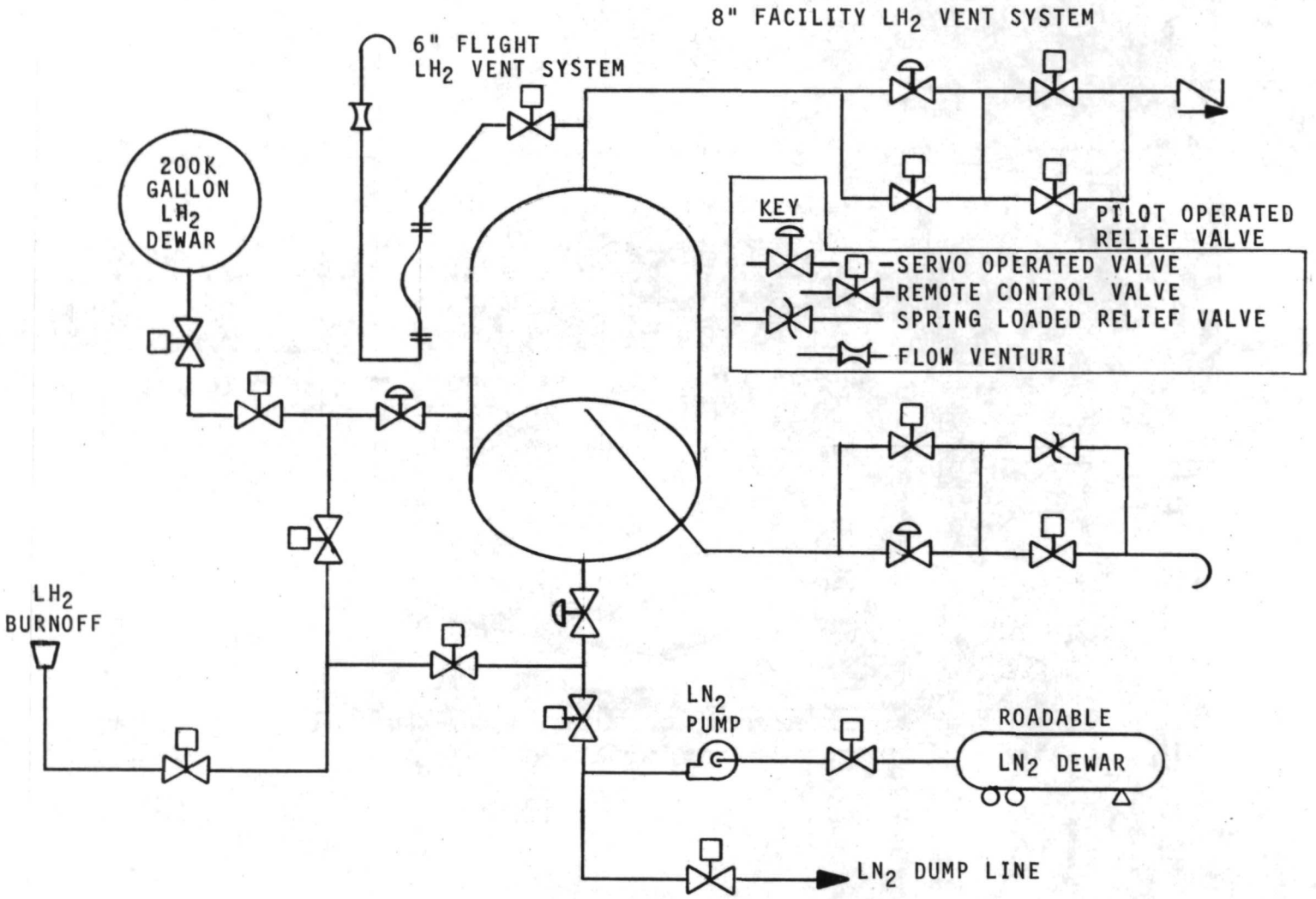

FIGURE C-2 CRYOGENIC FILL AND VENT LINES

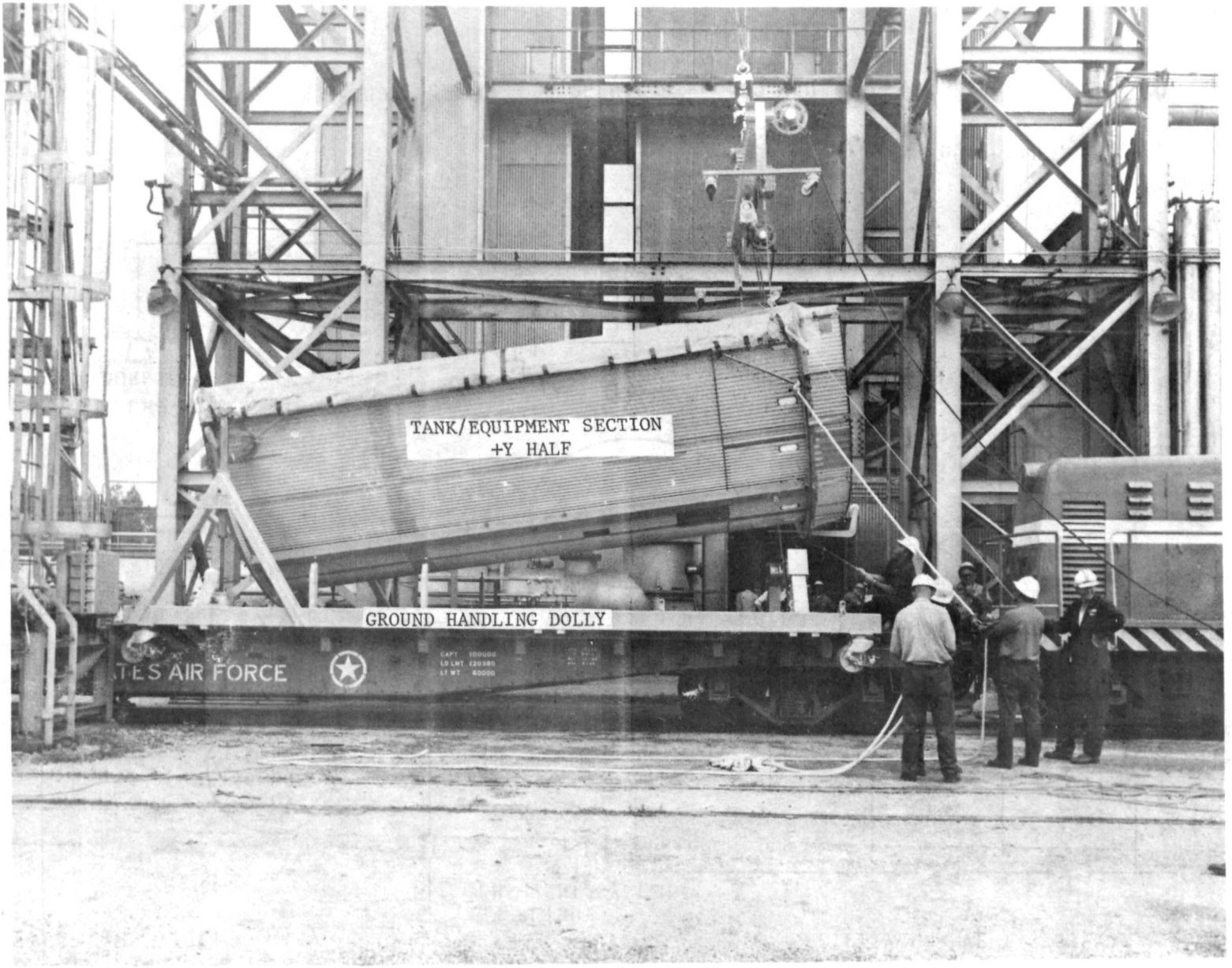

FIGURE C-3
SHROUD INSTALLATION - TANK/EQUIPMENT SECTION

FIGURE C-4
SHROUD INSTALLATION - TANK/EQUIPMENT SECTION

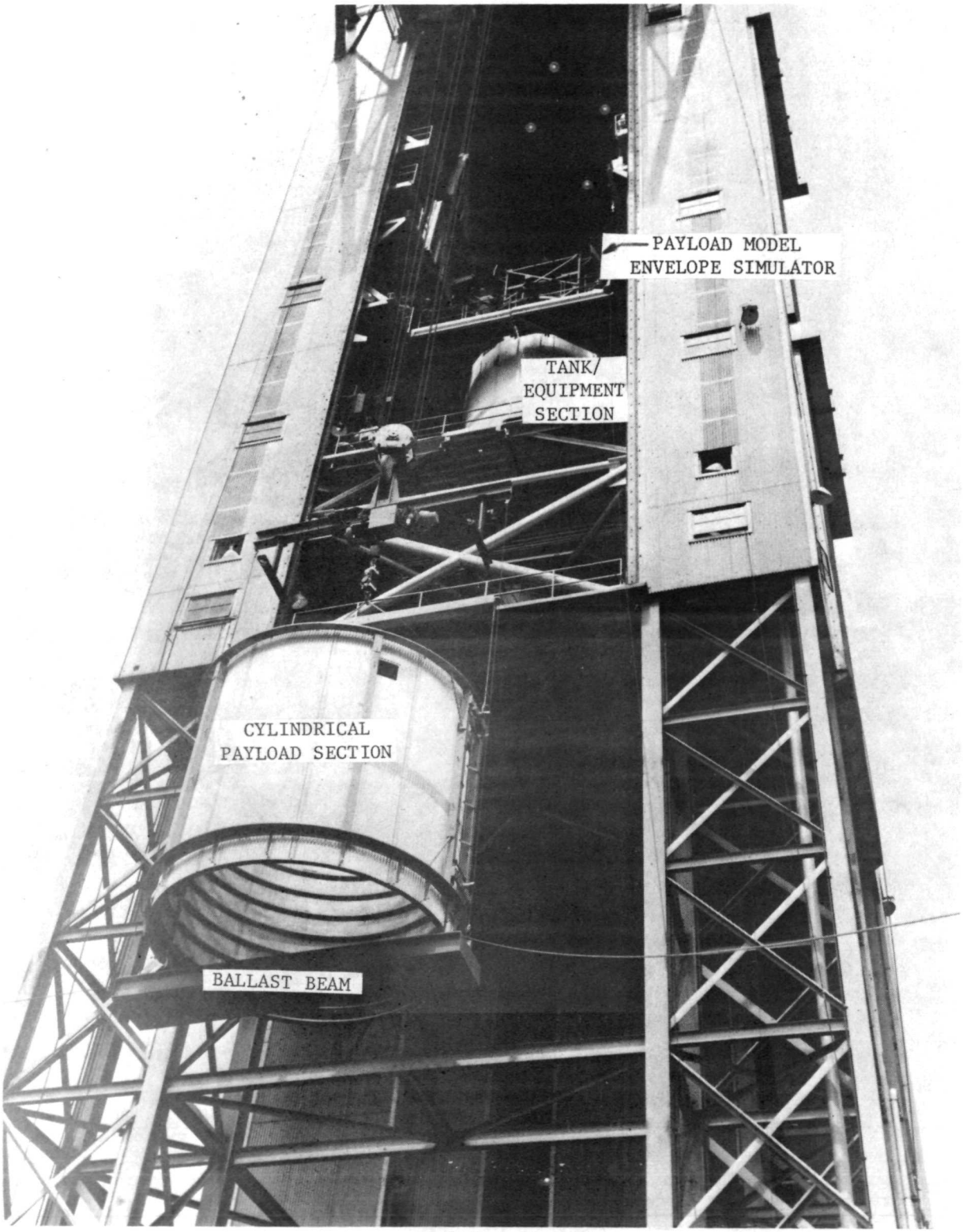

FIGURE C-5
SHROUD INSTALLATION-CYLINDRICAL PAYLOAD SECTION

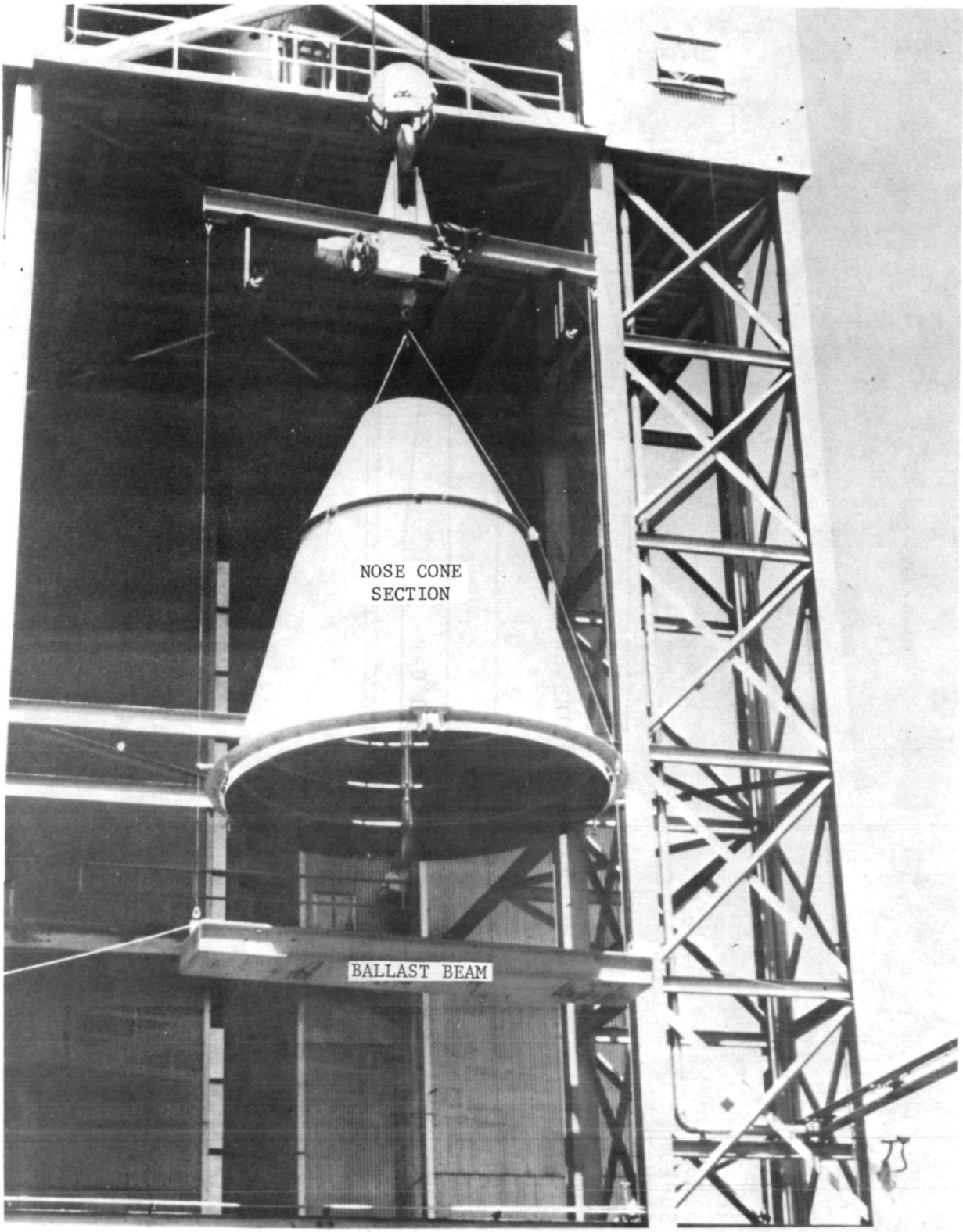

FIGURE C-6
SHROUD INSTALLATION - NOSE CONE SECTION

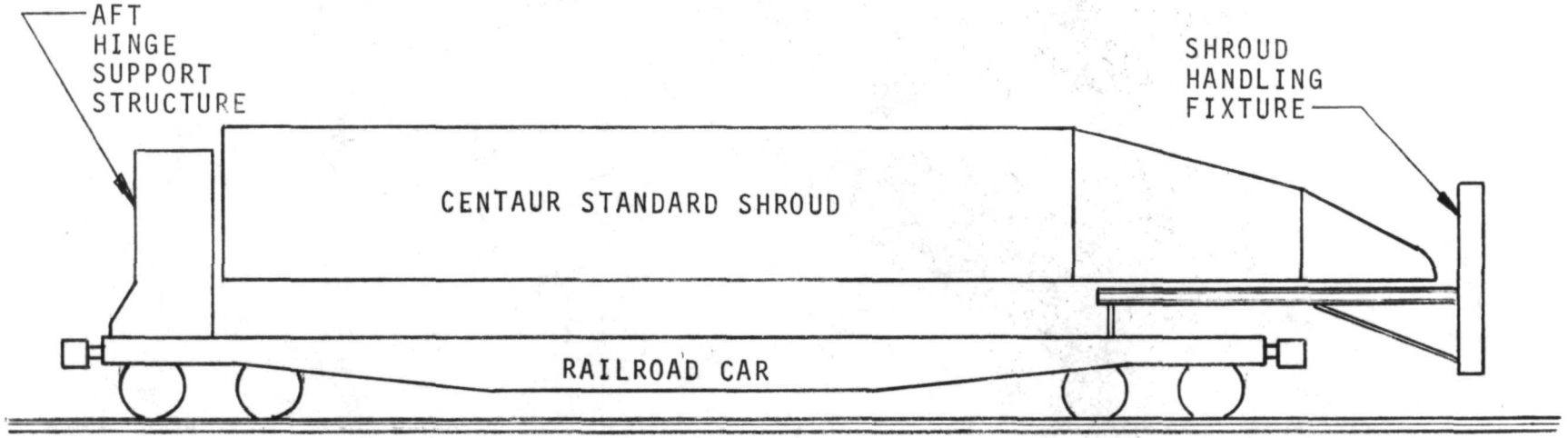

FIGURE C-7

SHROUD HALF ON RAILCAR

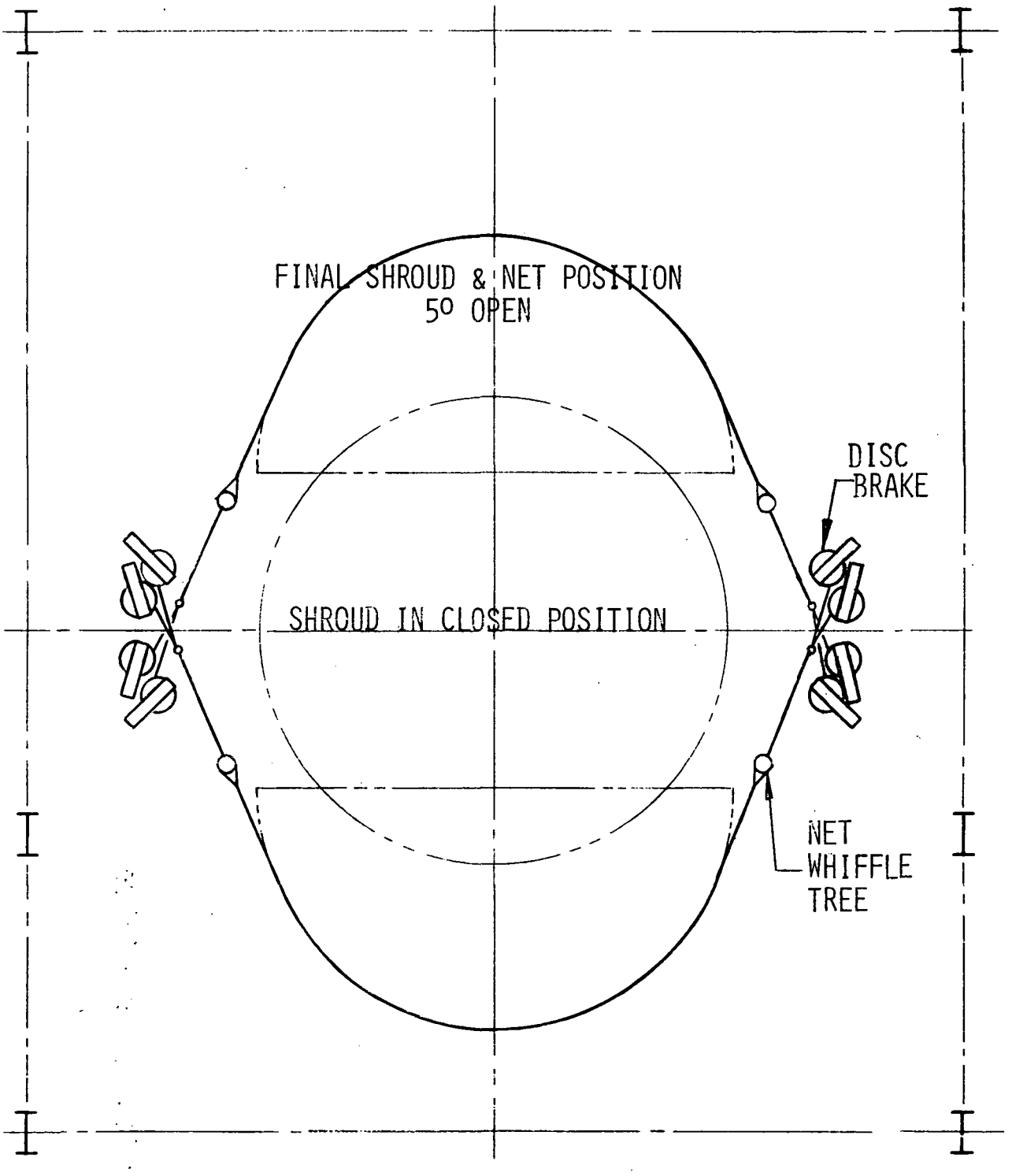

FIGURE C-8

PLAN VIEW OF CATCH SYSTEM

APPENDIX D

CHRONOLOGICAL RESUME OF EVENTS FOR EACH TEST

TABLE D-1

CHRONOLOGICAL RESUME OF CRYO-UNLATCH #1 TEST

WEEK OF 9/25/72

DATE:	TIME:	ELAPSED TIME:	EVENT
9/25/72 Mon.	0001	00:01	Started countdown operations. No check sheet work had been done the previous week. Instruments had remained setup from the Combined System Test conducted last week.
	0400	04:00	Problems with valve PIC-255 and HC-228. Will wait until day shift for valve shop to fix.
	1000	10:00	Readiness review meeting started. Went over C.S.T. data and reviewed status of facility and vehicle systems.
	1430	14:30	Readiness review meeting completed. All systems go for test.
	1500	15:00	Called in NASA, GD/CA and LMSC ordnance crew to run preloading checkout. Returned GD/CA ordnance to igloo after checkout.
	1600	16:00	**Finished facility roll door repairs**
	1800	18:00	Camera crew loading internal cameras.
	1830	18:30	Started shroud leak tests to see if repairs made on 9/22, 9/23 and 9/25 were good.
	2015	20:15	Shroud leak tests complete. Results were good.
			Adjustable vent / Flow Rate / Pressure Open — 52.5#/hr. Hel. — .93 psig Closed — 52.5#/hr. Hel. — 1.06 psig
	2200	22:00	Started ordnance loading procedure.
9/26/72 Tues.	0100	25:00	Started GN_2 purge of shroud. Test stand upper levels off limits to everyone except ordnance personnel.
	1515	39:15	F.B.R. cartridges installed and super-zip cord loaded in doubler strips. Continue with check sheet operation for facility setup.
	1630	40:30	Started procedures to cock lateral jettison springs and main shroud jettison springs.
	2010	44:10	Successfully remotely controlled all five roll doors for the first time.

TABLE D-1 Cont.

DATE:	TIME:	ELAPSED TIME:	EVENT
9/26/72 Tues.	2130	45:30	Finished spring cocking procedure.
	2200	46:00	Decided brake discs looked too rusty to run with. Will disassemble and clean up all 8 discs.
9/27/72 Wed.	0010	48:10	SEL not recording properly. Reloaded data pattern tape and it looked O.K.
	0100	49:00	Lightning in area. Keep a close watch on the weather.
	0125	49:25	All boattail access doors installed.
	0310	51:10	Brake discs on east side are finished. Starting on west side.
	0630	52:30	Called in ordnance crews for final loading of detonators.
	0655	52:55	Switched shroud purge from N_2 to helium.
	0920	57:20	SEL off line for a short period.
	1030	58:30	Readjusted catch nets.
	1035	58:35	Checked all external camera lights. Looked good.
	1145	59:45	Started final ordnance arming procedures.
	1340	61:40	FBR's were disarmed so LMSC could make an adjustment to the lateral jettison springs to keep them from striking the CSS at jettison.
	1600	64:00	CSS doors put in place at forward seal area. Began to get H_2 gas detector alarm due to helium gas affecting sensor over nose cone of shroud.
	2030	68:30	All check sheets complete except Cell Evacuation. Annunciator problems developing in control room. Called in electrician from home.
	2230	70:30	Helium supply becoming a matter of concern. Backed off purges to shroud to low flow rates to conserve helium.
9/28/72 Thurs.	0730	79:30	Annunciators repaired and back on-line. Problem traced to camera purge supply pressure switches at site. They somehow cause a short when the switch makes contact.
	0830	80:30	Started aft and forward seal warming purges.

TABLE D-1 Cont.

DATE:	TIME:	ELAPSED TIME:	EVENT
9/28/72 Thur.	0940	81:40	Mist on CSS and water dripping on cameras #8 and #9 and detonator blocks.
	1125	83:25	Started filling LOX tank with LN_2.
	1230	84:30	LOX tank fill complete.
	1500	87:00	Test stand evacuated.
	1725	89:25	Started filling LH_2 tank.
	1900	91:00	LH_2 tank fill complete.
	1915	91:15	Started LH_2 tank boiloff and pressurization tests.
	2325	95:25	Boiloff and pressurization tests completed.
	2345	95:45	Started detanking LH_2 for jettison test.
	2357	95:57	Successful jettison of shroud.
9/29/72 Fri.	0015	96:15	Started clean up of LH_2 tank and facility systems.
	0600	102:15	Ordnance crew in B-3 to remove detonators.
	0645	102:45	Preliminary inspection crew in test stand.
	0745	103:45	Preliminary inspection complete.
	1235	108:35	Finished ordnance disarmament.
	1300	109:00	Inspection team #2 enters test stand.
	1500	111:00	Inspection team has meeting in control room to report results of inspection.
	1535	111:15	Proceed with final test stand shutdown.
	2100	117:00	Test stand secure.

TABLE D-2

CHRONOLOGICAL RESUME OF CRYO-UNLATCH #2 TEST

11-4-72 to 11-9-72

Date:	Time:	Elapsed Time:	Event:
11/4/72 Sat.	1200	0	Started ordnance loading.
11/5/72 Sun.	0200	14	Stop loading ordnance for rest period.
	1000	14	Restarted ordnance loading.
	2000	24	Ordnance loading complete. (Super-zip cord and FBR pressure cartridges installed. No detonators installed)
11/6/72 Mon.	0000	00:00	Started countdown operations.
	0030	00:30	Started facility check sheets. Adjusting catch nets. Installing brake discs.
	0830	08:30	Vent and relief valves set up complete.
	1445	14:45	Centaur tanks on auto control.
	1615	16:15	All internal cameras loaded.
	1715	17:15	Centaur stretch set up complete.
	1730	17:30	Began GN_2 shroud purge.
	2000	20:00	Brake set up complete.
11/7/72 Tues.	0715	31:15	Shroud purge switched to helium.
	0845	32:45	GHe purge to radiation shield isolated.
	0900	33:00	Started loading detonators.
	1510	39:10	Detonator loading complete.
	1530	39:30	Started cell evacuation.
	1830	42:30	Cell evacuation upper levels complete.
	1945	43:45	Holding to fix TV camera monitoring manometers.
	2215	46:15	TV camera fixed.

TABLE D-2 Cont.

Date:	Time:	Elapsed Time:	Event:
11/7/72 Tues	2220	46:20	Started loading LO_2 tank with LN_2.
	2311	47:11	LO_2 tank filled to 44%.
	2320	47:20	Started final cell evacuation.
11/8/72 Wed.	0015	48:15	Final cell evacuation complete.
	0025	48:25	Started LH_2 tank fill.
	0155	49:55	Completed LH_2 tank fill.
	0234	50:34	Started LH_2 tank boiloff and pressurization tests.
	0751	55:51	Boiloff and pressurization test completed.
	0830	56:30	LH_2 tank retopped.
	0858	56:58	Started detanking LH_2 tank for jettison test.
	0915	*57:15*	*Successful jettison of shroud.*
	0918	57:18	Started cleanup of LH_2 tank and facility systems.
	1345	61:45	Preliminary inspection crew in test stand.
	1445	62:45	Preliminary inspection complete.
	1915	67:15	Finished ordnance checkout.
	1945	67:45	Fired second super-zip.
	2200	70:00	Completed all ordnance disarmament.
	2215	70:15	Start final CSS inspection.
	2315	71:15	Final CSS inspection finished.
11/9/72 Thur.	0400	76:00	Facility shutdown complete.

TABLE D-3

CHRONOLOGICAL RESUME OF LN_2/LN_2 SEAL RELEASE TEST

1/8/73 to 1/11/73

Date:	Time:	Elapsed Time:	Event:
1/8/73 Mon.	0000	00:00	Started countdown operations.
	0800	08:00	Started mechanical systems check sheets.
1/9/73 Tues.	0100	25:00	Vent and relief valves set up completed.
	0305	27:05	Centaur tanks on auto control.
	0530	29:30	Centaur stretch set up completed.
	0900	33:00	Found small slit in forward seal.
	1700	41:00	Seal repair completed.
	1815	42:15	Shroud leak check completed. Started GN_2 shroud purge.
1/10/73 Wed.	0205	50:05	Ordnance loading completed.
	0630	54:30	Switched shroud purge from GN_2 to GHe.
	0800	56:00	Camera film loading completed.
	0900	57:00	Upper levels of test stand evacuated.
	1030	58:30	406P bad. Changed signal conditioning equipment.
	1050	58:50	Started LO_2 tank fill with LN_2.
	1130	59:30	LO_2 tank filled to 44 per cent.
	1140	59:40	Started LH_2 tank fill with LN_2.
	1305	61:05	LH_2 tank filled to 85 per cent.
	1330	61:30	Started boiloff tests.
	1908	67:08	Started water spray test.
	2000	68:00	Water spray test completed.
	2120	69:20	Started detanking LH_2 tank.

TABLE D-3 Cont.

Date:	Time:	Elapsed Time:	Event:
1/10/73 Wed.	2143	69:43	Started autosequence.
	2230	70:30	Completed LO_2 tank dump. Started warming shroud for inspection.
1/11/73 Thurs.	0900	81:00	Completed safing ordnance system. Started main inspection. Started facility shutdown.
	1500	87:00	Facility shutdown completed.

TABLE D-4

CHRONOLOGICAL RESUME OF LH_2/LN_2 SEAL RELEASE TEST

1/22/73 to 1/24/73

Date:	Time:	Elapsed Time	Event:
1/22/73 Mon.	0000	00:00	Started countdown operations.
	0010	00:10	Started facility check sheets.
	0700	07:00	Vent and relief valves set up complete.
	0730	07:30	Found hydraulic leak on level 3. Oil splashed Titan skirt and floor.
	1330	13:30	Hydraulic leak repaired and oil cleaned up.
	1930	19:30	Centaur tanks on auto control.
	2100	21:00	Centaur stretch set up complete.
	2130	21:30	Started GN_2 shroud purge.
	2200	22:00	Camera film loading completed. Started loading ordnance.
	2400	24:00	Shroud ordnance loading complete.
1/23/73 Tues.	0400	28:00	Switched shroud purge from GN_2 to GHe.
	0723	31:23	Upper levels of test stand evacuated. Started LO_2 tank fill with LN_2.
	0755	31:55	LO_2 tank filled to 44 per cent.
	0800	32:00	Started final cell evacuation.
	0930	33:30	Final cell evacuation completed.
	1015	34:15	Started hold to straighten out electrical noise and other minor problems on TV's 2, 3, and 4.
	1115	35:15	TV problems resolved.
	1130	35:30	Started LH_2 tank fill.
	1245	36:45	LH_2 tank fill completed.
	1300	37:00	Started LH_2 boiloff tests.

TABLE D-4 Cont.

Date:	Time:	Elapsed Time:	Event:
1/23/73 Tues.	1806	42:06	Started water spray test.
	1910	43:10	Boiloff tests and water spray test completed.
	2232	46:32	Started detanking LH_2 tank.
	2242	46:42	Started autosequence.
	2250	46:50	Started LH_2 tank and systems inertion.
1/24/73 Wed.	0210	50:10	Started LO_2 tank dump.
	0215	50:15	Completed LO_2 tank dump.
	0235	50:35	Completed LH_2 system inertion. Started facility re-entry. Started shroud warming purge.
	0330	51:30	Completed facility re-entry.
	0800	56:00	Shroud warming completed. Started safing ordnance systems.
	0930	57:30	Completed safing ordnance systems.
	1320	61:20	Centaur tanks put on standby.
	1530	63:30	Facility shutdown complete.

TABLE D-5

CHRONOLOGICAL RESUME OF CRYO-UNLATCH #3 TEST

2-3-73 to 2-8-73

Date:	Time:	Elapsed Time:	Event:
2/3/73 Sat.	0805	00:00	Start ordnance loading.
	2235	14:30	Completed ordnance loading. (Super zip cord and FBR and FSR pressure cartridges installed. No detonators installed in CSS ordnance.)
2/5/73 Mon.	0000	00:00	Started countdown operations.
	0030	00:30	Started facility check sheets.
	0130	01:30	Vent and relief valves set up complete.
	0500	05:00	Moog on PIC 4187 oscillating at approximately 2 Hz when error monitor calls for PIC 4187 to be closed.
	1230	12:30	Lowered Moog drive current from error monitor system. Slower response, but system still satisfactory.
	1730	17:30	Centaur tanks on auto control.
	1800	18:00	Camera film loading complete.
	1850	18:50	Centaur stretch set up complete.
	2020	20:20	Performed shroud leak check with GHe.
	2045	20:45	Started GN_2 shroud purge.
2/6/73 Tues.	0330	27:30	Switched shroud purge from GN_2 to GHe.
	0530	29:30	Started loading CSS detonators.
	1200	36:00	Ordnance loading completed, started cell evacuation.
	1445	38:45	Upper levels of test stand evacuated.
	1530	39:30	Started "extra" ordnance system checkout. (Validation of computer relays and firing circuit.)
	1840	42:40	"Extra" ordnance checkout completed.

TABLE D-5 Cont.

Date:	Time:	Elapsed Time:	Event:
2/6/73 Tues.	1930	43:30	Started LO_2 tank fill with LN_2.
	2040	44:40	LO_2 tank filled to 44 per cent.
	2045	44:45	Started final cell evacuation.
	2120	45:20	Stopped evacuation to repair regulator for supply from GHe railcar.
	2310	47:10	Regulator repair completed.
	2325	47:25	Cell evacuation completed. Started LH_2 tank fill.
2/7/73 Wed.	0040	48:40	LH_2 tank fill completed.
	0050	48:50	Started LH_2 boiloff test.
	0145	49:45	Started water spray test.
	0245	50:45	Completed water spray test and LH_2 boiloff test.
	0300	51:00	Started detanking LH_2 tank.
	0324	*51:24*	*Started autosequence. FBR's fired, then sequence aborted. FBR #2 had hit limits, but came off, aborting sequence.*
	0340	51:40	Started LH_2 tank and systems inertion.
	0600	54:00	LH_2 systems inerted.
	0615	54:15	Started facility re-entry with LN_2 in LO_2 tank.
	0700	55:00	Facility re-entry completed. Started preliminary inspection.
	1130	59:30	Inspection completed. All FBR's fired successfully. Started evacuating upper levels.
	1200	60:00	Started purging shroud with GHe. (Minimum GN_2 purge rates had been maintained from end of LH_2 systems inertion.)
	1400	62:00	Upper level evacuated. Started re-topping LO_2 tank with LN_2.
	1430	62:30	Completed LO_2 tank re-topping. Started re-arming ordnance.
	1530	63:30	All ordnance re-armed.

TABLE D-5 Cont.

Date:	Time:	Elapsed Time:	Event:
2/7/73 Wed.	1620	64:20	Cell evacuation completed. Started LH_2 tank fill.
	1750	65:50	LH_2 tank fill completed.
	1830	66:30	Started LH_2 tank boiloff test.
	1930	67:30	Started water spray test.
	2020	68:20	LH_2 boiloff test and water spray test completed.
	2100	69:00	Started detanking LH_2 tank.
	2115	69:15	LH_2 detanking completed.
	2120	*69:20*	*Successful jettison of shroud.*
	2140	69:40	Started LH_2 system inertion.
2/8/73 Thurs.	0110	73:10	Completed LH_2 system inertion. Started LO_2 tank dump.
	0200	74:00	Completed LO_2 tank dump. Started facility re-entry.
	0320	75:20	Completed facility re-entry. Started preliminary inspection.
	0600	78:00	Completed preliminary inspection. Evacuated upper levels.
	0710	79:10	Fired secondary ordnance system.
	0715	79:15	Started preliminary inspection.
	0800	80:00	Completed preliminary inspection.
	0915	81:15	Completed safing ordnance system. Started main inspection. Started facility shutdown.
	1600	87:00	Facility shutdown complete.